**Calhoun: The NPS Institutional Archive**

**DSpace Repository**

Theses and Dissertations | 1. Thesis and Dissertation Collection, all items

1997

# Procedures to predict vertical differential soil movement for expansive soils

Naiser, Donald David

http://hdl.handle.net/10945/8855

*Downloaded from NPS Archive: Calhoun*

http://www.nps.edu/library

Calhoun is the Naval Postgraduate School's public access digital repository for research materials and institutional publications created by the NPS community. Calhoun is named for Professor of Mathematics Guy K. Calhoun, NPS's first appointed -- and published -- scholarly author.

Dudley Knox Library / Naval Postgraduate School
411 Dyer Road / 1 University Circle
Monterey, California USA 93943

NPS ARCHIVE
1997
NAISER, D.

DUDLEY KNOX LIBRARY
NAVAL POSTGRADUATE SCHOOL
MONTEREY CA 93943-5101

# PROCEDURES TO PREDICT VERTICAL DIFFERENTIAL SOIL MOVEMENT FOR EXPANSIVE SOILS

A Thesis

by

DONALD DAVID NAISER, JR.

Submitted to the Office of Graduate Studies of
Texas A&M University
in partial fulfillment of the requirements for the degree of

MASTER OF SCIENCE

December 1997

Major Subject: Civil Engineering

# PROCEDURES TO PREDICT VERTICAL DIFFERENTIAL SOIL MOVEMENT FOR EXPANSIVE SOILS

A Thesis

by

DONALD DAVID NAISER, JR.

Submitted to Texas A&M University
in partial fulfillment of the requirements
for the degree of

MASTER OF SCIENCE

NPS ARCHIVE
1997
NAISER, D.

DUDLEY KNOX LIBRARY
NAVAL POSTGRADUATE SCHOOL
MONTEREY CA 93943-5101



## ABSTRACT

Procedures to Predict Vertical Differential Soil Movement
For Expansive Soils. (December 1997)
Donald David Naiser, Jr., B.S., Texas A&M University
Chair of Advisory Committee: Dr. Robert L. Lytton

Damage to lightly loaded structures, paving and service piping in areas of expansive clay soils has occurred throughout the world. The cause of this damage has been the inability to accurately model expansive soil movement so that foundations are adequately designed to withstand the movement. The amount and rate of differential soil movement for expansive soils is due to a combination of soil characteristics, namely: suction compression index, unsaturated permeability, and diffusivity. Currently, geotechnical engineers run tests to measure the soil properties required to estimate differential soil movements. However, there seems to be apprehension toward attempting these soil movement calculations due to the perceived complexity of the calculations or a simple lack of understanding of the theory. The procedures delineating the step by step process used to calculate suction profiles and volume strains of expansive soils is presented. These procedures include the methodology to predict soil heave and shrink underneath shallow foundations which generate maximum center lift and maximum edge lift slab distortion modes. The main contributions of this research are: equations and procedures to calculate the equilibrium suction profile and depth to constant suction for a particular soil profile and location, equations to calculate the horizontal velocity flow of water in unsaturated soils, the methodology to predict differential soil movement shortly after a slab has been constructed and before the soil under the slab has reached an equilibrium moisture content, and the procedures to apply differential soil movement theory to soil profiles with multiple layers and moisture effect cases to be used for shallow foundation design.

## DEDICATION

This thesis is dedicated to my mother and father, Barbara and Don, my brother, his wife and their baby girl, Derek, Susan and Katie, my brother, his wife and their baby boy, Brian, Kristine and Logan and my youngest brother Mark. Their love, understanding, support and encouragement made this accomplishment possible.

# ACKNOWLEDGMENTS

I am very fortunate, blessed and privileged to be given the opportunity to work under the tutelage of Dr. Robert L. Lytton. I am grateful for the patience, support, encouragement, and guidance Dr. Lytton provided throughout my studies. I thank Dr. Glen R. Andersen for his encouragement and belief in my abilities to perform as a Master of Science candidate. I would also like to recognize Dr. Christopher Mathewson for his interests and support as a member of this advisory committee. Additionally, I thank Mr. Doug Lambert for his drafting assistance and expertise.

# TABLE OF CONTENTS

Page

ABSTRACT..... iii

DEDICATION..... iv

ACKNOWLEDGEMENTS..... v

TABLE OF CONTENTS..... vi

LIST OF TABLES..... viii

LIST OF FIGURES..... ix

LIST OF SYMBOLS..... xi

LIST OF DEFINITIONS..... xviii

INTRODUCTION..... 1

THE PROBLEM..... 4

The Magnitude and Description of the Problem..... 4

Expansive Soil, on a Molecular Level..... 6

The Building Blocks of Expansive Soil..... 6
Gilgai..... 11
Suction, Matrix and Osmotic..... 13
Components of Soil Suction..... 13
Typical Suction Levels in the Field..... 13

THE THEORY OF DIFFERENTIAL SOIL MOVEMENT..... 16

Soil Volume Strain..... 17

A Simplified Method for Identifying Predominant Clays..... 20

The Suction/Mean Principal Stress Compression Indexes..... 22

Estimates of Unsaturated Soil Properties..... 25

Edge Moisture Variation for Center Lift and Edge Lift Cases..... 26

Equilibrium Suction..... 30

Suction Profiles..... 35

Depth to Constant Suction..... 38

Horizontal Velocity in Expansive Soils..... 40

Page

Post Construction Theory..... 41

The "Damped" Slab Suction Profile..... 42
The Time Equation..... 45

THE PROCEDURES, IN A SOFTWARE DESIGN FORMAT..... 46

Introduction to the Software Design Approach..... 46

Input..... 47

Calculated Soil Properties and Soil Characteristics..... 51

Procedures to Calculate the Equilibrium Suction..... 52

Depth to Constant Suction..... 53

POST EQUILIBRIUM AND POST CONSTRUCTION SOLUTIONS..... 58

Post Equilibrium Approach..... 58

Equilibrium Suction Profiles..... 58
Suction Profiles Causing the Center Lift Distortion Mode..... 59
Suction Profiles Causing the Edge Lift Distortion Mode..... 59
Vertical Differential Soil Movement..... 61

Post Construction Approach..... 65

Post Construction Suction Profiles..... 65
Vertical Differential Soil Movement..... 67

MEASURED SUCTION PROFILES..... 69

DISCUSSION OF RESULTS..... 73

SUMMARY AND SUGGESTIONS FOR RESEARCH AND DEVELOPMENT... 76

REFERENCES..... 78

APPENDIX A..... 81

APPENDIX B..... 116

APPENDIX C..... 131

APPENDIX D..... 133

VITA..... 135

# LIST OF TABLES

Table Page

1. Soil profile considered in all sample calculations..... 50
2. Gardner's coefficients..... 54
3. Measured suction profile values..... 70
4. Summary of vertical differential soil movements for Appendix C.....74

# LIST OF FIGURES

Figure Page

1. United States map of expansive soils after Wiggins..... 4
2. Center lift distortion mode..... 6
3. Edge lift distortion mode..... 6
4. The structure of kaolinite (a) atomic structure (b) symbolic structure..... 7
5. The structure of serpentine (a) atomic structure (b) symbolic structure..... 8
6. Soil particles with water and ions (a) sodium montmorillonite (b) sodium kaolinite...9
7. The structure of pyrophyllite (a) atomic structure (b) symbolic structure..... 10
8. The structure of muscovite (a) atomic structure (b) symbolic structure..... 10
9. Gilgai stages..... 12
10. Suction vs volumetric water content curve..... 14
11. Edge heave and center heave distortion modes..... 17
12. Mean principal stress-volume-matrix suction diagram..... 18
13. Chart to identify predominant clays..... 22
14. Pressure-volume-suction surface..... 23
15. Chart to determine the suction compression index..... 24
16. Edge moisture variation distance for center lift conditions (50 yrs)..... 28
17. Edge moisture variation distance for edge lift conditions (50 yrs)..... 29
18. Edge moisture variation distances for edge/center lift conditions (10 yrs)..... 29
19. Domains of functions f(d) and g(T)..... 31
20. Theoretical relationships for mean annual moisture depth vs TMI..... 32
21. Moisture changes in unsaturated soils between typical wet and dry states..... 34
22. Typical dry limit suction profile for bare soil at the surface..... 37
23. Typical wet limit suction profile for bare soil at the surface..... 37
24. A weather cycle modeled by a cosine function, n = 1, June is the driest month..... 43
25. Domains of functions h, t, and f(h)..... 44

Figure Page

26. Thornthwaite index for Texas (20 year average 1955-1974)..... 50
27. Post equilibrium suction profiles for flower bed at the surface (dry limit)..... 60
28. Post equilibrium suction profiles for a tree at the surface (dry limit)..... 60
29. Post equilibrium suction profiles for a flower bed at the surface (wet limit)..... 61
30. Bare soil dry limit suction profiles for a slab with a 4ft vertical barrier..... 63
31. Suction profiles for flower bed at the slab edge with a 4 ft horizontal barrier..... 64
32. Suction profiles for a tree 4ft from the slab edge with a 4 ft vertical barrier..... 65
33. Initial and final measured suction profiles described in table 4..... 71

## LIST OF SYMBOLS

The page number in parenthesis after the definition of a symbol refers to the location the symbol was first used.

| | |
|---|---|
| A,B | Gardner's coefficients (pg 33) |
| $Ac(z_i)$ | Activity ratio for the $i^{th}$ soil increment (pg 20) |
| B | Number of boring samples (pg 48) |
| $BD_b$ | Depth of boring sample b (Appendix A-84) |
| $C_c$ | Soil compression index (pg 25) |
| $CEAc(z_i)$ | Cation exchange activity ratio for the $i^{th}$ soil increment (pg 20) |
| $CEC(z_i)$ | Cation exchange capacity for the $i^{th}$ soil increment (pg 21) |
| $Clay(z_i)$ | Percent fine clay for the $i^{th}$ soil increment (pg 21) |
| $D_c$ | Depth to the $c^{th}$ suction measurement in a sample (pg 48) |
| H | Relative humidity, in percent $H = \frac{\overline{u_v}}{u_{vo}}$ (pg 13) |
| $K_o(z_i)\lvert h_o\rvert$ | Mitchell's unsaturated permeability for the $i^{th}$ soil increment (pg 11) |
| $L_s$ | Depth to the bottom of layer s (pg 48) |
| $LL_s$ | Liquid limit for layer s, in percent (pg 48) |
| $LL(z_i)$ | Liquid limit for the $i^{th}$ soil increment, in percent (pg 21) |
| $M_b$ | Number of layers in the $b^{th}$ boring sample (pg 48) |
| N | Number of suction measurements in a sample (pg 48) |
| $P_i$ | Ratio of suction values between the top and bottom layers within the $i^{th}$ increment (pg 56) |
| $PI(z_i)$ | Plasticity Index for the $i^{th}$ soil increment, in percent (pg 20) |
| $PL_s$ | Plastic limit for layer s, in percent (pg 48) |
| $PL(z_i)$ | Plastic limit for the $i^{th}$ soil increment, in percent (pg 20) |
| $P(z_i)$ | Mitchell's unsaturated permeability for the $i^{th}$ soil increment (pg 25) |

| | |
|---|---|
| $R$ | Universal gas constant (pg 13) |
| $Slope_{c+1}$ | Slope of the line between suction values $h_c$ and $h_{c+1}$ (Appendix A) |
| $S(z_i)$ | Slope of the suction vs gravimetric water content wet line for the $i^{th}$ increment (pg 14) |
| $T$ | Conversion of TMI, T = TMI + 60 (pg 30) |
| TMI | Local annual Thornthwaite Moisture Index, (pg 30) |
| $T_1$ | An assumed value of TMI at the moisture depth $d_1$ (pg 30) |
| T' | Absolute temperature, degrees kelvin (pg. 13) |
| $U_{Li}$ | Suction amplitude at depth $L_i$ (pg 57) |
| $U_o$ | Suction amplitude at the top of the incremental layer being considered (pg 36) |
| $V_x(z_i)$ | Horizontal velocity of soil water at depth $z_i$ (pg 40) |
| $X_b$ | X coordinate for the $b^{th}$ boring sample (pg 48) |
| $Y_b$ | Y coordinate for the $b^{th}$ boring sample (pg 48) |
| a | Term used to damp the under slab suction profile toward the equilibrium suction profile (Appendix A-111) |
| b | The sequential number describing a boring sample (pg 48) |
| c | Suction measurement counter (pg 48) |
| d | Mean annual moisture depth, $d_m$ (pg 30) |
| $d_{am}$ | Available moisture depth of the soil mass (pg 30) |
| $d_{dry}$ | Available moisture depth of the soil mass associated with the dry limit (pg 33) |
| $d_{hbar}$ | Size of horizontal barrier (pg 48) |
| $d_m$ | Mean annual moisture depth (pg 33) |
| $d_{source}$ | Distance between a moisture effect source and edge of barrier/slab (pg 46) |
| $d_{vbar}$ | Depth of vertical barrier (pg 48) |
| $d_{wl}$ | Available moisture depth of the soil mass associated with the wet limit (pg 33) |
| $d_{zone}$ | Depth of the root or flower bed zone (pg 46) |

| | |
|---|---|
| $d_1$ | Moisture depth used to arrive at $T_1$ (pg 30) |
| $e_{mc}$ | Controlling center lift, edge moisture variation distance (pg 52) |
| $e_{mc}(z_i)$ | Center lift, edge moisture variation distance for the $i^{th}$ soil increment (pg 27) |
| $e_{me}$ | Controlling edge lift, edge moisture variation distance (pg 52) |
| $e_{me}(z_i)$ | Edge lift, edge moisture variation distance for the $i^{th}$ soil increment (pg 27) |
| $e_{m_r}$ | Edge moisture variation distance for return period r (pg 27) |
| $e_{m_{10}}$ | Edge moisture variation distance for a 10 year return period (pg 27) |
| $e_{m_{50}}$ | Edge moisture variation distance for a 50 year return period (pg 27) |
| $e_o$ | Soil void ratio (pg 25) |
| f(d) | A functional relationship between moisture depth d and T (pg 30) |
| $f_i$ | Cracked fabric factor for the $i^{th}$ soil increment (pg 20) |
| g | Conversion from gram mass to gram force (pg 13) |
| h | total suction, tension (usual units, pF) (pg. 13) |
| $h_c$ | $c^{th}$ suction measurement in a sample (usual units, pF) (pg 48) |
| $h_{const}$ | Soil suction value at the time of construction (pF units) (pg 44) |
| $h_{const}(z_i,t_{const})$ | Soil suction value at the time of construction for the $i^{th}$ soil increment (pF units) (pg 45) |
| $h_{dry}$ | Dry suction limit for soils in the field, bare soil at the surface usually has a value of 6.0pF and soil with vegetation at the surface usually has a value of 4.5pF (pF units) (pg 14) |
| $h_{edge}(z_i)$ | Soil suction profile at the edge of the slab at depth $z_i$ (pF units) (pg 63) |
| $h_{entry}(z_i)$ | Vertical soil suction profile at the entry point between two locations separated by a horizontal distance, when calculating the horizontal water flow (pF units) (pg 41) |
| $h_{exit}(z_i)$ | Vertical soil suction profile at the exit point between two locations separated by a horizontal distance, when calculating the horizontal water flow (pF units) (pg 41) |
| $h_F(z_i)$ | Final suction value at depth $z_i$ (pF units) (pg 19) |

| | |
|---|---|
| $h_{fb}(z_i,t)$ | Suction profile with respect to time and depth for a flower bed at the surface (pF units) (Appendix A-110) |
| $h_{fc}$ | Field capacity suction value of soil (pg 14) |
| $h_{grass}(z_i,t)$ | Suction profile with respect to time and depth for grass at the surface (pF units) (Appendix A-110) |
| $h_i(z_i)$ | Initial suction value at depth $z_i$ (pF units) (pg 19) |
| $h_m$ | Equilibrium suction value of the soil mass (pF units) (pg 30) |
| $h_m(z_i)$ | Equilibrium suction value at depth $z_i$ (pF units) (pg 30) |
| $h_{max}$ | Dry limit suction for soils in the field, bare soil at the surface usually has a value of 6.0pF and soil with vegetation at the surface usually has a value of 4.5pF (pg 30) |
| $h_{max}(z_i)/h_{dry}(z_i)$ | Dry limit suction value at depth $z_i$ (pF units) (pg 30) |
| $h_{min}$ | Wet limit suction of soils in the field, usually 2.5pF (pF units) (pg 30) |
| $h_{min}(z_i)/h_{wl}(z_i)$ | Wet limit suction value at depth $z_i$ (pF units) (pg 30) |
| $h_{slab}(z_i,t)$ | Suction profile with respect to time and depth for soil underneath a slab (pF units) (Appendix A-110) |
| $h_{slab}(z_i,t_{const/dry})$ | Suction profile with respect to depth of under slab soil at time of construction (pF units) (pg 42) |
| $h_{slab}(z_i,t_{vc/dry})$ | Suction profile with respect to depth of under slab soil at time the soil volume change is sought (pF units) (Appendix A-111) |
| $h_{soil}(z_i,t)$ | Suction profile with respect to time and depth for bare soil at the surface (pF units) (Appendix A-110) |
| $h_{tree}(z_i,t)$ | Suction profile with respect to time and depth for a tree at the surface (pF units) (Appendix A-110) |
| $h_{wl}$ | Wet limit suction for soils in the field, usually 2.5pF (pg 14) |
| $h(z_i,t)$ | Suction profile with respect to time and depth (pF units) (pg 30) |
| $h_1$ | Soil suction midway between the suction value at time of construction and the equilibrium suction value (pF units) (pg 44) |
| increment | Soil increment, 5 cm. (Appendix A) |

| | |
|---|---|
| $i$ | Incremental layer counter (pg 19) |
| $k_o$ | Lateral earth pressure coefficient (pg 19) |
| $m$ | Gram molecular weight of water, 18.02 gm/mole (pg 13) |
| $n$ | Local annual weather cycle (pg 36) |
| $r$ | Return period (in years) (pg 27) |
| $r$ | Dummy variable (pg 34) |
| $s$ | Soil layer counter (pg 48) |
| $t$ | Time in seconds (pg 38) |
| $t_{const}$ | The month the slab was constructed (pg 45) |
| $t_{const/dry}$ | Time elapsed between the driest month and the month of construction (pg 66) |
| $t_{dry}$ | Driest month of the year (pg 49) |
| test1 | Dummy time variable (Appendix A-107) |
| test2 | Dummy time variable (Appendix A-107) |
| $t_{new}$ | Dummy time variable (Appendix A-107) |
| $t_{vc}$ | The month the soil volume change is sought (pg 49) |
| $t_{vc/const}$ | Time elapsed between the month of construction and the month soil volume change is sought (pg 66) |
| $t_{vc/dry}$ | Time elapsed between the driest month of the year and the month soil volume change is sought (pg 66) |
| $t_1(z_i)$ | Time after construction when the value $h_1(z_i)$ is reached (pg 44) |
| $\overline{u_v}$ | Partial pressure of pore water vapor (pg xi) |
| $\overline{u_{vo}}$ | Saturation pressure of water vapor over a flat surface of pure water at the same temperature (pg xi) |
| $x$ | Horizontal distance (pg 40) |
| $z_c$ | The characteristic soil depth over which the available moisture depth is removed to achieve the driest soil state (pg 32) |
| $z_i$ | Depth to the $i^{th}$ soil increment (pg 19) |

$z_m$ Depth to constant suction (pg 11)

$z_r$ Scores computed for return period r for the Gumbel cumulative probability distribution curve (pg 27)

$z_{top}$ Depth to the top of the incremental soil layer being considered (Appendix A)

$z_{10}$ Scores computed for a 10 year return period for the Gumbel cumulative probability distribution curve (pg 27)

$z_{50}$ Scores computed for a 50 year return period for the Gumbel cumulative probability distribution curve (pg 27)

$\alpha(z_i)$ Mitchell's diffusion coefficient for the $i^{th}$ soil increment (pg 11)

$\beta$ Shape factor in Gumbel's cumulative probability equation (pg 28)

$\beta$ An exponent from Mitchell's equation set equal to 1 (pg 44)

$\left(\frac{\Delta H}{H}\right)_i$ Vertical strain for the $i^{th}$ soil increment (pg 20)

$\left(\frac{\Delta V}{V}\right)_h$ Volumetric strain due to suction for the $i^{th}$ soil increment (Appendix A-103)

$\left(\frac{\Delta V}{V}\right)_\sigma$ Volumetric strain correction due to overburden for the $i^{th}$ soil increment (Appendix A-103)

$\left(\frac{\Delta V}{V}\right)_i$ Volumetric strain due to suction and overburden for the $i^{th}$ soil increment (pg 19)

$\Delta z$ Total heave or shrinkage in the soil mass (pg 20)

$\Delta z_{edge}$ Vertical heave or shrinkage in the soil mass at the edge of the slab (pg 65)

$\Delta z_{slab}$ Vertical heave or shrinkage in the soil mass at the edge moisture variation distance measured to the center of the slab from the edge of the slab (pg 65)

$\Delta z_{total}$ The difference in vertical movement between the edge of the slab and a vertical movement at the edge moisture variation distance measured to the center of the slab from the edge of the slab (pg 65)

$\gamma$ Regression coefficient (pg 30)

| | |
|---|---|
| $\gamma_{ds}$ | Dry unit weight for layer s (Appendix A-84) |
| $\gamma_d(z_i)$ | Dry unit weight for the soil in the $i^{th}$ increment (pg 25) |
| $\gamma_h(z_i)$ | Matrix suction compression index for the $i^{th}$ soil increment (pg 11) |
| $\gamma_{h100}$ | Matrix suction compression for a soil consisting of 100% of a particular type of clay mineral (pg 52) |
| $\gamma_\pi(z_i)$ | Osmotic suction compression index for the $i^{th}$ soil increment (pg 19) |
| $\gamma_\sigma(z_i)$ | Mean principal stress compression index for the $i^{th}$ soil increment (pg 19) |
| $\gamma_t$ | Total unit weight (pg 19) |
| $\gamma_w$ | Unit weight of water (pg 25) |
| $\mu$ | Matrix suction (pg 13) |
| $\mu_s$ | Percent passing 2 micron for layer s (Appendix A-84) |
| $\mu(z_i)$ | Percent passing 2 micron for the $i^{th}$ soil increment (pg 21) |
| $\nu_s$ | Percent passing number 200 sieve for layer s (Appendix A-84) |
| $\nu(z_i)$ | Percent passing the number 200 sieve for the $i^{th}$ soil increment (pg 21) |
| $\pi$ | Osmotic suction (pg 13) |
| $\pi_F(z_i)$ | Final osmotic suction value a depth $z_i$ (pg 19) |
| $\pi_I(z_i)$ | Initial osmotic suction value a depth $z_i$ (pg 19) |
| $\theta_{dry}$ | Volumetric water content at depth $z_m$ corresponding to $h_{dry}$ (pg 32) |
| $\theta_m$ | Volumetric water content at depth $z_m$ corresponding to $h_m$ (pg 32) |
| $\theta_r$ | Residual volumetric water content for the soil at depth $z_m$ (pg 33) |
| $\theta_s$ | Saturated volumetric water content for the soil at depth $z_m$ (pg 33) |
| $\theta_{wl}$ | Volumetric water content at depth $z_m$ corresponding to $h_{wl}$ (pg 32) |
| $\rho$ | Shape factor in Gumbel's probability equation (pg 28) |
| $\sigma_F(z_i)$ | Applied octahedral normal stress at depth $z_i$ (pg 19) |
| $\sigma_I$ | Stress level below which there is no suppression of suction volume strain by overburden pressure (pg 19) |
| $\psi$ | Total suction (pg 13) |

## LIST OF DEFINITIONS

| | |
|---|---|
| Activity ratio | The ratio of the plasticity index to the percentage clay content (Skempton 1955). Percent clay is defined as the percentage less than 2m of the soil material passing the U.S. No. 200 sieve (Pearring 1968). |
| Cation exchange | The interchange between a cation in solution and another cation on a surface active material (Holt 1969). |
| Cation exchange activity | The ratio of the cation exchange capacity to the percentage clay content (Pearring 1968). |
| Cation exchange capacity | The total amount of exchangeable cations that a soil is capable of absorbing, measured in milliequivalents per 100 grams of soil (Mojekwu 1979). |
| Center lift distortion mode | This is a slab-on-ground distortion mode resulting from the soil at the perimeter being more dry (perimeter soil may be shrinking) than the soil beneath the slab (soil beneath the slab is either at equilibrium, shrinking at a rate slower than the exterior soil, or heaving). Refer to Fig. 2 (Castleberry 1974 and Mitchell 1980). |
| Clay | The soil particles smaller than 2μ which are derived from the chemical decomposition of rock. It consists, chiefly, of clay minerals but small amounts of quartz, feldspar, organic matter, soluble salts and amorphous materials are also present (Lambe and Whitman 1969). |
| Depth of available moisture | The maximum depth of moisture available for use by transpiring vegetation, which is stored within the soil zone up to the depth to constant suction (Ga.y 1994). |
| Depth to constant suction | The depth in a soil profile to which there is no longer a |

| | |
|---|---|
| | significant seasonal suction change (the seasonal change in suction is less than 0.2 pF (Lytton 1997)). |
| Edge lift distortion mode | This is a distortion mode resulting form the soil at the perimeter being more wet (perimeter soil may be heaving) than the soil beneath the slab (soil beneath the slab is either at equilibrium, heaving at a rate slower than the exterior soil, or shrinking). Refer to Fig. 3 (Mitchell 1980). |
| Edge moisture variation distance | For soil under an impervious membrane, the edge moisture variation distance is the distance from the edge of the barrier to the point where soil suction does not vary with season moisture variation (Jayatilaka et al. 1992). |
| Equilibrium suction profile | A suction profile generated by decreasing the equilibrium suction, $h_{m,}$ a centimeter in suction for every centimeter increase in depth (McQueen and Miller 1968). |
| Horizontal barrier | Any impervious barrier that is attached and sealed to the edge of the foundation and extends some distance, $d_{hbar,}$ horizontally from the edge of the slab. A sidewalk attached and sealed to the edge of a foundation is considered a horizontal barrier. Refer to the sidewalk shown in Appendix C-132. |
| Liquid limit | The water content, expressed as a percentage of the weight of the dry soil, at the boundary between the liquid and plastic states. The water content at this boundary is defined as the water content at which a groove, 1mm wide, cut in the soil sample with a standard grooving tool, closes for a length of ½ inch when a brass dish containing the soil is dropped 25 times, at a rate of 2 drops per second, through a distance of 1 cm on a standard hard rubber base (Mojekwu 1979). |
| Mean principal stress | The slope of the volume-total stress curve in the plane of |

| | |
|---|---|
| compression index | zero suction (Lytton 1994). |
| Plastic limit | The water content, expressed as a percentage of the dry weight of the soil at which the soil becomes crumbly and ceases to be plastic. The water content is defined as the water content at which the soil just begins to break apart and crumble when rolled, by hand, into threads one-eighth of an inch in diameter (Mojekwu 1979). |
| Plasticity index | The difference between the greater moisture content of the liquid limit and the less moisture content of the plastic limit. It is defined as the range in water contents through which the soil remains in the plastic state (Mojekwu 1979). |
| Post construction | This refers to the transient case for calculating volume strain of expansive soils immediately after construction, before the soil under the slab has reached an equilibrium moisture content. |
| Post equilibrium | This refers to the case for calculating volume strain of expansive soils after the soil under the slab has reached an equilibrium moisture content. |
| Soil suction | the negative gage pressure relative to the external gas pressure on the soil water to which a pool of pure water must be subjected in order to be in equilibrium through a semi-permeable membrane with the soil water. |
| Suction amplitude | The absolute value of the range between the maximum and the minimum suction values being considered in soil suction profile, (typically, $U_o = h_{max}(z_i) - h_{min}(z_i)$ or $U_o = h(z_i) - h_m(z_i)$). |
| Suction compression index | The slope of the volume-total suction curve in the plane of zero suction (Lytton 1994). |
| Suction profile | When the state of suction is measured at intervals of depth |

| | |
|---|---|
| | down the soil profile, the resulting relation between suction and depth is termed the suction profile (Mitchell 1981). |
| Thornthwaite Moisture Index | TMI is defined as a climatic index that measures the water balance of an area to determine if there is a deficiency or excess to ascertain if the climate should be classified as arid or humid (Thornthwaite 1948). |
| Vertical barrier | Any impervious barrier that extends some distance, $d_{vbar}$, vertically downward from the foundation edge. |
| Vertical differential Soil Movement | The total amount of vertical movement between two distinct locations separated by a characteristic distance. |

# INTRODUCTION

When a slab barrier is placed on an expansive soil, the immediate effect is that evaporation and precipitation cannot effect the soil beneath the slab. During subsequent weather events occurring to the surrounding soil, moisture differentials develop between the uncovered soil and the soil beneath the slab barrier. These differentials are largest when the climate is described by a distinct wet period followed by a hot dry period. Unless a foundation system is installed to prevent or reduce moisture movement, moisture redistribution occurs within the soil mass to reduce these differences in moisture content (Holland and Lawrance 1980). Damage caused by this type of moisture differential is considerable and warrants investigation in developing a more scientific and accurate methodology to address these problems.

The ability to predict differential soil movement is critical for engineers to formulate a picture of what the soil/structure interface will be. This information is necessary to adequately design foundations or other ground supported structures. In slab-on-ground design, the principal interest is in making an accurate estimate of the range of vertical movement that must be sustained by the foundation. The procedures contained herein are methods for defining envelopes of maximum heave and shrinkage so that adequate slab-on-ground designs are made. For highway and airport pavements, canals, and pipelines, the wave spectrum of differential movements versus wave lengths are the desirable design characteristics. Structural floors suspended above expansive clays must be provided with a gap that exceeds the total expected heave. Drilled piers (or shafts) must be designed to resist simultaneously a vertical movement profile and a horizontal pressure profile, both of which change with wetting and drying conditions. Retaining structures, basement walls, rip rap, and canal linings must be designed to withstand lateral movements. Finally, all foundations must be designed against the time-dependent vertical and horizontal curvature that is generated by down hill creep (Lytton 1994).

---

This thesis follows the style of the *Journal of Geotechnical Engineering*.

Each type of soil movement listed above and their effects on different types of ground structures is of sufficient importance and complexity to warrant research of its own. Addressed herein are the effects of vertical differential soil movement on commercial and residential types of slabs-on-ground. Vertical differential soil movement in these cases is defined as the total amount of vertical movement between two distinct locations separated by a characteristic distance. The characteristic distance is described as the edge moisture variation distance plus the distance a moisture effect source is away from the slab edge. The model used to predict differential movement of expansive soils is based on constitutive soil relationships derived primarily from works developed by C. W. Thornthwaite (1948), W. R. Gardner (1958), R. L. Lytton (1973, 1977, 1994, 1995, 1997), J. R. Pearring (1968), J. H. Holt (1969), E. C. Mojekwu (1979), J. L. Nieber (1981), R. G. McKeen (1981, 1992), P. W. Mitchell (1980, 1984), D. A. Gay (1994).

It has been well documented that the magnitude at which soil shrinks and swells is not exclusively based on the soils characteristics. The magnitude of differential soil movement in expansive soils is dominated by the following variables: soil characteristics, pre-construction and post construction vegetation, slope of perimeter surface grade, shape and age of slab and depth of soil moisture active zone (Castleberry 1974, Mathewson et al. 1975, Mathewson et al. 1980).

The methodology used to predict vertical differential soil movement involves using soil suction profiles under the foundation and at the edge of the foundation. These suction profiles are developed using the following variables: depth, time, local surface annual weather and vegetation conditions, and soil characteristics such as the suction compression index, unsaturated permeability, and soil diffusivity. Soil suction profiles combined with overburden stresses are used in volume strain equations developed by Lytton (1994) to predict the volumetric strain for an incremental layer of soil. The incremental layer movements are summed up and total vertical differential soil movement is predicted for a particular column of soil. These procedures are detailed in the chapter on "The Procedures, in a Software Design Format". These procedures address foundation perimeter moisture effect cases that are either very common with many foundation problems or have a

significant effect on vertical differential soil movement. Specifically, the foundation perimeter moisture effect cases that are addressed include: (1) bare soil at the surface, (2) grass at the surface, (3) flower bed at the surface with a defined moisture effect zone depth, (4) trees at the surface with a defined root zone depth, and (5) moisture effect zones that have been measured in the form of suction profiles. Included are methods for predicting the effects that vertical or horizontal barriers have on vertical differential soil movement. Additionally, methods to predict differential soil movement shortly after construction and before the soil has reached an equilibrium moisture content under the foundation are the highlights of this research and are presented.

In "The Problem" chapter, the theory and methodology used to predict differential soil movement is defined and described in order by which the theory was developed. These bits and pieces of theory are applied in step by step processes described in the procedures sections of this document to address all of the different moisture effect cases, with and without barriers imposed.

# THE PROBLEM

## The Magnitude and Description of the Problem

Since early 1950, damage to lightly loaded structures, paving and service piping in areas of expansive clay soils has occurred throughout the world. Estimates show that one in five Americans are affected by this type of damage while only one in ten are affected by major floods. Structural damage caused by expansive clay soils in the United States annually exceeds that caused by earthquakes, hurricanes, and floods combined (Jones and Holtz 1973.) Damage to residential and commercial structures caused by soil movement is estimated at 660 million dollars, almost one-third of the total monetary damage received by all structures as a result of soil movement. On a state-by-state basis, California and Texas account for 35% of all expansive soil losses in the United States. This becomes obvious from a map of the location of much of the expansive soils in the United States, see Fig. 1. Much of this soil is located in highly populated regions of both California and Texas.

**Fig. 1. United States Map of Expansive Soils After Wiggins (1976)**

When it is realized that most residences and light commercial buildings in these two states, which together had 430,000 new home starts in 1978, are constructed with slab-on-ground foundations, the need to develop a theoretical design approach based on physical and natural law for slab-on-ground design in expansive soil areas becomes evident.

The problem with slabs-on-ground built on expansive soils becomes manifested as excessive structural distortions in response to the subsoil undergoing volume changes induced by a change in subsoil moisture. If foundations are not of a stiffness to resist or span the gaps caused by differential soil movements, and if the superstructure is not of a suitable flexibility, the foundation distortions resulting from the soil movements can be of a magnitude to cause excessive cracking of walls and distortion of internal fittings. This type of differential shrink and heave of soils give rise to two distinct distortion modes which cause damage to the superstructure. Fig 2 shows typical superstructure damage that would occur in the case of center lift. Center lift is a distortion mode resulting from the soil at the perimeter being more dry (perimeter soil may be shrinking) than the soil beneath the slab (soil beneath the slab is either at equilibrium, shrinking at a rate slower than the exterior soil, or heaving.) Fig 3 shows typical superstructure damage that would occur in the case of edge lift. Edge lift is a distortion mode resulting from the soil at the perimeter being more wet (perimeter soil may be heaving) than the soil beneath the slab (soil beneath the slab is either at equilibrium, heaving at a rate slower than the exterior soil, or shrinking.) The engineering profession lacks a universal method of analysis within a theoretical framework that utilizes fundamental properties of soil and footing behavior to enable a footing design that is satisfactorily accurate without resorting to empirical methods (Mitchell 1980). Since the late 1970's strides have been made by the Post Tensioning Institute (PTI) to adopt a standard method for designing ground structures in expansive soils. The Post Tensioned Institute has adopted the methodology discussed herein and stipulates that post tensioned slab designs shall provide necessary rigidity to avoid damage to the buildings or houses when the supporting soil expands or contracts (PTI 1996). However, a theoretical approach to predict vertical differential soil movement, as presented herein, has not been widely adopted by today's practicing engineers.

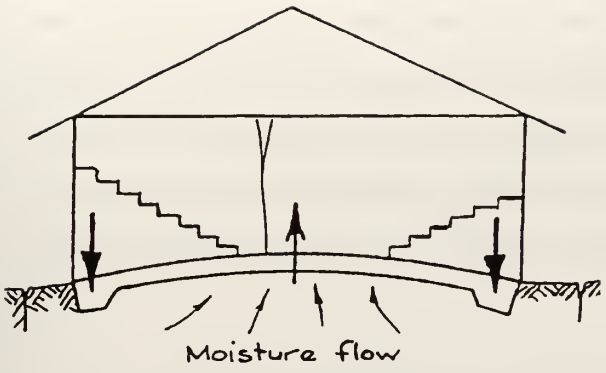


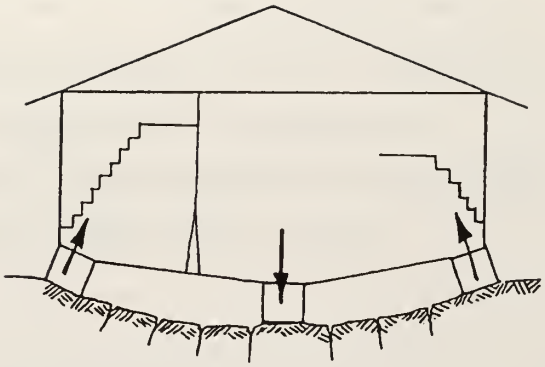

**Fig. 2. (Mitchell 1980) Center Lift Distortion Mode Fig. 3. (Mitchell 1980) Edge Lift Distortion Mode**

## Expansive Soil, on a Molecular Level

*The Building Blocks of Expansive Soil*

Why are "expansive soils" so expansive? The answer can be found in the material on a molecular level. The magnitude of the surface area per mass and the molecular composition of expansive soils plays a major role in the soil's ability to shrink and swell to such an impressive degree. "Expansive soils" are typically the fine grained soils as classified in the unified classification system. Fifty percent or more of a soil, by weight, in a sample that passes the number 200 sieve is classified as a fine grained soil. Fine grained soils are further broken down into categories of silts, clays and organics having either a high or low plasticity. The ability to break down and classify a soil according to the unified soil classification system provides an engineer with a wealth of information about the behavioral characteristics and how a particular soil may effect design. An in depth explanation of soil characteristics and the unified soil classification system can be found in Lambe and Whitman (1969).

The following clay structural unit explanation is idealized and simplified and are presented to provide a picture of the basic behavioral characteristics that give rise to clay's ability to undergo large changes in volume. The structural units that make up a clay particle are silicate sheets. Primarily, clays are made of sandwiches of: silica sheets,

gibbsite sheets, and brucite sheets. These sheets are combined in two distinct groups: two-layer sheet minerals, and three layer sheet minerals. The most important and most common two-layer sheet mineral is the kaolinite clay particle, see Fig. 4. Kaolinite is a two-layer mineral which consists of a silicate sheet bonded to a gibbsite sheet by hydrogen bonding and secondary valence forces. Another example of a two layer sheet mineral is serpentine which is formed by brucite bonding to silica, see Fig. 5.

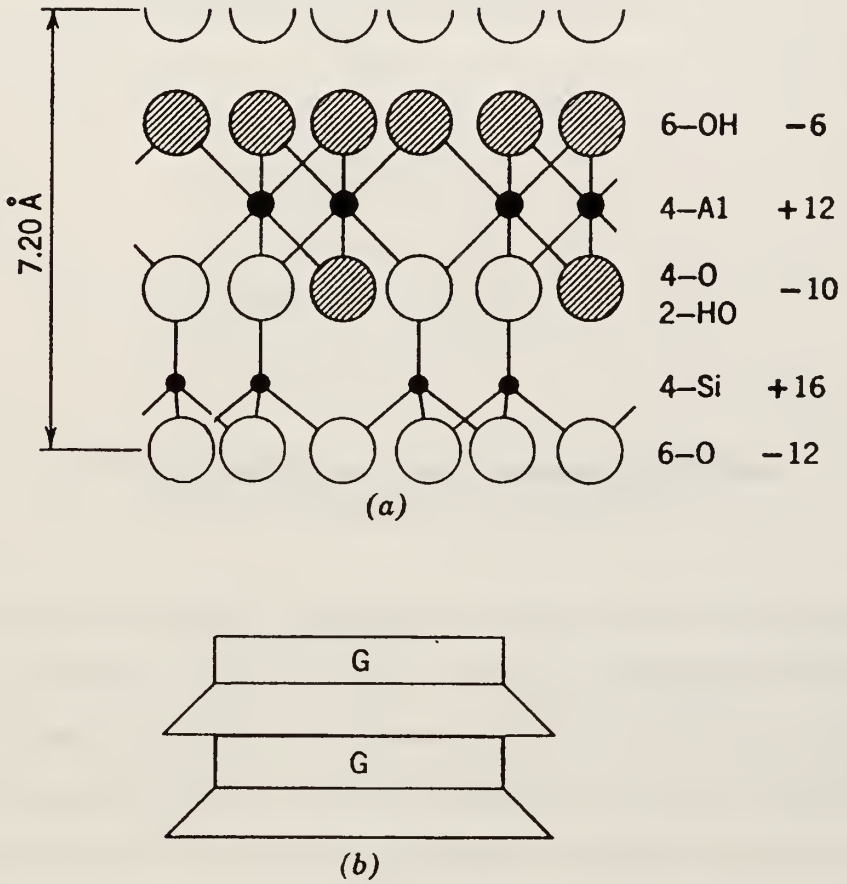


**Fig. 4. (Lambe and Whitman 1969) The Structure of Kaolinite**
**(a) Atomic Structure (b) Symbolic Structure**

In the actual formation of these silicate sheets there may be some isomorphous substitution. Isomorphous substitution is when one kind of atom is substituted for

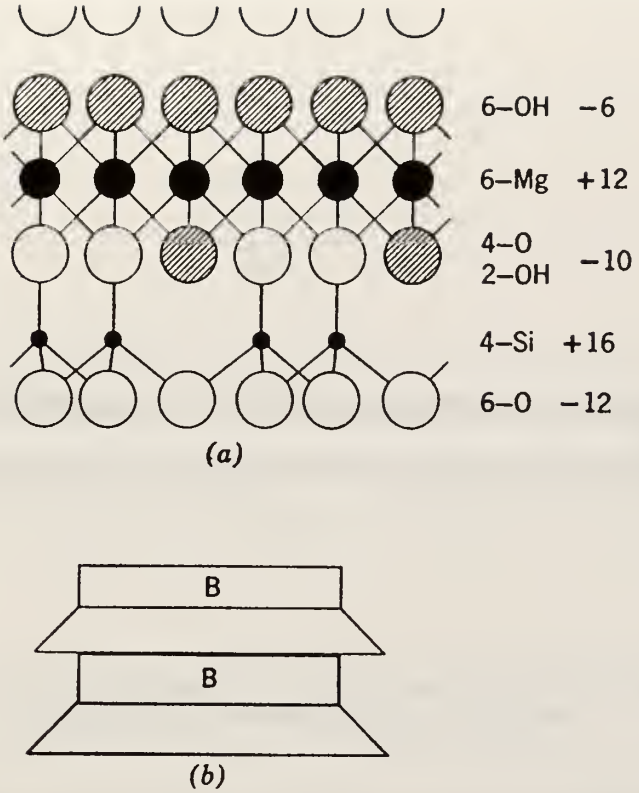


**Fig. 5. (Lambe and Whitman 1969) The Structure of Serpentine**
**(a) Atomic Structure (b) Symbolic Structure**

another atom that is very similar in structure and size. In other words aluminum may be substituted for silicon if there is a shortage of silicon and an abundance of aluminum during the formation stage of the clay mineral. This sort of substitution may give the mineral a net charge deficiency and may cause slight distortion in the crystal lattice due to the substituted atom's size difference. Isomorphous substitution that occurs giving the clay mineral a large negative charge will give the mineral the capacity to attract polar charged water molecules. A double layer of molecules, such as water molecules, will try to form around a clay mineral to neutralize the negatively charged clay particle. This great affinity for water due to isomorphous substitutions provides an explanation as to why clay minerals, like montmorillonite, can have large volume changes at high

volumetric water contents. In Fig. 6 the clay particles are shown with the fully developed double layers they would have in pure water.

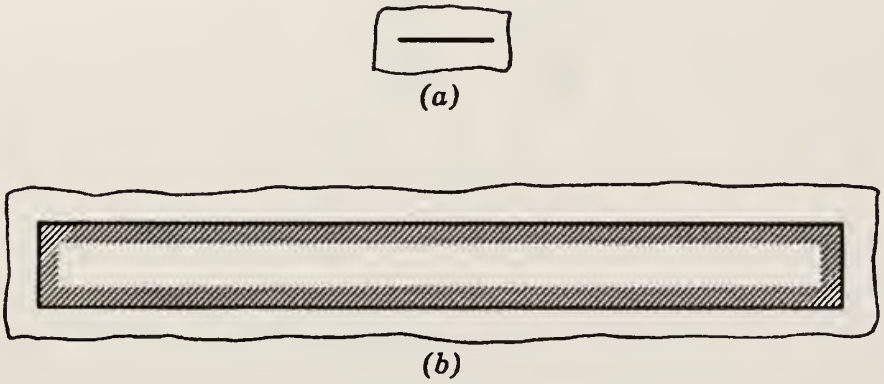


**Fig. 6. (Lambe and Whitman 1969) Soil Particles With Water and Ions (a) Sodium Montmorillonite (b) Sodium Kaolinite**

In kaolinite there is a very small amount of isomorphous substitution. However in the three layer sheet clay minerals there is much more isomorphous substitution. Three layer sheets are formed by placing a silica on the top of, and on the bottom of, either a gibbsite or brucite sheet. Fig. 7 shows the mineral pyrophyllite made of a gibbsite sheet sandwiched between two silica sheets. Fig. 8 shows the structure of the mineral muscovite, which is similar to pyrophyllite except that there has been isomorphous substitution of aluminum for silicon in muscovite. The net charge created by this substitution is balanced by potassium ions which serve to link the three layer sandwiches together. The most common three-layer minerals in soil are montmorillonite and illite. Montmorillonite is similar to pyrophyllite with the exception that there has been isomorphous substitution of magnesium for aluminum in the gibbsite sheets. Due to the isomorphous substitution the illite mineral has a moderately high capacity for volume change and montmorillonite has a very high capacity for volume change (Lambe and Whitman 1969).

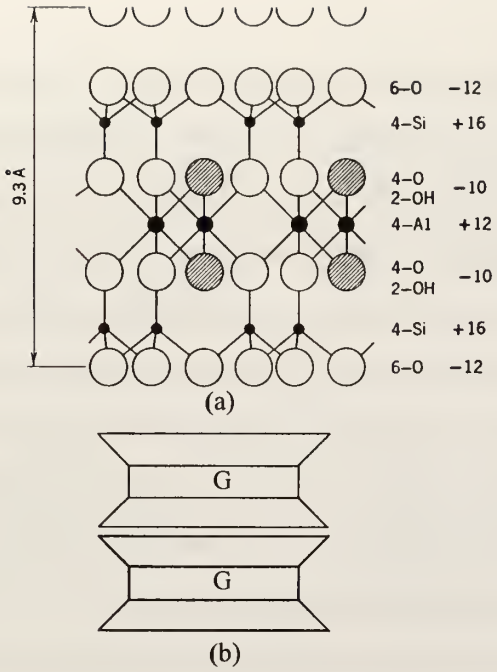


**Fig. 7. (Lambe and Whitman 1969) The Structure of Pyrophyllite**
**(a) Atomic Structure (b) Symbolic Structure**

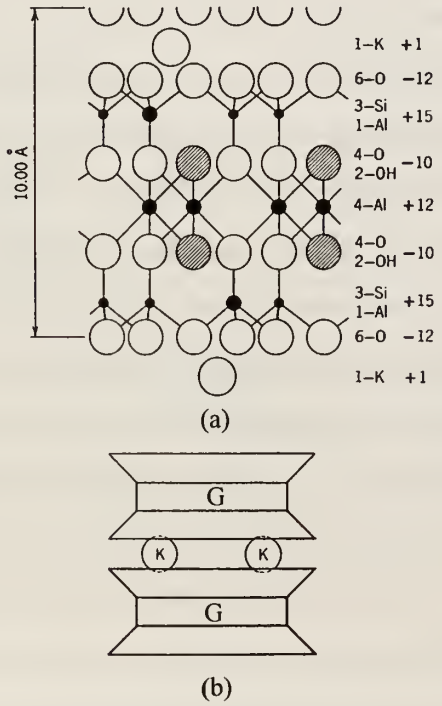


**Fig. 8. (Lambe and Whitman 1969) The Structure of Muscovite**
**(a) Atomic Structure (b) Symbolic Structure**

*Gilgai*

Clay soil left to interact with surface climate conditions will develop an irregular surface microrelief pattern called gilgai, which in colloquial terms is referred to as "hog wallows." This phenomenon is recognizable in areas where highly expansive soils are known to exist undisturbed for extended periods of time. These gilgai may be experienced while taking a very undulating ride: up the fairway of an old golf course, during farming evolutions in a native hay field, or down an old country road. As illustrated in Fig. 9 from Spotts (1974), the pattern develops in seven stages. First, the sedimentary clay is deposited. Following deposition, drying occurs, producing surface shrinkage cracks. Further desiccation results in the formation of major cracks penetrating far into the clay. The extent of penetration and spacing are determined by a number of factors of which the degree and rate of drying and the clay type are the most significant. Subsequent development of microrelief occurs as the clay is wetted and dried by cyclic variation of the climate. Because water penetrates deeper at the major cracks, greater swell occurs. As the next cycle of drying proceeds, the higher areas dry first, causing the major cracks to reappear in approximately the same locations. Thus, over a period of several years, an undulating surface pattern called gilgai develops on the soil surface (McKeen 1981). This phenomenon is important to realize since it is a natural occurrence of differential soil movement that must be understood by engineers so that appropriate models of this type of soil behavior can be properly applied to design. There are important parameters to consider when addressing volume strain that causes the gilgai phenomenon, such as: (1) The depth at which soil interacts with the climate, known as the depth to constant suction, $z_m$. (2) The climate, or the annual wetting and drying cycles at the surface. (3) The type of surface conditions, such as; vegetation growth, bare soil, slope, or barriers of some type. (4) The soil characteristics, namely: suction compression index, $\gamma_h(z_i)$, unsaturated permeability, $K_o(z_i)|h_o|$, and soil diffusivity, $\alpha(z_i)$. The roles that each of these parameters play in predicting differential soil movement are presented.

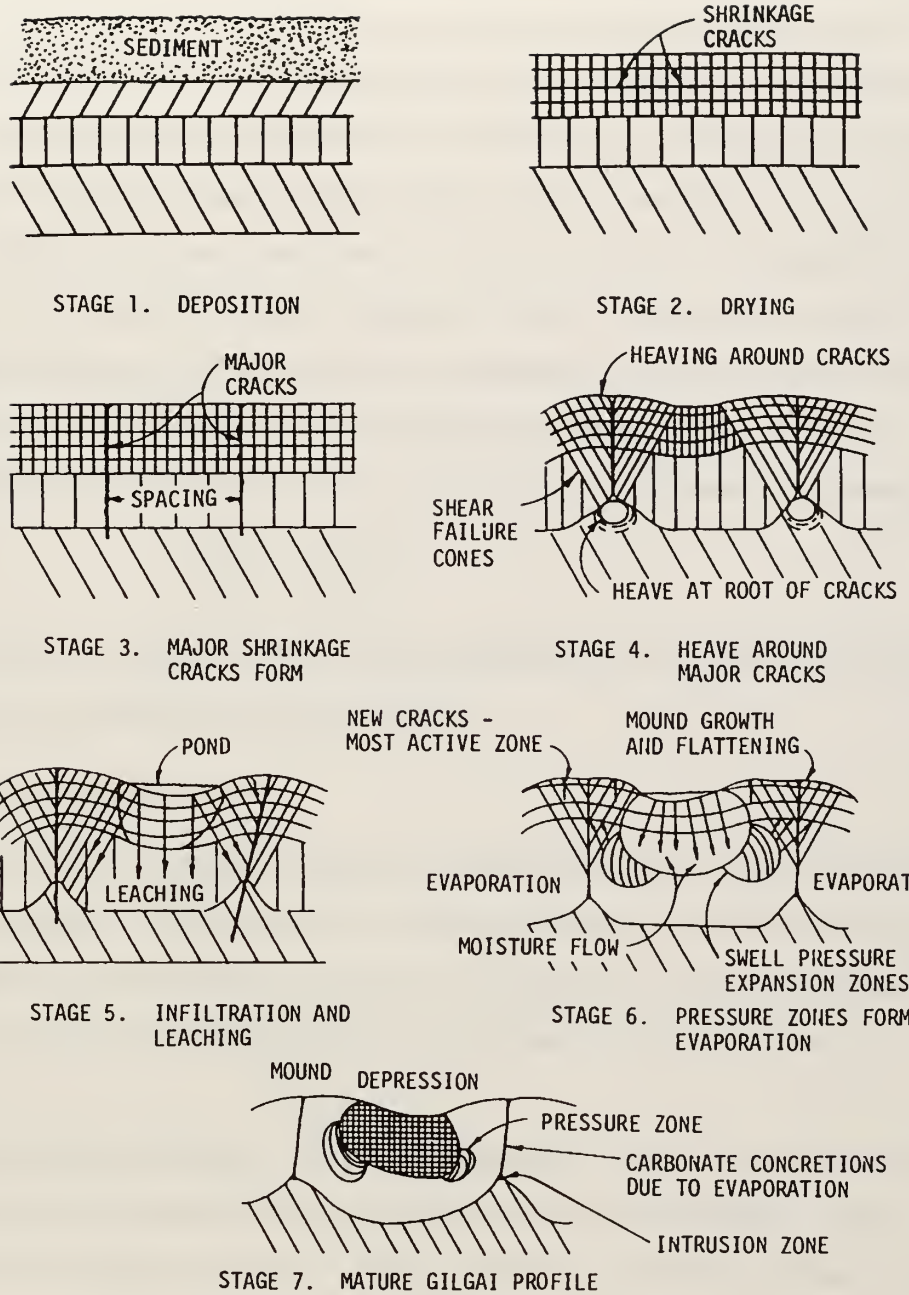


**Fig. 9. (Spotts 1974) Gilgai Stages**

*Suction, Matrix and Osmotic*

Soil suction is the measure of a soil's affinity for water. Soil suction is an energy: water always moves down an energy gradient and it takes energy to cause volume strain in any soil. Soil scientists and arboriculture scientists refer to soil suction in terms of water potential. As defined by the 1960 Moisture Equilibria Symposium, soil suction is the negative gage pressure relative to the external gas pressure on the soil water to which a pool of pure water must be subjected in order to be in equilibrium through a semi-permeable membrane with the soil water. Suction is the term used principally by engineers for the thermodynamic quantity, Gibb's free energy which is inherently negative, as seen in (1) below, and generates tension in the pore water stretching between soil particles (Lytton 1994). Soil suction is equal to 0.0 when the

$$h = \frac{R \cdot T'}{m \cdot g} \cdot \ln\left(\frac{H}{100}\right) \qquad (1)$$

relative humidity is equal to 100%. A relative humidity value less than 100% in a soil would indicate the presence of suction in the soil.

*Components of Soil Suction*

Soil suction is quantified in terms of the relative humidity (1) and is commonly called "total suction." "Total suction," $\psi$ , has two components, namely: matrix suction ($\mu$), which is due to the attraction of water to the soil particle surfaces, and osmotic suction ($\pi$), which is due to dissolved salts or other solutes in the pore water (2).

$$\psi = \mu + \pi. \qquad (2)$$

Matrix suction will have the most effect on the volumetric changes in soil due to the fact that this component varies with the changes in the moisture environment. Osmotic suction will not change unless there is a change in the salt concentration within a given soil layer.

*Typical Suction Levels in the Field*

Fig. 10 illustrates the suction-vs-volumetric water content curve for a natural soil under

wetting and drying conditions. A common measure of suction is the pF-scale, in which pF is defined as (3), where p refers to the logarithmic value analagous to pH, and the F refers to free energy.

$$\text{Suction in pF} = \log_{10}|\,h\,| \qquad (3)$$

Where $|\,h\,|$ equals the magnitude of suction in centimeters of water, a positive value. The various suction levels corresponding to field cases are listed below:

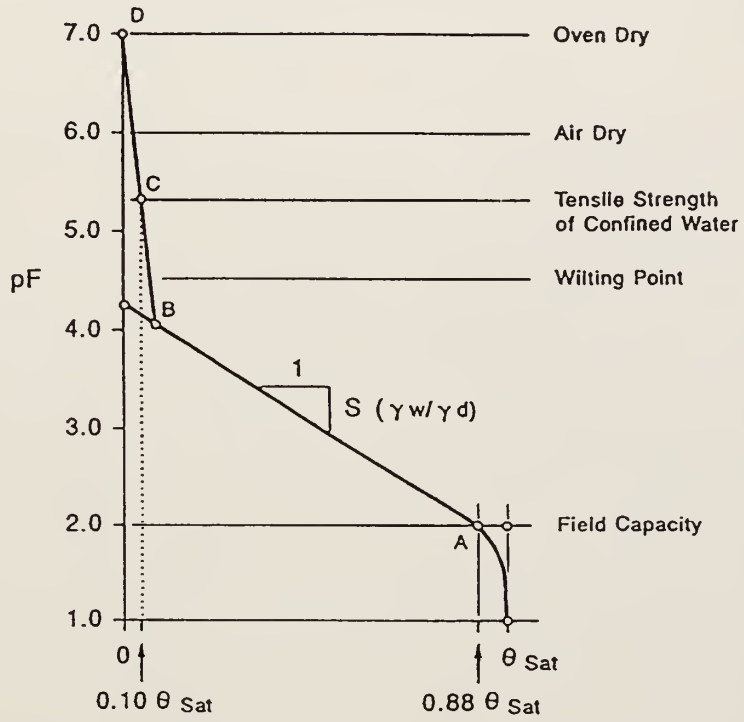


**Fig. 10. (Lytton 1994) Suction vs Volumetric Water Content Curve**

Field capacity ($h_{fc}$ = 2.0 pF)

Wet Limit for clays ($h_{wl}$ = 2.5 pF)

Plastic limit (3.5 pF)

Wilting point of plants ($h_{dry}$ = 4.5 pF for vegetation)

Tensile strength of confined water (5.3 pF)

Air dry at 50% relative humidity ($h_{dry}$ = 6.0 pF for bare soil)

Oven dry (7.0 pF)

Field capacity is an agricultural engineering term used to define the maximum amount of water that a soil can hold in the field. Fig. 10 shows field capacity to be a value of 2.0 pF, but actual field values never quite drop below a value of 2.5 pF for clays (Lytton 1995 and Mitchell 1980). Soil suction is a term that measures energy potential and is directly related to the soil's potential for volume change. This information is referred to repeatedly throughout this document.

## THE THEORY OF DIFFERENTIAL SOIL MOVEMENT

Some notable breakthroughs have been made pertaining to the topic of predicting differential soil movement and are described in this chapter. The real challenge in geotechnical engineering, especially in the area of expansive soils, is to develop a consistent body of theoretical mechanics which adequately explains the behavior of the soil mass and to develop methods of measuring the relevant material properties critical for making appropriate design decisions.

In the 1970's the first attempt was made to design slabs-on-ground using a scientifically based theoretical approach. In 1973, Lytton and Woodburn prepared a report which chronicles a successful school building foundation design. The school foundation design procedure considered differentially expanding and shrinking clay due to the changing suction of the soil beneath the foundation. The suction profiles of the soil were predicted using a rational method which relied upon suction profiles measured on samples taken on the site at different times in the year. These suction values were used to predict the differential soil movement, and the foundations were designed based on the distortion modes caused by the magnitude and location of the expansive soil movements. Lytton noted that this differentially expanding and shrinking effect caused "mounds" to form beneath the slab. The foundation interacts with these mounds pressing down on the high spots and bridging the low spots. The foundation design procedures considers the limit cases in which the mounds produce two types of distortion patterns: edge lift pattern and center lift pattern, as shown in Fig. 11. These two distortion modes were used to design the slabs so that the loads of the superstructure would be carried across a span generated by edge lift, or carried in a cantilevered fashion out to the edge of the foundation in the case of center lift. Woodburn recorded the performance of the foundation systems after the designs were built and the school was put into service. Lytton and Woodburn reported post construction edge shrink values to be 2.75 inches which compared favorably with the predicted value of 3.1 inches. Just as Lytton predicted, the worst case differential

movement occurred in the first dry season subsequent to the construction of the slab during the wettest time of the year. In this post construction case the soil was "capped" and the moisture content was preserved in a

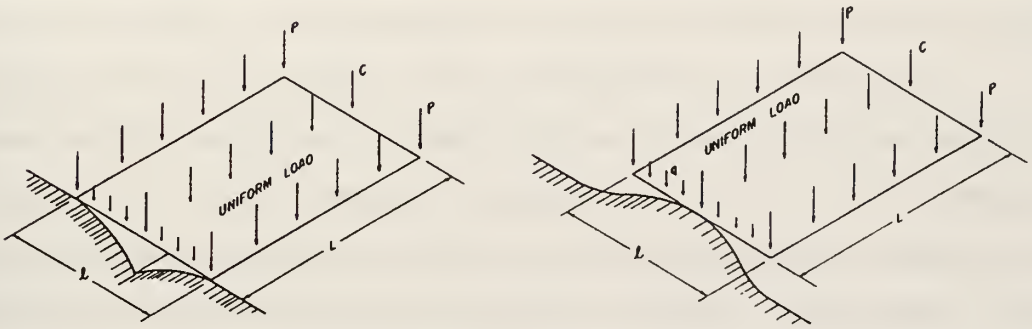


**Edge Heave** **Center Heave**

**Fig. 11. (Lytton 1973) Edge Heave and Center Heave Distortion Modes**

state of heave under the slab while the perimeter soil shrank as it dried. This post construction case produced the worst case center lift mode. Subsequent weather cycles did not produce such extreme cases of differential soil movements as compared to the post construction case. However, subsequent weather cycles did produce differential soil movements as predicted. The model to predict this type of post construction differential soil movement is presented in the Post Construction section of this chapter.

This design and research venture documented by Lytton and Woodburn's 1973 paper marked the beginning of a slab-on-ground design method that has been adopted by the Post Tensioning Institute as the standard for design of post-tensioned slabs-on-ground on expansive soils (PTI 1980, 1996). However, the objective of this research is to consider the methodology behind predicting the differential soil movement used to design such slabs.

**Soil Volume Strain**

Movements in expansive soils are generated by changes of suction which are brought about by the entry or loss of moisture or change in concentration of dissolved

salts in the pore water. The volume change that accompanies the change of suction (and water content) depends upon the total stress states that surround the soil. Within a soil mass, a decrease in the magnitude of suction results in an increase of water content. The volume of the soil also increases unless the surrounding pressure is sufficient to restrain the swelling. A conceptual graph of suction-vs-volume can be drawn using the relations of each to water content. This is illustrated in Fig. 12 on the plane corresponding to zero pressure. A similar graph can be drawn relating pressure (total stress) - versus - volume on the plane corresponding to zero suction. The simultaneous change of the magnitude of suction (decrease) and pressure (increase) results in a small change of volume, following the path from Point A to Point C on the pressure - suction - volume surface. The magnitude of suction decreases from Point A to Point B while the pressure increases from Point B to Point C. The volume change process can be viewed as the net result of two processes;

a. Increase of volume from A to B at constant mechanical pressure or total stress.
b. Decrease of volume from B to C at constant suction.

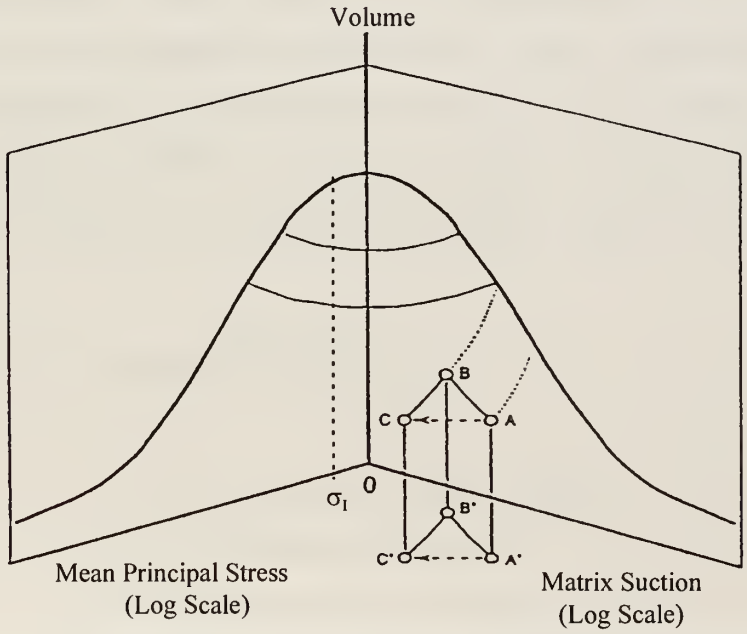


**Fig. 12. (Lytton 1994) Mean Principal Stress-Volume-Matrix Suction Diagram**

For small increments of volume change on this surface, the volume strain, is linearly related to the logarithms of both pressure and |suction|. The soil volume strain equation which shows the relation between matrix suction, mean principal stress, and osmotic suction is (4), (Lytton 1977, 1994).

$$\left(\frac{\Delta V}{V}\right)_i = -\gamma_h(z_i)\log_{10}\left(\frac{h_F(z_i)}{h_I(z_i)}\right) - \gamma_\sigma(z_i)\log_{10}\left(\frac{\sigma_F(z_i)}{\sigma_I}\right) - \gamma_\pi(z_i)\log_{10}\left(\frac{\pi_F(z_i)}{\pi_I(z_i)}\right) \quad (4)$$

In the procedures described herein the assumption will be made that the osmotic component has no change. If the case exists that the osmotic component has no real change, which is the case most of the time, then that term within the volume strain equation can be neglected. The suction compression index , $\gamma_h(z_i)$, and the mean principal stress compression index, $\gamma_\sigma(z_i)$, will be discussed in more detail in the section titled "The Suction/Mean Principal Stress Compression Indexes". The initial and final suction profiles, $h_I(z_i)$ and $h_F(z_i)$, will be discussed in more detail in the section titled "Suction Profiles". The initial mean principal stress, $\sigma_I$, is the stress level below which there is no suppression of volume strain by overburden pressure. This is the stress at which the curve in the pressure-volume plane in Fig 12 begins to depart from horizontal as pressure increases from zero and has been observed to be approximately 40 centimeters of soil (Lytton 1994). The final stress at depth $z_i$, $\sigma_F(z_i)$, is the mean principal stress at a depth $z_i$ at the time the volume strain is desired and is given by (5).

$$\sigma_F(z_i) = \left[\frac{1+2\cdot k_o}{3}\right]\cdot\gamma_t\cdot z_i \quad (5)$$

where $k_o$ is:

$k_o = 0.00$ when the soil is badly cracked.

$k_o = 0.33$ when the soil is drying.

$k_o = 0.67$ when the soil is wetting.

$k_o = 1.00$ when the cracks are closed and the soil is swelling.

Once the volume strain for an incremental layer of soil is known the vertical strain for that layer is estimated using a cracked fabric factor, $f_i$ , as shown in (6). The cracked fabric factor is the percent soil volume strain that is directed vertically in a soil column.

$$\left(\frac{\Delta H}{H}\right)_i = f_i\left(\frac{\Delta V}{V}\right)_i \tag{6}$$

McKeen (1981) back calculated vales of $f_i$ and found that $f_i = 0.5$ when soils are drying and $f_i = 0.8$ when soils are wetting. The total vertical differential movement in a soil mass, $\Delta z$ , is then found by summing the product of vertical strain and the incremental depth to which they apply as shown in (7).

$$\Delta z = \sum_{i=i}^{n}\left(\frac{\Delta H}{H}\right)_i \cdot \text{increment} \tag{7}$$

The volume strain theory previously described was developed by Lytton (1973, 1977, 1994, and 1995). All symbols are defined in the List of Symbols.

**A Simplified Method for Identifying Predominant Clays**

There are three areas of soil characteristics that must be known before the volume strain theory can be applied, namely: the soil suction compression index, the soil suction profiles, and the mean principal stresses within the soil. The mean principal stress was described earlier and suction profiles will be discussed in a later section. However, the soil suction compression index, as described in the next section, depends on proper identification of the predominant clays in soils. A simplified method for identifying these predominant clays is discussed in this section.

Before Lytton developed the methodology to predict vertical differential soil movement, Pearring (1968) and Holt (1969) had completed a correlation chart to aid in the identification of predominant clay mineral in a given soil. According to Pearring and Holt's research, the two parameters used to classify the clay minerals are the cation exchange activity, $CEAc(z_i)$, and activity ratio, $Ac(z_i)$. Obtaining the measure of these two parameters requires the plasticity index, $PI(z_i)$, the cation exchange capacity, $CEC(z_i)$, and the percent of clay in the soil passing the number 200 sieve, $Clay(z_i)$, (8),

(9), (10), (11).

$$PI(z_i) = LL(z_i) - PL(z_i) \tag{8}$$

$$Clay(z_i) = \frac{\mu(z_i)}{\nu(z_i)} \tag{9}$$

$$Ac(z_i) = \frac{PI(z_i)}{Clay(z_i)} \tag{10}$$

$$CEAc(z_i) = \frac{CEC(z_i)}{Clay(z_i)} \tag{11}$$

All symbols are defined in the List of Symbols. Once the cation exchange activity and the activity ratio are known for a given clay mineral the type of clay is determined from Fig 13.

The difficulty comes in arriving at the measure of cation exchange capacity. Until Pearring and Holt's method of identifying predominant clays came to light the geotechnical engineer had to rely on experience or the more reliable, expensive, and arcane techniques used by clay mineralogist and soil physicists. However, Pearring and Holt's method still required engineers to find the cation exchange capacity (CEC) of the soil, which is a soil property not typically evaluated in normal soils test laboratories. Mojekwu (1979) realized this problem and developed a simplified way to arrive at the CEC. His work involved data collected for a wide range and number of soil samples taken in the state of Texas. Among other data, Mojekwu collected and analyzed the Atterberg limits of these soils and found that very good correlations could be made that linked the plastic limit and the liquid limit to the CEC of a specific soil. The method he developed requires the simple Atterberg limits tests to find the plastic limit, PL, and the liquid limit, LL. Mojekwu ran a simple regression analysis, the dependent variable being CEC, the independent variables being PL and LL respectively, and produced very high R squared values of .9941 and .9942 for (12) and (13) respectively.

$$CEC(z_i) = PL(z_i)^{1.17} \tag{12}$$

$$CEC(z_i) = LL(z_i)^{0.912} \tag{13}$$

The larger of these two approximated values of CEC is used to find the CEAc, which is then used along with Ac to determine the predominant clay minerals in Fig. 13. These findings by Pearring, Holt, and Mojekwu paved the way for research by McKeen in developing a simplified method to identify the suction compression index, which is critical to predicting differential soil movements.

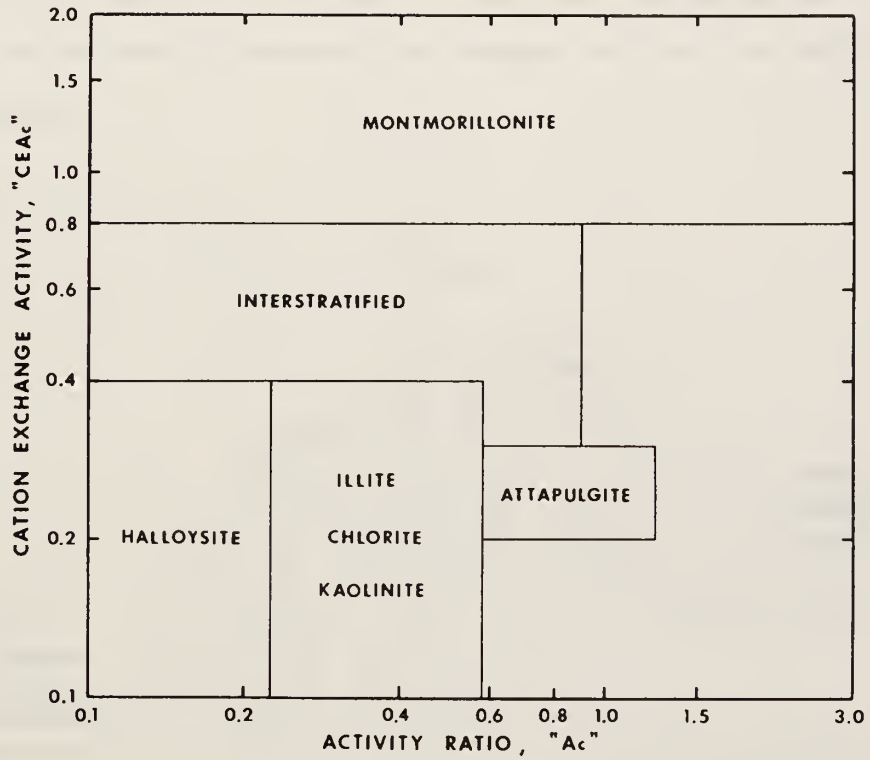


**Fig. 13. (Pearring 1968 and Holt 1969) Chart to Identify Predominant Clays**

## The Suction/Mean Principal Stress Compression Indexes

Suction forces on a soil element are body forces rather than externally applied forces at the surface of the element. Because the suction stresses are dominating the effective stresses in expansive soils, volume change studies are made using total suction values. It is the slope of the volume change versus suction curve that quantifies soil response to moisture changes. Thus, the suction compression index, $\gamma_h(z_i)$, is defined as the slope of the volume-total suction curve, see Fig 14 (Lytton 1977). McKeen (1981)

analyzed soils data in which he measured volume strain corresponding to soil suction values to arrive at a corresponding suction compression index for particular types of expansive soils. In McKeen's study, he measured the soil volume change using the conventional oedometer for cases when the soil was un-cracked and using the coefficient of linear extensibility (COLE) method when the clay was cracked. The measurements of soil suction were taken utilizing a variety of methods as well. The primary methods were the thermocouple psychrometer and filter paper methods. Using the basic concept

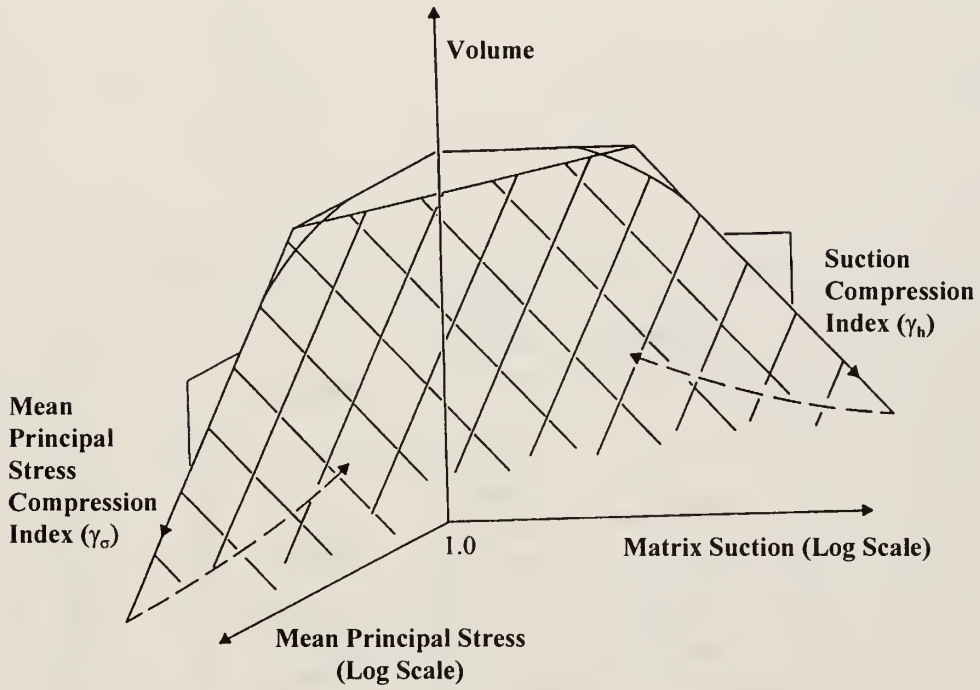


**Fig. 14. (Lytton 1977) Pressure-Volume-Suction Surface**

described above, McKeen developed the chart method to determine $\gamma_h$ by analyzing a large number of Soil Survey samples, adopting the methodology for determining predominant clays by Pearring (1968), Holt (1969) and Mojekwu (1979), and produced Fig 15 which gives values of $\gamma_{h100}$ without requiring suction tests. The value of $\gamma_{h100}$

typically ranges from .033 to .220. This method requires only the activity ratio and the cation exchange activity of the soil to find the corresponding $\gamma_h$ for particular soils. The chart method is used in the procedures to calculate $\gamma_h$ in the software design format procedures.

Another factor to consider in calculating soil volume strain is the effect of applied loads in suppressing the suction volume strain by overburden pressure. The mean principal stress compression index is required to complete the term to calculate the amount of suppression to the suction volume strain by overburden pressure. The mean principal stress compression index is calculated by (14) (Lytton 1977).

$$\gamma_\sigma = \frac{\left(\frac{\Delta V}{V}\right)_i}{\log_{10}\left(\frac{\sigma_F}{\sigma_I}\right)} \tag{14}$$

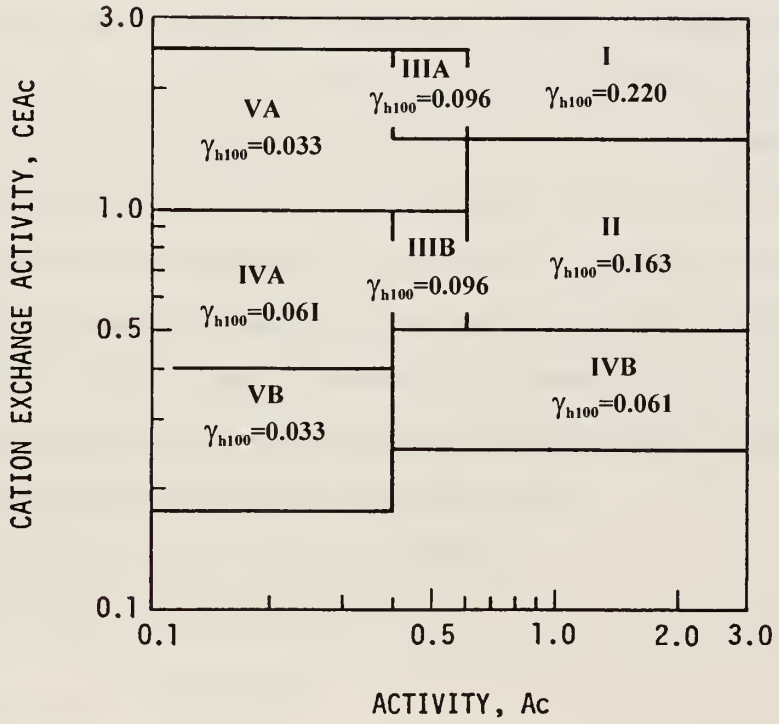


**Fig. 15. (McKeen 1981) Chart to Determine the Suction Compression Index**

The mean principal compression index is also calculated by the commonly used compression index, $C_c$, by (15) (Lytton 1994).

$$\gamma_\sigma = \frac{C_c}{1+e_o} \tag{15}$$

Typical values of $\gamma_\sigma$ were calculated from results of swell tests and swell pressure tests reported by Vigayvergiya and Ghazzaly (1973) according to (14). The range of these calculated values of $\gamma_\sigma$ fell between 0.02 and 0.09 indicating that the ratio of $\gamma_h/\gamma_\sigma$ is typically at or slightly below 1.0. Therefore it is slightly conservative but convenient to assume $\gamma_h$ is equal to $\gamma_\sigma$. Until there is research that develops a more practical and cost effective method for obtaining more accurate values of $\gamma_\sigma$, that coefficient will assume the value of $\gamma_h$ for calculations of volume strain in the software design format procedures described in this document (Vigayvergiya and Ghazzaly 1973).

**Estimates of Unsaturated Soil Properties**

Before a clear explanation of the remaining sections is possible, estimates of unsaturated soil properties must be defined. Specifically, definitions are required for the following soil properties, namely: the slope of the suction versus volumetric water content wetting line shown in Fig. 10, $S(z_i)$, Mitchell's diffusion coefficient, $\alpha(z_i)$, and Mitchell's unsaturated permeability, $K_o(z_i)|h_o|$ or $P(z_i)$. The slope of the suction versus volumetric water content wetting line is given by (16). Mitchell's diffusion coefficient is given by (17). Finally, Mitchell's unsaturated permeability is given by (18). The process flow sheet that describes procedures for calculating all soil properties required for the software design can be found in Appendix A-88.

$$S(z_i) = -20.29 + 0.1555 \cdot LL(z_i) - 0.117 \cdot PI(z_i) + 0.0684 \cdot \nu(z_i) \tag{16}$$

$$\alpha(z_i) = 0.0029 - 0.000162 \cdot S(z_i) - 0.0122 \cdot \gamma_h(z_i) \tag{17}$$

$$K_o(z_i) \cdot |h_o| = 0.4343 \cdot \frac{\alpha(z_i) \cdot \gamma_d(z_i)}{|S(z_i)| \cdot \gamma_w} \tag{18}$$

The above equations were developed by Jayatilaka et al. (1992) and Lytton (1994). All symbols are defined in the list of symbols.

**Edge Moisture Variation for Center Lift and Edge Lift Cases**

As discussed earlier, the effects of vertical differential soil movement on commercial and residential types of slabs-on-ground is dictated by the perimeter moisture effect cases and the total amount of vertical movement between two distinct locations separated by a characteristic distance. The characteristic distance is described as the edge moisture variation distance. At some time after construction, the soil under the slab will reach an equilibrium moisture content. However, the soil at the edge will vary in moisture content dependent on the local annual weather cycle. Additionally, the soil underneath the slab will vary in moisture content up to a distinct distance, the edge moisture variation distance, that is controlled by the permeability and diffusivity of the soil. This differential in moisture content of soil underneath the slab and the edge of the slab is what causes the center lift and edge lift distortion modes. As part of research conducted by Jayatilaka et al. (1992) a calibrated finite element program with coupled transient moisture flow and elasticity that had been used in the study of vertical moisture barriers provided an ideal means to study the edge moisture variation distance. The unsaturated soil properties discussed in the previous section in addition to the Thornthwaite Moisture Index were used to determine the relation of the edge moisture variation distance.

The Thornthwaite Moisture Index (TMI), which measures the location's potential for evapotranspiration, is defined as a climatic index that measures the water balance of an area to determine if there is a water deficiency or water excess.

Both edge lift and center lift conditions were explored using several hundred runs with the program (Jayatilaka et al. 1992). Center lift conditions were simulated by a one year dry spell following a wet suction profile condition. Edge lift conditions were simulated by a one year wet spell following a dry suction profile condition. The edge moisture variation distance was considered to be that distance between the edge of the foundation and the point beneath the covered area where the suction changed no more that .2 pF during the entire period of simulation (Lytton 1994).

The dry and wet conditions used annual suction variation patterns that were appropriate for each of nine different climatic zones ranging from a Thornthwaite Moisture Index of -46.5 to +26.8, spanning the range found in Texas. The resulting edge moisture variation distances are shown in Figs. 16 and 17. No distance less that 2.0 feet should be considered for design purposes (Lytton 1994). In the procedures for the software design, the edge moisture variation distances, $e_{me}(z_i)$ and $e_{mc}(z_i)$, are calculated using Figs. 16 and 17.

In 1997 Lytton developed a method to determine the edge moisture variation distance for a particular design return period $e_{m_r}$. In designing slabs-on-ground recognition must be taken of the length of the time these structures must be in service, and of the severity of the weather patterns that may occur during the expected life of the structure. The return period of hydrologic events is appropriate to use in estimating the design criteria for slabs-on-ground on unsaturated soils. Determining the edge moisture variation distance for a selected return period involves applying an equation that relates the edge moisture variation values for the 10-year and 50-year return periods to the design edge moisture variation value for the selected return period, (19).

$$e_{m_r} = e_{m_{10}} + \left(e_{m_{50}} - e_{m_{10}}\right) \cdot \left(\frac{z_r - z_{10}}{z_{50} - z_{10}}\right) \qquad (19)$$

The edge moisture variation distance for a 10 year return period can be obtained from Fig. 18. These edge moisture variation distances were derived by back calculation from slabs which were performing successfully in San Antonio, Dallas, and Houston. None of the slabs were more than 10 years old at the time. It can be argued that the design values of edge moisture variation distance represent a 10 year return period, $e_{m_{10}}$. The edge moisture variation distance charts shown in Fig. 16 and Fig. 17 represent a 50 year return period, $e_{m_{50}}$. The use of the Gumbel probability density function, which is commonly used to represent the probability of weather events, may be used to establish the risk level that is desired for design in accordance with the expected service life. The $z_r$ scores used in (19) are computed from the Gumbel cumulative probability

distribution curve, (20). The return period is represented by the variable r. ρ and β are

$$z_r = \frac{\rho}{\left(-\ln\left(1-\frac{1}{r}\right)\right)^{\frac{1}{\beta}}} \qquad (20)$$

both shape factors and can be assumed as one. Solving for an edge moisture variation distance for a particular return period between 10 and 50 years is a simple two step process: (1) simply substitute the return periods of 10, 50 and the selected return period r into (20) and solve for $z_{10}$, $z_{50}$ and $z_r$ respectively, and (2) Substitute values of $e_{m_{10}}$ from Fig. 18, $e_{m_{50}}$ from Fig. 16 or Fig. 17, and values of $z_{10}$, $z_{50}$, and $z_r$ previously calculated into equation (19) and solve for the $e_{m_r}$. A common design period for residential and light commercial structures is r = 20 years (5 percent risk).

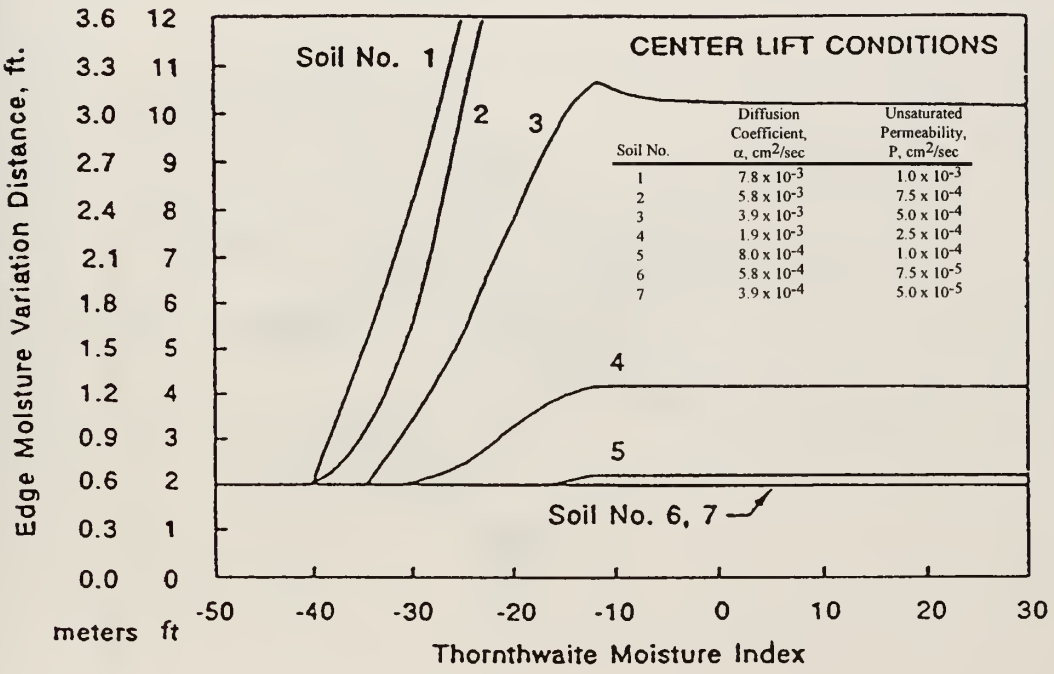
Edge Moisture Variation Distance, ft.
3.6 12
3.3 11
3.0 10
2.7 9
2.4 8
2.1 7
1.8 6
1.5 5
1.2 4
0.9 3
0.6 2
0.3 1
0.0 0
meters ft
Soil No. 1
2
3
4
5
Soil No. 6, 7
CENTER LIFT CONDITIONS
Soil No. | Diffusion Coefficient, α, cm²/sec | Unsaturated Permeability, P, cm²/sec
1 | 7.8 x 10⁻³ | 1.0 x 10⁻³
2 | 5.8 x 10⁻³ | 7.5 x 10⁻⁴
3 | 3.9 x 10⁻³ | 5.0 x 10⁻⁴
4 | 1.9 x 10⁻³ | 2.5 x 10⁻⁴
5 | 8.0 x 10⁻⁴ | 1.0 x 10⁻⁴
6 | 5.8 x 10⁻⁴ | 7.5 x 10⁻⁵
7 | 3.9 x 10⁻⁴ | 5.0 x 10⁻⁵
-50 -40 -30 -20 -10 0 10 20 30
Thornthwaite Moisture Index

**Fig. 16. (Lytton 1994) Edge Moisture Variation Distance for Center Lift Conditions (50 yrs)**

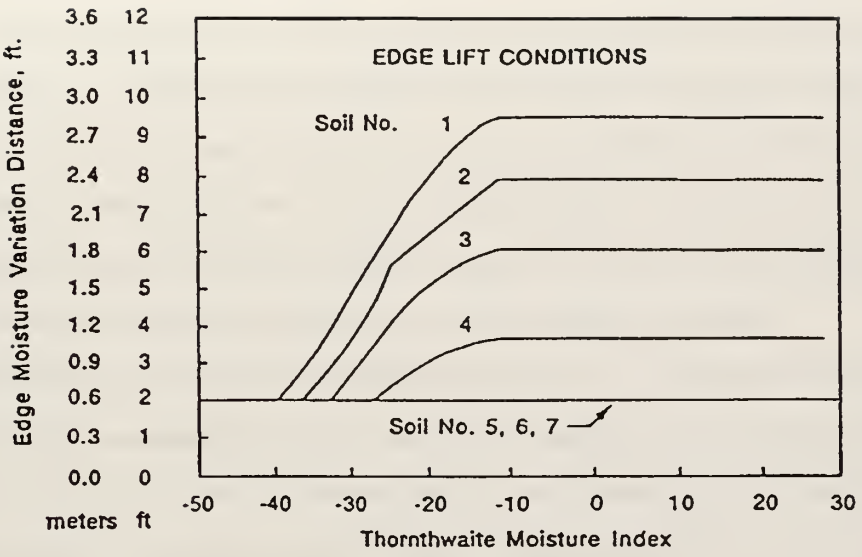


**Fig. 17. (Lytton 1994) Edge Moisture Variation Distance for Edge Lift Conditions (50 yrs)**

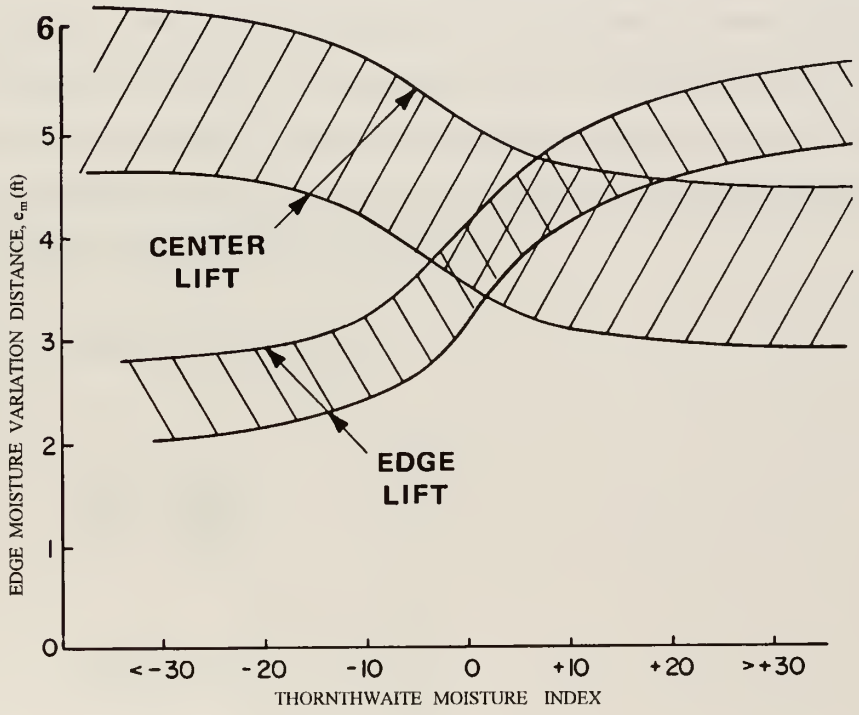


**Fig. 18. (Wray 1978) Edge Moisture Variation Distances for Edge/Center Lift Conditions (10yrs)**

**Equilibrium Suction**

Before the equilibrium suction profiles, $h_m(z_i)$, wet and dry limit suction profiles, $h_{min}(z_i)$ and $h_{max}(z_i)$, transient state suction profiles, $h(z_i,t)$, and depth to constant suction, $z_m$ can be generated, the equilibrium suction , $h_m$, must be known for particular soil profiles and surface conditions. Gay (1994) did extensive work in the area of calculating the mean volumetric moisture content for a given soil mass dependent upon the soil's depth of available moisture, $d_{am}$, and the location's potential evapotranspiration. The depth of available moisture, $d_{am}$, is defined as the maximum depth of moisture available for use by transpiring vegetation, which is stored within the soil zone down to the depth to constant suction. The Thornthwaite Moisture Index is used to ascertain if a climate is arid or humid (Thornthwaite 1948). Gay's theory considers $d_{am}$ and TMI. With these, he developed a set of functional relationships that are used to calculate the mean volumetric moisture content, which are then used to calculate the equilibrium suction value for a particular soil profile and location. The approach he used to solve for these equations was developed by Juarez-Badillo (1975) in which functional domains for the problem are first established as shown in Fig. 19. Function (21) was developed to satisfy the boundary conditions in Fig. 19. Then through an assumption of linear proportionality of the rates of change of the two complete functions, Gay obtained, (22) and (23).

$$f(d) = \left( \frac{1}{d_{am} - d} - \frac{1}{d_{am}} \right) \tag{21}$$

$$\gamma \frac{dT}{T} = \frac{df(d)}{f(d)} \tag{22}$$

$$\gamma \ln\left(\frac{T}{T_1}\right) = \ln\left( \frac{\frac{1}{d_{am} - d} - \frac{1}{d_{am}}}{\frac{1}{d_{am} - d_1} - \frac{1}{d_{am}}} \right) \tag{23}$$

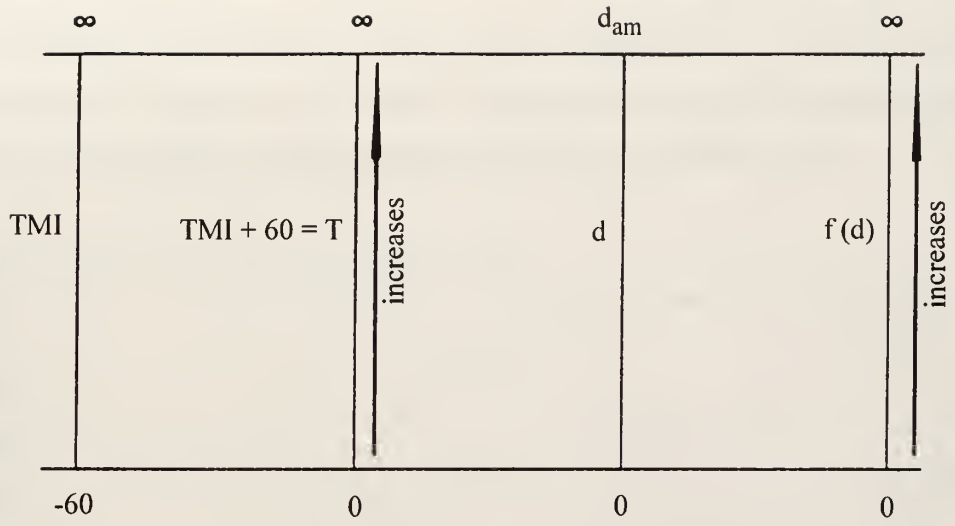


**Fig. 19. (Gay 1994) Domains of Functions f(d) and g(T)**

Solving (23) for d gives (24).

$$d = \frac{d_{am}}{1 + \frac{d_{am} - d_1}{d_1 \left( \frac{T}{T_1} \right)^{\gamma}}} \tag{24}$$

All symbols are defined in the list of symbols. Gay then determined how the coefficients $\gamma$, $d_1$, and $T_1$ depend upon $d_{am}$ using the pattern search technique and arrived at the expressions (25), (26), and (27).

$$\gamma = 0.039337 d_{am} + 1.357033 \tag{25}$$

$$d_1 = 0.449079 d_{am} + 0.304560 \tag{26}$$

$$T_1 = 0.062651 d_{am} + 59.53593 \tag{27}$$

These relationships facilitate the calculation of mean moisture depths, $d_m$, for all values of TMI for any value of available moisture depth between 10cm and 50cm, as illustrated

in Fig. 20 (Gay 1994). The development of (24) is important because it is used to solve for the mean volumetric water content, $\theta_m$. The value $\theta_m$ is applied as a target to solve for $h_m$ in an iterative process using Nieber's (1981) equation (34). Nieber's equation relates suction to volumetric water content. The method to apply this iterative process to solve for the equilibrium suction value can be found in Appendix A-90.

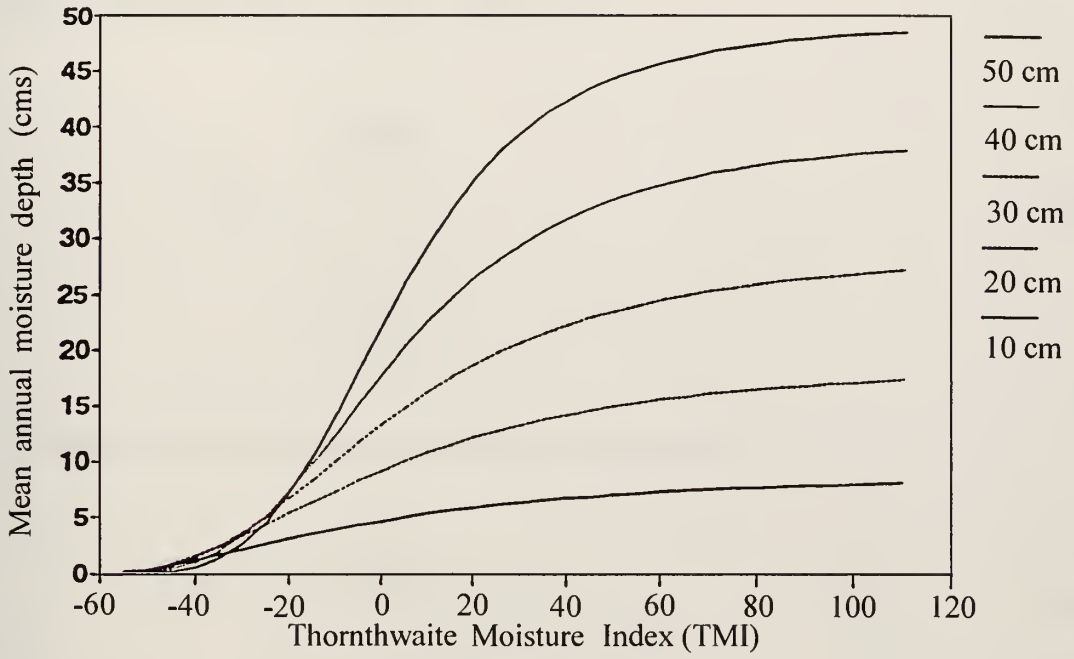


**Fig. 20. (Gay 1994) Theoretical Relationships for Mean Annual Moisture Depth vs TMI**

The equation used to solve for the mean annual moisture depth, (24), developed by Gay is rearranged to arrive at the mean volumetric water content, (32). Below is the step by step process to obtain the equation to solve for $\theta_m$. First note the following equations from Gay (1994), (28), (29), (30), (31). Fig 21 provides a graphical explanation for some of the symbols in these equations. All symbols are defined in the list of symbols.

$$z_c = \frac{d_{am}}{\theta_{wl} - \theta_{dry}} \tag{28}$$

$$\theta_m = \frac{d_m + d_{dry}}{z_c} \tag{29}$$

$$\theta_{wl} = \frac{d_{wl}}{z_c} \tag{30}$$

$$\theta_{dry} = \frac{d_{dry}}{z_c} \tag{31}$$

Dividing through equation (24) by $z_c$ gives (32).

$$\frac{d_m}{z_c} = \frac{\frac{d_{am}}{z_c}}{\left(1 + \frac{d_{am} - d_1}{d_1\left(\frac{T}{T_1}\right)^{\gamma}}\right)} \tag{32}$$

Solving for $d_m/z_c$ in (29) and substituting in (32) gives (33).

$$\theta_m = \frac{\theta_{wl} - \theta_{dry}}{\left(1 + \frac{d_{am} - d_1}{d_1\left(\frac{T}{T_1}\right)^{\gamma}}\right)} + \theta_{dry} \tag{33}$$

The steps to arrive at equations which solve for $\theta_{wl}$, $\theta_{dry}$, and $\theta_m$ using Nieber's equation (34) are given below.

$$|h_m| = \left[A\left(\frac{\theta_s - \theta_r}{\theta - \theta_r} - 1\right)\right]^{\frac{1}{B}} \tag{34}$$

Introduce dummy variable r, (35).

$$r = \frac{|h_m|^B}{A} = \frac{\theta_s - \theta}{\theta - \theta_r} \tag{35}$$

Solving (34) for θ gives (36).

$$\theta = \frac{\theta_s + r \cdot \theta_r}{1 + r} \tag{36}$$

Substituting $\frac{|h_m|^B}{A}$, $\frac{|h_{wl}|^B}{A}$, or $\frac{|h_{dry}|^B}{A}$ back into (36) for r gives (37), (38), or (39) depending on which volumetric moisture content is to be found.

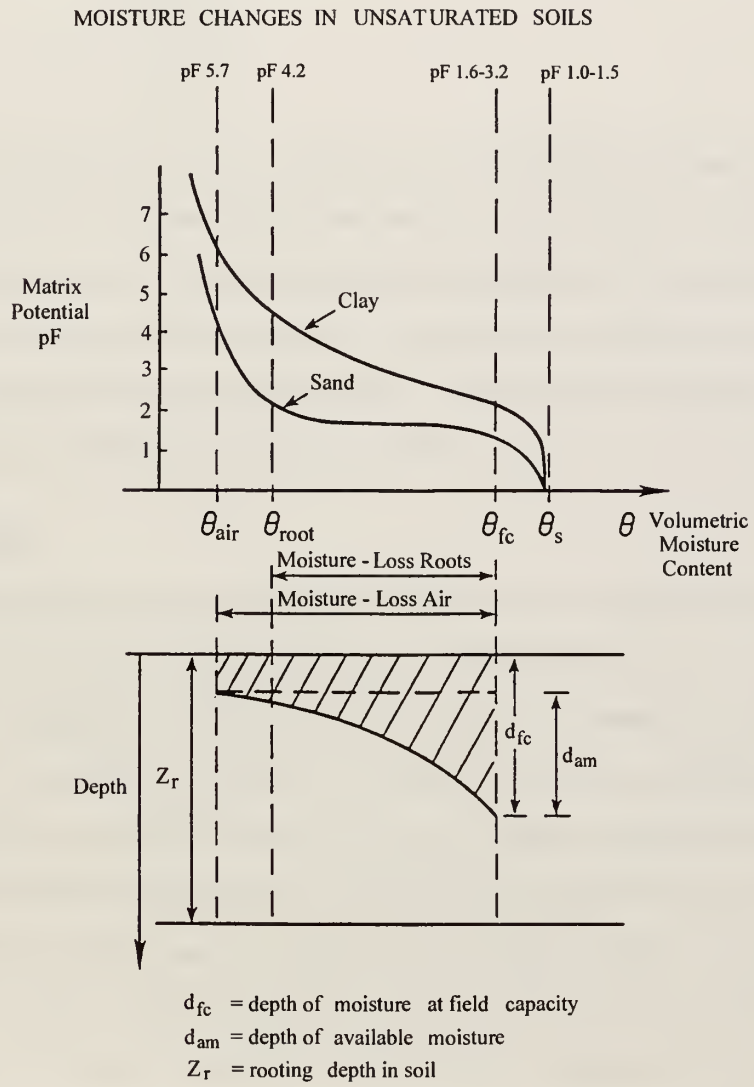


**Fig. 21. (Lytton 1994) Moisture Changes in Unsaturated Soils Between Typical Wet and Dry States**

$$\theta_m = \frac{\theta_s + \frac{|h_m|^B}{A}\theta_r}{1 + \frac{|h_m|^B}{A}} \quad (37)$$

$$\theta_{wl} = \frac{\theta_s + \frac{|h_{wl}|^B}{A}\theta_r}{1 + \frac{|h_{wl}|^B}{A}} \quad (38)$$

$$\theta_{dry} = \frac{\theta_s + \frac{|h_{dry}|^B}{A}\theta_r}{1 + \frac{|h_{dry}|^B}{A}} \quad (39)$$

The equilibrium suction value, $h_m$, can then be solved through an iterative process using equations (33), (37), (38) and (39) as described in Appendix A-90. The equilibrium suction profile, $h_m(z_i)$ for any pervious soil profile is defined by decreasing the equilibrium suction value at the surface, $h_{m,}$ a centimeter in suction for every centimeter increase in depth (McQueen and Miller 1968). The process for determining the equilibrium suction profile is detailed in Appendix A-96.

**Suction Profiles**

It is important to note that moisture changes within a natural soil are determined by the ratio of the period of evaporation to the period of precipitation. A measure of this period of evaporation to the period of precipitation is determined through a method developed by Thornthwaite (1948). In the previous section the equilibrium suction is determined based on relations to the climatic water balance expressed in terms of the Thornthwaite Moisture Index (1948). When a marked separation occurs between wet and dry seasons, a large seasonal variation in soil moisture content occurs, whereas in areas which are either predominantly dry or predominantly wet for most part of the year, the changes in soil moisture content is not so marked. A location where predominant clays are abundant in which the climate is marked by this large separation in the periods of evaporation and periods of precipitation will experience problems with differential

movement to the greatest degree. The state of moisture is dependent on the state of suction and tends towards an equilibrium suction profile, as defined in the previous section, with a moisture source either at the boundaries or within the soil mass. When the state of suction is measured at intervals of depth in a soil profile, the resulting relation between suction and depth is termed the suction profile. Mitchell measured actual suction profiles in the area of Adelaide, South Australia and found a very consistent and typical trend that could be modeled. In his study he developed a method based on constitutive soil properties to model the suction profile within a soil profile base on the local annual weather cycle, n, soil diffusion, $\alpha(z_i)$, equilibrium suction value, $h_m$, and the amplitude suction value, $U_o$. The maximum limit suction profile, $h_{max}(z_i)$, and minimum limit suction profile, $h_{min}(z_i)$ begin at the limiting field condition suction value at the surface, and decrease at an exponential rate toward the equilibrium profile, $h_m(z_i)$. These limit suction profiles will approach the equilibrium suction profile at the depth to constant suction, $z_m$, which will be defined in the next section. The limit suction value depends on the type of surface conditions and is defined in the section titled "Typical Suction Levels in the Field". The dry limit suction value is usually 4.5 pF for soil with vegetation at the surface and 6.0 pF for bare soil at the surface. Refer to Fig. 22 for a typical maximum limit suction profile. The wet limit suction value, which is somewhat drier than the field capacity suction value, is usually 2.5 pF. Refer to Fig. 23 for a typical minimum limit suction profile. Mitchell uses an idealized model of the annual weather surface cycle which he represents by (40). This is a good representation for design because it assumes that soil at the surface approaches the maximum and minimum moisture conditions at two distinct and separate times of the year. As stated earlier, this separation between wet and dry periods produces worst case differential soil movement scenarios. Mitchell combines the soil suction relationship with the relationship that describes the local surface weather cycle and arrives at equation (42).

Mitchell found that the suction change due to the effects of climate, drainage and site cover is a periodic function of time. The suction at any time and at any depth in the

soil profile is determined by solving the diffusion equation, (41), for a particular

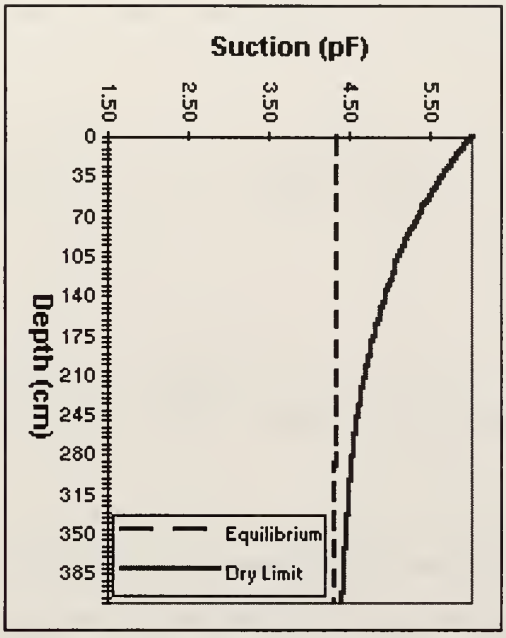


**Fig. 22. Typical Dry Limit Suction Profile for Bare Soil at the Surface**

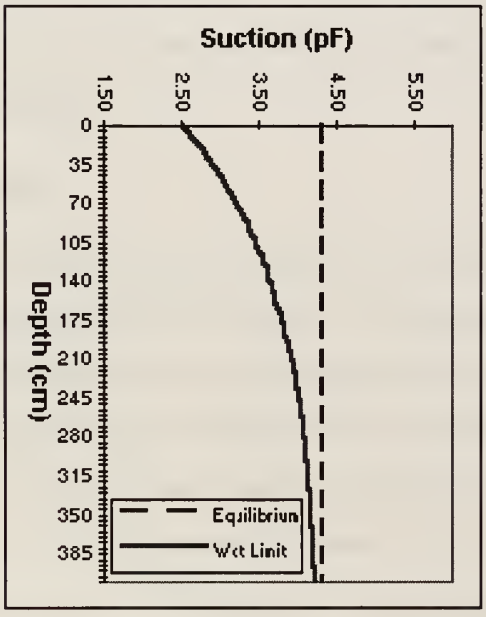


**Fig. 23. Typical Wet Limit Suction Profile for Bare Soil at the Surface**

set of boundary conditions. The solution to arrive at the soil suction profile equation (42) can be found in Mitchell's 1981 report (values of $h(z_i,t)$, $h_m(z_i,t)$, and $U_o$ are all in units of pF).

$$h(z_i = 0,t) = \cos\left(2\pi \cdot n \cdot t - (z_i = 0) \cdot \sqrt{\frac{n \cdot \pi}{\alpha(z_i = 0)}}\right) \tag{40}$$

$$\frac{\partial h}{\partial t} = \alpha \frac{\partial^2 h}{\partial z^2} \tag{41}$$

$$h(z_i,t) = h_m(z_i) + U_o e^{-(z_i)\sqrt{\frac{n\cdot\pi}{\alpha(z_i)}}} \cdot \cos\left(2\pi \cdot n \cdot t - (z_i) \cdot \sqrt{\frac{n \cdot \pi}{\alpha(z_i)}}\right) \tag{42}$$

Based on the surface and depth boundary conditions, referred to as moisture effect cases, (42) is applied to produce suction profiles for many surface conditions and soil profiles. Appendix A contains detailed algorithms that describe precisely how to apply (42) to arrive at suction profiles resulting from combinations of different moisture effect cases and soil profiles. Later sections in "The Procedures, in a Software Design Format" chapter will provide a more detailed discussion with respect to application of (42) in producing suction profiles.

**Depth to Constant Suction**

The depth to constant suction is the depth in a soil profile to which there is no longer a significant seasonal change in soil suction. This depth has been reported to be anywhere from 6 feet to as much as 26 feet dependent upon the type of soil, seasonal weather trends, and the type of surface conditions such as vegetation and slope. Mohan and Rao reported where the active zone extended to a depth of 13 to 16 feet, in the black cotton soils of India. Kassiff reported movement of an exposed clay at depths up to 20 feet in Israel, with the largest differential movements being measured within an active zone of 6 ½ feet, where moisture changes are maximal (Mitchell 1980). As one

uses the procedures contained herein to predict the differential movement in soils, it becomes clear that most of the movement does in fact occur nearer the surface. This reduction in the amount of differential soil movement with an increase in depth is attributable to the combination of small seasonal changes in soil moisture content with an increase in depth, and the increase in restriction to volume strain due to overburden stresses with an increase in depth. The algorithm to solve for the depth to constant suction is based primarily on Mitchell's equation (42) that is described in the previous section.

Lytton and the author are responsible for developing the following steps to arrive at the equation to calculate the depth to constant suction. Only the limit profile aspect of Mitchell's equation, (42), will be used. Setting the cosine term equal to one forces this equation to generate only the maximum and or minimum suction envelopes. Refer to (43).

$$h(z_i,t) = h_m(z_i) + U_o e^{-(z_i)\sqrt{\frac{n\cdot\pi}{\alpha(z_i)}}} \cdot \cancel{\cos\left(2\pi\cdot n\cdot t - (z_i)\cdot\sqrt{\frac{n\cdot\pi}{\alpha(z_i)}}\right)} \quad 1.0 \qquad (43)$$

Mitchell's equation in the form of (43) is used in most of the algorithms to calculate the volume strain for post equilibrium moisture effect cases. Equation (43) is rearranged to isolate the exponent term, (44).

$$h(z_i,t) - h_m(z_i) = U_o e^{-(z_i)\sqrt{\frac{n\cdot\pi}{\alpha(z_i)}}} \qquad (44)$$

(44) is then divided through by $U_o$, (45).

$$\frac{h(z_i,t) - h_m(z_i)}{U_o} = P = e^{-(z_i)\sqrt{\frac{n\cdot\pi}{\alpha(z_i)}}} \qquad (45)$$

The last step is to take the natural log of both sides and solve for $z_i$, (46).

$$z_m = -\ln\left(\frac{h(z_i,t) - h_m(z_i)}{U_o}\right) \cdot \frac{1}{\sqrt{\frac{n \cdot \pi}{\alpha(z_i)}}} \tag{46}$$

The depth to constant suction, $z_m$, has been obtained when the amplitude at depth $z_i$ is equal to 0.2 pF. Later sections in "The Procedures, in a Software Design Format" chapter will provide a more detailed discussion with respect to application of (45) and (46) in calculating the depth to constant suction.

**Horizontal Velocity in Expansive Soils**

The ability to calculate horizontal velocity of water flow in soils is critical for the application of the soil volume strain theory. Predicting vertical differential soil movement when a horizontal barrier is employed, or when a moisture effect case is located a distinct distance from the slab's edge depends upon the soil's horizontal water flow characteristics. The horizontal velocity is calculated and then used to calculate a suction profile a distinct distance from another known suction profile. Lytton and the author developed the horizontal velocity equation by applying Darcy's law, (47), to the unsaturated permeability relationship for clay soils developed by Mitchell, (18), to arrive at the horizontal velocity equation for unsaturated soils, (52). The steps to derive (52) are described below. First Darcy's law, (47), is solved for dh, (48).

$$V_x(z_i) = -k \cdot \left(\frac{dh}{dx}\right) \tag{47}$$

$$dh = -\frac{V_x(z_i)}{k} \cdot dx \tag{48}$$

Darcy's permeability constant is set equal to Mitchell's unsaturated permeability, (49).

$$k = \frac{K_o(z_i) \cdot h_o}{h} \tag{49}$$

Substitute (49) in for Darcy's permeability in (48) and separate variables dependent on distance and variables dependent on suction to arrive at (50).

$$-\frac{V_x(z_i)}{K_o(z_i) \cdot h_o} \cdot dx = \frac{dh}{h} \tag{50}$$

Integrate the left side of (50) from zero to a distance x, and the right side of (50) from an entry suction value, $h_{entry}(z_i)$, to an exit suction value, $h_{exit}(z_i)$. Refer to equation (51).

$$-\frac{V_x(z_i)}{K_o(z_i) \cdot h_o} \int_0^x dx = \int_{h_{entry}(z_i)}^{h_{exit}(z_i)} \frac{dh}{h} \tag{51}$$

Solve equation (51) for $V_x(z_i)$ to arrive at equation (52).

$$V_x(z_i) = \frac{K_o(z_i) \cdot h_o}{x} \cdot \ln\left(\frac{h_{entry}(z_i)}{h_{exit}(z_i)}\right) \tag{52}$$

The entry suction value is the suction value at x = 0. The exit suction value is the suction value at x. Once the horizontal velocity is known between two distinct locations in an incremental soil layer, the suction value for any point between those two distinct locations is solved for using equation (53). Equation (53) is derived by solving for the exit suction in (52).

$$h_{exit}(z_i) = h_{entry}(z_i) \cdot e^{-\frac{V_x(z_i) \cdot x}{K_o(z_i) \cdot h_o}} \tag{53}$$

**Post Construction Theory**

The worst case differential soil movement may occur in the first dry season subsequent to the construction of the slab during the wettest time of the year, or during the first wet season subsequent to construction of the slab during the driest time of the year. This type of moisture effect case is referred to as the post construction case. The post construction case is a transient case for calculating volume strain of

expansive soils immediately after construction and before the soil under the center of the slab has reached an equilibrium moisture content. For example, when a slab is constructed the soil is "capped" and the moisture content changes slowly toward its equilibrium value while the perimeter soil shrinks and swells with the change in seasonal moisture. This type of scenario provides conditions for the post construction moisture effect case. The moisture content of the "capped" soil looses or gains moisture for some period of time until the soil under the center of the slab reaches an equilibrium moisture content. The rate at which the soil approaches equilibrium is dictated by the soil's diffusivity and unsaturated permeability. Once the soil under the slab reaches the equilibrium moisture content, subsequent suction distributions and differential movements must be determined using the post equilibrium methodology.

*The "Damped" Slab Suction Profile*

Lytton and the author developed the following set of equations to model the soil under the slab subsequent to construction in a transient case in which a soil suction profile approaches an equilibrium suction profile. The idea is to calculate the soil suction profile under the slab at the time of construction, $h_{slab}(z_i,t_{const/dry})$, and then dampen this profile until it approaches the equilibrium profile. The soil suction profiles under the slab and at the slab edge are solved, with respect to time, based on some knowledge of the number of annual weather cycles. The annual weather cycle will be assumed to vary according to the function described by (40). To demonstrate this method, the annual weather cycle is assumed to be one, n = 1. This means that, in one year there will be one wet season and one dry season. The driest, or wettest, month of the year must be known. In this case, June is selected as the driest month of the year. Fig. 24 is an example of a weather cycle modeled using (40) for bare soil at the surface (n = 1, and June is the driest month of the year).

The approach used to derive the equations to damp the suction profile at time of construction back to the equilibrium suction profile was developed by Juarez-Badillo

(1975) in which functional domains for the problem are first established as shown in Fig. 25. Function (54) was developed to satisfy the boundary conditions in Fig. 25.

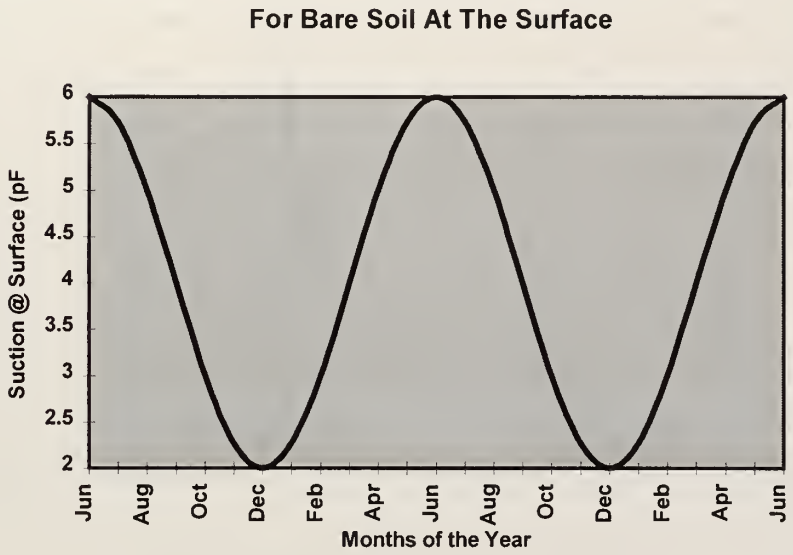


**Fig. 24. A Weather Cycle Modeled by a Cosine Function, n = 1, June is the Driest Month**

$$f(h) = \frac{1}{h_m - h} - \frac{1}{h_m - h_{const}} \quad \text{(Case 1, when } h_m \text{ is greater than } h_{const}\text{.)} \qquad (54)$$

$$f(h) = \frac{1}{h_m - h} - \frac{1}{h_m - h_{const}} \quad \text{(Case 2, when } h_m \text{ is less than } h_{const}\text{.)} \qquad (54)$$

The suction value with respect to time and depth for a profile that is modeled to tend toward an equilibrium suction was solved for cases 1 and 2. Both cases arrived at the same expression (59). The steps to arrive at (59) are described below. Through an assumption of linear proportionality of the rates of change of the function equations (55) is established, and the constant of proportionality, β, is equal to 1.

$$\frac{df(h)}{f(h)} = \beta \frac{dt}{t} \qquad (55)$$

**Fig. 25. Domains of Functions h, t, and f(h)**

The left side of equation (55) is integrated from an arbitrarily chosen suction value, h, to a suction value half way between $h_m$ and $h_{const}$, $h_1$. The right side of equation (55) is integrated from a time corresponding to $h_1$, $t_1$, to the time required to approach h, t. This integration is given by equation (56).

$$\ln \frac{\frac{1}{h_m - h} - \frac{1}{h_m - h_{const}}}{\frac{1}{h_m - h_1} - \frac{1}{h_m - h_{const}}} = \beta \cdot \ln \frac{t}{t_1} \tag{56}$$

Equation (56) is rearranged to collect all constant variables on one side of the equation and set equal to a variable, r. Refer to equation (57).

$$\left(\frac{h - h_{const}}{h_m - h}\right) = \left(\frac{h_1 - h_m}{h_m - h_1}\right) \cdot \left(\frac{t}{t_1}\right)^{\beta} = r \tag{57}$$

Now equation (57) is rearranged to solve for the suction value, h, given by (58).

$$h = \frac{h_{const} + r \cdot h_m}{1 + r} \tag{58}$$

Substitute (57) back in to (58) to arrive at the equation used to solve for the suction profile under the slab some time, t, after the slab was "capped" as a result of slab construction, (59).

$$h(z,t) = \frac{h_{const}(z, t_{const}) + h_m(z)\left(\frac{h_1 - h_m}{h_m - h_1}\right)\cdot t_1^{-\beta}\cdot t^{\beta}}{1 + \left(\frac{h_1 - h_m}{h_m - h_1}\right)\cdot t_1^{-\beta}\cdot t^{\beta}} \tag{59}$$

*The Time Equation*

Before equation (59) can be applied, a relationship must be derived to determine the amount of time required for water to move upward or downward to change the suction at any given depth half way between its initial value and the equilibrium value of suction. This time equation for $t_1$ is given by (61). The derivation of (61) is as follows. Darcy's law of permeability is the relationship used to introduce the time variable. Velocity is defined as a distance through which water flows in soil, x, traveled in some amount of time, $t_1$. Velocity described in terms of permeability of water in expansive soils in which the time, $t_1$, required to obtain half of the change in suction (the time to obtain half of the change in suction was arbitrarily chosen), $0.5\cdot\Delta h$, is given by (60)

$$V = \frac{x}{t_1} = k\cdot\frac{dh}{dx} = P(z_i)\cdot\left(\frac{0.5\cdot\Delta h}{x}\right) \tag{60}$$

Equation (60) is solved for $t_1$, (61). In equation (60), the variable x is replaced with equation (44), where the ratio of suction values is set equal to one half.

$$t_1 = \frac{\left(-\sqrt{\frac{\alpha(z_i)}{n\cdot\pi}}\cdot\ln(0.5)\right)^2}{0.5\cdot\frac{K_o(z_i)\cdot h_o}{0.4343}\cdot\left(h(z_i, t_{const}) - h_m(z)\right)} \tag{61}$$

The time variable represented by (61) is used in (59) to solve for the suction profile some time, t, after soil is "capped" as a result of slab construction.

## THE PROCEDURES, IN A SOFTWARE DESIGN FORMAT

### Introduction to the Software Design Approach

The tools described in "The Theory of Differential Soil Movement" chapter are all that is needed to develop the equations and terms used in the procedures described in this chapter. Appendix B is a graphic representation suggested as a flow of vertical differential soil movement algorithms in a windows environment type software design layout. The suggested software design layout, Appendix B, is modeled after the PTISLAB WIN 1.0 software package owned by Geostructural Tool Kit, Inc. (1996). The focus of this document is not software design or marketing, those skills are left to experts in that area of work. The focus is to present the equations and terms in easy to follow algorithms, as described in Appendix A, so that engineers or programmers can apply this soil volume strain technology in everyday practice.

A question that a practicing engineer may ask is, "What practical engineering cases can these procedures address?" The answer is, cases involving a surface drained soil profile in which the slope is stable and surface conditions are those described below:

1. Bare soil at the surface.
2. Grass at the surface with shallow roots.
3. A flower bed at the surface with a known depth of flower bed zone, $d_{zone}$.
4. A tree with a known depth of root zone, $d_{zone}$.

The procedures consider design effects that are introduced to change the magnitude of the vertical differential soil movement. These design effects include: vertical barriers, horizontal barriers, and the effects of locating the surface moisture effect a distinct distance from the foundation, $d_{source}$. All of these design effects can be rigorously analyzed to enable an engineer the ability to choose the effect which will provide the

desired design results.

The algorithms contained herein address all cases and design effects listed above by way of two design approaches: (1) the post construction approach, and (2) the post equilibrium approach. An engineer would apply the algorithms, used in both approaches, to address all possible combinations of cases and design effects presented. The engineer compares the results of these cases to find scenarios that produce vertical differential soil movement that generates maximum bending, shear and deflection. This information is used to generate adequate foundation designs. The most promising scenario is to use the power of today's computing technology to perform the iterative calculations and tests required to arrive at these design quantities. A programmer could apply software technology, such as PTISLAB WIN 1.0, to model a slab's interaction with the differential soil movements produced by the algorithms contained herein to arrive at these maximum design cases.

The algorithms are presented in a format that can be easily programmed using simple spreadsheet type software. First, input required for all calculations are entered. Soil properties and other related soil characteristics are calculated and stored for use in algorithms presented later. Equilibrium suction values, $h_m$, and depth to constant suction values, $z_m$, are calculated for a specific location and specific sets of surface conditions. With the above complete, all moisture effect cases and design effects listed previously are addressed using the post construction solutions and the post equilibrium solutions.

**Input**

When considering all cases and all calculations required to complete algorithms, an accounting of the variables required for input becomes important. Great effort is made to keep the complex nature of data required for input down to a minimum. The goal, relative to input of data, is to ensure that all variables required for input are items that are easy and economical for practicing engineers to obtain. This is the same goal authors had in mind while developing the simplified method for identifying

predominant clay minerals (Pearring 1968, Holt 1969 and Mojekwu 1979), the methods for obtaining the suction compression index and the mean principal stress compression index (McKeen 1981 and Viayvergiya and Ghazzaly 1973), and the method for obtaining the edge moisture variation distance (Jayatilaka et al.1992). Below is a full list of items required for input to perform every calculation in the algorithms described in Appendix A.

| | |
|---|---|
| A,B | Gardner's coefficients (Appendix A-90 and Table 2) |
| B | Number of boring samples (Appendix A-84) |
| $D_c$ | Depth to the $c^{th}$ suction measurement in a sample (Appendix A-87) |
| $L_s$ | Depth to the bottom of layer s (Appendix A-84) |
| $LL_s$ | Liquid limit for layer s, in percent (Appendix A-84) |
| $M_b$ | Number of layers in the $b^{th}$ boring sample (Appendix A-84) |
| N | Number of suction measurements in a sample (Appendix A-87) |
| $PL_s$ | Plastic limit for layer s, in percent (Appendix A-84) |
| TMI | Local annual Thornthwaite Moisture Index, (Fig. 26 and Appendix A-83) |
| $X_b$ | X coordinate for the $b^{th}$ boring sample (Appendix A-84) |
| $Y_b$ | Y coordinate for the $b^{th}$ boring sample (Appendix A-84) |
| $d_{am}$ | Available moisture depth of the soil mass (Appendix A-90) |
| $d_{hbar}$ | Size of horizontal barrier (Appendix A-86) |
| $d_{source}$ | Distance effect is away from the edge of barrier/slab (Appendix A-86) |
| $d_{vbar}$ | Depth of vertical barrier (Appendix A-86) |
| $d_{zone}$ | Depth of the root or flower bed zone (Appendix A-86) |
| $h_c$ | $c^{th}$ suction measurement in a sample (Appendix A-87) |
| $h_{dry}$ | Dry suction limit for soils in the field, bare soil at the surface usually has a value of 6.0pF and soil with vegetation at the surface usually has a value of 4.5pF (It may be requested in various algorithms. Appendix A-90 is the first time $h_{dry}$ is requested as input). |

$h_{wl}$ Wet limit suction for soils in the field, usually 2.5pF (It may be requested in various algorithms. Appendix A-90 is the first time $h_{wl}$ is used).

n Local annual weather cycle (Appendix A-83).

$t_{const}$ The month the slab was constructed (Appendix A-107)

$t_{dry}$ Driest month of the year (Appendix A-107)

$t_{vc}$ The month the soil volume change is sought (Appendix A-107)

$\mu_s$ Percent passing 2 micron for layer s (Appendix A-84)

$\nu_s$ Percent passing number 200 sieve for layer s (Appendix A-84)

More detailed explanations of how these variables are used is described in the following sections of this document. Appendix A gives a complete process flow detailing the use of the variables listed above and the variables listed in the list of symbols.

Input, as requested by the process flow in Appendix A and as graphically represented in the software design layout sheets in Appendix B, is broken down into six major categories:

1. **Project Information input.** This includes project name, date the project started, name of the engineer assigned to the project, and the site location. This information is basic information an engineering firm may want to establish in a database so that information can be readily accessed. The only information critical to calculating differential soil movement is the site location. The site location can be used as the means to locate the TMI for a site without requiring the user to manually research this bit of information. Refer to Appendix A-82 for a process flow and Appendix B-117 for a program design layout. The TMI for a particular site is found in Fig.26.
2. **Foundation Layout.** This is basic surveying information to establish a three dimensional grid for logging information related to appropriate physical locations. Refer to Appendix A-83 for process flow and Appendix B-118 for program design layout.
3. **Soil Layer Property Input.** These values include boring sample data and soil layer property data. The data entered here will provide enough information to generate a

three dimensional picture of the soil profile. Refer to Appendix A-84 for a process flow and Appendix B-119, 120, 126 for program design layouts. The soil profile used in all example calculations is shown in Table 1.

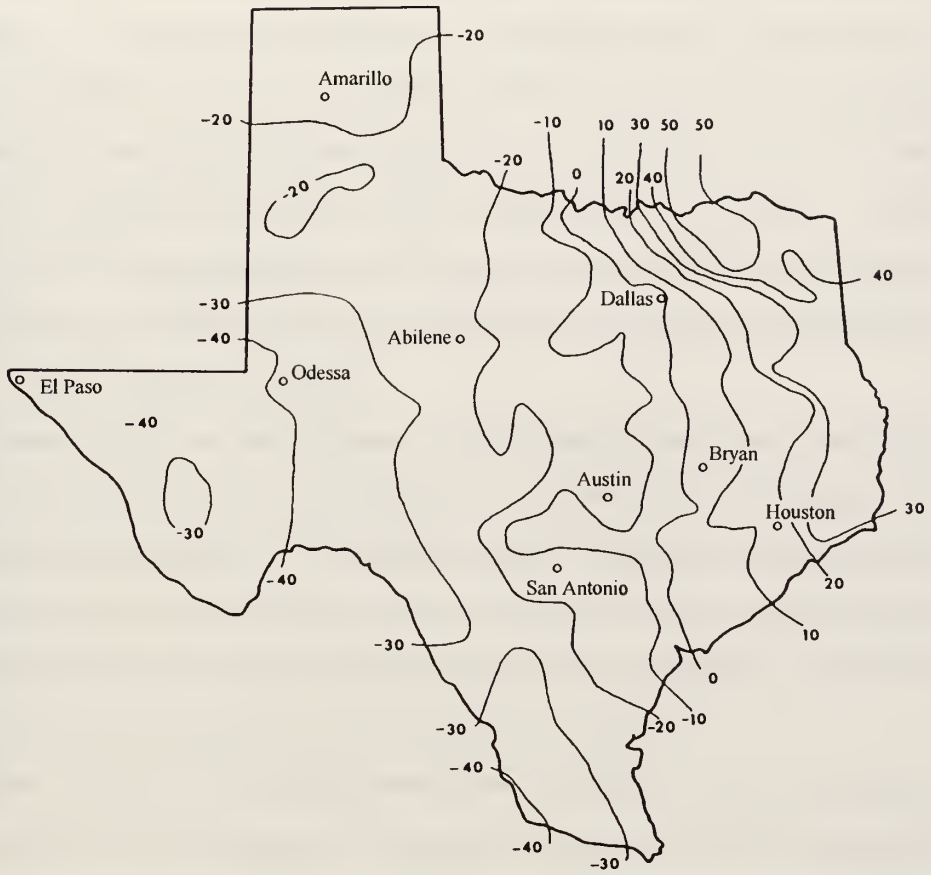


**Fig. 26. (Wray 1978) Thornthwaite Index for Texas (20 year average 1955-1974)**

**Table 1. Soil Profile Considered in all Sample Calculations**

| Soil Layer No. | $L_s$ ft | $LL_s$ % | $PL_s$ % | $\nu_s$ % | $\mu_s$ % | $\gamma_d$ lbs/ft$^3$ |
|---|---|---|---|---|---|---|
| s = 1 | 5 | 56.0% | 22.0% | 65.0% | 25.0% | 120 |
| s = 2 | 9 | 67.0% | 24.0% | 76.0% | 46.0% | 120 |
| s = 3 | 13 | 44.0% | 18.0% | 47.0% | 18.0% | 120 |
| s = 4 | 30 | 53.0% | 20.0% | 64.0% | 31.0% | 120 |

4. **Moisture Effect Input.** This gives the user the option to input the type and location of the moisture effect cases considered in vertical differential soil movement calculations. Refer to the plan view, Appendix C-132, for a view of the foundation used as the example throughout this document. The input for location and moisture effect case type can be found listed on the program design layout Appendix B-121. For example, case "1-5" describes the sidewalk with grass covered lawn on the north and west portions of the building shown in Appendix C-132. The number "1", in "1-5", describes this case as the first sequential case of this type. The number "5", in "1-5", describes this case to be grass at the surface with a horizontal barrier. Additional information is shown in Appendix B-121 and is described in the process flow sheets Appendix A-85, 86.
5. **Measured Suction Profile Input.** Geotechnical engineers may identify some unique moisture effect cases that cannot be modeled in the procedures to address the typical moisture effect cases contained herein. Those special cases are addressed using initial and final measured suction profiles. The input of these measured suction profiles is described in the process flow sheet Appendix A-87, and shown in the program design layout sheet, Appendix B-122, 123.
6. **Time Input for Post Construction Cases.** Algorithms for post construction solutions are time dependent. Calculating the post construction differential soil movements can only be accomplished if the driest (or wettest) time of year is known, $t_{dry}$, the month of year the foundation was built is known, $t_{const}$, and the month the soil volume change is sought is known, $t_{vc}$. Input of these quantities is described in the process flow sheet Appendix A-107.

**Calculated Soil Properties and Soil Characteristics**

Once the liquid limit, the plastic limit, the percent passing the number 200 sieve, the percent smaller than two microns, and the dry unit weight is entered for the soil profile considered, the remainder of the required soil properties and characteristics are

solved. The process flow sheet, Appendix A-88, describes the algorithm by which these remaining soil characteristics are solved. Definitions for all symbols are found in the list of symbols.

The plasticity index, $PI(z_i)$, is the difference between the liquid limit, $LL(z_i)$, and the plastic limit, $PL(z_i)$. The percent fine clay, $Clay(z_i)$, is calculated by dividing the percent smaller than two microns, $\mu(z_i)$, by the percent passing the number 200 sieve, $\nu(z_i)$. The activity ratio, $Ac(z_i)$, is calculated by dividing the $PI(z_i)$ by $Clay(z_i)$. The cation exchange capacity, $CEC(z_i)$, is the larger of the values $PL(z_i)^{1.17}$ or $LL(z_i)^{0.912}$. The cation exchange activity, $CEAc(z_i)$, is calculated by dividing $CEC(z_i)$ by $Clay(z_i)$. Using Fig. 15, the matrix suction compression index, $\gamma_{h100}$, is the value found at the intersection of $CEAc(z_i)$ and $Ac(z_i)$. To obtain the $\gamma_h(z_i)$ simply multiply Clay(zi) by $\gamma_{h100}$. The slope of the suction versus the gravimetric water content line, $S(z_i)$, is approximated by (16). Mitchell's diffusion coefficient, $\alpha(z_i)$, is approximated by (17). Mitchell's unsaturated permeability, $K_o(z_i)\cdot|h_o|$, is calculated by (18). Using Fig. 16 for center lift conditions and Fig. 17 for edge lift conditions, the edge moisture variation is found by finding the curve that corresponds with the soil's diffusion coefficient, $\alpha(z_i)$, then finding the intersection made by drawing a vertical line corresponding to the local TMI (for locations in Texas the local TMI can be found in Fig. 26), and finally drawing a horizontal line from that intersection across to the y axis identifies the appropriate edge moisture variation distance. For each case of center lift and edge lift, the largest edge moisture variation value, considering all incremental soil layers, is the soil profile's edge moisture variation distance, $e_{mc}$ and $e_{me}$.

**Procedures to Calculate the Equilibrium Suction**

The next step in the process of calculating the vertical differential soil movement is to establish a baseline equilibrium suction, $h_m$ (units of pF). All suction profiles are calculated relative to this baseline. The equilibrium suction, $h_m$, is calculated for the soil layer located at the depth to constant suction. The depth to constant suction, $z_m$, is

dependent upon the $h_m$. Therefore, if the depth to constant suction, $z_m$, does not fall within the soil layer in which the $h_m$ was calculated, then the $h_m$ must be re-calculated for the soil layer located at the depth to constant suction. This is an iterative process. The process flow sheet which describes the procedure for calculating $h_m$ is found on Appendix A-90. The procedures for calculating $z_m$ are found in the next section. The equilibrium suction value is dependent upon the following inputs: TMI, $d_{am}$, $h_{wl}$, $h_{dry}$, $\theta_s$, $\theta_r$, A, and B. For the state of Texas the TMI is obtained from Fig. 26. Values for $\theta_s$, $\theta_r$, A, and B for a particular classification of soil are listed in Table 2. As reported by Gay (1994), a conservative estimate for the $d_{am}$ can be taken as 30 cm for all expansive soils in which the $d_{am}$ is not known. All variables have default values. Refer to Appendix A-90. Once all input is entered $\gamma$, $d_1$, $T_1$, $\theta_{wl}$, $\theta_{dry}$ are calculated using (25), (26), (27), (38), and (39) respectively. These values are used in equations (33) and (37) to solve for $h_m$. A value of $h_m$ is picked and an iterative process for solving for $\theta_m$ is performed until equal values of $\theta_m$ satisfies both equations (33) and (37).

**Depth to Constant Suction**

The depth to constant suction is the depth in a soil profile to which there is no longer a significant seasonal suction change. The definition of no significant seasonal suction change is 0.2 pF from Lytton's 1994 paper. Depth to constant suction is dependent upon the diffusivity of the soil, the number of local annual weather cycles, and the suction amplitude at the surface. As discussed in the "Soil Volume Strain" section, the soil's ability to change volume is dependent upon the seasonal change of moisture and the magnitude of the mean principal stress present to suppress the volume change. Using Mitchell's equation (42) there will always be a reduction in the suction amplitude with an increase of depth. Additionally, an increase in depth introduces added restraint to soil volume strain due to the effect of overburden. Considering these two aspects of the soil volume change equation it becomes apparent that for depths greater than 30 feet there is usually no longer any significant changes in suction. The

depth to constant suction, $z_m$, will be used as the depth beyond which there is no significant change in suction.

**Table 2. (Lytton et al. 1989) Gardner's Coefficients**

| No | Unified Soil Class. | Void ratio e | AWL | XWL | Porosity $n = \theta_s$ | $\theta_r = 0.1\theta_s$ | A | B |
|---|---|---|---|---|---|---|---|---|
| GM-GC1 | GM-GC | 0.42 | 0.004 | 0.637 | 0.296 | 0.0296 | 1083.777 | 0.637 |
| GM1 | GM | 0.259 | 0.152 | 0.269 | 0.206 | 0.0206 | 12.2224 | 0.269 |
| GM2 | GM | 0.382 | 0.04 | 0.648 | 0.276 | 0.0276 | 111.1578 | 0.648 |
| GM3 | GM | 0.451 | 0.066 | 0.251 | 0.311 | 0.0311 | 27.00574 | 0.251 |
| GM4 | GM | 0.608 | 0.043 | 0.478 | 0.378 | 0.0378 | 69.90875 | 0.478 |
| GP1 | GP | 0.255 | 0.065 | 0.55 | 0.203 | 0.0203 | 54.58668 | 0.55 |
| GW1 | GW | 0.443 | 0.039 | 0.302 | 0.307 | 0.0307 | 51.39672 | 0.302 |
| GW2 | GW | 0.506 | 0.596 | 0.318 | 0.416 | 0.0416 | 3.489424 | 0.318 |
| GW3 | GW | 0.252 | 0.309 | 0.319 | 0.355 | 0.0355 | 6.745925 | 0.319 |
| SM-SC1 | SM-SC | 0.656 | 0.013 | 0.77 | 0.396 | 0.0396 | 452.9567 | 0.77 |
| SM1 | SM | 0.396 | 0.016 | 0.562 | 0.284 | 0.0284 | 227.9712 | 0.562 |
| SM2 | SM | 0.619 | 0.001 | 1.023 | 0.382 | 0.0382 | 10543.87 | 1.023 |
| SM3 | SM | 1.192 | 0.11 | 0.339 | 0.544 | 0.0544 | 19.843 | 0.339 |
| SM4 | SM | 0.655 | 0.039 | 0.468 | 0.396 | 0.0396 | 75.32435 | 0.468 |
| SM5 | SM | 0.623 | 0.015 | 0.835 | 0.384 | 0.0384 | 455.9411 | 0.835 |
| SM6 | SM | 1.024 | 0.011 | 0.671 | 0.506 | 0.0506 | 426.194 | 0.671 |
| SM7 | SM | 0.72 | 0.023 | 0.549 | 0.419 | 0.0419 | 153.9119 | 0.549 |
| SM8 | SM | 0.831 | 0.208 | 0.436 | 0.454 | 0.0454 | 13.12009 | 0.436 |
| SM9 | SM | 0.721 | 0.01 | 0.835 | 0.419 | 0.0419 | 683.9116 | 0.835 |
| SM10 | SM | 0.818 | 0.018 | 0.806 | 0.45 | 0.045 | 355.4082 | 0.806 |
| SM11 | SM | 1.132 | 0.029 | 0.745 | 0.531 | 0.0531 | 191.6911 | 0.745 |
| SM12 | SM | 2.16 | 0.042 | 0.501 | 0.684 | 0.0684 | 75.46589 | 0.501 |
| SP-SM1 | SP-SM | 0.574 | 0.048 | 0.769 | 0.365 | 0.0365 | 122.3936 | 0.769 |
| SP-SM2 | SP-SM | 0.583 | 0.095 | 0.613 | 0.368 | 0.0368 | 43.17938 | 0.613 |
| SP1 | SP | 0.712 | 0.0554 | 0.79 | 0.416 | 0.0416 | 111.2987 | 0.79 |
| SP2 | SP | 0.736 | 0.024 | 0.951 | 0.424 | 0.0424 | 372.2106 | 0.951 |
| SP3 | SP | 0.818 | 0.042 | 0.9 | 0.45 | 0.045 | 189.1258 | 0.9 |
| SP4 | SP | 0.593 | 0.076 | 0.665 | 0.372 | 0.0372 | 60.83961 | 0.665 |
| SP5 | SP | 0.583 | 0.053 | 0.809 | 0.368 | 0.0368 | 121.5414 | 0.809 |
| SW-SP1 | SW-SP | 0.773 | 0.012 | 1.082 | 0.296 | 0.0296 | 1006.512 | 1.082 |
| SW1 | SW | 0.551 | 0.162 | 0.5852 | 0.355 | 0.0355 | 23.75117 | 0.5852 |
| SW3 | SW | 0.385 | 0.111 | 0.616 | 0.278 | 0.0278 | 37.21149 | 0.616 |
| CL1 | CL | 1.183 | 0.065 | 0.417 | 0.542 | 0.0542 | 40.1871 | 0.417 |
| CL2 | CL | 0.621 | 0 | 0.976 | 0.383 | 0.0383 | 0 | 0.976 |
| CL3 | CL | 0.785 | 0.004 | 0.61 | 0.44 | 0.044 | 1018.451 | 0.61 |
| CL4 | CL | 0.61 | 0 | 0.957 | 0.379 | 0.0379 | 0 | 0.957 |
| CL5 | CL | 0.825 | 0.018 | 0.523 | 0.452 | 0.0452 | 185.2369 | 0.523 |
| CL6 | CL | 0.964 | 0 | 1.91 | 0.491 | 0.0491 | 0 | 1.91 |
| CL7 | CL | 0.808 | 0 | 1.593 | 0.447 | 0.0447 | 0 | 1.593 |
| CL8 | CL | 0.972 | 0.028 | 0.344 | 0.493 | 0.0493 | 78.85731 | 0.344 |

Table 2. Continued

| No | Unified Soil Class. | Void ratio e | AWL | XWL | Porosity $n = \theta_s$ | $\theta_r=0.1\theta_s$ | A | B |
|---|---|---|---|---|---|---|---|---|
| CL9 | CL | 0.562 | 6.9E-06 | 1.551 | 0.36 | 0.036 | 5154077 | 1.551 |
| CL10 | CL | 0.517 | 0.024 | 0.359 | 0.341 | 0.0341 | 95.23328 | 0.359 |
| CL11 | CL | 0.415 | 0.064 | 0.247 | 0.293 | 0.0293 | 27.59434 | 0.247 |
| ML8 | ML | 0.858 | 0.003 | 0.973 | 0.462 | 0.0462 | 3132.411 | 0.973 |
| ML9 | ML | 0.606 | 0.022 | 0.707 | 0.377 | 0.0377 | 231.514 | 0.707 |
| ML10 | ML | 2.163 | 0.038 | 0.61 | 0.684 | 0.0684 | 107.2053 | 0.61 |
| ML11 | ML | 0.603 | 0.031 | 0.722 | 0.376 | 0.0376 | 170.0741 | 0.722 |
| ML12 | ML | 0.821 | 0 | 2.059 | 0.451 | 0.0451 | 0 | 2.059 |
| CL12 | CL | 0.972 | 0.004 | 0.474 | 0.493 | 0.0493 | 744.6291 | 0.474 |
| ML-OL1 | ML-OL | 1.721 | 0.064 | 0.535 | 0.632 | 0.0632 | 53.55747 | 0.535 |
| ML-OL2 | ML-OL | 0.885 | 0 | 1.362 | 0.469 | 0.0469 | 0 | 1.362 |
| ML-CL1 | ML-CL | 0.692 | 0.066 | 0.365 | 0.409 | 0.0409 | 35.11204 | 0.365 |
| ML-CL2 | ML-CL | 0.642 | 0.013 | 0.634 | 0.391 | 0.0391 | 331.1743 | 0.634 |
| ML-CL3 | ML-CL | 0.645 | 0.001 | 1.052 | 0.392 | 0.0392 | 11271.97 | 1.052 |
| ML1 | ML | 1.015 | 0.003 | 1.054 | 0.504 | 0.0504 | 3774.668 | 1.054 |
| ML2 | ML | 1.067 | 0 | 1.257 | 0.516 | 0.0516 | 0 | 1.257 |
| ML3 | ML | 1.119 | 0.032 | 0.681 | 0.528 | 0.0528 | 149.9167 | 0.681 |
| ML4 | ML | 1.558 | 0.065 | 0.411 | 0.609 | 0.0609 | 39.63571 | 0.411 |
| ML5 | ML | 0.88 | 0 | 1.019 | 0.468 | 0.0468 | 0 | 1.019 |
| ML6 | ML | 0.825 | 0 | 1.474 | 0.452 | 0.0452 | 0 | 1.474 |
| ML7 | ML | 0.783 | 0.012 | 0.575 | 0.439 | 0.0439 | 313.1978 | 0.575 |

The depth to constant suction varies dependent upon the soil strata, the local weather conditions, and the type of soil surface conditions. The depth to constant suction, $z_m$, will be calculated for the following cases of soil surface conditions, Appendix A-91:

1. Bare soil at the surface (Appendix A-92).
2. Grass at the surface with shallow roots (Appendix A-92).
3. Flower bed at the surface with a known flower bed zone depth, $d_{zone}$ (Appendix A-93).
4. A tree at the surface with a known depth of root zone, $d_{zone}$ (Appendix A-93).
5. And measured suction profiles (Appendix A-94).

The simplest case would be that of bare soil or grass at the surface with only one soil layer the entire depth of moisture active zone. For this case equation (46) is all that

is needed to solve for $z_m$. Simply replace the numerator in the natural log function with 0.2 pF, substitute entered or previously calculated values for all other variables and solve for $z_m$. The suction amplitude, $U_o$, is the difference between maximum and the minimum surface soil suction values. For bare soils the suction amplitude is $U_o = h_{dry} - h_{wl,}$ where $h_{dry} = 6.0$ pF. For soils with grass at the surface the suction amplitude is $U_o = h_{dry} - h_{wl}$, where $h_{dry} = 4.5$ pF. Refer to the "Typical Suction Levels in the Field" for typical values of suction.

In most soil profiles there is usually at least two soil layers to consider. In cases considering bare soil or grass at the surface, with multiple soil layers, the algorithms in Appendix A-92 are used to solve for $z_m$. The procedures are simple.

1. First solve for the ratio of the suction difference between the top increment and bottom increment of a soil layer, $P_s$, using equation (45).
2. Multiply $P_s$ by the suction amplitude at the top of the layer which gives the suction amplitude at the bottom of the layer, $U_{Ls}$.
3. Test $U_{Ls}$:
    a. If $U_{Ls}$ is less than 0.2 pF, then the depth to constant suction is in this layer, in which case $z_m$ is solved using (46). The initial $U_o$ is the same as the one described in the previous paragraph. All subsequent $U_o$'s are solved using the procedure in paragraph 3.b. described below.
    b. If $U_{Ls}$ is grater than 0.2 pF, then set $U_o$ equal to $U_{Ls}$ and repeat these three steps.

The depth to constant suction is the $z_m$ calculated for the last layer added to the value of the depth to the top of this layer.

The procedures for calculating the $z_m$ for flower beds and trees is basically the same with two distinct differences: (1) The suction amplitude is the difference between the limit suction value and the equilibrium suction value. (2) The suction amplitude at the surface is constant to the depth of moisture effect zone, $d_{zone}$. For a flower bed at the surface the suction amplitude is the difference between the equilibrium suction value and the wet limit suction value, $U_o = h_m - h_{wl}$. For a tree at the surface the suction

amplitude is the difference between the dry limit suction value for vegetation and equilibrium suction value, $U_o = h_{dry} - h_m$. Refer to Appendix A-93 for a detailed process flow of these procedures. Refer to "Typical Suction Levels in the Field" and "Procedures to Calculate the Equilibrium Suction" for values of ($h_{wl}$ and $h_{dry}$) and $h_m$ respectively.

When making calculations of the depth to constant suction, $z_m$, for the case of measured suction profiles, the depth to constant suction can be taken as the value of $z_m$ calculated for one of the four previously explained cases if the surface conditions are the same. However, a check must be made to ensure that the $z_m$ in a particular measured suction profile case does not extend beyond those values of $z_m$ in the previously described cases. If the $z_m$ extends beyond those values calculated using the procedures described in the previous four cases then the $z_m$ must be calculated using the procedures described in Appendix A-94. The procedures are the same as those described above for bare soil and grass at the surface with one major difference. The difference is that the process is initiated at the bottom of the measured suction profile. This $z_m$ value calculated for a measured suction profile is then compared to the $z_m$ for the surface conditions most similar to the measured profile surface conditions. The depth to constant suction is taken as the larger of these values.

## POST EQUILIBRIUM AND POST CONSTRUCTION SOLUTIONS

At this point in the procedures all inputs and calculated values required to generate suction profiles for soil volume strain calculations have been explained. The procedures to generate soil suction profiles and the corresponding soil movement for moisture effect cases and design effects are explained using the following two procedural approaches: (1) the post equilibrium approach, and (2) the post construction approach. The post equilibrium approach refers to procedures to solve for differential movement of expansive soils after the soil under the slab has reached an equilibrium moisture content. When a slab is placed on an expansive soil, there is a time period in which the moisture content under the slab changes from the suction profile as it was when the slab was placed to approach the equilibrium suction value. The algorithms to solve for differential soil movement during this time period are handled by the post construction approach.

### Post Equilibrium Approach

Once the soil under the slab reaches the equilibrium suction value, the differential soil movement is calculated using the differential in soil suction profiles between the equilibrium suction profile under the slab and the suction profile at the edge of the slab. The suction profile at the edge of the slab is dependent upon the seasonal moisture change. The restraint to soil volume increase at any depth is dictated by the amount of overburden and surcharge stress. The post equilibrium algorithms to solve for the limit cases are: (1) differential soil movement causing a maximum center lift distortion mode, and (2) differential soil movement causing a maximum edge lift distortion mode.

#### *Equilibrium Suction Profiles*

The first calculations that are made in the post equilibrium approach are the base line equilibrium suction profiles. The equilibrium suction profile is generated by reducing the equilibrium suction value calculated for a specific moisture effect case by one centimeter in suction for every centimeter of descent in soil depth. Care should be taken to convert the calculated equilibrium suction value from units of pF to units of centimeters.

Once the equilibrium suction profile is generated these values of suction in units of centimeters should be converted back to units of pF to make further calculations. Refer to Appendix A-96 for algorithms to calculate equilibrium suction profiles.

*Suction Profiles Causing The Center Lift Distortion Mode*

Center lift distortion modes are caused by a differential in the equilibrium suction profile under the slab and the dry limit suction profile at the edge of the slab. Once the equilibrium suction profiles are calculated for each case considered, the dry limit suction profiles for the slab edge moisture effect conditions are calculated. The dry limit suction profiles for bare soil and grass at the slab edge are calculated using Appendix A-97, using variables unique to the specific moisture effect case and location. The dry limit suction profiles for a flower bed and a tree at the edge of slab are calculated using the Appendix A-98. The suction profiles are calculated by the application of (43). The differences in these processes, dependent upon moisture effect case and location are: the surface suction values, the soil properties, the baseline equilibrium suction profiles, and depth to constant suction values. For all moisture effect cases, the suction amplitude change and the depth are initialized at every soil layer change. The cases of a tree and a flower bed at the surface have one other major difference, these cases include the depth of moisture effect zone. The suction profile within the tree root or flower bed zone is constant and equal to the limit suction value for the full depth of the moisture effect zone, $d_{zone}$. Refer to Fig. 27 for an example of the dry limit post equilibrium suction profiles for a flower bed at the surface with a 4 foot moisture effect zone depth. Refer to Fig. 28 for an example of the dry limit post equilibrium suction profiles for a tree at the surface with 20 foot deep roots.

*Suction Profiles Causing The Edge Lift Distortion Mode*

Edge lift distortion modes are caused by a differential in the equilibrium suction profile under the slab and the wet limit suction profile at the edge of the slab. Once the equilibrium suction profiles are calculated for each case considered, the suction profiles for the slab edge moisture effect conditions are calculated. The wet limit suction profiles for bare soil, grass, and trees at the slab's edge are calculated using Appendix A-99. The wet

limit suction profiles for a flower bed at the edge of the slab is calculated using the algorithm described in Appendix A-100. The differences in these processes which depend

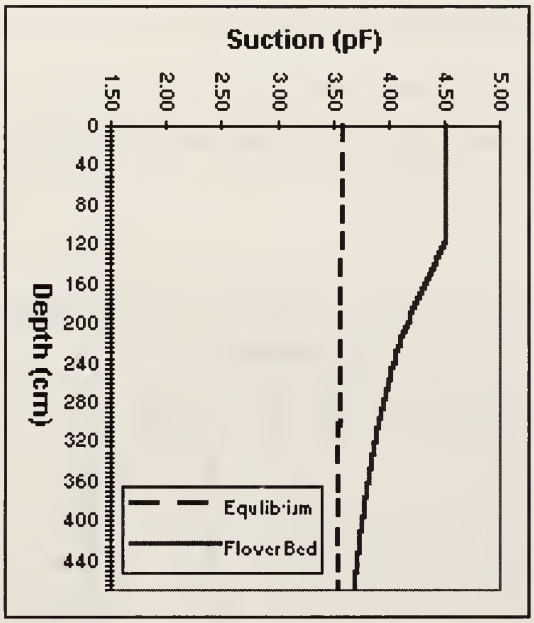


**Fig. 27. Post Equilibrium Suction Profiles for Flower Bed at the Surface (Dry Limit)**

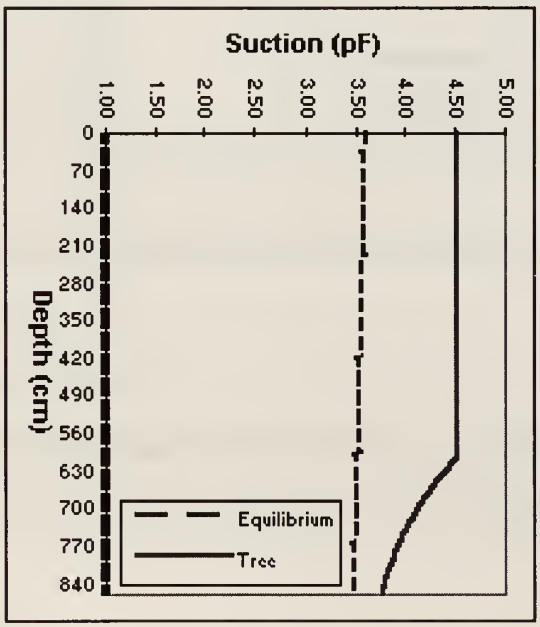


**Fig. 28. Post Equilibrium Suction Profiles for a Tree at The Surface (Dry Limit)**

upon the moisture effect case and location are: the soil properties, the baseline equilibrium suction profiles, and depth to constant suction values. Note that the suction profile is constant and equal to the limit suction value for the full depth of the flower bed zone, $d_{zone}$. The suction amplitude change and the depth are initialized at every soil layer change. Refer to Fig. 29 for an example of the wet limit post equilibrium suction profiles for a flower bed at the surface.

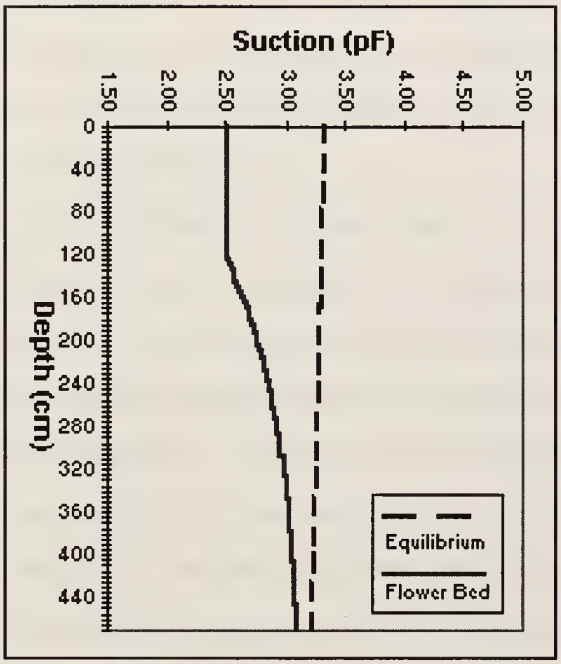


**Fig. 29. Post Equilibrium Suction Profiles for a Flower Bed at The Surface (Wet Limit)**

*Vertical Differential Soil Movement*

Expansive soil volume change is predicted by applying the theory explained in the "Soil Volume Strain" section of the previous chapter. The moisture effect cases considered consist of:

1. Bare soil at the surface,
2. Grass at the surface with shallow roots,

3. A flower bed at the surface with a known depth of flower bed zone, $d_{zone}$, and
4. A tree at the surface with a known depth of root zone, $d_{zone}$.

The procedures also consider the application of design effects to provide the best possible conditions so foundation design performance is at a pinnacle. The design effects considered include:

1. Vertical barriers,
2. Horizontal barriers, and
3. The effect of locating the moisture effect case a distinct distance from the slab edge.

Explanation of the procedures to predict vertical differential soil movement is broken down into three categories: (1) all moisture effect cases with or without a vertical barrier, (2) moisture effect cases with or without a horizontal barrier, and (3) moisture effect cases located a distinct distance from the slab edge.

Post equilibrium vertical differential soil movement can be determined for all moisture effect cases with or without a vertical barrier by simply applying the algorithms described by Appendix A-103. This process can be broken down into three basic steps: (1) All pertinent variables and information collected or calculated in previous procedural steps are retrieved for use in this process. (2) Tests are performed on variables to ensure the appropriate calculations and quantities are used, based on Lytton's volume strain theory. (3) Incremental strain and corresponding vertical soil movement is summed up for every soil increment within the moisture active zone of the soil profile. The total vertical differential soil movement quantity is defined by the variable $\Delta z$. Refer to Fig. 30 for an example of bare soil dry limit suction profiles (center lift distortion mode) for a slab edge that has a four foot deep vertical barrier.

Post equilibrium vertical differential soil movement can be computed for all moisture effect cases, except the tree case, with or without a horizontal barrier by simply applying the algorithms described by Appendix A-104. The case of the tree is unique in that the tree roots will be active regardless of whether a horizontal barrier exists or not. If the tree is killed because of the placement of the horizontal barrier then the point becomes mute. The process in Appendix A-104 is broken down into four basic steps: (1) All

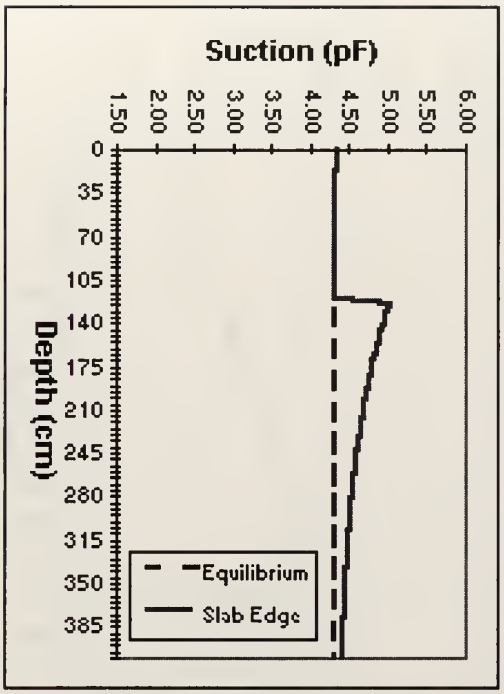


**Fig. 30 Bare Soil Dry Limit Suction Profiles for a Slab with a 4ft Vertical Barrier**

pertinent variables and information collected or calculated in previous procedural steps are retrieved for use in this process. (2) The horizontal velocity for each incremental soil layer is calculated based on the edge moisture variation distance and the size of horizontal barrier. This step is based on equation (52). (3) The suction at the slab edge is calculated using equation (53). (4) This slab edge suction value, $h_{edge}(z_i)$, is used in the place of the final suction value in Appendix A-103 to make vertical differential soil movement calculations, $\Delta z$. Refer to Fig. 31 for an example of wet limit suction profiles (edge lift distortion mode) for a four foot deep flower bed at the edge of a four foot horizontal barrier constructed adjacent to the edge of the slab.

If a flower bed or tree is located a distinct distance from the slab edge, the vertical differential soil movement is calculated by applying Appendix A-104. These are the only two cases that can be located a distance from the slab and still have an effect on vertical differential soil movement under the slab. The differential movement caused by the tree or flower bed located a distance from the slab edge should be compared to the differential

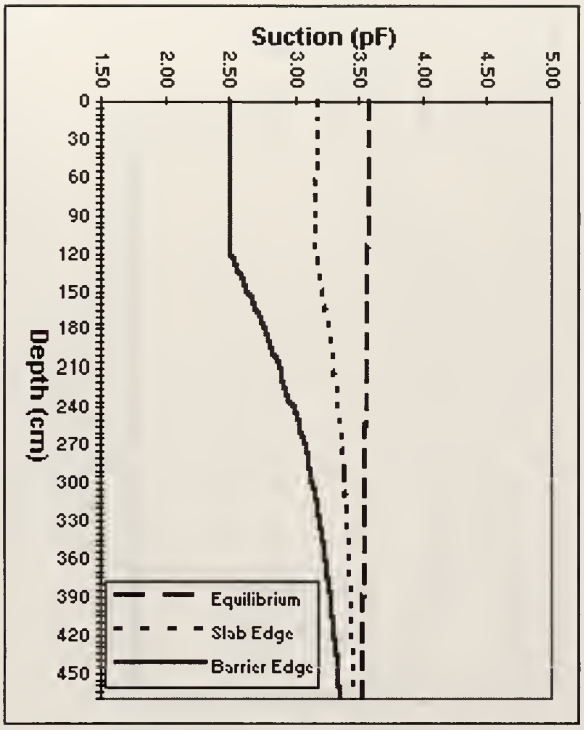


**Fig. 31. Suction Profiles for Flower Bed at the Slab Edge with a 4 ft Horizontal Barrier**

movement caused by the surface condition that exists between the slab edge and the tree/flower bed. The maximum differential soil movement produced by either the tree/flower bed case or the conditions between the slab edge and the tree/flower bed case controls. This process is broken down into four basic steps: (1) All pertinent variables and information collected or calculated in previous procedural steps are retrieved for use in this process. (2) The horizontal velocity for each incremental soil layer is calculated based on the edge moisture variation distance and the distance the moisture effect is away from the slab edge, $d_{source.}$ This step is based on equation (52). (3) The suction at the slab edge is calculated using equation (53). (4) This slab edge suction value, $h_{edge}(z_i)$, is used in the place of the final suction value in Appendix A-103 to make vertical differential soil movement calculations, $\Delta z$. Refer to Fig. 32 for a dry limit suction profiles (center lift distortion mode) for tree roots that are 20 ft deep and located four feet away from the edge of a slab with a four foot vertical barrier.

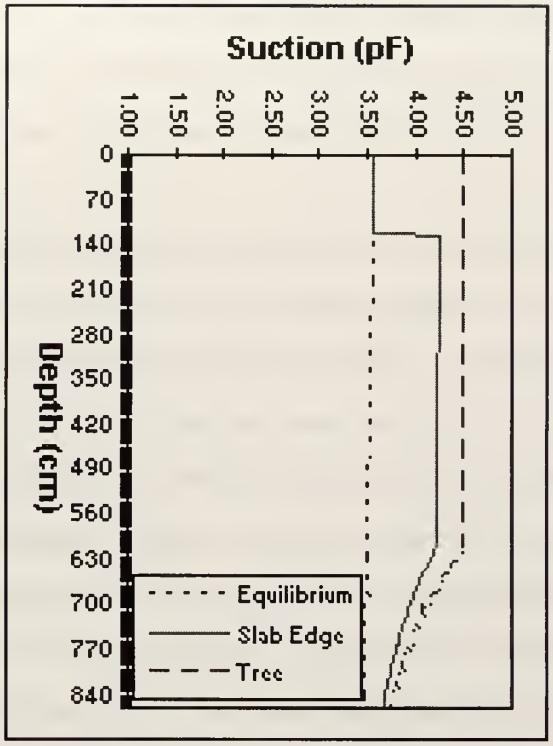


**Fig. 32. Suction Profiles for a Tree 4ft From the Slab Edge with a 4ft Vertical Barrier**

## Post Construction Approach

As described in the "Post Construction Theory" section earlier, the worst case of vertical soil movement in expansive soils may occur in the post construction time period of the life of a structure. Lytton and Woodburn's 1973 paper provides a perfect illustration of this worst case scenario occurring in the post construction time period during the life of a school building. The procedures to apply the post construction theory is basically a two step process. First, all suction profiles considered are calculated. Second, these suction profiles are used to calculate vertical soil movement at the center of the slab, $\Delta z_{slab}$, and combined with the vertical soil movement at the slab edge, $\Delta z_{edge}$, to arrive at a total vertical differential soil movement quantity, $\Delta z_{total}$.

### *Post Construction Suction Profiles*

The suction profiles must be calculated for two time periods: soil suction profiles at the time of construction, $t_{const}$, and soil suction profiles at the time the vertical differential

soil movement is sought, $t_{vc}$. Soil suction profiles at the edge of the slab are generated for the time at which the vertical differential soil movement is sought. Soil suction profiles beneath the slab are generated at the time of construction and at the time the vertical differential soil movement is sought.

Appendix A-107 is the process flow sheet that: describes the time variables, lists a step by step process for entering the required times, and lists the steps to calculate the time periods needed to make soil suction profile calculations. Appendix B-127 is a picture of the program design layout sheet for the time input and display of suction profiles both under the slab and at the edge of the slab for time that transpires from the driest month to the month the volume change is sought. In Appendix B-127, the suction profile under the slab at the time of construction is the thin solid line. The dashed line is the suction profile under the slab six months after construction. Notice that this dashed line is tending toward equilibrium. The equilibrium profiles are the vertical thin lines with tick marks. Finally, the thick solid line is the suction at the edge of the slab with a vertical barrier. To generate suction profiles illustrated in Appendix B-127 the following time inputs are required: (1) the driest month of the year, $t_{dry}$, (2) the month the slab is constructed, $t_{const}$, and (3) the month the soil volume change is sought, $t_{vc}$. These entered values of time are required for two primary purposes: (1) to establish a baseline time to enable application of the surface annual weather cycle model developed by Mitchell, (40), and (2) to establish time periods used in the procedures to calculate suction profiles for each case at times required to make calculations for the post construction algorithms. Appendix A-107 is broken down into two basic steps. First, the times required for input are entered. Second, three time periods are calculated using the driest month of the year as the baseline. The time period used to calculate the suction profile under the slab at the time of construction is represented by the variable $t_{const/dry}$, as calculated in Appendix A-107. The time period between the time of construction and the time at which the soil volume change is sought is represented by the variable $t_{vc/const}$, as calculated in Appendix A-107. Finally, the variable $t_{vc/dry}$ describes the time transpired from the driest month of the year to the month the soil volume change is sought.

All soil suction profiles with respect to surface conditions, time and depth are calculated using the algorithms in Appendix A-109 and Appendix A-110. The process by which post construction soil suction profiles are generated consist of the following basic steps:

1. All values required to make calculations are retrieved for each particular moisture effect case and time the suction profile is sought, Appendix A-109.
2. Suction values, for each particular moisture effect case, are calculated for 5 centimeter thick incremental soil layers.
3. For every incremental soil layer cycle, variables are re-initialized and pertinent equations are activated based on: the location within the soil profile, the moisture effect case type, and the type and size of design effect implemented (If a horizontal barrier is implemented or if a moisture effect case is located a distance from the edge, Appendix A-104 will be used to augment the procedures described in Appendix A-110.)

Once all soil suction profiles are generated, the soil suction profile at the slab center is damped from time $t_{const}$ to time $t_{vc}$ by applying the algorithms described by Appendix A-111. This process takes the soil suction profile under the slab at the time of construction, $h_{slab}(z_i,t_{const/dry})$, and dampens it based on equations (59) and (61). These equations model the soil suction profile under the center of the slab at time $t_{const}$ so that the soil suction in each incremental soil layer approaches the equilibrium suction profile. The rate of approach depends on unsaturated soil profile properties, surface weather conditions, and time. The process in Appendix A-111 is broken down into two basic steps. First, all required variables are retrieved. Second, the dampened suction value for every incremental soil layer is calculated for the time transpired from the time of construction to the time the soil volume change is sought.

*Vertical Differential Soil Movement*

Once all soil suction profiles are calculated, the expansive volume strain theory developed by Lytton is applied. All moisture effect cases are applied to the same vertical differential soil movement algorithms which are broken down into a four step process.

First, all variables and quantities required for calculations are retrieved, as described in Appendix A-113, depending on which moisture effect case and design effect scenario is chosen. Second, vertical differential soil movement is calculated for soil at the edge of the foundation by way of steps described in Appendix A-114. Third, vertical differential soil movement is calculated for soil under the center of the foundation by way of steps described in Appendix A-115. Finally, the two quantities of vertical differential soil movement are summed together to arrive at the total differential soil movement for the soil under the slab at a specified time after construction, as described in Appendix A-115.

Appendix B-128 is a program design layout sheet that illustrates the results of the post construction procedures when applied to calculate the worst case center lift mode for case "1-6". The moisture effect case considered in Appendix B-128 is grass at the surface with a 4 ft vertical barrier, case "1-6". The vertical soil movement calculated at the edge moisture variation distance under the slab is $\Delta z_{slab}$ = -0.13 inches (shrink). The vertical soil movement calculated at the edge of the slab is $\Delta z_{edge}$ = -0.61 inches. The total vertical differential soil movement for this moisture effect case using Table 2 as the soil profile is $\Delta z_{total}$ = 0.48 inches (shrink). This quantity, $\Delta z_{total}$ , is the difference between the values of $\Delta z_{slab}$ and $\Delta z_{edge}$.

## MEASURED SUCTION PROFILES

When cases exist that can not be modeled by one of the moisture effect cases discussed in the previous procedures, vertical differential soil movement can be calculated by the measured suction profile method. This is a method to solve for the differential soil movement by measuring the initial and final suction profiles and applying those profiles to the volume strain theory developed by Lytton. The procedures are broken down into three broad steps: (1) The measured suction values for a sample are entered and stored for later use, Appendix A-87. (2) The entered measured suction values for a sample are converted into a measured suction profile, Appendix A-101. (3) The measured suction profiles are used to solve for vertical differential soil movement for a specific column of soil, Appendix A-105 and Appendix A-106.

The first step to applying this methodology is to input measured suction values for a sample of soil. There are a number of methods to measure the matrix suction in a soil sample. One of the more accurate means for measuring total soil suction is the thermocouple psychrometer. The thermocouple psychrometer sensor and data logging equipment is not inexpensive and requires some expertise and maintenance to operate. For these reasons the filter paper is becoming a more widely accepted method in practice. The filter paper is inexpensive, requires practically no maintenance, and requires very little expertise to obtain results nearly as accurate as the thermocouple psychrometer (McKeen 1981).

The process of inputting measured suction values occurs as part of the process to input moisture effect cases. Appendix B-121 is a program design layout sheet that illustrates the choices for the moisture effect case input. The program user would select "12. Measured Suction Profile" and the next screen that appears is illustrated by Appendix B-122. Appendix B-122 and 123 are a program design layout sheets that illustrate windows environment screens for inputting the measured suction profiles. Appendix A-87 is the process flow describing measured suction profile input. It is important to note that a surface suction value must be entered or a default value equal to the equilibrium suction

will be assumed.

Appendix A-101 is the process flow describing the steps to generate a measured suction profile based on the entered suction values. The procedures are broken down into two basic steps: (1) The slope of a line connecting adjacent suction values within a sample is calculated. (2) The measured suction profile is generated, using this previously calculated slope, by connecting a line to adjacent suction values in the sample. Table 3 is an example of values used to generate a measured suction profile. Fig. 33 is a graph of the initial and final measured suction profiles generated by the values listed in Table 3

**Table 3 Measured Suction Profile Values**

| Input Suction Values | | | | | | | |
|---|---|---|---|---|---|---|---|
| Initial | | | | Final | | | |
| (ft) Depth | (cm) Depth | (pF) Suction | (cm) Suction | (ft) Depth | (cm) Depth | (pF) Suction | (cm) Suction |
| 0 | 0 | 4.5 | 31622.78 | 0 | 0 | 2.5 | 316.2278 |
| 3 | 91.44 | 4.3 | 19952.62 | 3 | 91.44 | 3 | 1000 |
| 12 | 365.76 | 4 | 10000 | 12 | 365.76 | 3.3 | 1995.262 |
| 16 | 487.68 | 3.7 | 5011.872 | 16 | 487.68 | 3.5 | 3162.278 |
| 20 | 609.6 | 3.57 | 3715.352 | 20 | 609.6 | 3.57 | 3715.352 |

| | Slope | |
|---|---|---|
| | Initial | Final |
| (ft) Depth | | |
| 0 | -0.00219 | 0.005468 |
| 3 | -0.00109 | 0.001094 |
| 12 | -0.00246 | 0.00164 |
| 16 | -0.00107 | 0.000574 |
| 20 | | |

| Given Values | |
|---|---|
| $z_m$ = | 20 ft |
| $h_m$ = | 3.57 pF |
| $\sigma_i$ = | 40 cm |
| $K_{o\,(dry)}$ = | 0.33 |
| $K_{o\,(wet)}$ = | 0.67 |
| $f_{(dry)}$ = | 0.5 |
| $f_{(wet)}$ = | 0.8 |

Applying the measured suction profiles to predict vertical differential soil movement is probably the simplest of all procedures contained herein. The procedures are broken down into two basic steps: (1) select an initial and final suction profile to accurately model the moisture change scenario being considered, Appendix A-105, and (2)

apply the algorithms to calculate vertical differential soil movement based on these measured suction profiles, Appendix A-106.

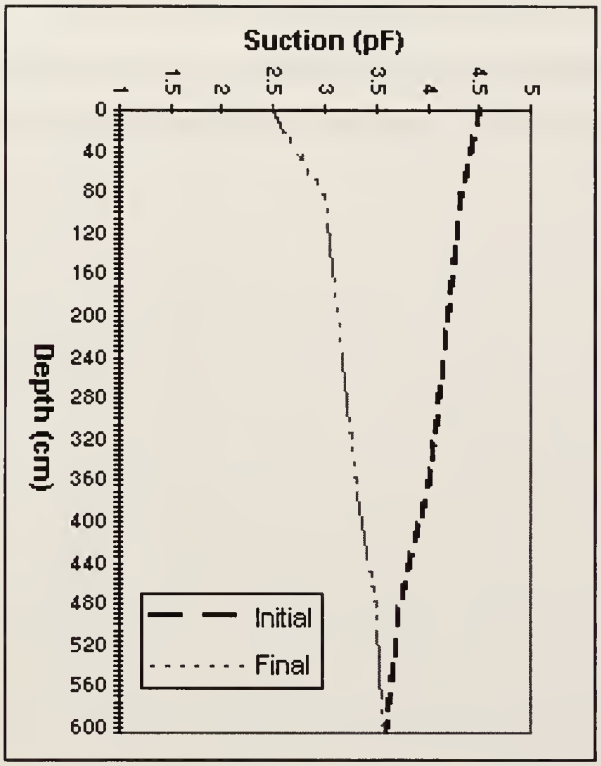


**Fig. 33. Initial and Final Measured Suction Profiles Described in Table 4**

The challenge is in deciding what suction profiles are used as the initial and final suction profile to accurately model the soil conditions which produce reasonable limit conditions used for design. The answer should come from knowledge about history of the site, to include: surface drainage conditions, soil characteristics in the soil profile, surface weather conditions, and type of structure placed. For example, consider the construction site described by the following: the site is located in College Station, the site is surface drained, the soil profile is described by Table 1, and the measured suction profile is located where a large oak tree was removed as a result of pre-construction clearing. The measured suction profile at this location is a dry profile. This profile will tend toward equilibrium and may approach the wet limit state subsequent to a wet season. A conservative approach

for calculating vertical differential soil movement is to set the initial suction profile equal to the measured suction profile and set the final suction profile equal to the wet limit state for the surface conditions that exist after the construction project is complete. This scenario produces heave values of vertical differential soil movement. Table 3 and Fig. 33 are values used to obtain results for vertical differential soil movement in the example described above. The vertical differential soil movement in this case is 5.48 inches of heave.

## DISCUSSION OF RESULTS

The procedures to predict vertical differential soil movement were developed based on the breakthroughs mentioned earlier. These procedures consider moisture effect cases that are common with light commercial and residential structures, such as: (1) bare soil at the surface, (2) grass at the surface, (3) tree at the surface, and (4) flower bed at the surface. Additionally, these procedures include calculating the effects of differential soil movement caused by the introduction of design effects, such as, vertical barriers and horizontal barriers. The methodology to handle these moisture effect cases and design effects are quite delineated in detail in the process flow of detailed algorithms, Appendix A. A graphical representation of the program design layout is illustrated in Appendix B.

The algorithms in Appendix A were programmed in a spreadsheet software package. The author used this package to analyze the moisture effect cases illustrated in Appendix C which consists of the soil profile described in Table 1. Table 4 is a summary of vertical differential soil movements for the site described by Appendix C. This summary illustrates the worst cases of edge lift and center lift distortion modes for all moisture effect cases. Post equilibrium and post construction approaches were used to solve for all cases so that the worst possible case of vertical differential soil movement is identified. Additional analyses were performed using different sizes of vertical and horizontal barriers to define the effects that these design features have on soil movement. An engineer may use the maximum cases of edge lift and center lift caused by the combination of moisture effect cases and the desired design effects to design an adequate foundation.

Table 4 is set up in chronological order beginning with the post construction differential soil movements and concluding with the post equilibrium soil movements.

The post construction numbers in Table 4 were generated for June as the driest month of the year and for a slab built in January (the wettest month of the year). The slab is placed on "wet" soil and this soil is allowed to approach an equilibrium moisture content based on the soil characteristics and the post construction theory described earlier. The soil

at the edge of the slab continues to fluctuate with the seasonal weather changes. Applying this post construction scenario to the "1-7 Tree" case produces the maximum differential soil movement compared to all other cases which cause a center lift distortion mode. The differential soil movement in this case is 4.32 inches and occurs the first August after construction. Note that a reduction to 2.44 inches of differential soil movement is made possible by introducing a four foot vertical barrier at the edge of the slab where the tree is located.

**Table 4. Summary of Vertical Differential Soil Movements for Appendix C**

## Post Construction

| | |
|---|---|
| **Driest Month of the year.....** | **June** |
| **Month of Construction.....** | **January** |

### Worst Case Center Lift Distortion Mode

| Moisture Effect Case/Design Scenario | Differential Soil Movement (units in inches) | Number of Months after Const. Worst Case Occurs |
|---|---|---|
| 1-4 Grass | **2.34** | **6** |
| 1-5 Grass with 4 ft Horizontal Barrier | **1.19** | **6** |
| 1-6 Grass with 4 ft Vertical Barrier | **0.48** | **7** |
| 1-7 Tree | **4.32** | **7** |
| 1-8 Tree with 4 ft Vertical Barrier | **2.44** | **7** |
| 1-9 Flower Bed | **3.30** | **6** |

### Worst Case Edge Lift Distortion Mode

| Moisture Effect Case/Design Scenario | Differential Soil Movement (units in inches) | Number of Months after Const. Worst Case Occurs |
|---|---|---|
| 1-4 Grass | **0.43** | **11** |
| 1-5 Grass with 4 ft Horizontal Barrier | **0.31** | **11** |
| 1-6 Grass with 4 ft Vertical Barrier | **0.23** | **14** |
| 1-7 Tree | **0.43** | **11** |
| 1-8 Tree with 4 ft Vertical Barrier | **0.23** | **14** |
| 1-9 Flower Bed | **0.92** | **12** |
| 1-11 Flower Bed with 4 ft Vertical Barrier | **0.20** | **12** |

Table 4. Continued

## Post Equilibrium

### Worst Case Differential Soil Movement

| Moisture Effect Case/Design Scenario | Edge Heave (in) | Edge Shrink (in) |
|---|---|---|
| 1-4 Grass | **1.65** | **1.03** |
| 1-5 Grass with 4 ft Horizontal Barrier | **0.47** | **0.56** |
| 1-6 Grass with 4 ft Vertical Barrier | **0.07** | **0.09** |
| 1-7 Tree | **1.64** | **3.67** |
| 1-8 Tree with 4 ft Vertical Barrier | **0.07** | **2.36** |
| 1-9 Flower Bed | **2.89** | **1.86** |
| 1-11 Flower Bed with 4 ft Vertical Barrier | **0.68** | **0.55** |
| 1-12 Measured Suction Profile (Point Water Source) | **4.40** | **NA** |
| 2-12 Measured Suction Profile (Point Water Source) | **4.40** | **NA** |
| 3-12 Measured Suction Profile (Tree Removal) | **1.62** | **NA** |

An inspection of Table 4 shows that the differential soil movement is greatest when there are no vertical or horizontal barriers in place. In the "1-4 Grass" case, the edge heave is 1.65 inches and edge shrink is 1.03 inches. When a four foot horizontal barrier is added the edge heave is reduced to 0.47 inches and the edge shrink is reduced to 0.56 inches, as described in the Table 4 case "1-5 Grass with 4 ft Horizontal Barrier". A further reduction in soil movement is obtained by adding a four foot vertical barrier as shown in Table 4 case "1-6 Grass with 4 ft Vertical Barrier". This latter case reduces the edge heave to 0.07 inches and the edge shrink to 0.09 inches.

As shown in Table 4, the worst case edge heave occurs in the post equilibrium case of the measured suction profiles produced at the locations of the leaking pipes. The leaking pipes produced a "wet" spot that caused the soil to heave 4.40 inches at those two locations. This type of heave at the edge caused the worst case edge lift distortion mode. Refer to Appendix B-130 for a conceptual illustration of the post construction case of vertical differential soil movement that can be predicted by applying the procedures contained herein. These procedures for analyzing vertical differential soil movements should be applied to a soil profile to enable an engineer to maximize resources ensuring that the best foundation is designed.

## SUMMARY AND SUGGESTIONS FOR RESEARCH AND DEVELOPMENT

The theory to predict differential soil movement of expansive soils has evolved since the 1970's. The engineering profession is at a juncture today in which engineers have the technology to apply this information to maximize resources and produce high performing ground structures. The evolution of this theory began in the early 1970's with the advent of the volume strain theory for expansive soils which was developed by Lytton (1973). In the decade of the 1970's, great strides were made by Pearring (1968), Holt (1969), and Mojekwu (1979) to enable engineers to identify predominant clays. In 1981, McKeen used these newfound procedures to identify predominant clays and developed a correlation to link groups of clays to suction compression indices. The suction compression index is used in the soil volume strain equations developed by Lytton to predict vertical differential soil movement for particular types of expansive soils. In the 1980's, although the volume strain theory was well based, its application was limited by the lack of knowledge and methodology to predict the equilibrium suction and soil suction profiles for a particular soil profile and location. This is when work by Mitchell and later Gay opened the door for major advancements in this area of expansive soils. In 1980, Mitchell developed and applied simple mathematical methods for predicting soil suction profiles. Then in 1994, Gay developed a way to predict the mean volumetric water content for soils dependent upon the location and climatic conditions. Jayatilaka, Gay, Lytton, and Wray (1992) then developed and calibrated to field data a finite element method for determining the edge moisture variation distance. They also devised methods to predict a number of unsaturated soil properties using simple index properties.

Based on the wealth of information and breakthroughs in the areas of expansive soils listed above, Lytton and the author made five critical advancements necessary to effectively and easily apply this theory:

1. The means to calculate the equilibrium suction for a particular soil profile and location.
2. The means to calculate depth to constant suction for a soil profile with multiple layers.
3. The equation to calculate horizontal velocity of water flow in unsaturated soils.

4. A method to consider the transient case for calculating vertical differential soil movement for expansive soils immediately after construction and before the soil under the center of the slab has reached an equilibrium moisture content.
5. Procedures to apply all of the theory discussed herein to predict differential soil movement for expansive soils considering all of the moisture effect cases and design effects that have been mentioned.

The theory discussed herein represents physical behavioral characteristics of expansive and unsaturated soils and is well documented. Those contributing to this vertical differential soil movement theory have approached the problem with a theoretically sound yet practical mindset. Additionally, this expansive soil theory has been developed in a way to enable practicing engineers to run simple, common and economical geotechnical engineering lab tests to adequately define all necessary soils profile information. This soil profile information is applied in the vertical differential soil movement theory and should be used to make sound geotechnical engineering designs.

Further development needs to be made in the areas of enhancements to the present programs, materials characterization testing, in situ testing, and foundation structural analysis models for stiffened plates and drilled shafts in expansive soils. The program enhancements should include the choice to use the Gardner, as well as the Mitchell, unsaturated permeability options. Materials characterization testing developments that are needed are more convenient methods of measuring the volume change, diffusion, and soil-water characteristics of expansive soils directly. In situ testing developments that are needed include methods of measuring suction profiles on site and preferably down hole; lateral earth pressure coefficient; and of detecting the presence of roots and voids, either air-filled or water-conducting; in the field and non-destructively. Stiffened plate models which incorporate non-rectangular geometry need to be coupled with this program or its enhancements to determine design quantities of moment, shear, and deflection. Drilled shaft models with interface elements need to be coupled with the enhanced program to determine the design quantities for both shrinking and expanding soils.

## REFERENCES

Castleberry, J. P. II, (1974). "An engineering geology analysis of home foundations on expansive clays." M.S thesis, Dept.of Geology, Texas A&M University, College Station.

Gardner, W. R., (1958). "Some steady state solutions of the unsaturated moisture flow equation with application to evaporation from a water table." *Soil Science,* 85(4), 223-232.

Gay, D. A., (1994). "Development of a predictive model for pavement roughness on expansive clay." PhD dissertation, Dept. of Civ. Engrg., Texas A&M University, College Station.

Geostructural Tool Kit, Inc., (1996). *PTISLAB WIN 1.0.* Geostructural Tool Kit, Inc., Austin.

Holland, J. E. and Lawrance, C. E. (1980). "Seasonal heave of Australian clay soils." *Proc., Fifth Int.Conf. on Expansive Soils.* ASCE, Denver, 302-321.

Holt, J. H., (1969). "A study of physico-chemical, mineralogical, and engineering index properties of fine-grained soils in relation to their expansive characteristics." PhD dissertation, Dept. of Civ. Engrg., Texas A&M University, College Station, Texas.

Jayatilaka, R., Gay, D. A., Lytton, R. L., and Wray, W. K. (1992). "Effectiveness of controlling pavement roughness due to expansive clays with vertical moisture barriers." *Research Report No. 1165-2F*, Texas Transportation Institute, College Station.

Jones, D. E. and Holtz, W. G. (1973). "Expansive soils - the hidden disaster", *Civil Engineering*, ASCE, August, 49-51.

Juarez-Badillo, E. (1975). "Constitutive relationships for soils." *Proc., Symposium on Recent Developments in the Analysis of Soil Behavior and their Applications to Geotechnical Structures*, The University of New South Wales, Kensington, N.S.W., Australia, 231-257.

Lambe, T. W. and Whitman, R. V. (1969). *Soil mechanics.* John Wiley & Sons, New

York, New York.

Lytton, R. L. and Woodburn, J. A., (1973). "Design and performance of mat foundations on expansive clay." *Proc., Third Int. Conf. on Expansive Soils.* American Society of Civil Engineers, Haifa, Israel, 301-307.

Lytton, R. L., (1977). "The characterization of expansive soils in engineering." *Presentation at the Symposium on Water Movement and Equilibrium in Swelling Soils,* American Geophysical Union, San Francisco.

Lytton, R. L., Pufahl, D. E., Michalak, C. H., Liang, H. S., and Dempsey, B. J., (1989). "An integrated model of the climatic effects on pavements." *Rep. FHWA-RD-90-033 to Federal Highway Admin.,* Civ. Engrg., Texas A&M Univ., College Station.

Lytton, R. L., (1994). "Prediction of movement in expansive clays." *Geotechnical Special Publication No. 40*, Yeung, A.T., and Felio, G.Y., eds., ASCE, New York, Vol. 2, 1827-1845.

Lytton, R. L., (1995). "Foundations and pavements on unsaturated soils." *Proc., First Int. Conf. on Unsaturated Soils,* E.E. Alonso and P. Delage, eds., Vol. 3, 1201-1220.

Lytton, R. L., (1997). "Engineering structures in expansive soils." *Proc., Third Brazilian Symposium on Unsaturated Soils,* De Campos, T.M.P., and Vargas, E.A. Jr., eds., Rio De Janeiro, Brazil, Vol. 2, 550-562.

Mathewson, C. C., Castleberry, J. P. II, and Lytton, R.L., (1975). "Analysis and modeling of the performance of home foundations on expansive soils in central Texas." *Bulletin of the Association of Engineering Geologists,* Vol. 12, No. 4, 275-302.

Mathewson, C. C., Dobson, B. M., Dyke, L. D., and Lytton, R. L., (1980). "System interaction of expansive soils with light foundations." *Bulletin of the Association of Engineering Geologists,* Vol. 17, No. 2, 55-94.

McKeen, R. G. (1981). "Design of airport pavements on expansive soils." U.S. Department of Transportation, Federal Aviation Administration, Washington D.C.

McQueen, I. S. and Miller, R. F., (1968). "Calibration and evaluation of a wide-range gravimetric method for measuring moisture stress." *Soil Science*, Vol. 106, No. 3,

225-231.

Mitchell, P. W. (1980). *The structural analysis of footings on expansive soil 2nd edition*, K.W.G. Smith and Associates, Newton, South Australia.

Mojekwu, E. C. (1979). "A simplified method for identifying the predominant clay mineral in soil." M.S thesis, Dept. of Civ. Engrg., Texas Tech University, Lubbock.

Nieber, J. L., (1981). "Simulation of infiltration into cracked soils." Presented at the 1981 Summer Meeting, American Society of Agricultural Engineers, Orlando.

Pearring, J. R, (1968). "A study of basic mineralogical, physical-chemical, and engineering index properties of laterite soils." PhD dissertation, Dept. of Civ. Engrg., Texas A&M University, College Station.

Post-Tensioning Institute, (1980). *Design and construction of post-tensioned slabs-on-ground, 1st edition.* Post Tensioning Institute, Phoenix.

Post-Tensioning Institute, (1996). *Design and construction of post-tensioned slabs-on-ground, 2nd edition.* Post Tensioning Institute, Phoenix.

Skempton, A. W., (1955). "The colloidal activity of clays." *Proc., Third Int. Conf. On Soil Mechanics and Foundation Engineering,* Vol. 1, Switzerland, 57.

Spotts, J. W., (1974). "The role of water in gilgai formation." PhD dissertation, Texas A&M University, College Station.

Thornthwaite, C. W., (1948). "An approach toward a rational classification of climate." *The Geographical Review 38*, 55-94.

Viayvergiya, V. N., and Ghazzaly, O. I., (1973). "Prediction of swelling potential for natural clays." *Proc., Third Int. Conf. on Expansive Soils,* Haifa, Israel, Vol. 1, 227-236.

Wiggins, J. H., (1976). "Natural hazards, an unexpected building loss assessment." *Technical Report No. 1246*, J. H. Wiggins Co., Redondo Beach, California.

Wray, W. K. (1978). "Development of a design procedure for residential and light commercial slabs-on-ground constructed on expansive clays." PhD dissertation, Texas A&M University, College Station.

# APPENDIX A

## PROCEDURES TO CALCULATE VERTICAL DIFFERENTIAL SOIL MOVEMENT

# Start of Program and Project Input

© by Donald Naiser, Jr. 5 Aug 97

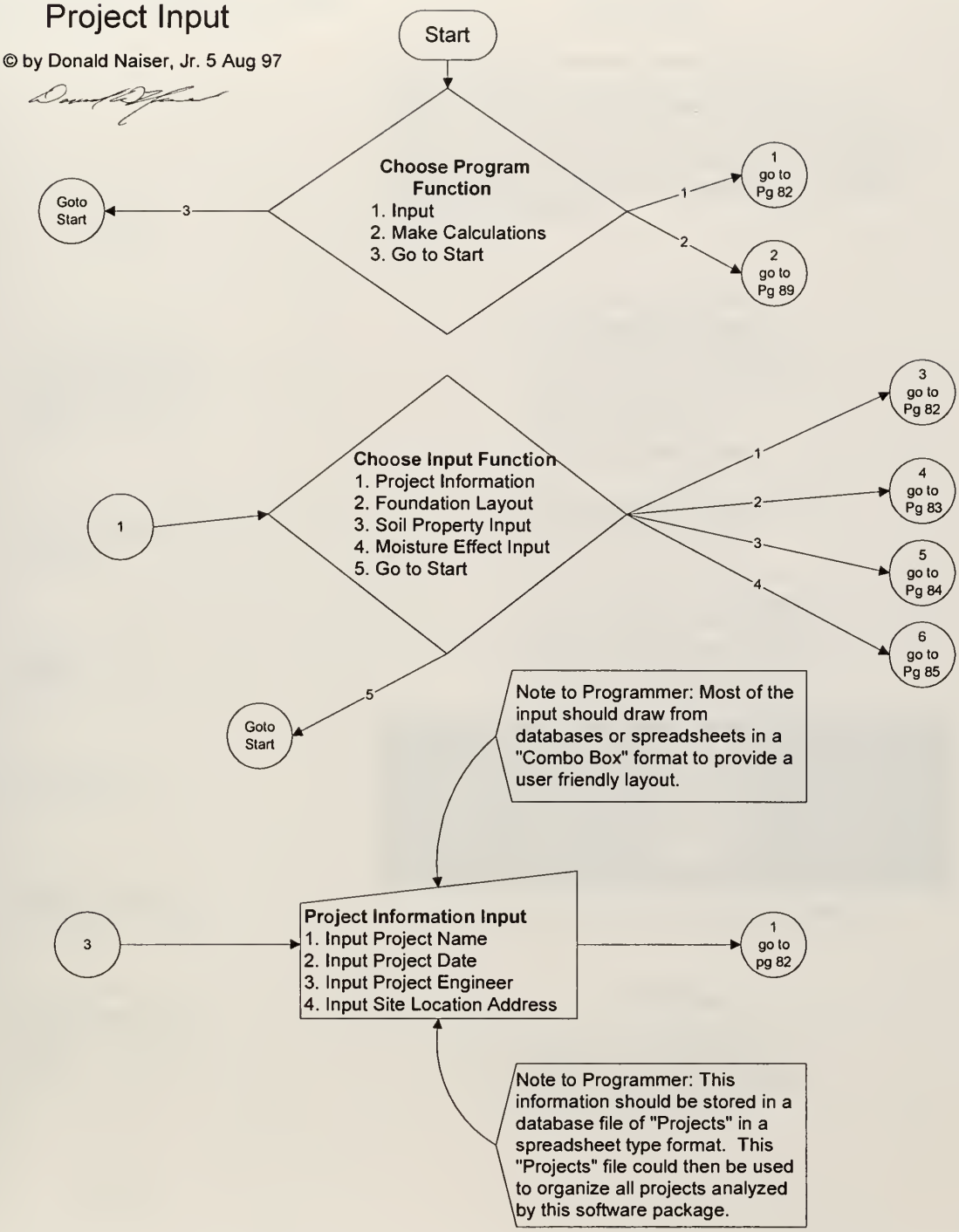
Start
Choose Program Function
1. Input
2. Make Calculations
3. Go to Start
Goto Start
3
1
1 go to Pg 82
2
2 go to Pg 89
1
Choose Input Function
1. Project Information
2. Foundation Layout
3. Soil Property Input
4. Moisture Effect Input
5. Go to Start
1
2
3
4
5
3 go to Pg 82
4 go to Pg 83
5 go to Pg 84
6 go to Pg 85
Goto Start
Note to Programmer: Most of the input should draw from databases or spreadsheets in a "Combo Box" format to provide a user friendly layout.
3
Project Information Input
1. Input Project Name
2. Input Project Date
3. Input Project Engineer
4. Input Site Location Address
1 go to pg 82
Note to Programmer: This information should be stored in a database file of "Projects" in a spreadsheet type format. This "Projects" file could then be used to organize all projects analyzed by this software package.

# Foundation Layout Input

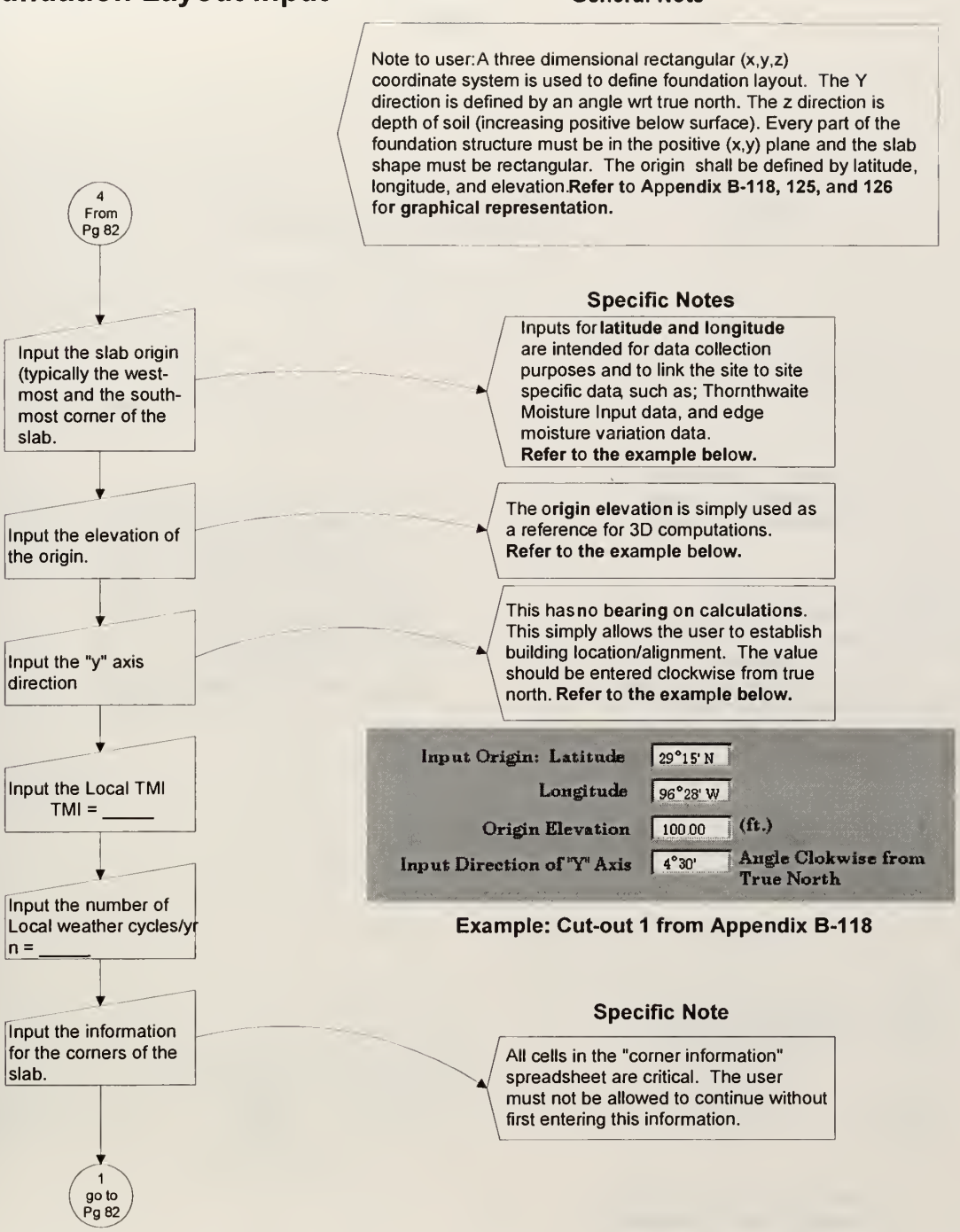
General Note
Note to user:A three dimensional rectangular (x,y,z) coordinate system is used to define foundation layout. The Y direction is defined by an angle wrt true north. The z direction is depth of soil (increasing positive below surface). Every part of the foundation structure must be in the positive (x,y) plane and the slab shape must be rectangular. The origin shall be defined by latitude, longitude, and elevation.Refer to Appendix B-118, 125, and 126 for graphical representation.
4 From Pg 82
Input the slab origin (typically the west-most and the south-most corner of the slab.
Specific Notes
Inputs for latitude and longitude are intended for data collection purposes and to link the site to site specific data, such as; Thornthwaite Moisture Input data, and edge moisture variation data. Refer to the example below.
Input the elevation of the origin.
The origin elevation is simply used as a reference for 3D computations. Refer to the example below.
Input the "y" axis direction
This has no bearing on calculations. This simply allows the user to establish building location/alignment. The value should be entered clockwise from true north. Refer to the example below.
Input the Local TMI
TMI = _____
Input the number of Local weather cycles/yr
n = _____
Input the information for the corners of the slab.
Specific Note
All cells in the "corner information" spreadsheet are critical. The user must not be allowed to continue without first entering this information.
1 go to Pg 82

Input Origin: Latitude 29°15' N
Longitude 96°28' W
Origin Elevation 100.00 (ft.)
Input Direction of "Y" Axis 4°30' Angle Clokwise from True North

**Example: Cut-out 1 from Appendix B-118**

# Soil Layer Property Input

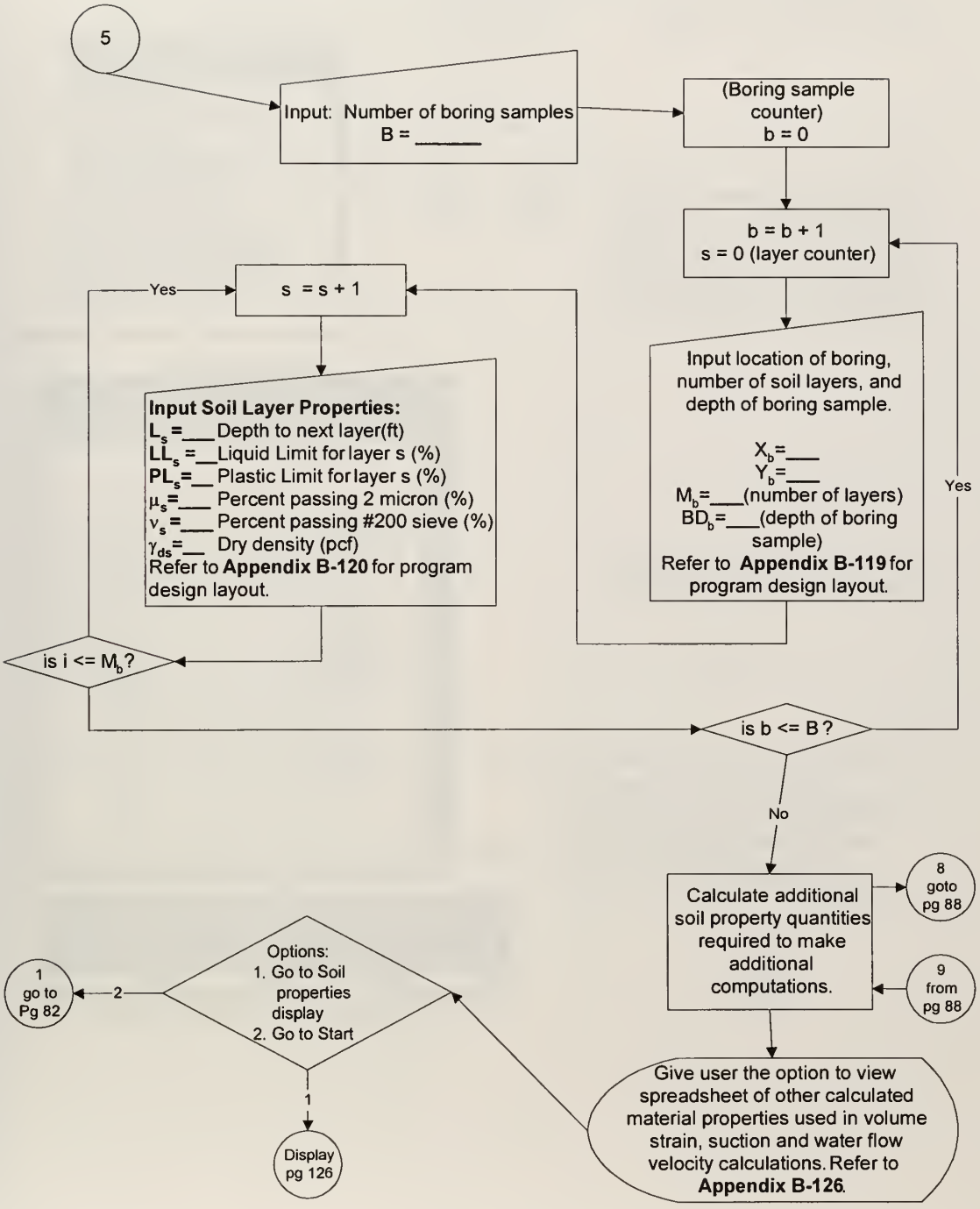
5
Input: Number of boring samples
B = _____
(Boring sample counter)
b = 0
b = b + 1
s = 0 (layer counter)
Yes
s = s + 1
Input location of boring, number of soil layers, and depth of boring sample.
$X_b$=___
$Y_b$=___
$M_b$=___(number of layers)
$BD_b$=___(depth of boring sample)
Refer to Appendix B-119 for program design layout.
Input Soil Layer Properties:
$L_s$=___Depth to next layer(ft)
$LL_s$ =__Liquid Limit for layer s (%)
$PL_s$=__ Plastic Limit for layer s (%)
$\mu_s$=___ Percent passing 2 micron (%)
$\nu_s$=___ Percent passing #200 sieve (%)
$\gamma_{ds}$=__ Dry density (pcf)
Refer to Appendix B-120 for program design layout.
Yes
is i <= $M_b$?
is b <= B?
No
Calculate additional soil property quantities required to make additional computations.
8 goto pg 88
9 from pg 88
Options:
1. Go to Soil properties display
2. Go to Start
2
1 go to Pg 82
1
Display pg 126
Give user the option to view spreadsheet of other calculated material properties used in volume strain, suction and water flow velocity calculations. Refer to Appendix B-126.

# Moisture Effect Input

6

Select Moisture Case: Refer to Cut-out 2 below for possible selections, or return to start.

As the Moisture Effect Case types are selected a database spreadsheet row is generated and a counter is initiated for each case.

Example

For example, the first "flowerbed" moisture effect case selected would be given the "case number" name (1-6) [and the second would be (2-6) and so on]. A row would be established to contain all pertinent cells of information required for computations made by this software package for that particular case. Refer to cut-out 7 on the next page.

12 → 10 go to pg 87

start → Start go to pg 82

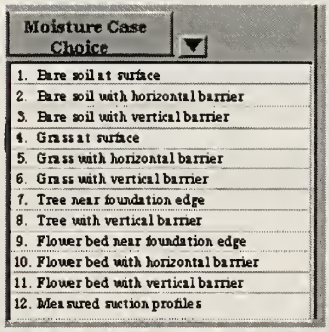
Moisture Case Choice
1. Bare soil at surface
2. Bare soil with horizontal barrier
3. Bare soil with vertical barrier
4. Grass at surface
5. Grass with horizontal barrier
6. Grass with vertical barrier
7. Tree near foundation edge
8. Tree with vertical barrier
9. Flower bed near foundation edge
10. Flower bed with horizontal barrier
11. Flower bed with vertical barrier
12. Measured suction profiles

**Example: Cut-out 2 from Appendix B-121**

Program Design Layout

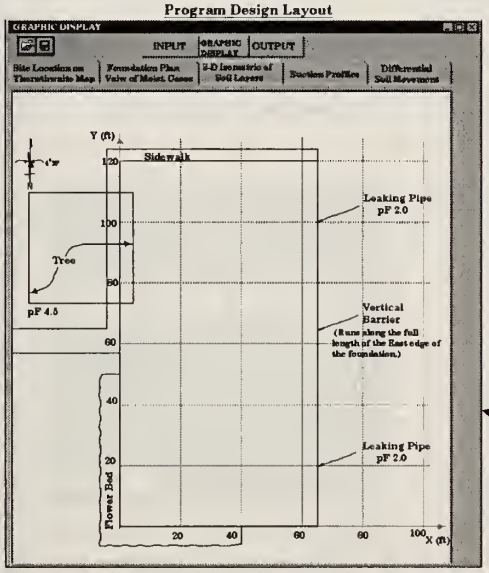


**Example: Cut-out 3 from Appendix B-125**

Prompt user to input a "start" and "end" location for all moisture effect cases.

Example

For example, the "start" and "end" points for the flower bed are (40,0) and (0,50) respectively. If the moisture effect is a point source then the two inputs will be the same. **Refer to the cut-out 3 and cut-out 4 for location of flowerbed on grid and example of coordinate inputs respectively.**

Example

Example

| Start Location of Effect | | End Location of Effect | |
|---|---|---|---|
| X Coord. | Y Coord. | X Coord. | Y Coord. |
| 40 | 0 | 0 | 50 |

**Example: Cut-out 4 from Appendix B-121**

7 go to pg 86

# Moisture Effect Input Continued

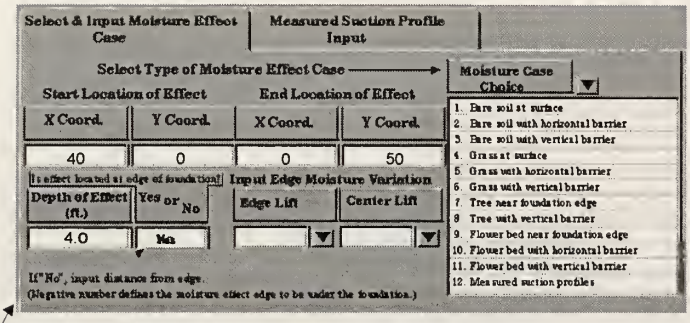
Select & Input Moisture Effect Case
Measured Suction Profile Input
Select Type of Moisture Effect Case
Moisture Case Choice
Start Location of Effect
End Location of Effect
X Coord.
Y Coord.
X Coord.
Y Coord.
40
0
0
50
Is effect located at edge of foundation?
Input Edge Moisture Variation
Depth of Effect (ft.)
Yes or No
Edge Lift
Center Lift
4.0
Yes
If "No", input distance from edge.
(Negative number defines the moisture effect edge to be under the foundation.)
1. Bare soil at surface
2. Bare soil with horizontal barrier
3. Bare soil with vertical barrier
4. Grass at surface
5. Grass with horizontal barrier
6. Grass with vertical barrier
7. Tree near foundation edge
8. Tree with vertical barrier
9. Flower bed near foundation edge
10. Flower bed with horizontal barrier
11. Flower bed with vertical barrier
12. Measured suction profiles

**Example: Cut-out 5 from Appendix B-121**

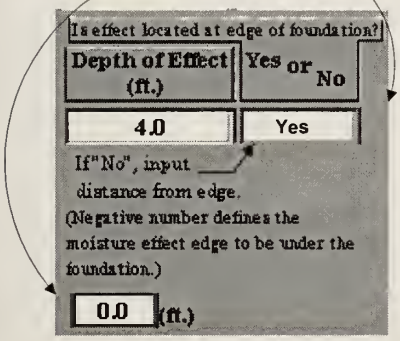
Is effect located at edge of foundation?
Depth of Effect (ft.)
Yes or No
4.0
Yes
If "No", input distance from edge.
(Negative number defines the moisture effect edge to be under the foundation.)
0.0
(ft.)

**Example: Cut-out 6 from Appendix B-121**

| Case # | Start X Coord | Start Y Coord | End X Coord | End Y Coord | Barrier Size (ft.) | Moist Effect Depth (ft.) | Edge Location |
|---|---|---|---|---|---|---|---|
| 1-5 | 0 | 56 | 65 | 120 | 4 | 0 | 0 |
| 1-7 | 0 | 75 | 0 | 110 | | 20 | -7.5 |
| 1-9 | 40 | 0 | 0 | 50 | | 4 | 0 |
| 1-6 | 65 | 120 | 65 | 0 | 4 | | 0 |
| 1-12 | 65 | 100 | | | | | |
| 2-12 | 65 | 20 | | | | | |
| 3-12 | 45 | 60 | | | | | |

**Example: Cut-out 7 from Appendix B-121**

7 from pg 85

Perform the following function for moisture effect cases 7 thru 11.

Prompt user to input the depth of the moisture effect zone.
$d_{zone}$ = ____

Example

For example, the depth of the flower bed in this case is 4 feet. Refer to cut-out 5 shown above.

Is the effect case at the edge of slab?

Example

Refer to cut-out 6 for example of edge location input for the flower bed.

No

Prompt user to enter location wrt slab. (-) number indicates the zone is under the slab, (+) number indicates the zone is away from the slab.
$d_{source}$ = ____

Yes

When yes is selected this indicates the effect is at the edge of the slab.

Does the location have a barrier?

No

Default size of barrier is zero.
$d_{vbar}$ = 0 (vertical)
$d_{hbar}$ = 0 (horizontal)

Yes

Input size of barrier.
$d_{vbar}$ = ____
$d_{hbar}$ = ____

Example/ Note

Provide the user opportunity to review spreadsheet of moisture effect input data. Refer to cut-out 7.

6 go to pg 85

# Measured Suction Profile Input

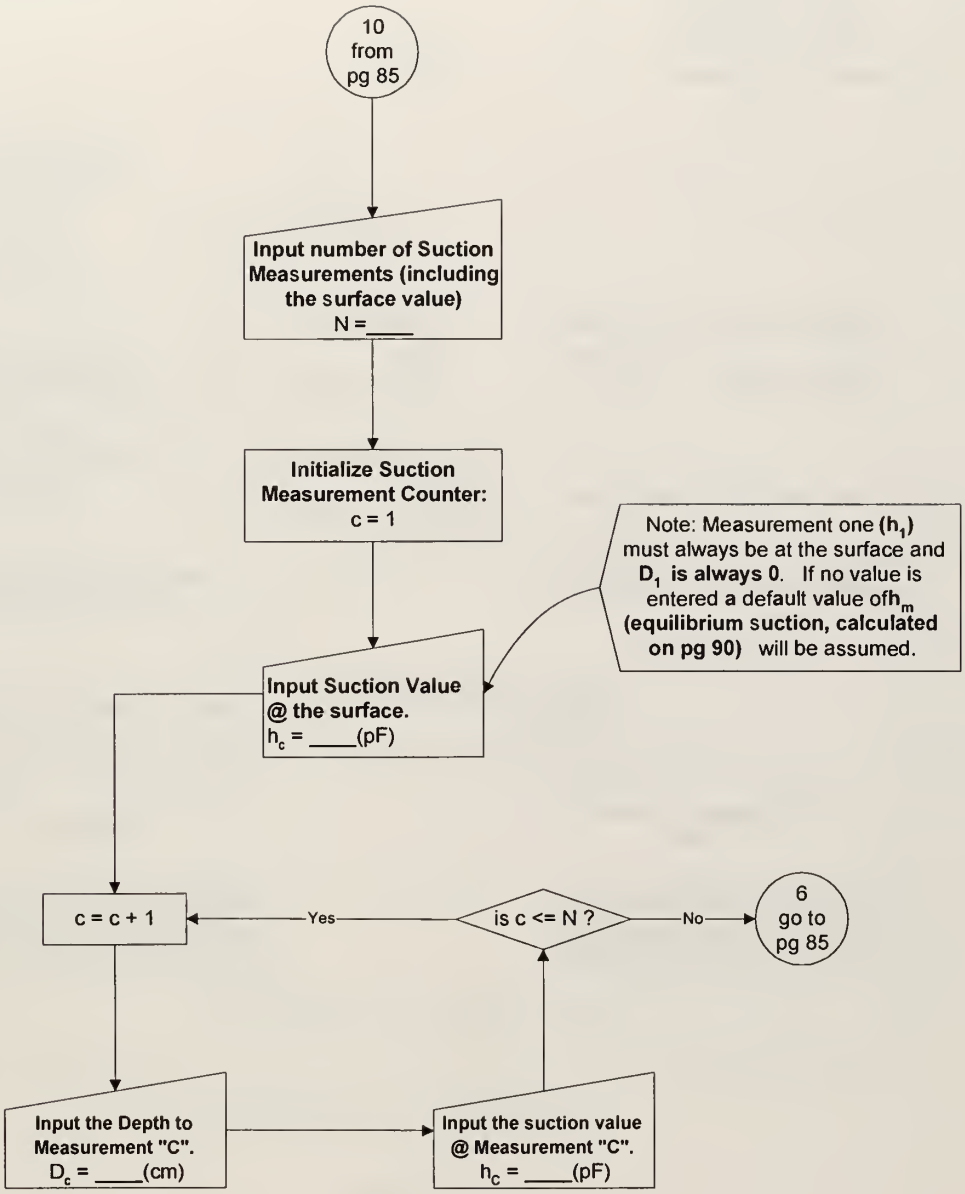
10 from pg 85
Input number of Suction Measurements (including the surface value) N = ____
Initialize Suction Measurement Counter: c = 1
Note: Measurement one ($h_1$) must always be at the surface and $D_1$ is always 0. If no value is entered a default value of $h_m$ (equilibrium suction, calculated on pg 90) will be assumed.
Input Suction Value @ the surface. $h_c$ = ____(pF)
c = c + 1
Yes
is c <= N ?
No
6 go to pg 85
Input the Depth to Measurement "C". $D_c$ = ____(cm)
Input the suction value @ Measurement "C". $h_c$ = ____(pF)

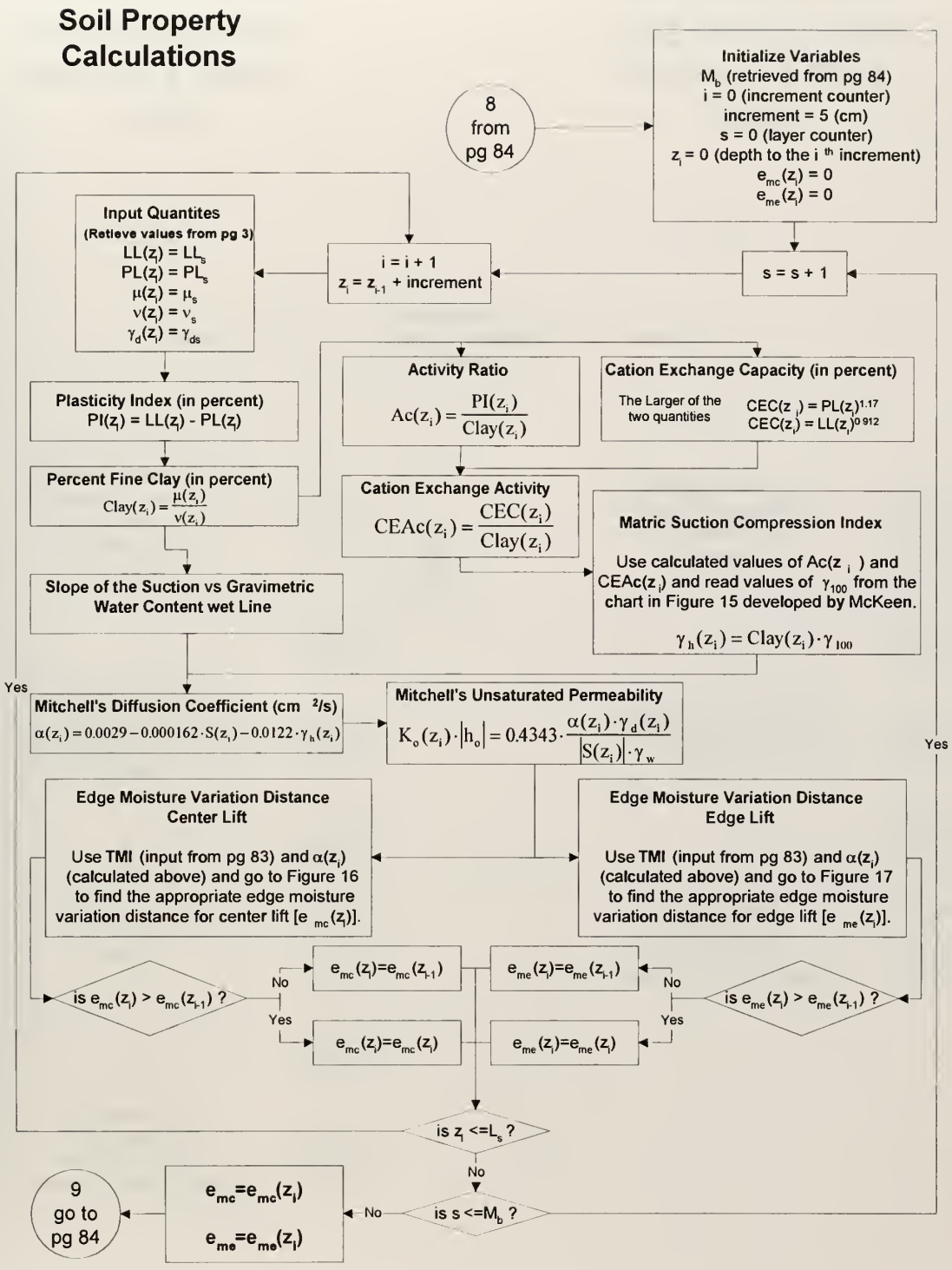
Soil Property Calculations
8 from pg 84
Initialize Variables
$M_b$ (retrieved from pg 84)
i = 0 (increment counter)
increment = 5 (cm)
s = 0 (layer counter)
$z_i$ = 0 (depth to the i th increment)
$e_{mc}(z_i)$ = 0
$e_{me}(z_i)$ = 0
s = s + 1
i = i + 1
$z_i = z_{i-1}$ + increment
Input Quantites
(Retieve values from pg 3)
$LL(z_i) = LL_s$
$PL(z_i) = PL_s$
$\mu(z_i) = \mu_s$
$\nu(z_i) = \nu_s$
$\gamma_d(z_i) = \gamma_{ds}$
Plasticity Index (in percent)
$PI(z_i) = LL(z_i) - PL(z_i)$
Percent Fine Clay (in percent)
$Clay(z_i) = \frac{\mu(z_i)}{\nu(z_i)}$
Slope of the Suction vs Gravimetric Water Content wet Line
Activity Ratio
$Ac(z_i) = \frac{PI(z_i)}{Clay(z_i)}$
Cation Exchange Capacity (in percent)
The Larger of the two quantities
$CEC(z_i) = PL(z_i)^{1.17}$
$CEC(z_i) = LL(z_i)^{0.912}$
Cation Exchange Activity
$CEAc(z_i) = \frac{CEC(z_i)}{Clay(z_i)}$
Matric Suction Compression Index
Use calculated values of $Ac(z_i)$ and $CEAc(z_i)$ and read values of $\gamma_{100}$ from the chart in Figure 15 developed by McKeen.
$\gamma_h(z_i) = Clay(z_i) \cdot \gamma_{100}$
Yes
Mitchell's Diffusion Coefficient ($cm^2/s$)
$\alpha(z_i) = 0.0029 - 0.000162 \cdot S(z_i) - 0.0122 \cdot \gamma_h(z_i)$
Mitchell's Unsaturated Permeability
$K_o(z_i) \cdot |h_o| = 0.4343 \cdot \frac{\alpha(z_i) \cdot \gamma_d(z_i)}{|S(z_i)| \cdot \gamma_w}$
Yes
Edge Moisture Variation Distance Center Lift
Use TMI (input from pg 83) and $\alpha(z_i)$ (calculated above) and go to Figure 16 to find the appropriate edge moisture variation distance for center lift [$e_{mc}(z_i)$].
Edge Moisture Variation Distance Edge Lift
Use TMI (input from pg 83) and $\alpha(z_i)$ (calculated above) and go to Figure 17 to find the appropriate edge moisture variation distance for edge lift [$e_{me}(z_i)$].
is $e_{mc}(z_i) > e_{mc}(z_{i-1})$ ?
No
Yes
$e_{mc}(z_i)=e_{mc}(z_{i-1})$
$e_{mc}(z_i)=e_{mc}(z_i)$
$e_{me}(z_i)=e_{me}(z_{i-1})$
$e_{me}(z_i)=e_{me}(z_i)$
No
Yes
is $e_{me}(z_i) > e_{me}(z_{i-1})$ ?
is $z_i <= L_s$ ?
No
is $s <= M_b$ ?
No
$e_{mc}=e_{mc}(z_i)$
$e_{me}=e_{me}(z_i)$
9 go to pg 84

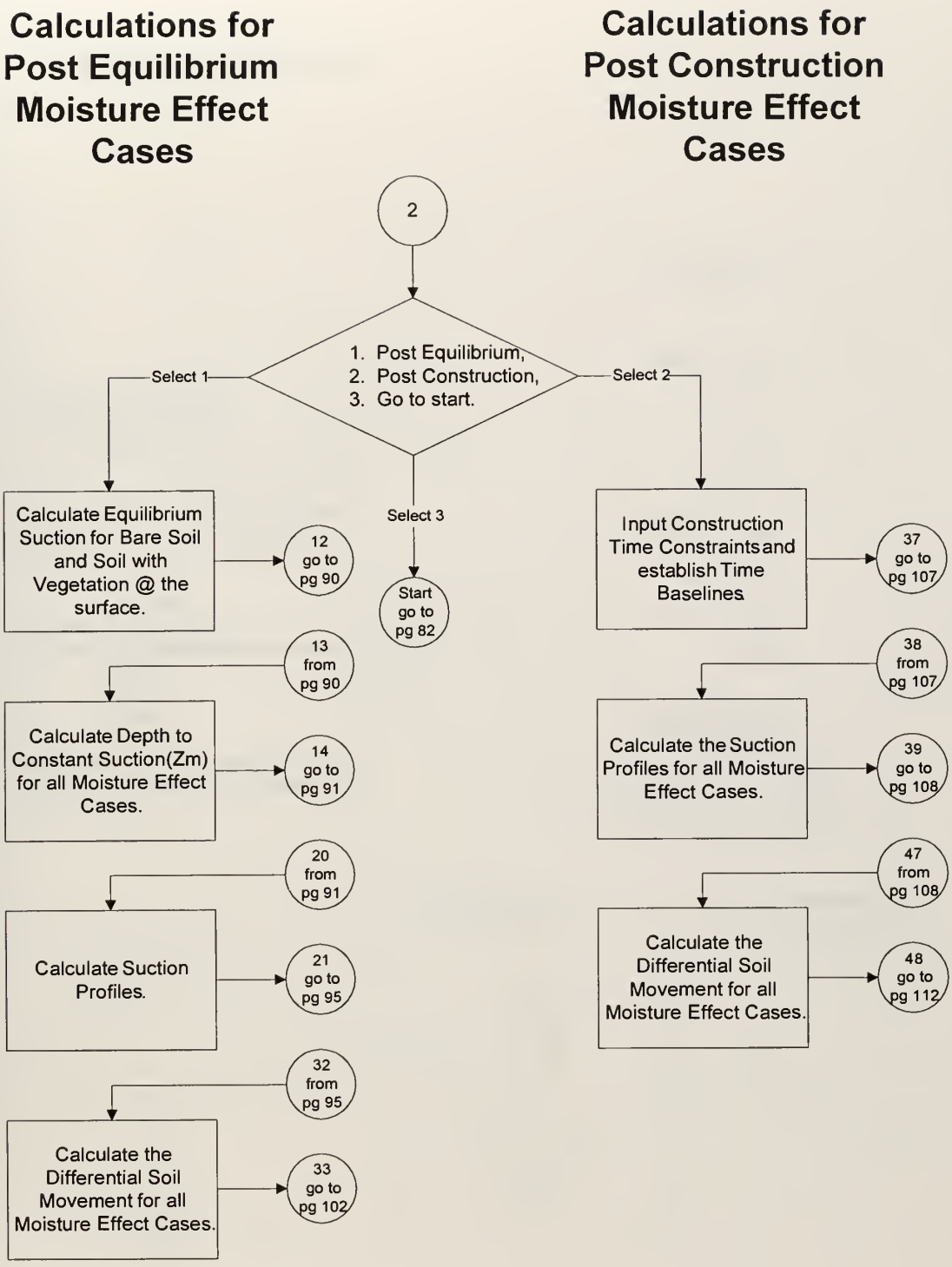
Calculations for Post Equilibrium Moisture Effect Cases
Calculations for Post Construction Moisture Effect Cases
2
1. Post Equilibrium,
2. Post Construction,
3. Go to start.
Select 1
Select 2
Select 3
Calculate Equilibrium Suction for Bare Soil and Soil with Vegetation @ the surface.
12 go to pg 90
Start go to pg 82
13 from pg 90
Calculate Depth to Constant Suction(Zm) for all Moisture Effect Cases.
14 go to pg 91
20 from pg 91
Calculate Suction Profiles.
21 go to pg 95
32 from pg 95
Calculate the Differential Soil Movement for all Moisture Effect Cases.
33 go to pg 102
Input Construction Time Constraints and establish Time Baselines
37 go to pg 107
38 from pg 107
Calculate the Suction Profiles for all Moisture Effect Cases.
39 go to pg 108
47 from pg 108
Calculate the Differential Soil Movement for all Moisture Effect Cases.
48 go to pg 112

# Equilibrium Suction $h_m$

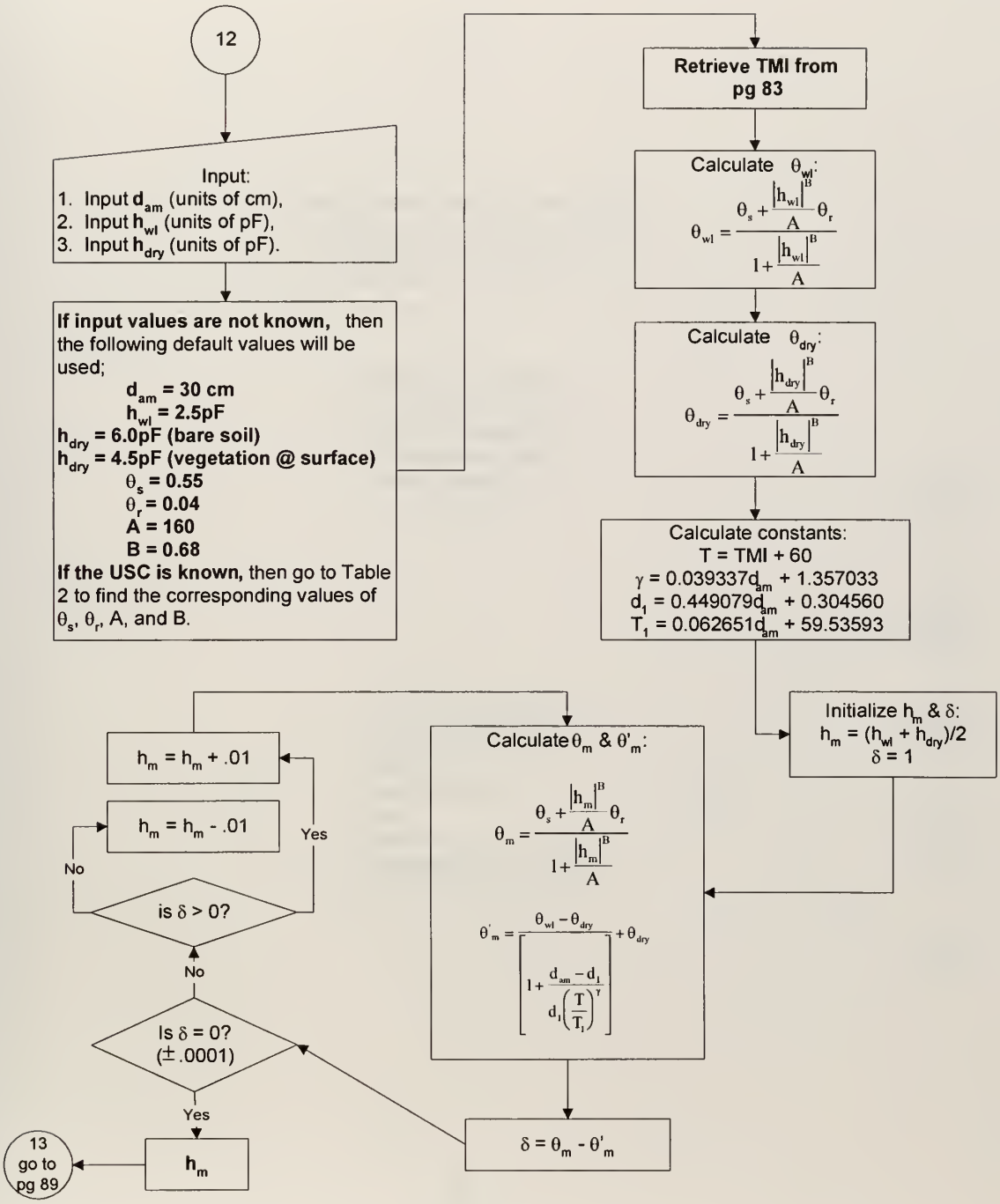
12
Input:
1. Input $d_{am}$ (units of cm),
2. Input $h_{wl}$ (units of pF),
3. Input $h_{dry}$ (units of pF).
If input values are not known, then the following default values will be used;
$d_{am}$ = 30 cm
$h_{wl}$ = 2.5pF
$h_{dry}$ = 6.0pF (bare soil)
$h_{dry}$ = 4.5pF (vegetation @ surface)
$\theta_s$ = 0.55
$\theta_r$ = 0.04
A = 160
B = 0.68
If the USC is known, then go to Table 2 to find the corresponding values of $\theta_s$, $\theta_r$, A, and B.
Retrieve TMI from pg 83
Calculate $\theta_{wl}$:
$\theta_{wl} = \frac{\theta_s + \frac{|h_{wl}|^B}{A}\theta_r}{1 + \frac{|h_{wl}|^B}{A}}$
Calculate $\theta_{dry}$:
$\theta_{dry} = \frac{\theta_s + \frac{|h_{dry}|^B}{A}\theta_r}{1 + \frac{|h_{dry}|^B}{A}}$
Calculate constants:
T = TMI + 60
$\gamma = 0.039337 d_{am} + 1.357033$
$d_1 = 0.449079 d_{am} + 0.304560$
$T_1 = 0.062651 d_{am} + 59.53593$
Initialize $h_m$ & $\delta$:
$h_m = (h_{wl} + h_{dry})/2$
$\delta = 1$
Calculate $\theta_m$ & $\theta'_m$:
$\theta_m = \frac{\theta_s + \frac{|h_m|^B}{A}\theta_r}{1 + \frac{|h_m|^B}{A}}$
$\theta'_m = \frac{\theta_{wl} - \theta_{dry}}{\left[1 + \frac{d_{am} - d_1}{d_1\left(\frac{T}{T_1}\right)^\gamma}\right]} + \theta_{dry}$
$\delta = \theta_m - \theta'_m$
Is $\delta$ = 0? ($\pm$.0001)
No
is $\delta$ > 0?
No
Yes
$h_m = h_m$ + .01
$h_m = h_m$ - .01
Yes
$h_m$
13 go to pg 89

# Depth to Constant Suction

## $z_m$

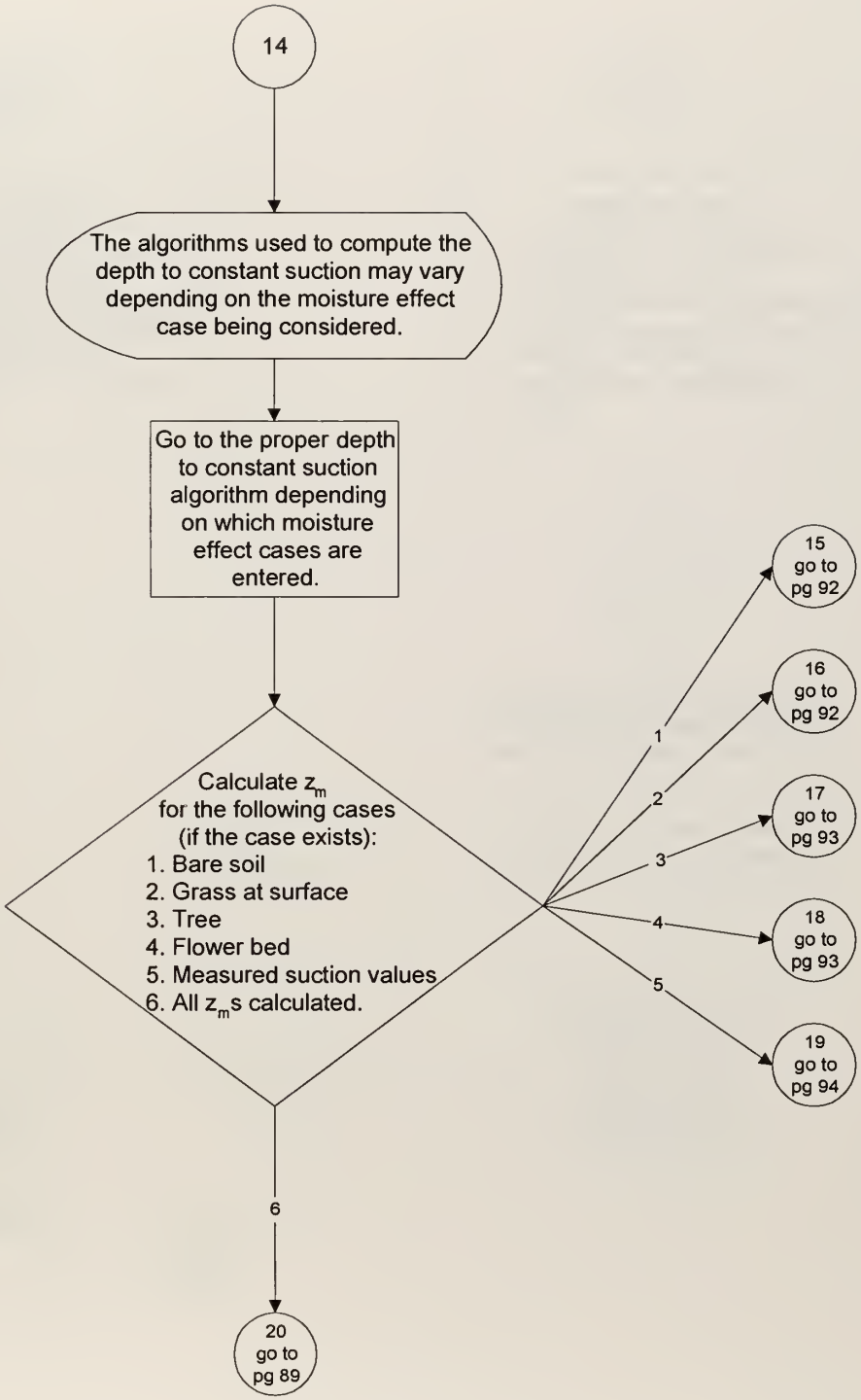
14
The algorithms used to compute the depth to constant suction may vary depending on the moisture effect case being considered.
Go to the proper depth to constant suction algorithm depending on which moisture effect cases are entered.
Calculate $z_m$ for the following cases (if the case exists):
1. Bare soil
2. Grass at surface
3. Tree
4. Flower bed
5. Measured suction values
6. All $z_m$s calculated.
1
2
3
4
5
6
15 go to pg 92
16 go to pg 92
17 go to pg 93
18 go to pg 93
19 go to pg 94
20 go to pg 89

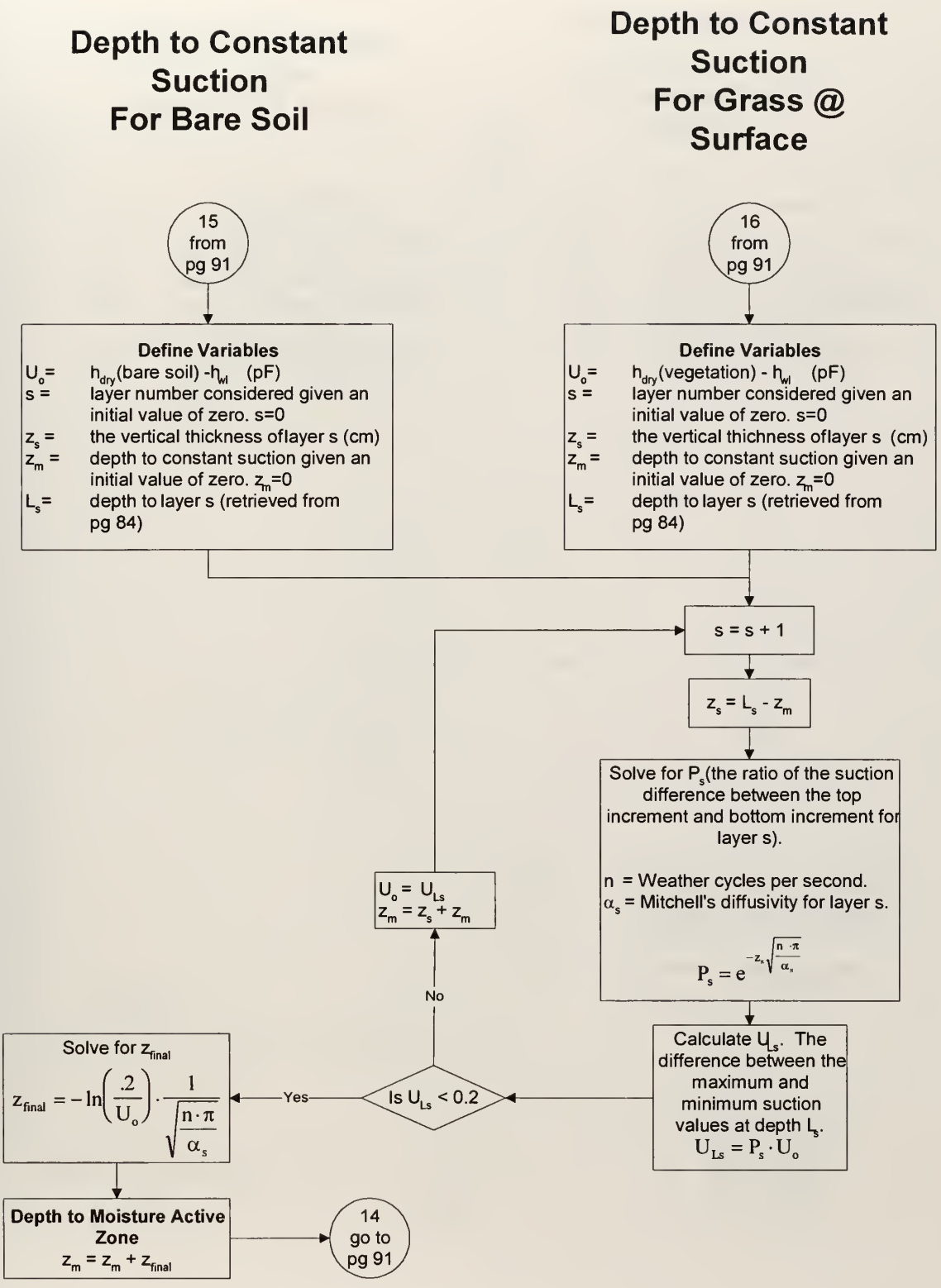
Depth to Constant Suction For Bare Soil
Depth to Constant Suction For Grass @ Surface
15 from pg 91
16 from pg 91
Define Variables
$U_o$= $h_{dry}$(bare soil) -$h_{wl}$ (pF)
s = layer number considered given an initial value of zero. s=0
$z_s$ = the vertical thickness oflayer s (cm)
$z_m$ = depth to constant suction given an initial value of zero. $z_m$=0
$L_s$= depth to layer s (retrieved from pg 84)
Define Variables
$U_o$= $h_{dry}$(vegetation) - $h_{wl}$ (pF)
s = layer number considered given an initial value of zero. s=0
$z_s$ = the vertical thichness oflayer s (cm)
$z_m$ = depth to constant suction given an initial value of zero. $z_m$=0
$L_s$= depth to layer s (retrieved from pg 84)
s = s + 1
$z_s = L_s - z_m$
Solve for $P_s$(the ratio of the suction difference between the top increment and bottom increment for layer s).
n = Weather cycles per second.
$\alpha_s$ = Mitchell's diffusivity for layer s.
$P_s = e^{-z_s\sqrt{\frac{n\cdot\pi}{\alpha_s}}}$
Calculate $U_{Ls}$. The difference between the maximum and minimum suction values at depth $L_s$.
$U_{Ls} = P_s \cdot U_o$
Is $U_{Ls}$ < 0.2
Yes
No
$U_o = U_{Ls}$
$z_m = z_s + z_m$
Solve for $z_{final}$
$z_{final} = -\ln\left(\frac{.2}{U_o}\right)\cdot\frac{1}{\sqrt{\frac{n\cdot\pi}{\alpha_s}}}$
Depth to Moisture Active Zone
$z_m = z_m + z_{final}$
14 go to pg 91

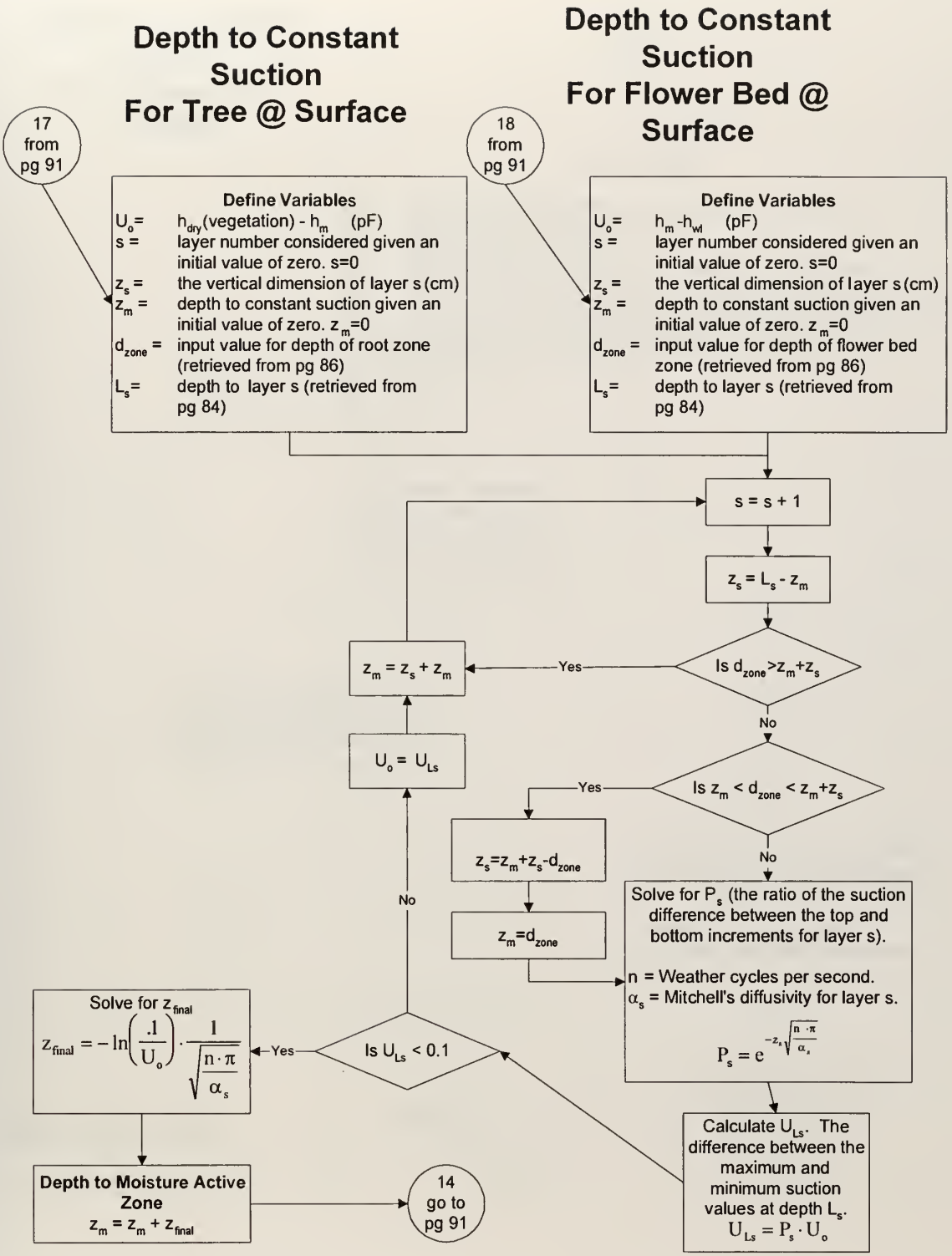
Depth to Constant Suction For Tree @ Surface
17 from pg 91
Define Variables
$U_o$= $h_{dry}$(vegetation) - $h_m$ (pF)
s = layer number considered given an initial value of zero. s=0
$z_s$ = the vertical dimension of layer s (cm)
$z_m$ = depth to constant suction given an initial value of zero. $z_m$=0
$d_{zone}$ = input value for depth of root zone (retrieved from pg 86)
$L_s$= depth to layer s (retrieved from pg 84)
Depth to Constant Suction For Flower Bed @ Surface
18 from pg 91
Define Variables
$U_o$= $h_m$-$h_{wl}$ (pF)
s = layer number considered given an initial value of zero. s=0
$z_s$ = the vertical dimension of layer s (cm)
$z_m$ = depth to constant suction given an initial value of zero. $z_m$=0
$d_{zone}$ = input value for depth of flower bed zone (retrieved from pg 86)
$L_s$= depth to layer s (retrieved from pg 84)
s = s + 1
$z_s = L_s - z_m$
Is $d_{zone} > z_m + z_s$
Yes
$z_m = z_s + z_m$
No
Is $z_m < d_{zone} < z_m + z_s$
Yes
$z_s = z_m + z_s - d_{zone}$
$z_m = d_{zone}$
No
$U_o = U_{Ls}$
Solve for $P_s$ (the ratio of the suction difference between the top and bottom increments for layer s).
n = Weather cycles per second.
$\alpha_s$ = Mitchell's diffusivity for layer s.
$P_s = e^{-z_s\sqrt{\frac{n\cdot\pi}{\alpha_s}}}$
Calculate $U_{Ls}$. The difference between the maximum and minimum suction values at depth $L_s$.
$U_{Ls} = P_s \cdot U_o$
Is $U_{Ls} < 0.1$
Yes
No
Solve for $z_{final}$
$z_{final} = -\ln\left(\frac{.1}{U_o}\right)\cdot\frac{1}{\sqrt{\frac{n\cdot\pi}{\alpha_s}}}$
Depth to Moisture Active Zone
$z_m = z_m + z_{final}$
14 go to pg 91

# Depth to Constant Suction For a Measured Profile

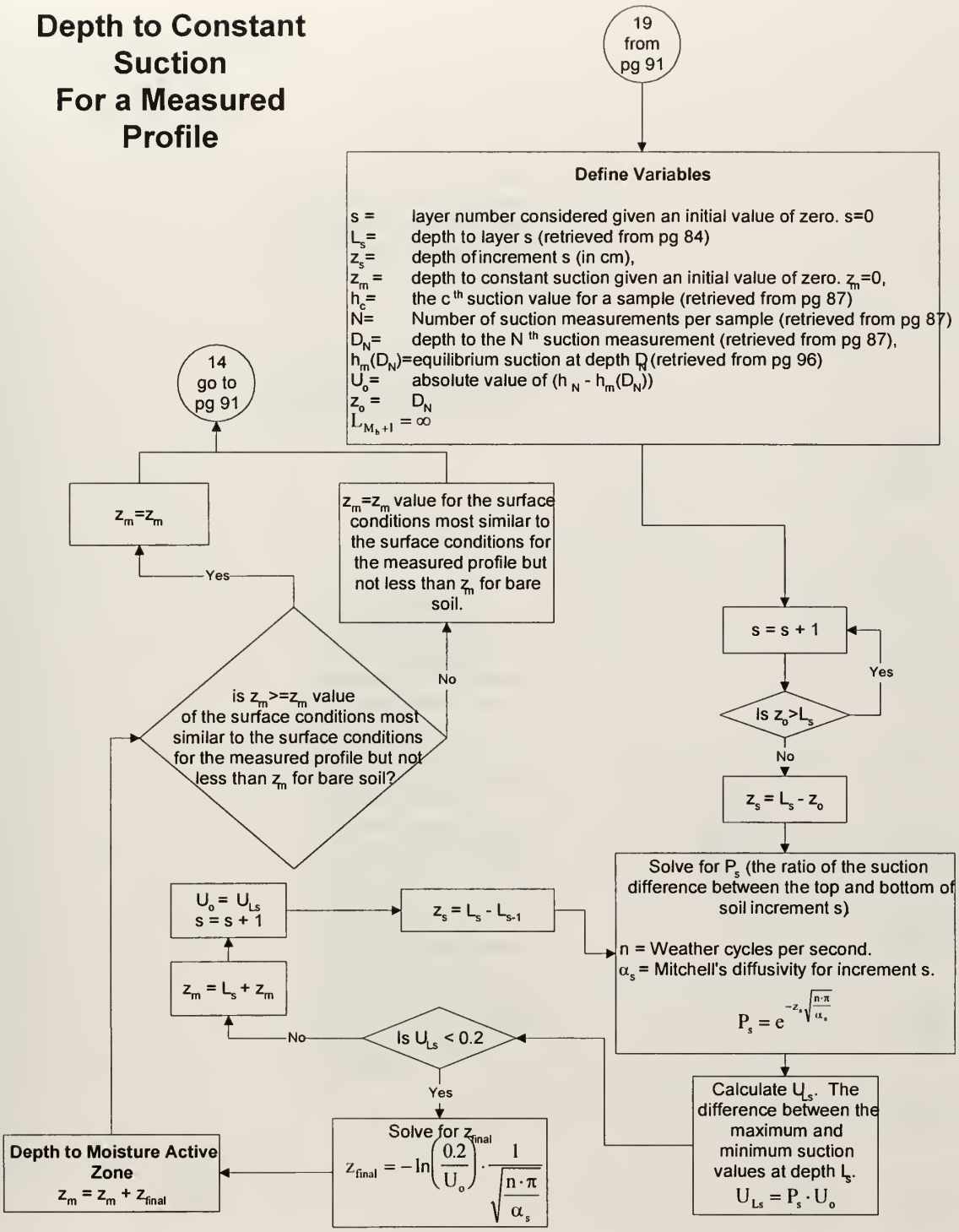
19 from pg 91
Define Variables
s = layer number considered given an initial value of zero. s=0
$L_s$= depth to layer s (retrieved from pg 84)
$z_s$= depth of increment s (in cm),
$z_m$ = depth to constant suction given an initial value of zero. $z_m$=0,
$h_c$= the c th suction value for a sample (retrieved from pg 87)
N= Number of suction measurements per sample (retrieved from pg 87)
$D_N$= depth to the N th suction measurement (retrieved from pg 87),
$h_m(D_N)$=equilibrium suction at depth $D_N$ (retrieved from pg 96)
$U_o$= absolute value of ($h_N$ - $h_m(D_N)$)
$z_o$ = $D_N$
$L_{M_b+1} = \infty$
14 go to pg 91
$z_m$=$z_m$
$z_m$=$z_m$ value for the surface conditions most similar to the surface conditions for the measured profile but not less than $z_m$ for bare soil.
Yes
No
is $z_m$>=$z_m$ value of the surface conditions most similar to the surface conditions for the measured profile but not less than $z_m$ for bare soil?
s = s + 1
Yes
Is $z_o$>$L_s$
No
$z_s$ = $L_s$ - $z_o$
Solve for $P_s$ (the ratio of the suction difference between the top and bottom of soil increment s)
n = Weather cycles per second.
$\alpha_s$ = Mitchell's diffusivity for increment s.
$P_s = e^{-z_s\sqrt{\frac{n\cdot\pi}{\alpha_s}}}$
$U_o$ = $U_{Ls}$
s = s + 1
$z_s$ = $L_s$ - $L_{s-1}$
$z_m$ = $L_s$ + $z_m$
No
Is $U_{Ls}$ < 0.2
Yes
Calculate $U_{Ls}$. The difference between the maximum and minimum suction values at depth $L_s$.
$U_{Ls} = P_s \cdot U_o$
Solve for $z_{final}$
$z_{final} = -\ln\left(\frac{0.2}{U_o}\right)\cdot\frac{1}{\sqrt{\frac{n\cdot\pi}{\alpha_s}}}$
Depth to Moisture Active Zone
$z_m = z_m + z_{final}$

# Calculate Suction Profiles Menu Page

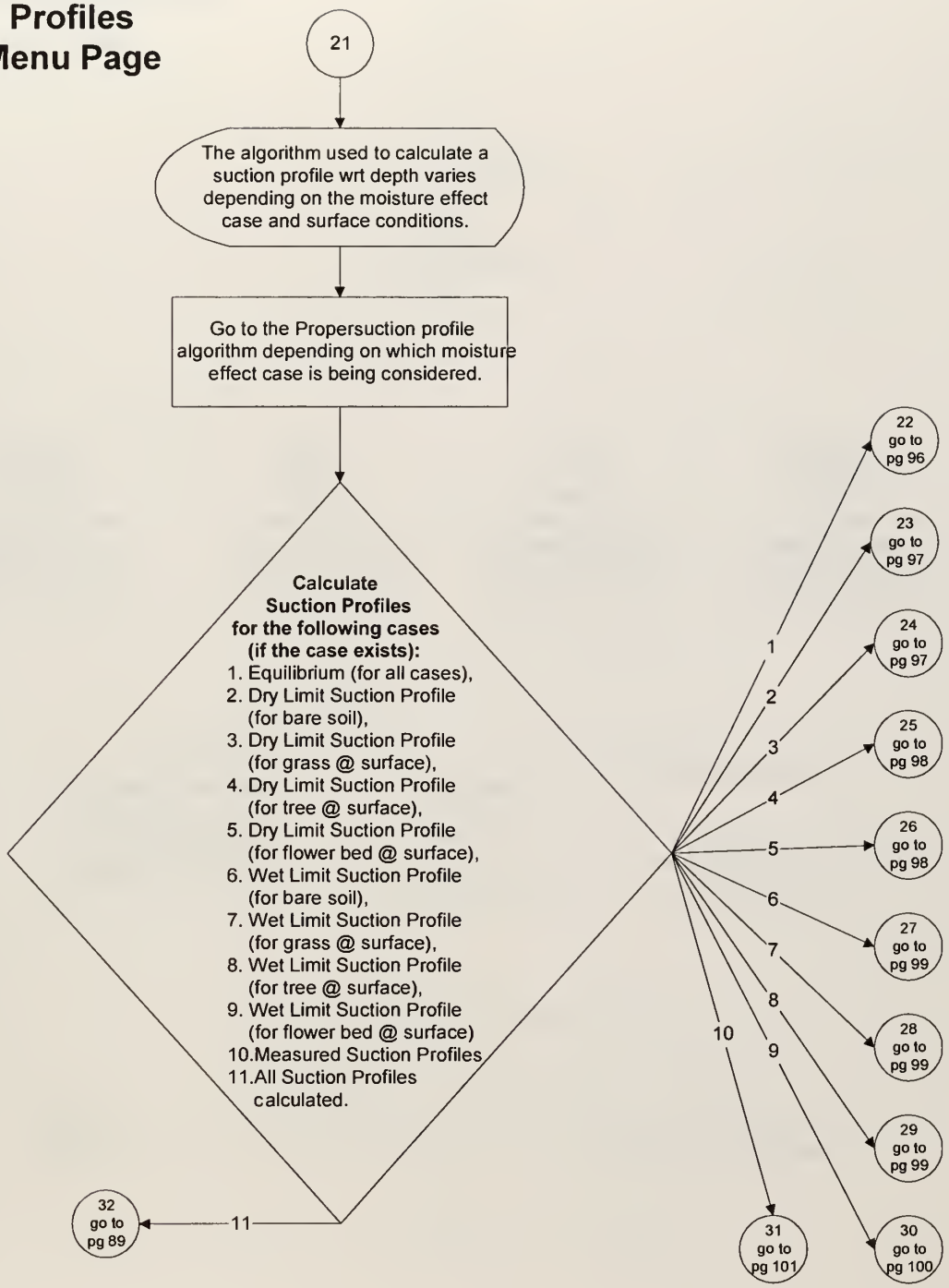
21
The algorithm used to calculate a suction profile wrt depth varies depending on the moisture effect case and surface conditions.
Go to the Propersuction profile algorithm depending on which moisture effect case is being considered.
Calculate Suction Profiles for the following cases (if the case exists):
1. Equilibrium (for all cases),
2. Dry Limit Suction Profile (for bare soil),
3. Dry Limit Suction Profile (for grass @ surface),
4. Dry Limit Suction Profile (for tree @ surface),
5. Dry Limit Suction Profile (for flower bed @ surface),
6. Wet Limit Suction Profile (for bare soil),
7. Wet Limit Suction Profile (for grass @ surface),
8. Wet Limit Suction Profile (for tree @ surface),
9. Wet Limit Suction Profile (for flower bed @ surface)
10. Measured Suction Profiles
11. All Suction Profiles calculated.
1
2
3
4
5
6
7
8
9
10
11
22 go to pg 96
23 go to pg 97
24 go to pg 97
25 go to pg 98
26 go to pg 98
27 go to pg 99
28 go to pg 99
29 go to pg 99
30 go to pg 100
31 go to pg 101
32 go to pg 89

# Equilibrium Suction Profiles

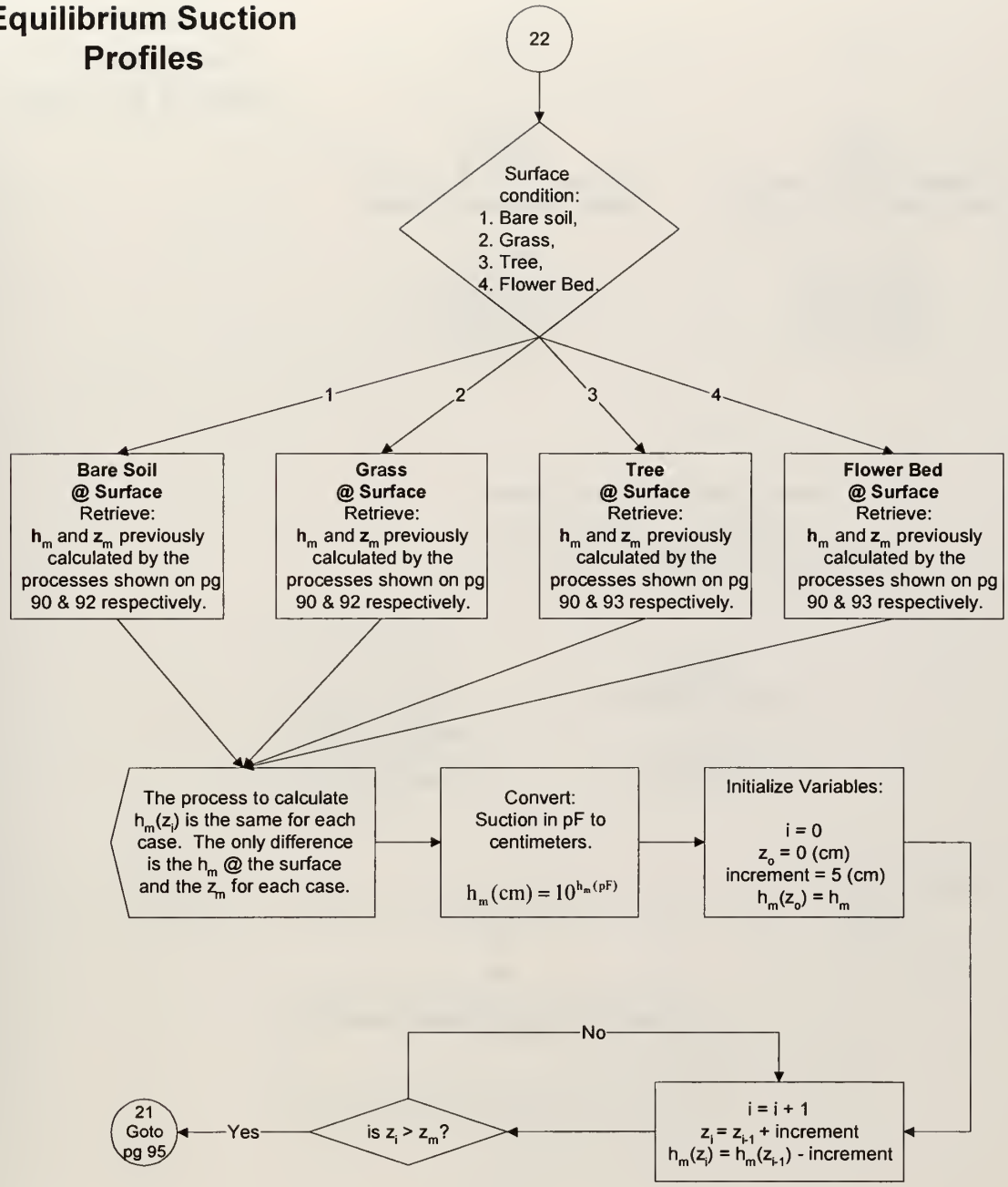
22
Surface condition:
1. Bare soil,
2. Grass,
3. Tree,
4. Flower Bed.
1
2
3
4
Bare Soil @ Surface
Retrieve:
$h_m$ and $z_m$ previously calculated by the processes shown on pg 90 & 92 respectively.
Grass @ Surface
Retrieve:
$h_m$ and $z_m$ previously calculated by the processes shown on pg 90 & 92 respectively.
Tree @ Surface
Retrieve:
$h_m$ and $z_m$ previously calculated by the processes shown on pg 90 & 93 respectively.
Flower Bed @ Surface
Retrieve:
$h_m$ and $z_m$ previously calculated by the processes shown on pg 90 & 93 respectively.
The process to calculate $h_m(z_i)$ is the same for each case. The only difference is the $h_m$ @ the surface and the $z_m$ for each case.
Convert:
Suction in pF to centimeters.
$h_m(cm) = 10^{h_m(pF)}$
Initialize Variables:
i = 0
$z_o$ = 0 (cm)
increment = 5 (cm)
$h_m(z_o) = h_m$
No
i = i + 1
$z_i = z_{i-1}$ + increment
$h_m(z_i) = h_m(z_{i-1})$ - increment
is $z_i > z_m$?
Yes
21
Goto pg 95

# Dry Limit Suction Profile For Bare Soil & Grass @ Surface

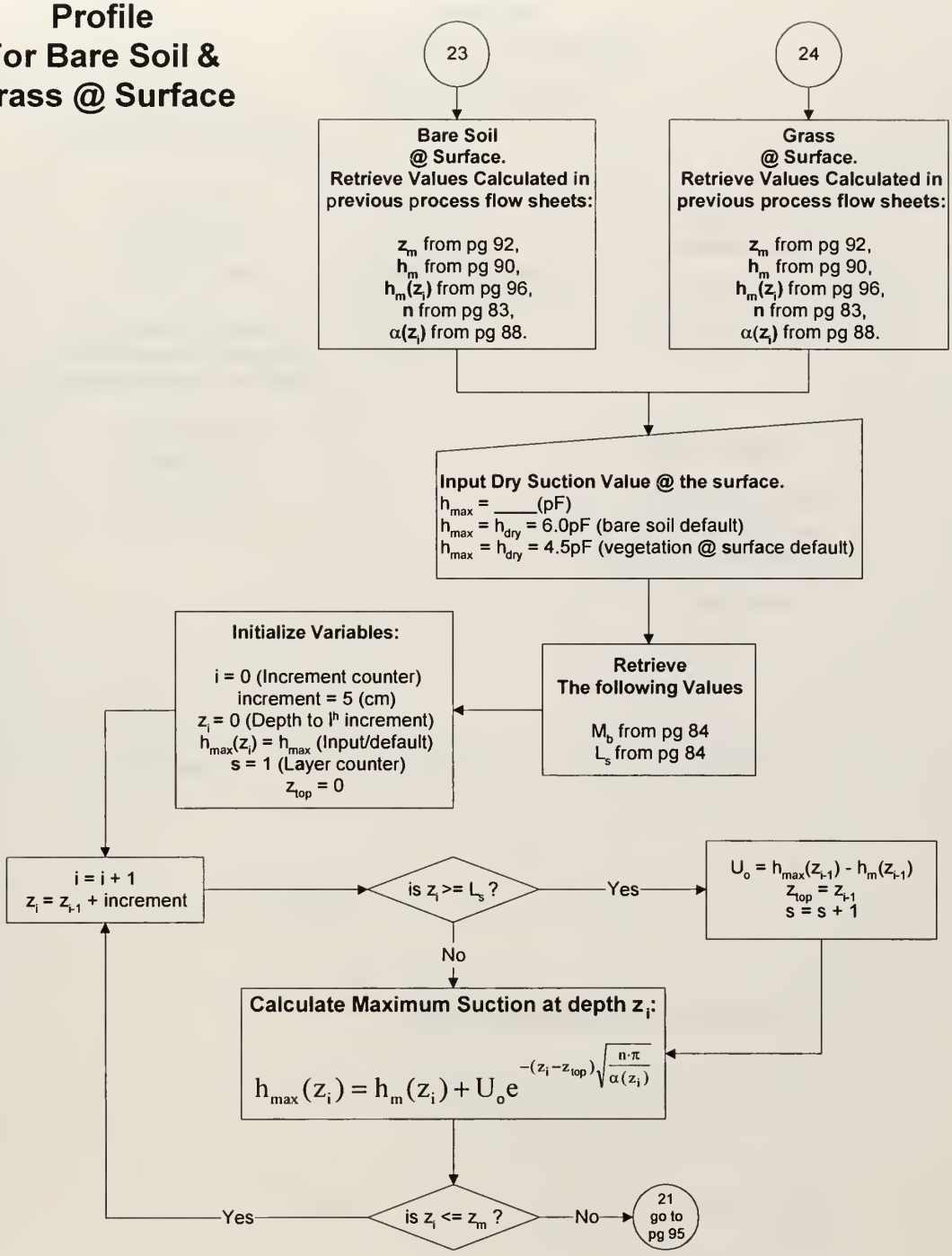
23
24
Bare Soil @ Surface. Retrieve Values Calculated in previous process flow sheets:
$z_m$ from pg 92,
$h_m$ from pg 90,
$h_m(z_i)$ from pg 96,
n from pg 83,
$\alpha(z_i)$ from pg 88.
Grass @ Surface. Retrieve Values Calculated in previous process flow sheets:
$z_m$ from pg 92,
$h_m$ from pg 90,
$h_m(z_i)$ from pg 96,
n from pg 83,
$\alpha(z_i)$ from pg 88.
Input Dry Suction Value @ the surface.
$h_{max}$ = ____(pF)
$h_{max} = h_{dry}$ = 6.0pF (bare soil default)
$h_{max} = h_{dry}$ = 4.5pF (vegetation @ surface default)
Retrieve The following Values
$M_b$ from pg 84
$L_s$ from pg 84
Initialize Variables:
i = 0 (Increment counter)
increment = 5 (cm)
$z_i$ = 0 (Depth to $i^{th}$ increment)
$h_{max}(z_i) = h_{max}$ (Input/default)
s = 1 (Layer counter)
$z_{top}$ = 0
i = i + 1
$z_i = z_{i-1}$ + increment
is $z_i >= L_s$ ?
Yes
$U_o = h_{max}(z_{i-1}) - h_m(z_{i-1})$
$z_{top} = z_{i-1}$
s = s + 1
No
Calculate Maximum Suction at depth $z_i$:
$h_{max}(z_i) = h_m(z_i) + U_o e^{-(z_i - z_{top})\sqrt{\frac{n \cdot \pi}{\alpha(z_i)}}}$
is $z_i <= z_m$ ?
Yes
No
21 go to pg 95

# Dry Limit Suction Profile For Tree and Flower Bed @ Surface

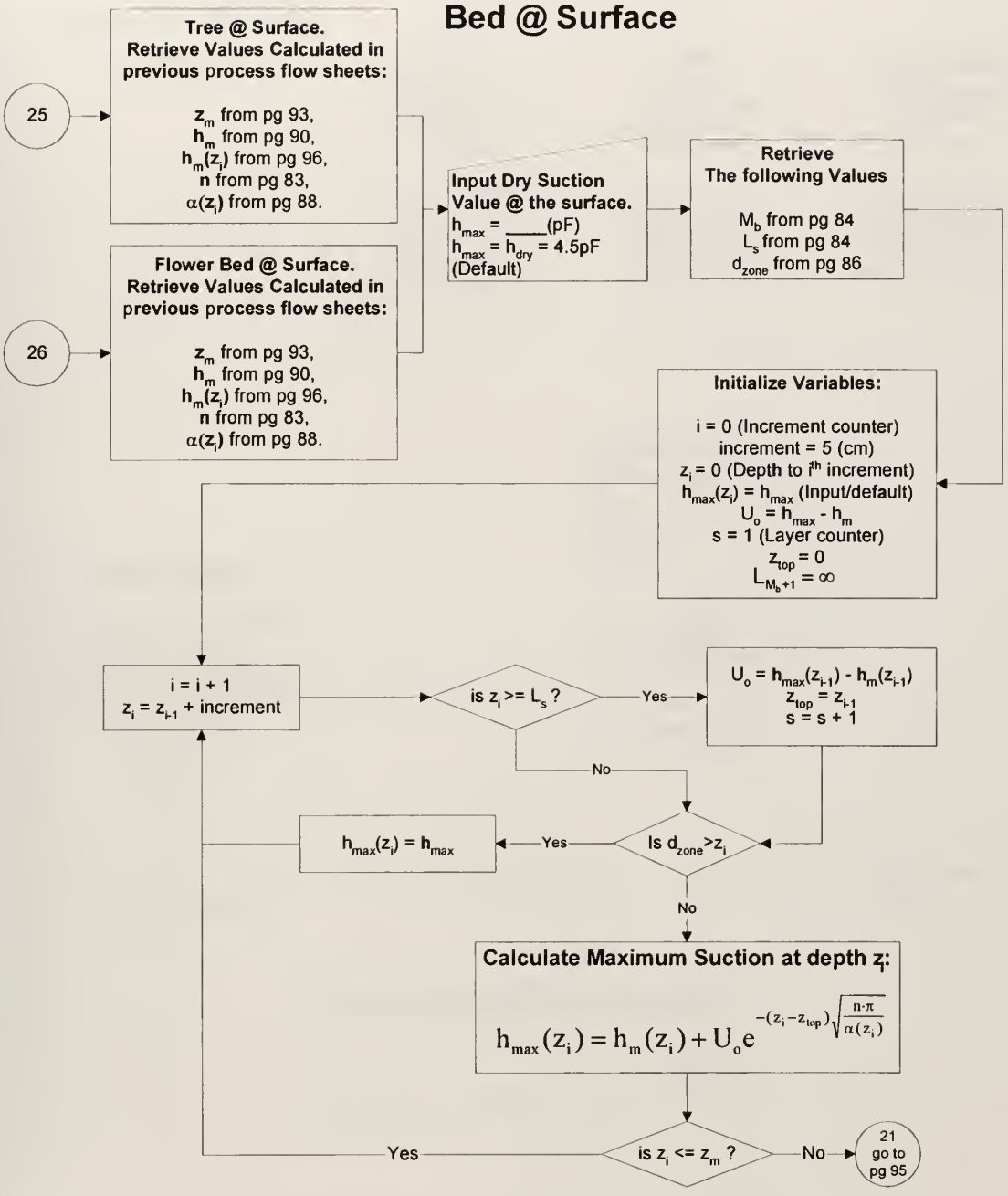
25
Tree @ Surface.
Retrieve Values Calculated in previous process flow sheets:
$z_m$ from pg 93,
$h_m$ from pg 90,
$h_m(z_i)$ from pg 96,
n from pg 83,
$\alpha(z_i)$ from pg 88.
26
Flower Bed @ Surface.
Retrieve Values Calculated in previous process flow sheets:
$z_m$ from pg 93,
$h_m$ from pg 90,
$h_m(z_i)$ from pg 96,
n from pg 83,
$\alpha(z_i)$ from pg 88.
Input Dry Suction Value @ the surface.
$h_{max}$ = ____(pF)
$h_{max} = h_{dry}$ = 4.5pF (Default)
Retrieve The following Values
$M_b$ from pg 84
$L_s$ from pg 84
$d_{zone}$ from pg 86
Initialize Variables:
i = 0 (Increment counter)
increment = 5 (cm)
$z_i$ = 0 (Depth to $i^{th}$ increment)
$h_{max}(z_i) = h_{max}$ (Input/default)
$U_o = h_{max} - h_m$
s = 1 (Layer counter)
$z_{top}$ = 0
$L_{M_b+1} = \infty$
i = i + 1
$z_i = z_{i-1}$ + increment
is $z_i >= L_s$ ?
Yes
$U_o = h_{max}(z_{i-1}) - h_m(z_{i-1})$
$z_{top} = z_{i-1}$
s = s + 1
No
Is $d_{zone} > z_i$
Yes
$h_{max}(z_i) = h_{max}$
No
Calculate Maximum Suction at depth $z_i$:
$h_{max}(z_i) = h_m(z_i) + U_o e^{-(z_i - z_{top})\sqrt{\frac{n \cdot \pi}{\alpha(z_i)}}}$
is $z_i <= z_m$ ?
Yes
No
21
go to pg 95

# Wet Limit Suction Profile For Bare Soil, Grass, & Tree @ Surface

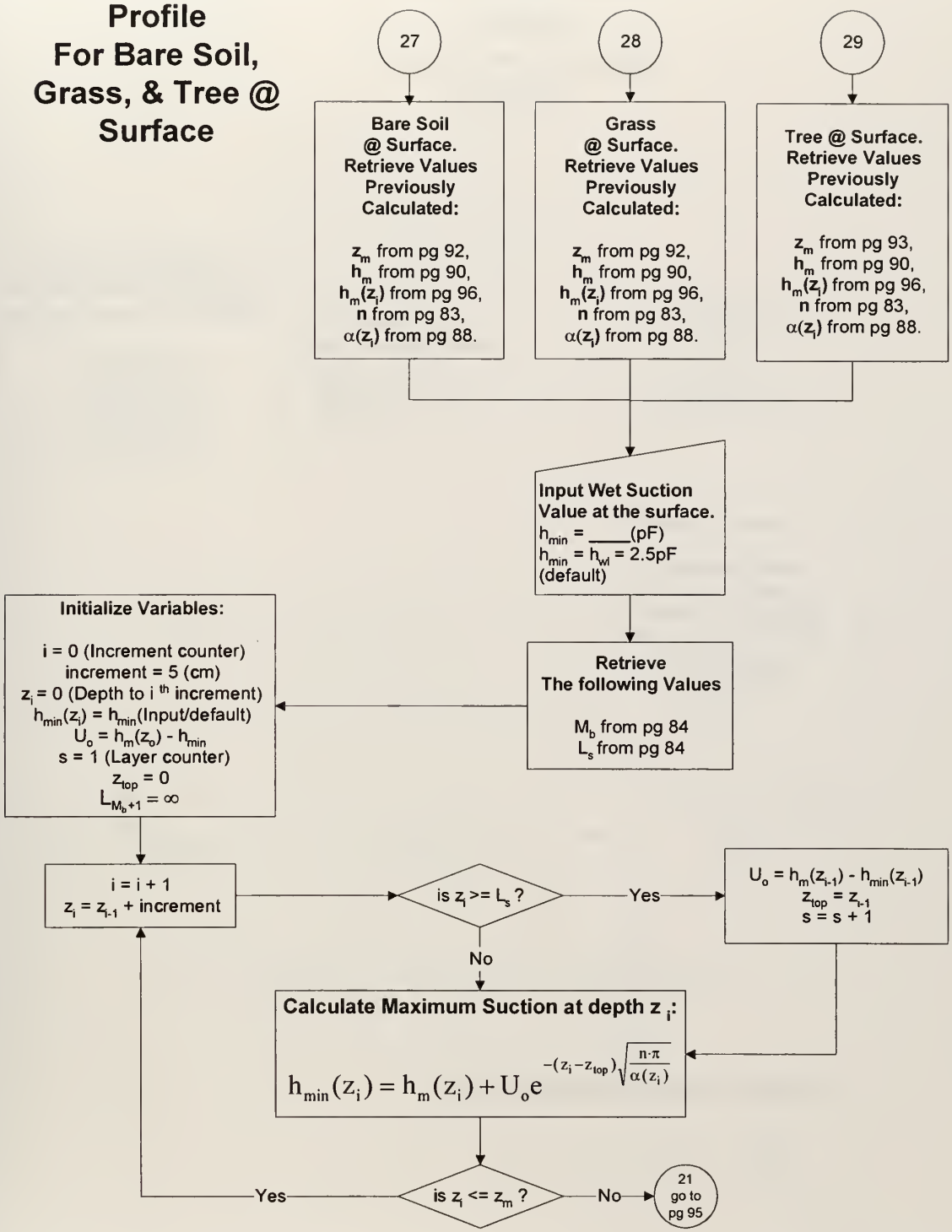
27
28
29
Bare Soil @ Surface. Retrieve Values Previously Calculated:
$z_m$ from pg 92,
$h_m$ from pg 90,
$h_m(z_i)$ from pg 96,
n from pg 83,
$\alpha(z_i)$ from pg 88.
Grass @ Surface. Retrieve Values Previously Calculated:
$z_m$ from pg 92,
$h_m$ from pg 90,
$h_m(z_i)$ from pg 96,
n from pg 83,
$\alpha(z_i)$ from pg 88.
Tree @ Surface. Retrieve Values Previously Calculated:
$z_m$ from pg 93,
$h_m$ from pg 90,
$h_m(z_i)$ from pg 96,
n from pg 83,
$\alpha(z_i)$ from pg 88.
Input Wet Suction Value at the surface.
$h_{min}$ = ____(pF)
$h_{min} = h_{wl}$ = 2.5pF (default)
Retrieve The following Values
$M_b$ from pg 84
$L_s$ from pg 84
Initialize Variables:
i = 0 (Increment counter)
increment = 5 (cm)
$z_i$ = 0 (Depth to i th increment)
$h_{min}(z_i) = h_{min}$(Input/default)
$U_o = h_m(z_o) - h_{min}$
s = 1 (Layer counter)
$z_{top}$ = 0
$L_{M_b+1} = \infty$
i = i + 1
$z_i = z_{i-1}$ + increment
is $z_i >= L_s$ ?
Yes
$U_o = h_m(z_{i-1}) - h_{min}(z_{i-1})$
$z_{top} = z_{i-1}$
s = s + 1
No
Calculate Maximum Suction at depth $z_i$:
$h_{min}(z_i) = h_m(z_i) + U_o e^{-(z_i - z_{top})\sqrt{\frac{n \cdot \pi}{\alpha(z_i)}}}$
is $z_i <= z_m$ ?
Yes
No
21
go to pg 95

# Wet Limit Suction Profile For Flower Bed @ Surface

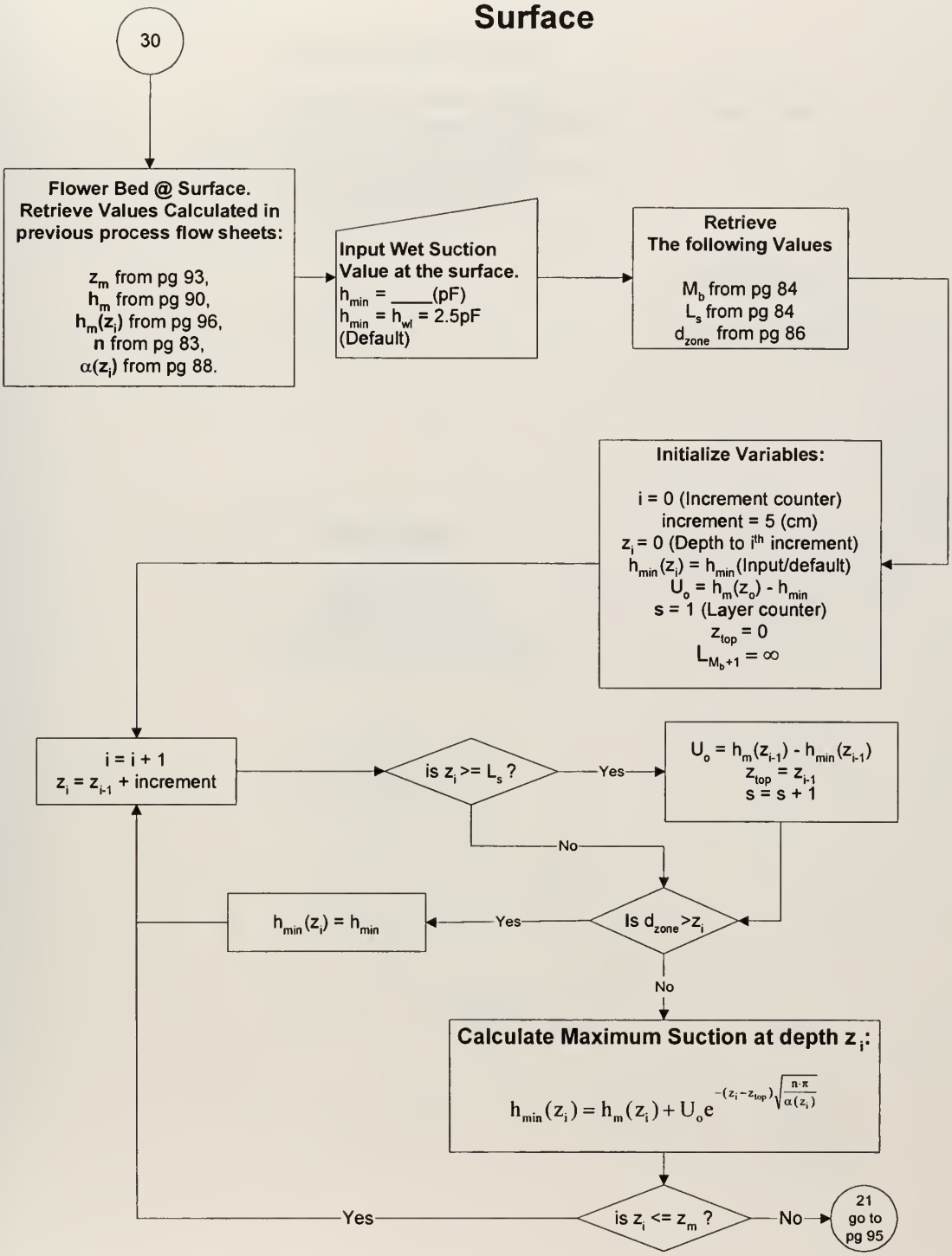
30
Flower Bed @ Surface. Retrieve Values Calculated in previous process flow sheets:
$z_m$ from pg 93,
$h_m$ from pg 90,
$h_m(z_i)$ from pg 96,
n from pg 83,
$\alpha(z_i)$ from pg 88.
Input Wet Suction Value at the surface.
$h_{min}$ = ____(pF)
$h_{min} = h_{wl}$ = 2.5pF (Default)
Retrieve The following Values
$M_b$ from pg 84
$L_s$ from pg 84
$d_{zone}$ from pg 86
Initialize Variables:
i = 0 (Increment counter)
increment = 5 (cm)
$z_i$ = 0 (Depth to $i^{th}$ increment)
$h_{min}(z_i) = h_{min}$(Input/default)
$U_o = h_m(z_o) - h_{min}$
s = 1 (Layer counter)
$z_{top}$ = 0
$L_{M_b+1} = \infty$
i = i + 1
$z_i = z_{i-1}$ + increment
is $z_i >= L_s$ ?
Yes
$U_o = h_m(z_{i-1}) - h_{min}(z_{i-1})$
$z_{top} = z_{i-1}$
s = s + 1
No
Is $d_{zone} > z_i$
Yes
$h_{min}(z_i) = h_{min}$
No
Calculate Maximum Suction at depth $z_i$:
$h_{min}(z_i) = h_m(z_i) + U_o e^{-(z_i - z_{top})\sqrt{\frac{n \cdot \pi}{\alpha(z_i)}}}$
is $z_i <= z_m$ ?
Yes
No
21 go to pg 95

# Suction Profile For a Measured Profile

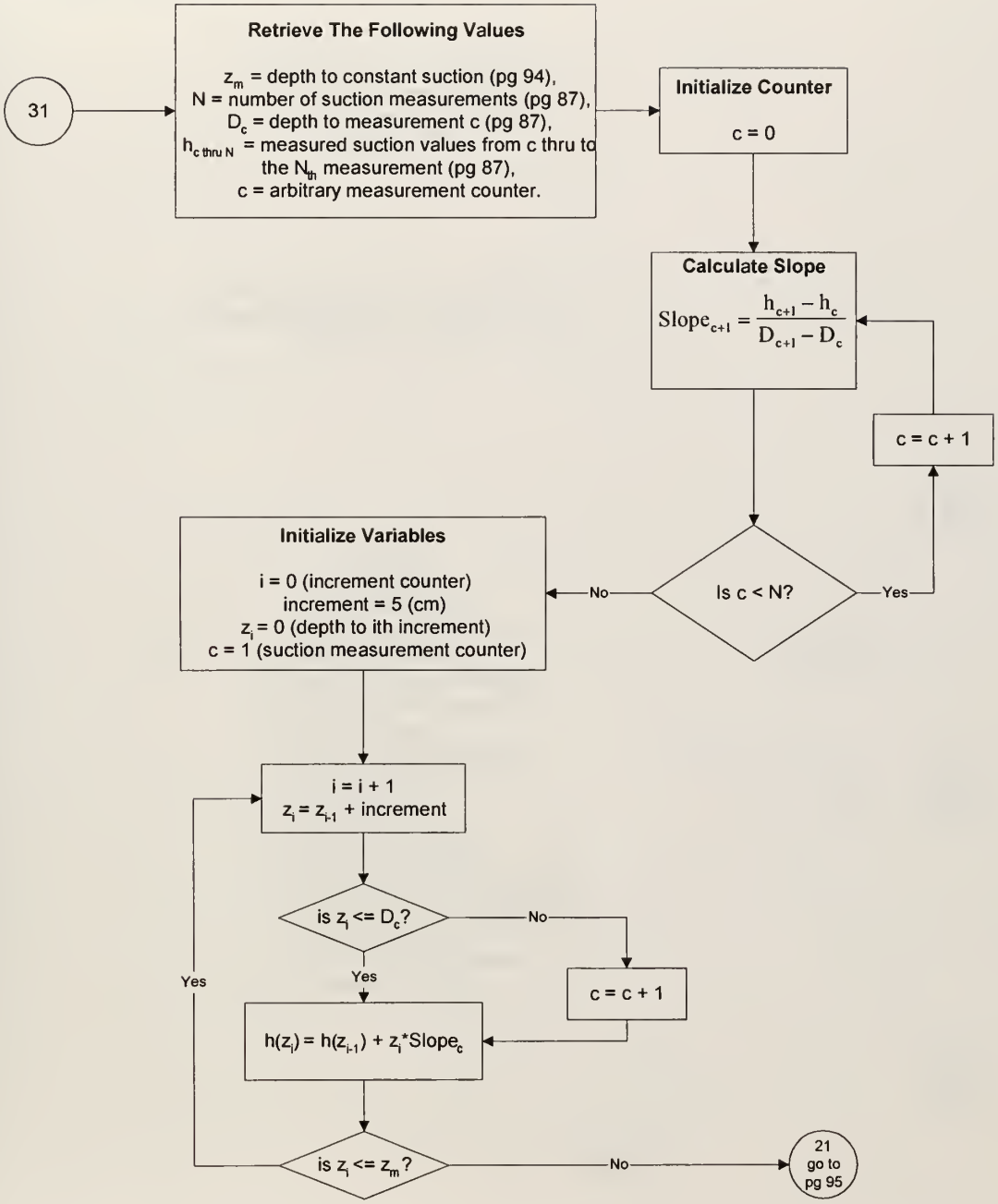
31
Retrieve The Following Values
$z_m$ = depth to constant suction (pg 94),
N = number of suction measurements (pg 87),
$D_c$ = depth to measurement c (pg 87),
$h_{c\ thru\ N}$ = measured suction values from c thru to the $N_{th}$ measurement (pg 87),
c = arbitrary measurement counter.
Initialize Counter
c = 0
Calculate Slope
$Slope_{c+1} = \frac{h_{c+1} - h_c}{D_{c+1} - D_c}$
c = c + 1
Is c < N?
No
Yes
Initialize Variables
i = 0 (increment counter)
increment = 5 (cm)
$z_i$ = 0 (depth to ith increment)
c = 1 (suction measurement counter)
i = i + 1
$z_i = z_{i-1}$ + increment
is $z_i$ <= $D_c$?
No
Yes
c = c + 1
$h(z_i) = h(z_{i-1}) + z_i * Slope_c$
is $z_i$ <= $z_m$?
Yes
No
21
go to
pg 95

# Calculate Soil Volume change Menu Page

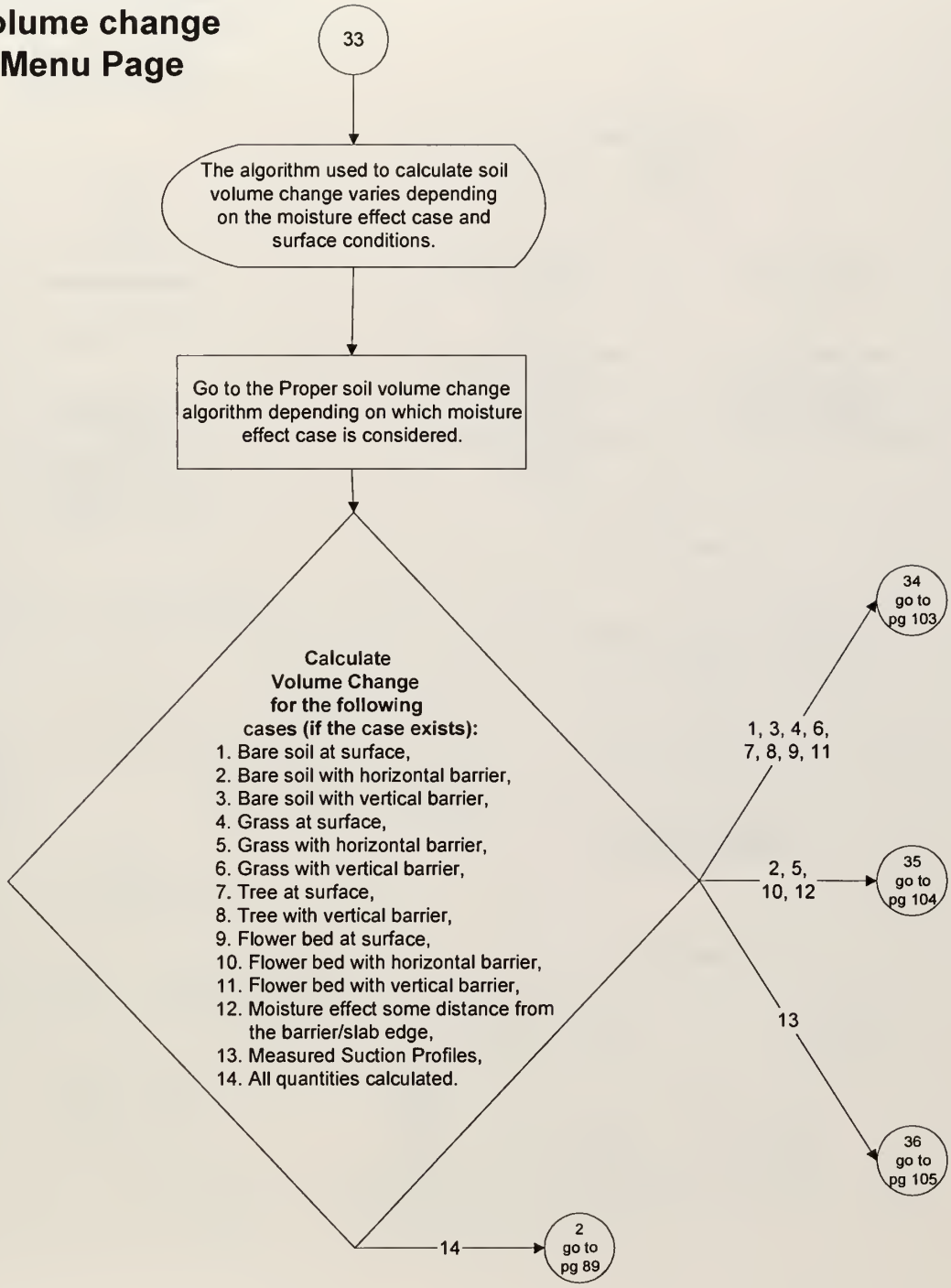
33
The algorithm used to calculate soil volume change varies depending on the moisture effect case and surface conditions.
Go to the Proper soil volume change algorithm depending on which moisture effect case is considered.
Calculate Volume Change for the following cases (if the case exists):
1. Bare soil at surface,
2. Bare soil with horizontal barrier,
3. Bare soil with vertical barrier,
4. Grass at surface,
5. Grass with horizontal barrier,
6. Grass with vertical barrier,
7. Tree at surface,
8. Tree with vertical barrier,
9. Flower bed at surface,
10. Flower bed with horizontal barrier,
11. Flower bed with vertical barrier,
12. Moisture effect some distance from the barrier/slab edge,
13. Measured Suction Profiles,
14. All quantities calculated.
1, 3, 4, 6, 7, 8, 9, 11
34 go to pg 103
2, 5, 10, 12
35 go to pg 104
13
36 go to pg 105
14
2 go to pg 89

# Soil Volume Change for Bare Soil, Grass, Tree and Flower bed at the surface with Vertical Barrier

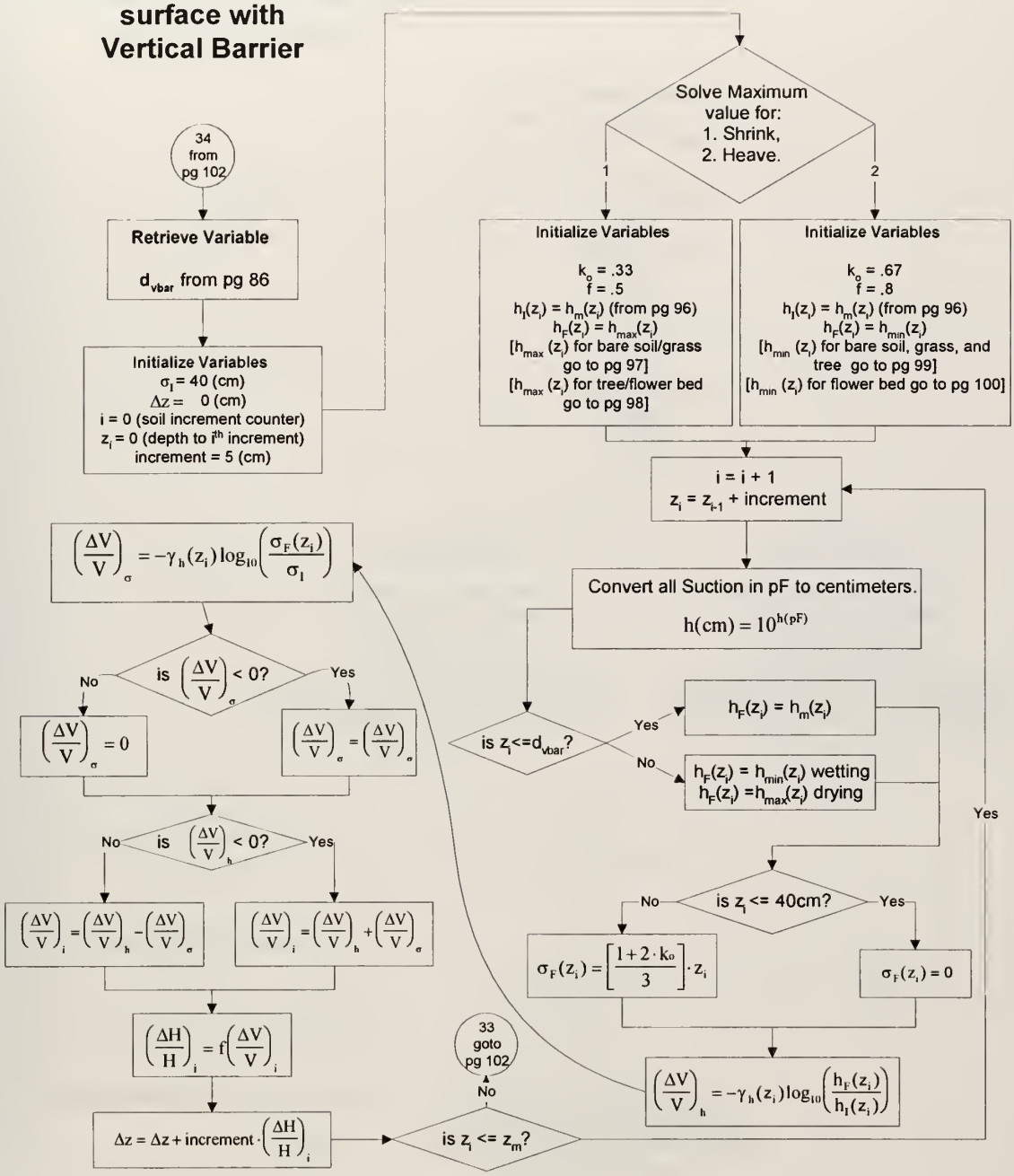

# Soil Volume Change for Bare Soil, Grass, Tree and Flower Bed at Surface with Horizontal Barrier

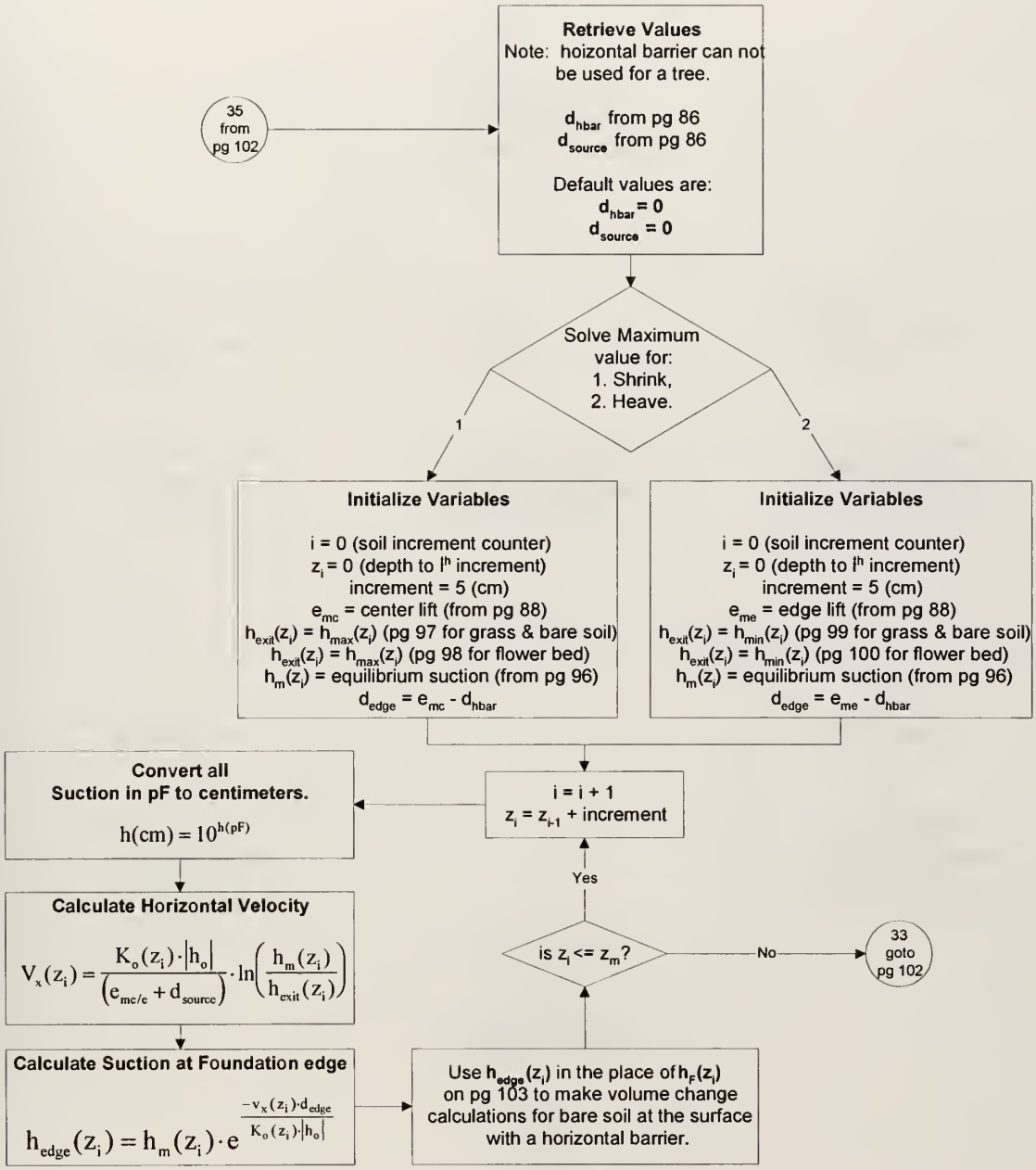
35 from pg 102
Retrieve Values
Note: hoizontal barrier can not be used for a tree.
$d_{hbar}$ from pg 86
$d_{source}$ from pg 86
Default values are:
$d_{hbar} = 0$
$d_{source} = 0$
Solve Maximum value for:
1. Shrink,
2. Heave.
1
2
Initialize Variables
i = 0 (soil increment counter)
$z_i$ = 0 (depth to $i^h$ increment)
increment = 5 (cm)
$e_{mc}$ = center lift (from pg 88)
$h_{exit}(z_i) = h_{max}(z_i)$ (pg 97 for grass & bare soil)
$h_{exit}(z_i) = h_{max}(z_i)$ (pg 98 for flower bed)
$h_m(z_i)$ = equilibrium suction (from pg 96)
$d_{edge} = e_{mc} - d_{hbar}$
Initialize Variables
i = 0 (soil increment counter)
$z_i$ = 0 (depth to $i^h$ increment)
increment = 5 (cm)
$e_{me}$ = edge lift (from pg 88)
$h_{exit}(z_i) = h_{min}(z_i)$ (pg 99 for grass & bare soil)
$h_{exit}(z_i) = h_{min}(z_i)$ (pg 100 for flower bed)
$h_m(z_i)$ = equilibrium suction (from pg 96)
$d_{edge} = e_{me} - d_{hbar}$
Convert all Suction in pF to centimeters.
$h(cm) = 10^{h(pF)}$
i = i + 1
$z_i = z_{i-1}$ + increment
Yes
Calculate Horizontal Velocity
$V_x(z_i) = \frac{K_o(z_i)\cdot|h_o|}{(e_{mc/e} + d_{source})} \cdot \ln\left(\frac{h_m(z_i)}{h_{exit}(z_i)}\right)$
is $z_i <= z_m$?
No
33 goto pg 102
Calculate Suction at Foundation edge
$h_{edge}(z_i) = h_m(z_i)\cdot e^{\frac{-v_x(z_i)\cdot d_{edge}}{K_o(z_i)\cdot|h_o|}}$
Use $h_{edge}(z_i)$ in the place of $h_F(z_i)$ on pg 103 to make volume change calculations for bare soil at the surface with a horizontal barrier.

# Soil Volume Change for Measured Suction Profiles

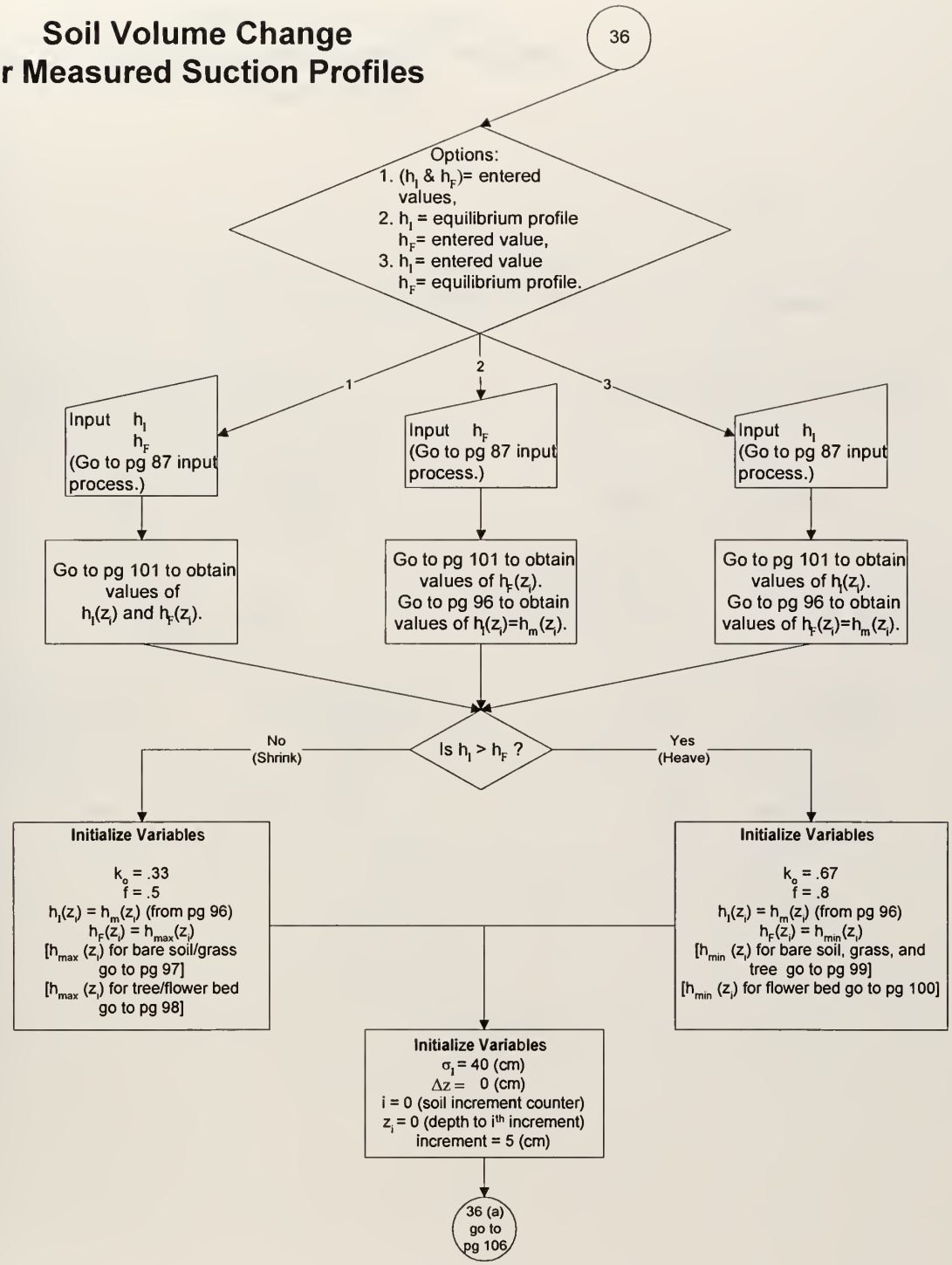
36
Options:
1. ($h_I$ & $h_F$)= entered values,
2. $h_I$ = equilibrium profile
$h_F$= entered value,
3. $h_I$= entered value
$h_F$= equilibrium profile.
1
2
3
Input $h_I$ $h_F$ (Go to pg 87 input process.)
Input $h_F$ (Go to pg 87 input process.)
Input $h_I$ (Go to pg 87 input process.)
Go to pg 101 to obtain values of $h_I(z_i)$ and $h_F(z_i)$.
Go to pg 101 to obtain values of $h_F(z_i)$. Go to pg 96 to obtain values of $h_I(z_i)=h_m(z_i)$.
Go to pg 101 to obtain values of $h_I(z_i)$. Go to pg 96 to obtain values of $h_F(z_i)=h_m(z_i)$.
No (Shrink)
Is $h_I > h_F$ ?
Yes (Heave)
Initialize Variables
$k_o$ = .33
f = .5
$h_I(z_i) = h_m(z_i)$ (from pg 96)
$h_F(z_i) = h_{max}(z_i)$
[$h_{max}$ ($z_i$) for bare soil/grass go to pg 97]
[$h_{max}$ ($z_i$) for tree/flower bed go to pg 98]
Initialize Variables
$k_o$ = .67
f = .8
$h_I(z_i) = h_m(z_i)$ (from pg 96)
$h_F(z_i) = h_{min}(z_i)$
[$h_{min}$ ($z_i$) for bare soil, grass, and tree go to pg 99]
[$h_{min}$ ($z_i$) for flower bed go to pg 100]
Initialize Variables
$\sigma_I$ = 40 (cm)
$\Delta z$ = 0 (cm)
i = 0 (soil increment counter)
$z_i$ = 0 (depth to $i^{th}$ increment)
increment = 5 (cm)
36 (a) go to pg 106

# Soil Volume Change for Measured Suction Profiles (Continued)

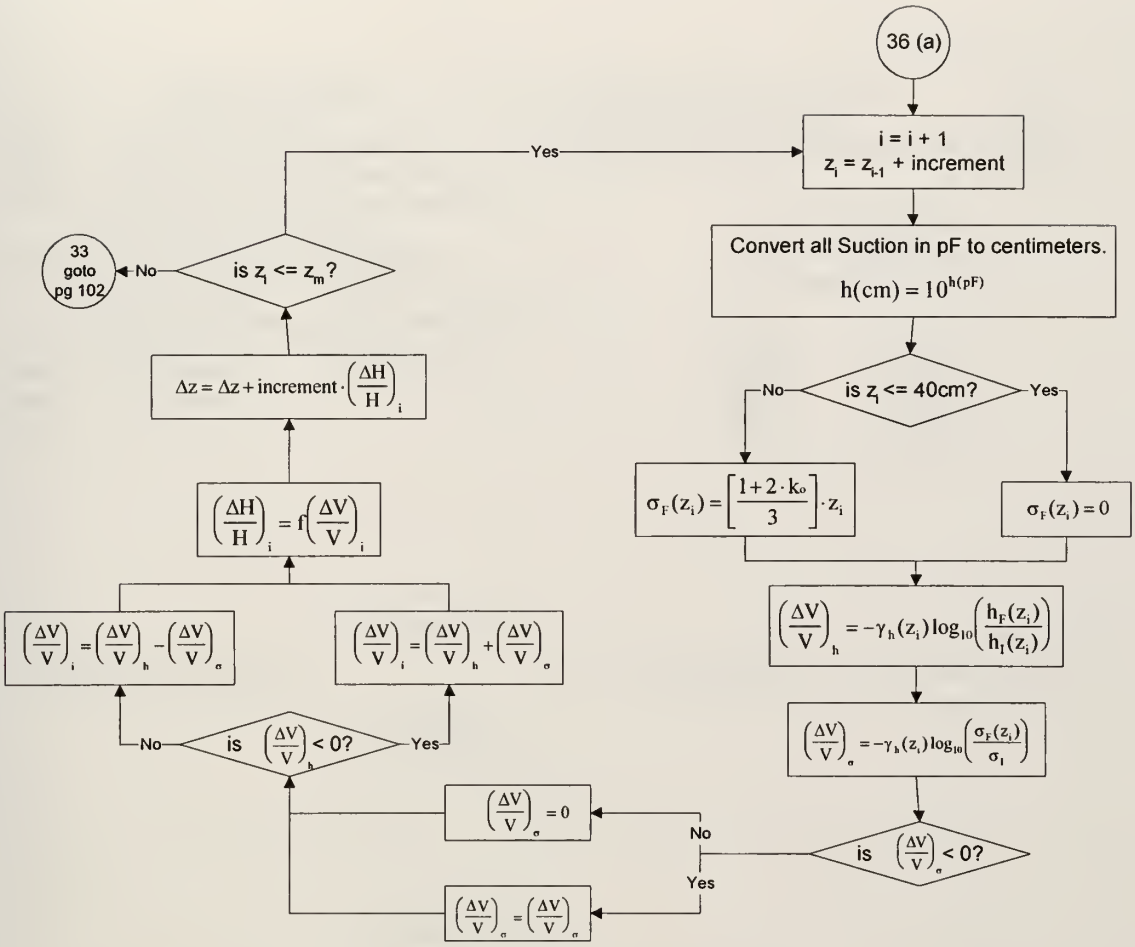

# Post Construction Time Constraint Input and Calculations

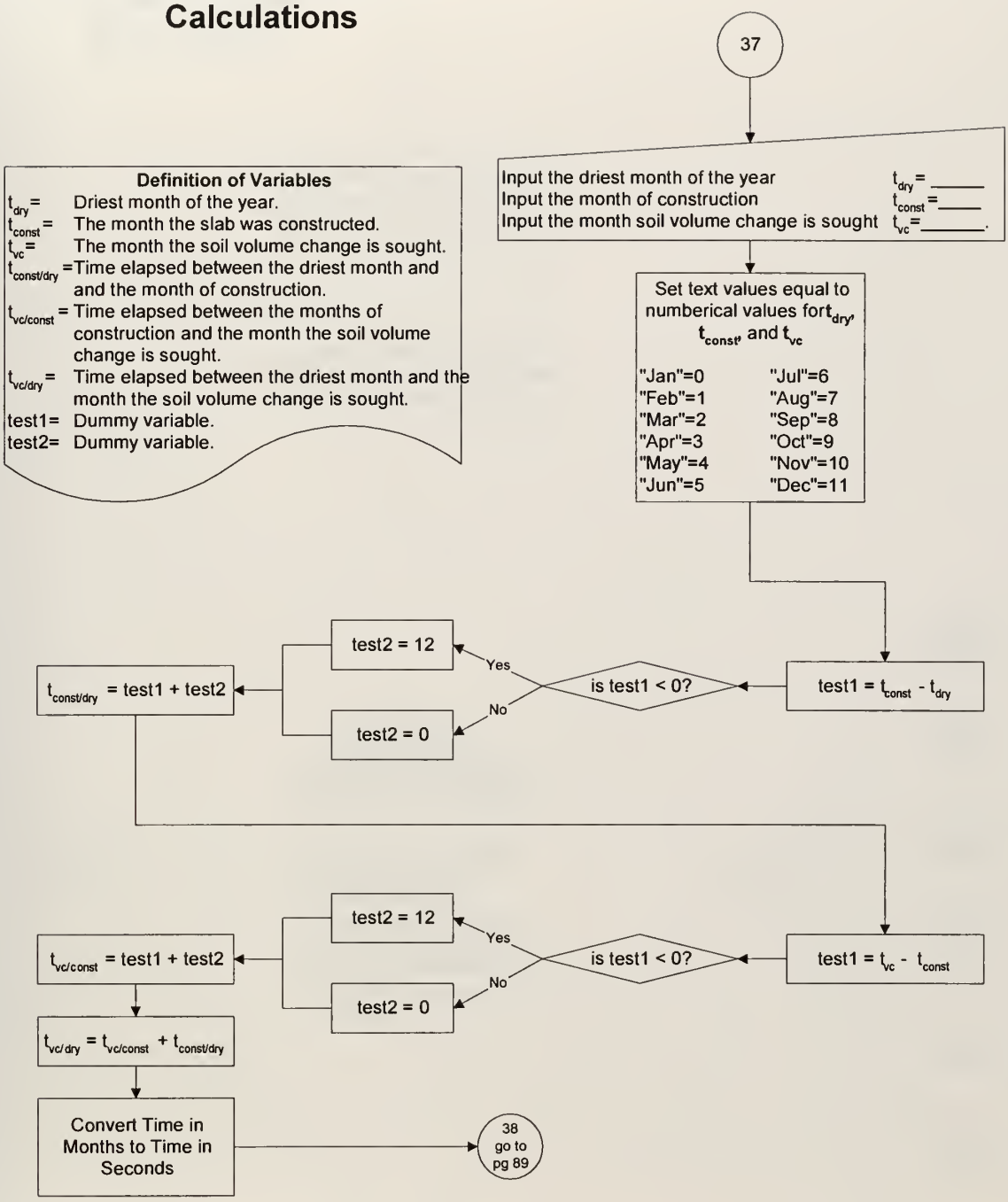
37
Definition of Variables
$t_{dry}$ = Driest month of the year.
$t_{const}$ = The month the slab was constructed.
$t_{vc}$ = The month the soil volume change is sought.
$t_{const/dry}$ = Time elapsed between the driest month and and the month of construction.
$t_{vc/const}$ = Time elapsed between the months of construction and the month the soil volume change is sought.
$t_{vc/dry}$ = Time elapsed between the driest month and the month the soil volume change is sought.
test1= Dummy variable.
test2= Dummy variable.
Input the driest month of the year $t_{dry}$ = _____
Input the month of construction $t_{const}$ = _____
Input the month soil volume change is sought $t_{vc}$ = _____.
Set text values equal to numberical values for $t_{dry}$, $t_{const}$, and $t_{vc}$
"Jan"=0 "Jul"=6
"Feb"=1 "Aug"=7
"Mar"=2 "Sep"=8
"Apr"=3 "Oct"=9
"May"=4 "Nov"=10
"Jun"=5 "Dec"=11
$t_{const/dry}$ = test1 + test2
test2 = 12
test2 = 0
Yes
No
is test1 < 0?
test1 = $t_{const}$ - $t_{dry}$
$t_{vc/const}$ = test1 + test2
test2 = 12
test2 = 0
Yes
No
is test1 < 0?
test1 = $t_{vc}$ - $t_{const}$
$t_{vc/dry}$ = $t_{vc/const}$ + $t_{const/dry}$
Convert Time in Months to Time in Seconds
38
go to
pg 89

# Calculate Post Construction Suction Profiles Menu Page

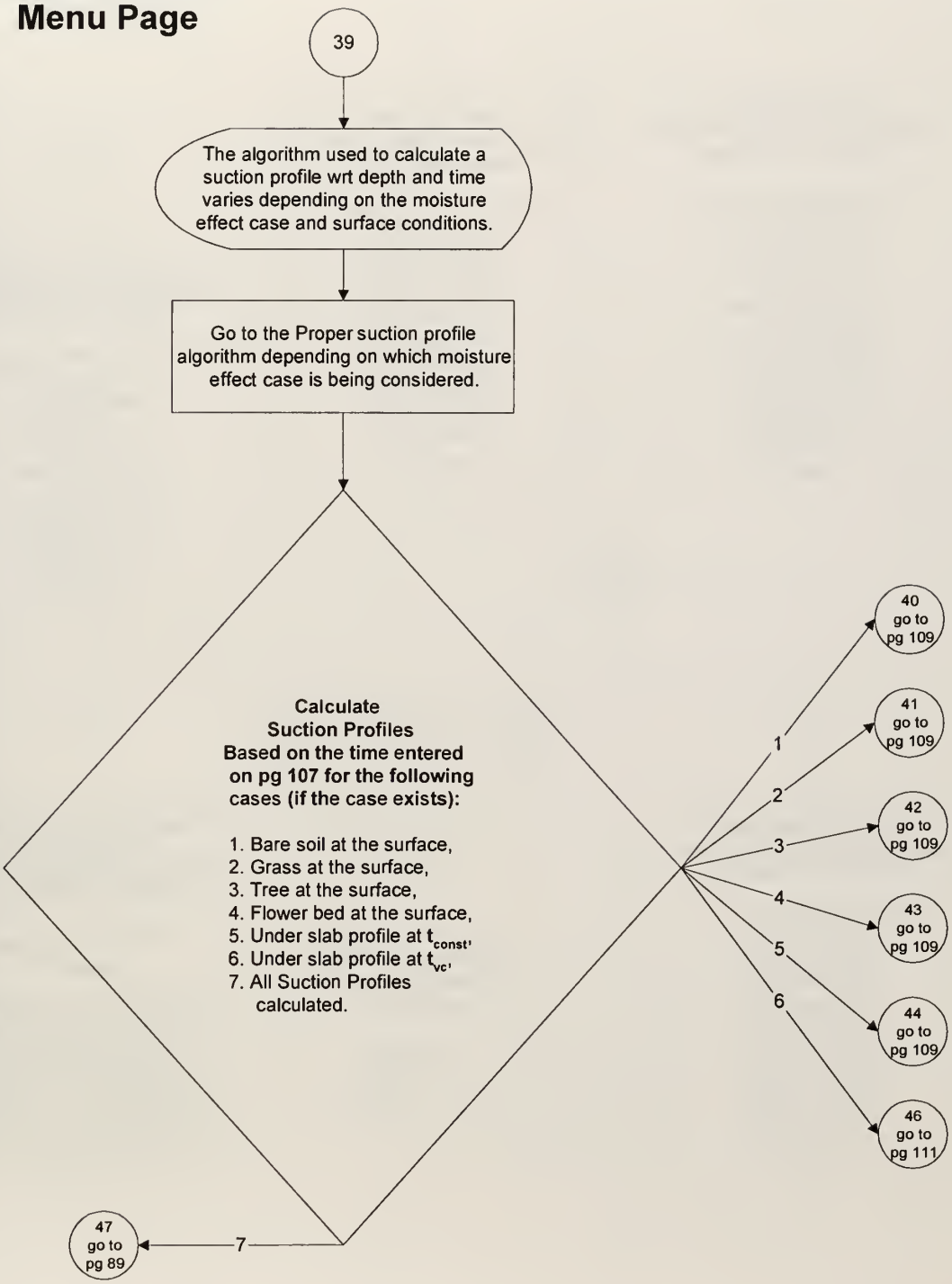
39
The algorithm used to calculate a suction profile wrt depth and time varies depending on the moisture effect case and surface conditions.
Go to the Proper suction profile algorithm depending on which moisture effect case is being considered.
Calculate
Suction Profiles
Based on the time entered on pg 107 for the following cases (if the case exists):
1. Bare soil at the surface,
2. Grass at the surface,
3. Tree at the surface,
4. Flower bed at the surface,
5. Under slab profile at $t_{const}$,
6. Under slab profile at $t_{vc}$,
7. All Suction Profiles calculated.
1
2
3
4
5
6
7
40 go to pg 109
41 go to pg 109
42 go to pg 109
43 go to pg 109
44 go to pg 109
46 go to pg 111
47 go to pg 89

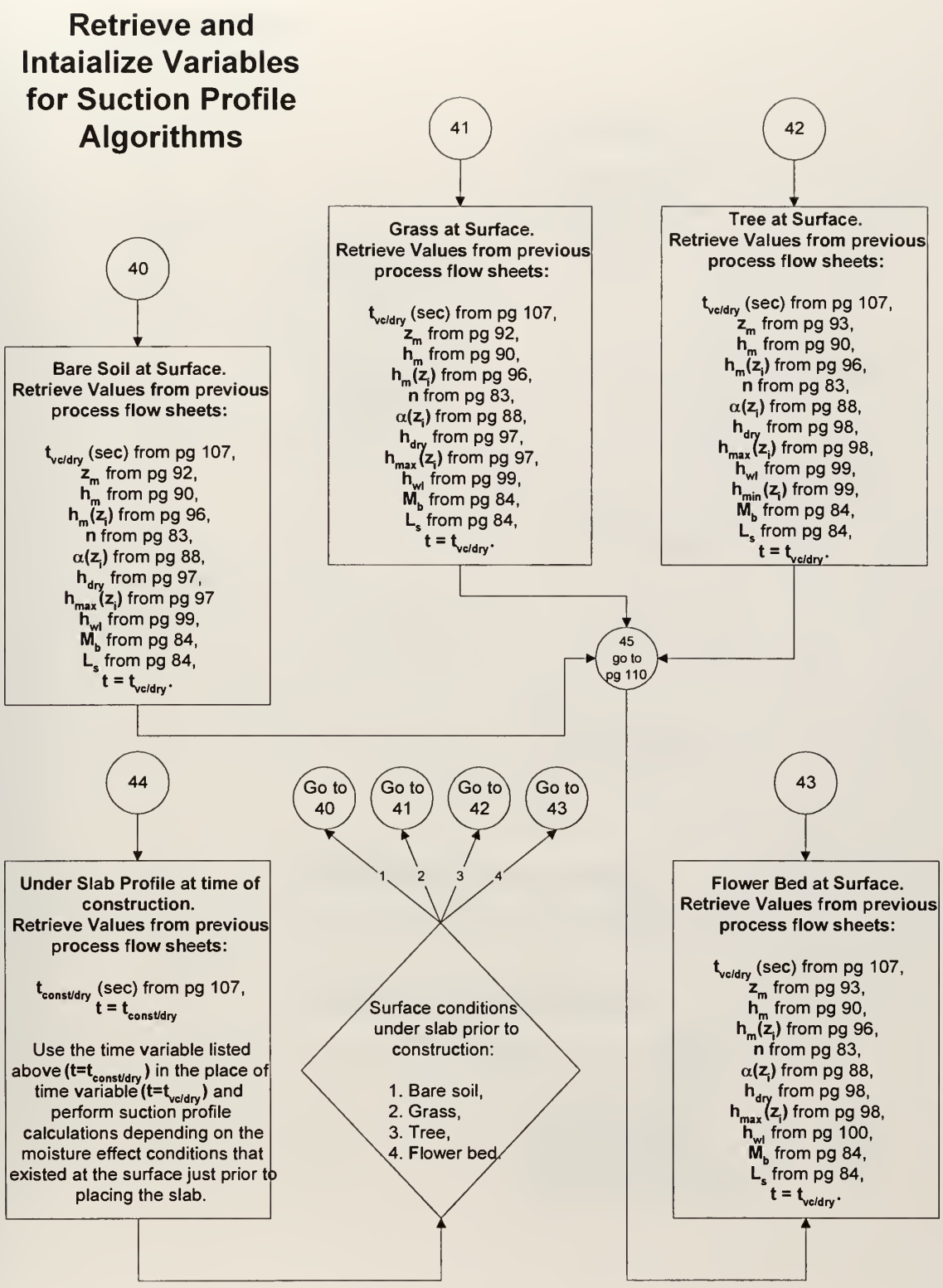
Retrieve and Intaialize Variables for Suction Profile Algorithms
41
42
40
Grass at Surface. Retrieve Values from previous process flow sheets:
$t_{vc/dry}$ (sec) from pg 107,
$z_m$ from pg 92,
$h_m$ from pg 90,
$h_m(z_i)$ from pg 96,
n from pg 83,
$\alpha(z_i)$ from pg 88,
$h_{dry}$ from pg 97,
$h_{max}(z_i)$ from pg 97,
$h_{wl}$ from pg 99,
$M_b$ from pg 84,
$L_s$ from pg 84,
$t = t_{vc/dry}$.
Tree at Surface. Retrieve Values from previous process flow sheets:
$t_{vc/dry}$ (sec) from pg 107,
$z_m$ from pg 93,
$h_m$ from pg 90,
$h_m(z_i)$ from pg 96,
n from pg 83,
$\alpha(z_i)$ from pg 88,
$h_{dry}$ from pg 98,
$h_{max}(z_i)$ from pg 98,
$h_{wl}$ from pg 99,
$h_{min}(z_i)$ from 99,
$M_b$ from pg 84,
$L_s$ from pg 84,
$t = t_{vc/dry}$.
Bare Soil at Surface. Retrieve Values from previous process flow sheets:
$t_{vc/dry}$ (sec) from pg 107,
$z_m$ from pg 92,
$h_m$ from pg 90,
$h_m(z_i)$ from pg 96,
n from pg 83,
$\alpha(z_i)$ from pg 88,
$h_{dry}$ from pg 97,
$h_{max}(z_i)$ from pg 97
$h_{wl}$ from pg 99,
$M_b$ from pg 84,
$L_s$ from pg 84,
$t = t_{vc/dry}$.
45 go to pg 110
44
43
Go to 40
Go to 41
Go to 42
Go to 43
1
2
3
4
Surface conditions under slab prior to construction:
1. Bare soil,
2. Grass,
3. Tree,
4. Flower bed.
Under Slab Profile at time of construction. Retrieve Values from previous process flow sheets:
$t_{const/dry}$ (sec) from pg 107,
$t = t_{const/dry}$
Use the time variable listed above ($t=t_{const/dry}$) in the place of time variable ($t=t_{vc/dry}$) and perform suction profile calculations depending on the moisture effect conditions that existed at the surface just prior to placing the slab.
Flower Bed at Surface. Retrieve Values from previous process flow sheets:
$t_{vc/dry}$ (sec) from pg 107,
$z_m$ from pg 93,
$h_m$ from pg 90,
$h_m(z_i)$ from pg 96,
n from pg 83,
$\alpha(z_i)$ from pg 88,
$h_{dry}$ from pg 98,
$h_{max}(z_i)$ from pg 98,
$h_{wl}$ from pg 100,
$M_b$ from pg 84,
$L_s$ from pg 84,
$t = t_{vc/dry}$.

# Suction Profile Algorithms

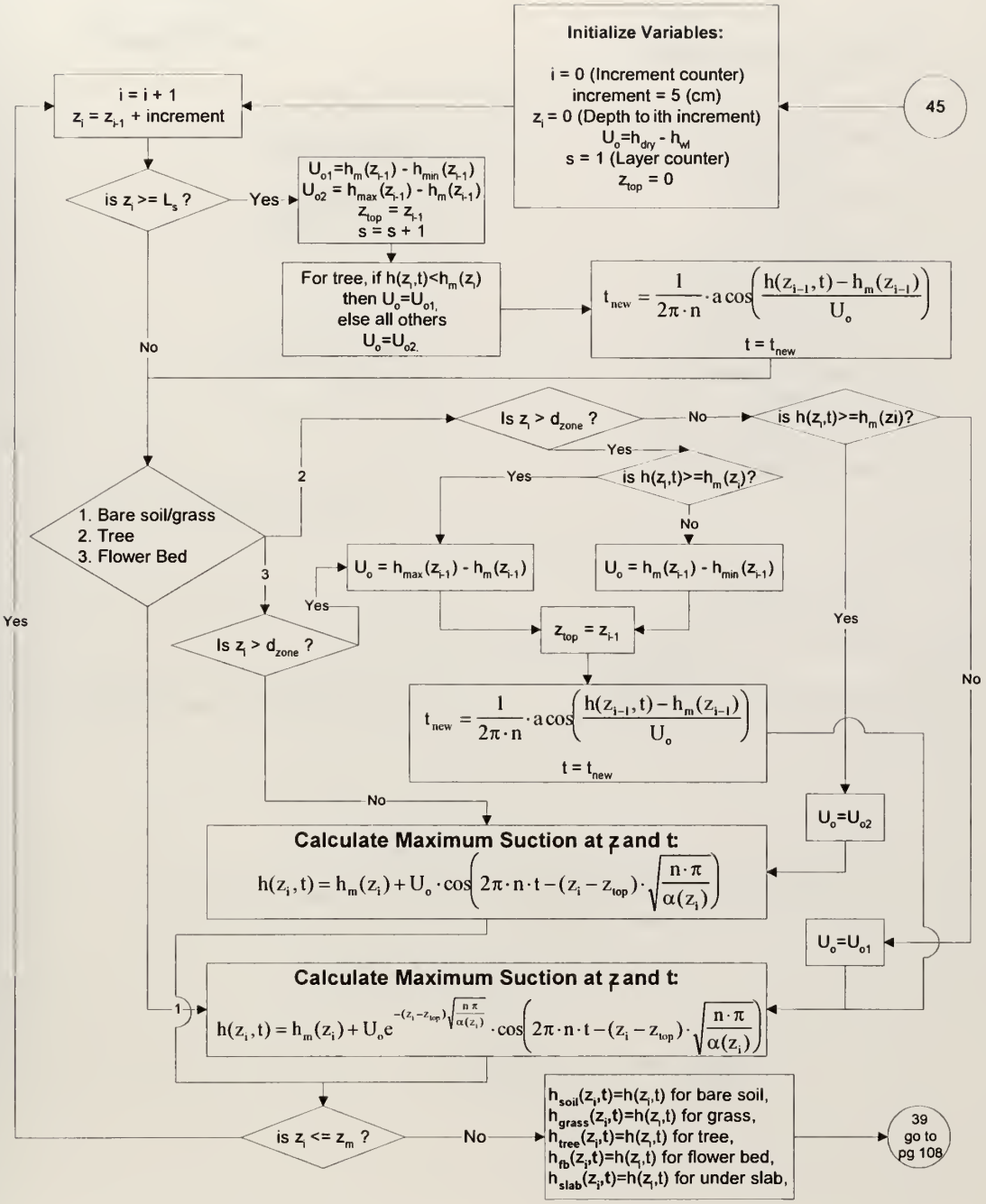

# "Damped" Suction Profile Underneath the Slab "$h_{slab}(z_i,t_{vc/dry})$"

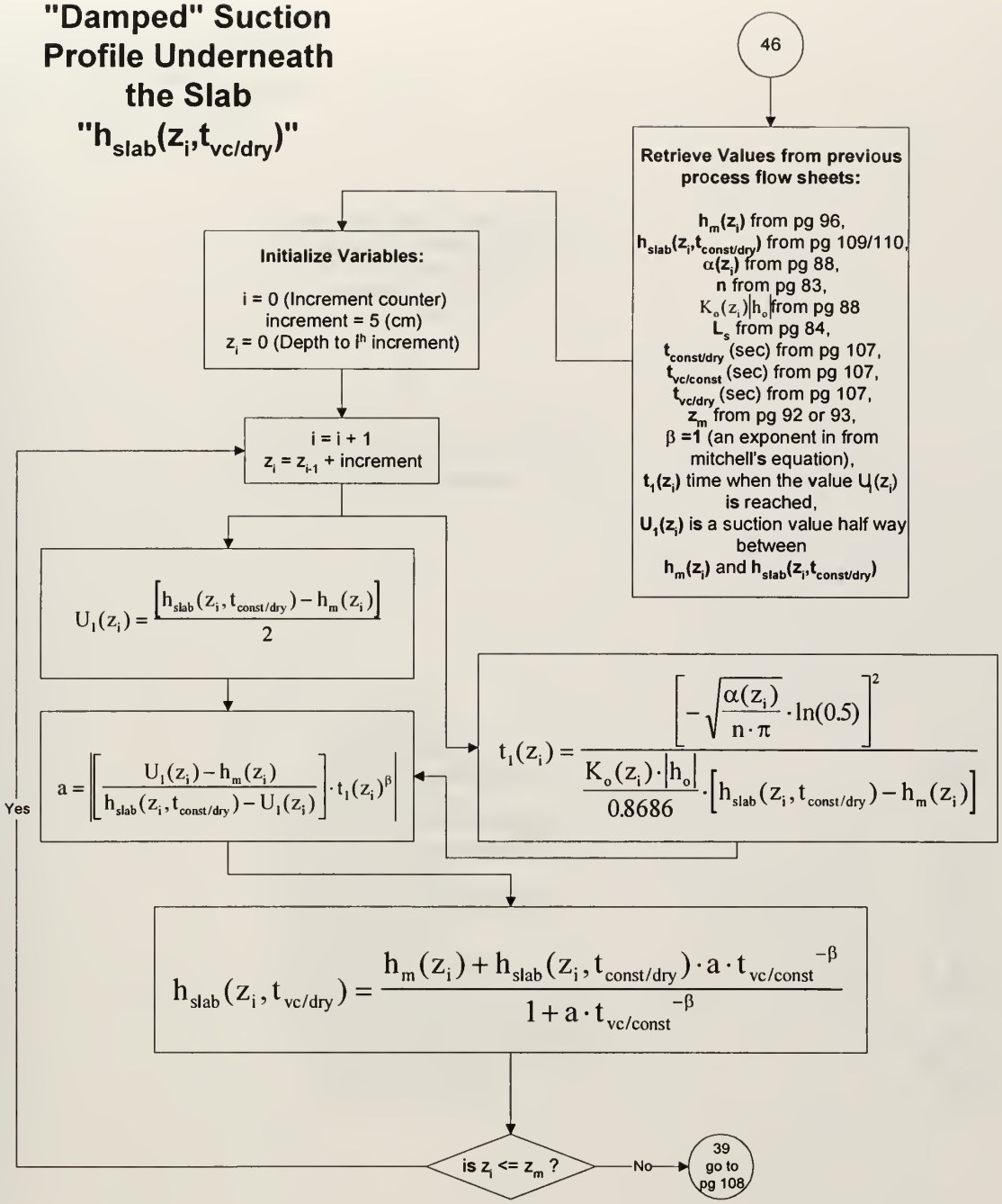
46
Retrieve Values from previous process flow sheets:
$h_m(z_i)$ from pg 96,
$h_{slab}(z_i,t_{const/dry})$ from pg 109/110,
$\alpha(z_i)$ from pg 88,
n from pg 83,
$K_o(z_i)|h_o|$ from pg 88
$L_s$ from pg 84,
$t_{const/dry}$ (sec) from pg 107,
$t_{vc/const}$ (sec) from pg 107,
$t_{vc/dry}$ (sec) from pg 107,
$z_m$ from pg 92 or 93,
$\beta$ =1 (an exponent in from mitchell's equation),
$t_1(z_i)$ time when the value $U_1(z_i)$ is reached,
$U_1(z_i)$ is a suction value half way between $h_m(z_i)$ and $h_{slab}(z_i,t_{const/dry})$
Initialize Variables:
i = 0 (Increment counter)
increment = 5 (cm)
$z_i$ = 0 (Depth to $i^{th}$ increment)
i = i + 1
$z_i = z_{i-1}$ + increment
$U_1(z_i) = \frac{\left[h_{slab}(z_i,t_{const/dry}) - h_m(z_i)\right]}{2}$
$t_1(z_i) = \frac{\left[-\sqrt{\frac{\alpha(z_i)}{n\cdot\pi}}\cdot\ln(0.5)\right]^2}{\frac{K_o(z_i)\cdot|h_o|}{0.8686}\cdot\left[h_{slab}(z_i,t_{const/dry}) - h_m(z_i)\right]}$
$a = \left|\left[\frac{U_1(z_i) - h_m(z_i)}{h_{slab}(z_i,t_{const/dry}) - U_1(z_i)}\right]\cdot t_1(z_i)^{\beta}\right|$
Yes
$h_{slab}(z_i,t_{vc/dry}) = \frac{h_m(z_i) + h_{slab}(z_i,t_{const/dry})\cdot a\cdot t_{vc/const}^{-\beta}}{1 + a\cdot t_{vc/const}^{-\beta}}$
is $z_i$ <= $z_m$ ?
No
39
go to
pg 108

# Post Construction Soil Volume Change Menu Page

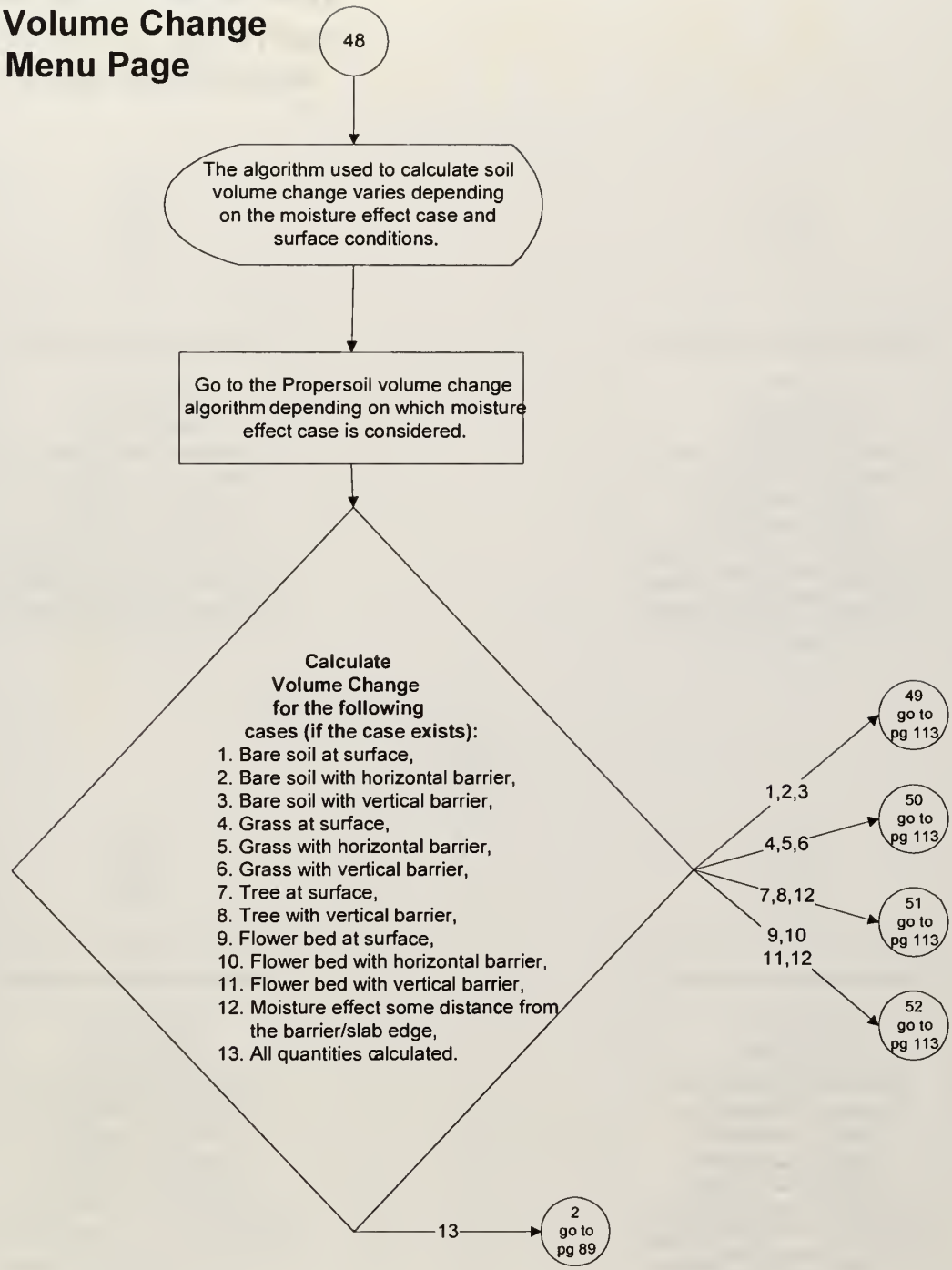
48
The algorithm used to calculate soil volume change varies depending on the moisture effect case and surface conditions.
Go to the Propersoil volume change algorithm depending on which moisture effect case is considered.
Calculate Volume Change for the following cases (if the case exists):
1. Bare soil at surface,
2. Bare soil with horizontal barrier,
3. Bare soil with vertical barrier,
4. Grass at surface,
5. Grass with horizontal barrier,
6. Grass with vertical barrier,
7. Tree at surface,
8. Tree with vertical barrier,
9. Flower bed at surface,
10. Flower bed with horizontal barrier,
11. Flower bed with vertical barrier,
12. Moisture effect some distance from the barrier/slab edge,
13. All quantities calculated.
1,2,3
4,5,6
7,8,12
9,10
11,12
49 go to pg 113
50 go to pg 113
51 go to pg 113
52 go to pg 113
13
2 go to pg 89

# Retrive Values for a Particular Case of Post Construction Soil Volume Change Calculations

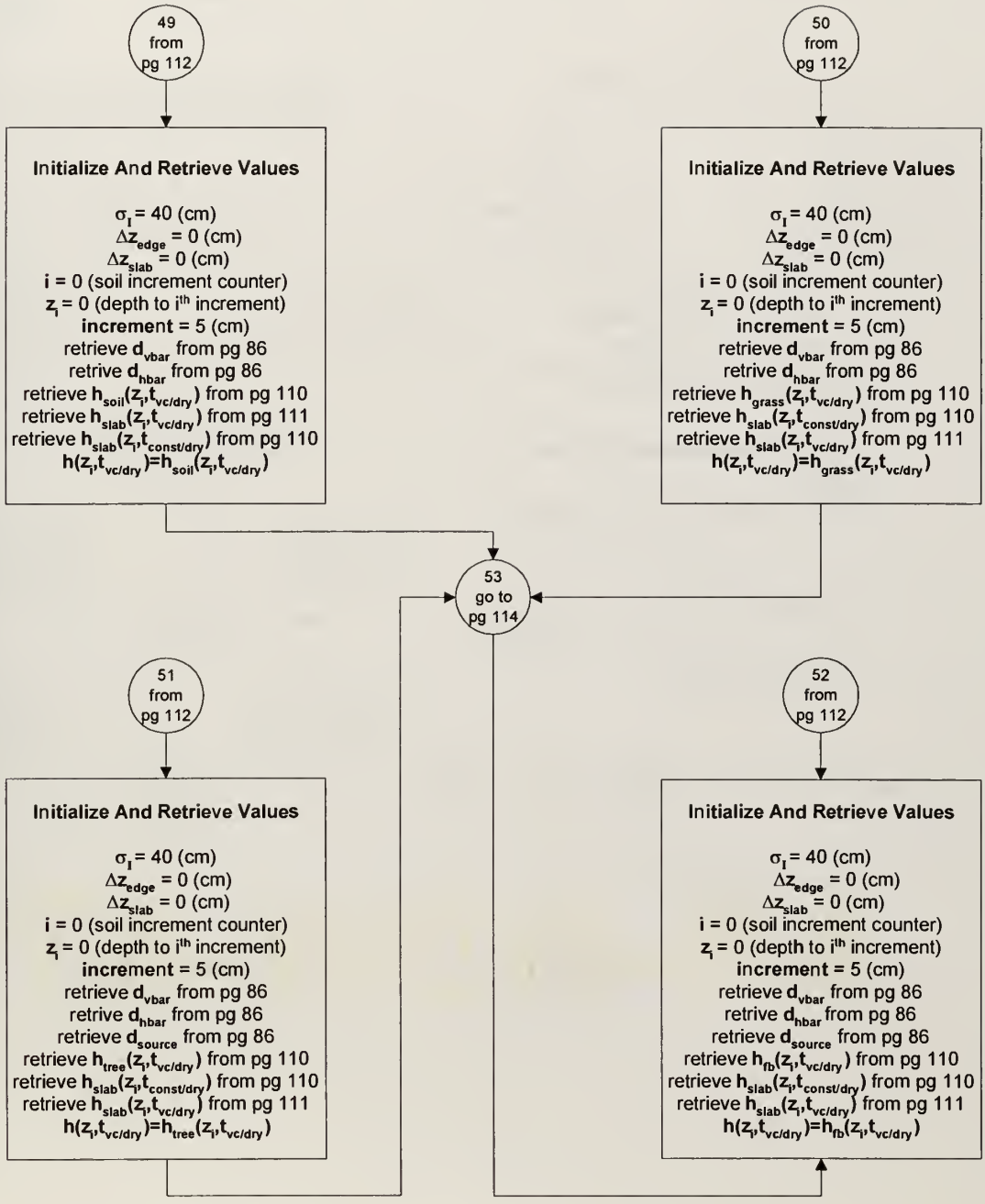
49 from pg 112
Initialize And Retrieve Values
$\sigma_1$ = 40 (cm)
$\Delta z_{edge}$ = 0 (cm)
$\Delta z_{slab}$ = 0 (cm)
i = 0 (soil increment counter)
$z_i$ = 0 (depth to $i^{th}$ increment)
increment = 5 (cm)
retrieve $d_{vbar}$ from pg 86
retrive $d_{hbar}$ from pg 86
retrieve $h_{soil}(z_i,t_{vc/dry})$ from pg 110
retrieve $h_{slab}(z_i,t_{vc/dry})$ from pg 111
retrieve $h_{slab}(z_i,t_{const/dry})$ from pg 110
$h(z_i,t_{vc/dry})=h_{soil}(z_i,t_{vc/dry})$
50 from pg 112
Initialize And Retrieve Values
$\sigma_1$ = 40 (cm)
$\Delta z_{edge}$ = 0 (cm)
$\Delta z_{slab}$ = 0 (cm)
i = 0 (soil increment counter)
$z_i$ = 0 (depth to $i^{th}$ increment)
increment = 5 (cm)
retrieve $d_{vbar}$ from pg 86
retrive $d_{hbar}$ from pg 86
retrieve $h_{grass}(z_i,t_{vc/dry})$ from pg 110
retrieve $h_{slab}(z_i,t_{const/dry})$ from pg 110
retrieve $h_{slab}(z_i,t_{vc/dry})$ from pg 111
$h(z_i,t_{vc/dry})=h_{grass}(z_i,t_{vc/dry})$
53 go to pg 114
51 from pg 112
Initialize And Retrieve Values
$\sigma_1$ = 40 (cm)
$\Delta z_{edge}$ = 0 (cm)
$\Delta z_{slab}$ = 0 (cm)
i = 0 (soil increment counter)
$z_i$ = 0 (depth to $i^{th}$ increment)
increment = 5 (cm)
retrieve $d_{vbar}$ from pg 86
retrive $d_{hbar}$ from pg 86
retrieve $d_{source}$ from pg 86
retrieve $h_{tree}(z_i,t_{vc/dry})$ from pg 110
retrieve $h_{slab}(z_i,t_{const/dry})$ from pg 110
retrieve $h_{slab}(z_i,t_{vc/dry})$ from pg 111
$h(z_i,t_{vc/dry})=h_{tree}(z_i,t_{vc/dry})$
52 from pg 112
Initialize And Retrieve Values
$\sigma_1$ = 40 (cm)
$\Delta z_{edge}$ = 0 (cm)
$\Delta z_{slab}$ = 0 (cm)
i = 0 (soil increment counter)
$z_i$ = 0 (depth to $i^{th}$ increment)
increment = 5 (cm)
retrieve $d_{vbar}$ from pg 86
retrive $d_{hbar}$ from pg 86
retrieve $d_{source}$ from pg 86
retrieve $h_{fb}(z_i,t_{vc/dry})$ from pg 110
retrieve $h_{slab}(z_i,t_{const/dry})$ from pg 110
retrieve $h_{slab}(z_i,t_{vc/dry})$ from pg 111
$h(z_i,t_{vc/dry})=h_{fb}(z_i,t_{vc/dry})$

# Post construction Soil Volume Change Calculations With or Without Barriers (Part I of II)

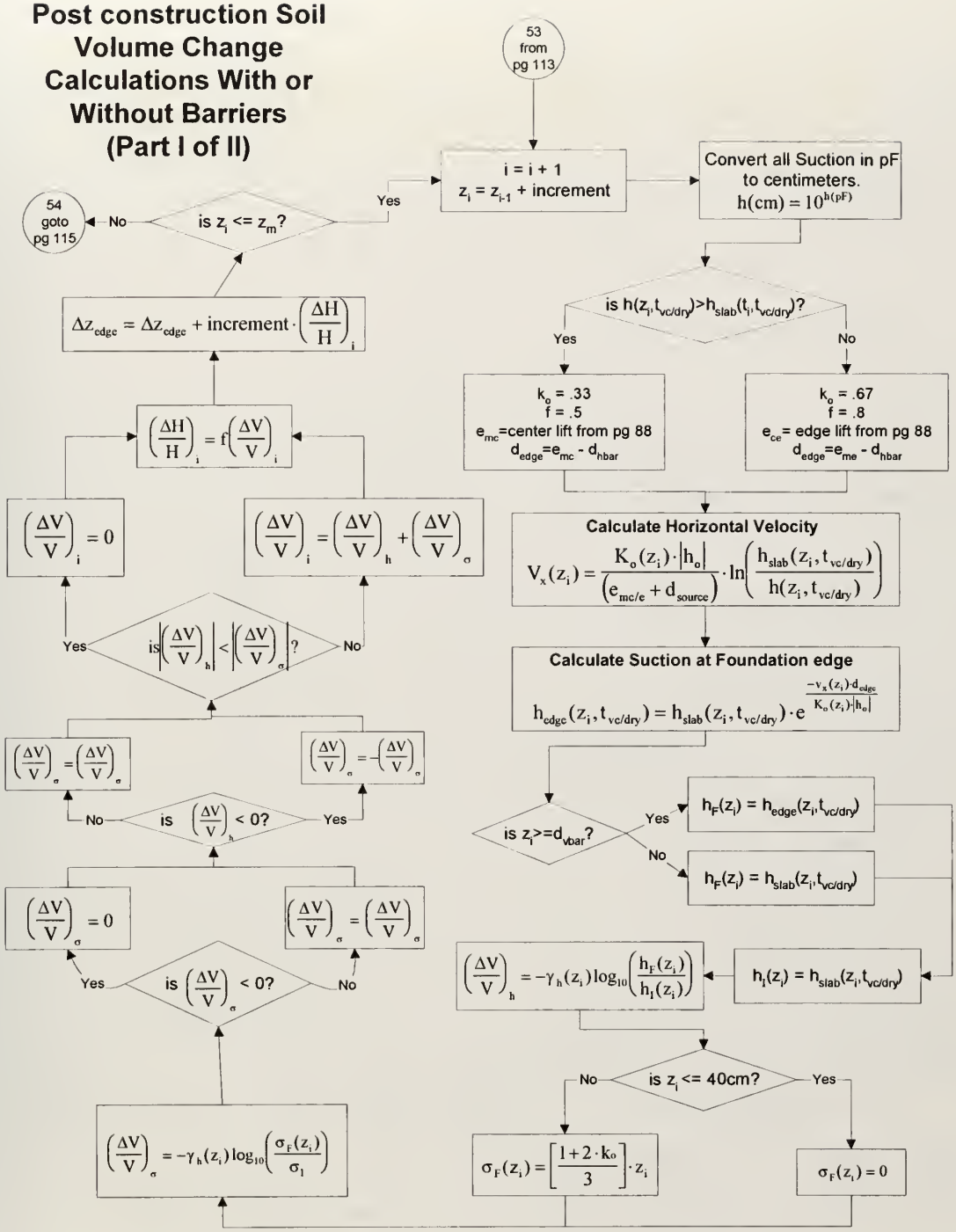
53 from pg 113
i = i + 1
$z_i = z_{i-1}$ + increment
Convert all Suction in pF to centimeters.
$h(cm) = 10^{h(pF)}$
is $z_i <= z_m$?
Yes
No
54 goto pg 115
is $h(z_i, t_{vc/dry}) > h_{slab}(t_i, t_{vc/dry})$?
Yes
No
$k_o$ = .33
f = .5
$e_{mc}$=center lift from pg 88
$d_{edge}=e_{mc} - d_{hbar}$
$k_o$ = .67
f = .8
$e_{ce}$= edge lift from pg 88
$d_{edge}=e_{me} - d_{hbar}$
$\Delta z_{edge} = \Delta z_{edge} + \text{increment} \cdot \left(\frac{\Delta H}{H}\right)_i$
$\left(\frac{\Delta H}{H}\right)_i = f\left(\frac{\Delta V}{V}\right)_i$
Calculate Horizontal Velocity
$V_x(z_i) = \frac{K_o(z_i) \cdot |h_o|}{(e_{mc/e} + d_{source})} \cdot \ln\left(\frac{h_{slab}(z_i, t_{vc/dry})}{h(z_i, t_{vc/dry})}\right)$
$\left(\frac{\Delta V}{V}\right)_i = 0$
$\left(\frac{\Delta V}{V}\right)_i = \left(\frac{\Delta V}{V}\right)_h + \left(\frac{\Delta V}{V}\right)_\sigma$
Yes
is $\left|\left(\frac{\Delta V}{V}\right)_h\right| < \left|\left(\frac{\Delta V}{V}\right)_\sigma\right|$?
No
Calculate Suction at Foundation edge
$h_{edge}(z_i, t_{vc/dry}) = h_{slab}(z_i, t_{vc/dry}) \cdot e^{\frac{-v_x(z_i) \cdot d_{edge}}{K_o(z_i) \cdot |h_o|}}$
$\left(\frac{\Delta V}{V}\right)_\sigma = \left(\frac{\Delta V}{V}\right)_\sigma$
$\left(\frac{\Delta V}{V}\right)_\sigma = -\left(\frac{\Delta V}{V}\right)_\sigma$
No
is $\left(\frac{\Delta V}{V}\right)_h$ < 0?
Yes
is $z_i >= d_{vbar}$?
Yes
No
$h_F(z_i) = h_{edge}(z_i, t_{vc/dry})$
$h_F(z_i) = h_{slab}(z_i, t_{vc/dry})$
$\left(\frac{\Delta V}{V}\right)_\sigma = 0$
$\left(\frac{\Delta V}{V}\right)_\sigma = \left(\frac{\Delta V}{V}\right)_\sigma$
Yes
is $\left(\frac{\Delta V}{V}\right)_\sigma$ < 0?
No
$\left(\frac{\Delta V}{V}\right)_h = -\gamma_h(z_i) \log_{10}\left(\frac{h_F(z_i)}{h_i(z_i)}\right)$
$h_i(z_i) = h_{slab}(z_i, t_{vc/dry})$
No
is $z_i <= 40cm$?
Yes
$\left(\frac{\Delta V}{V}\right)_\sigma = -\gamma_h(z_i) \log_{10}\left(\frac{\sigma_F(z_i)}{\sigma_1}\right)$
$\sigma_F(z_i) = \left[\frac{1 + 2 \cdot k_o}{3}\right] \cdot z_i$
$\sigma_F(z_i) = 0$

# Post construction Soil Volume Change Calculations With or Without Barriers (Part II of II)

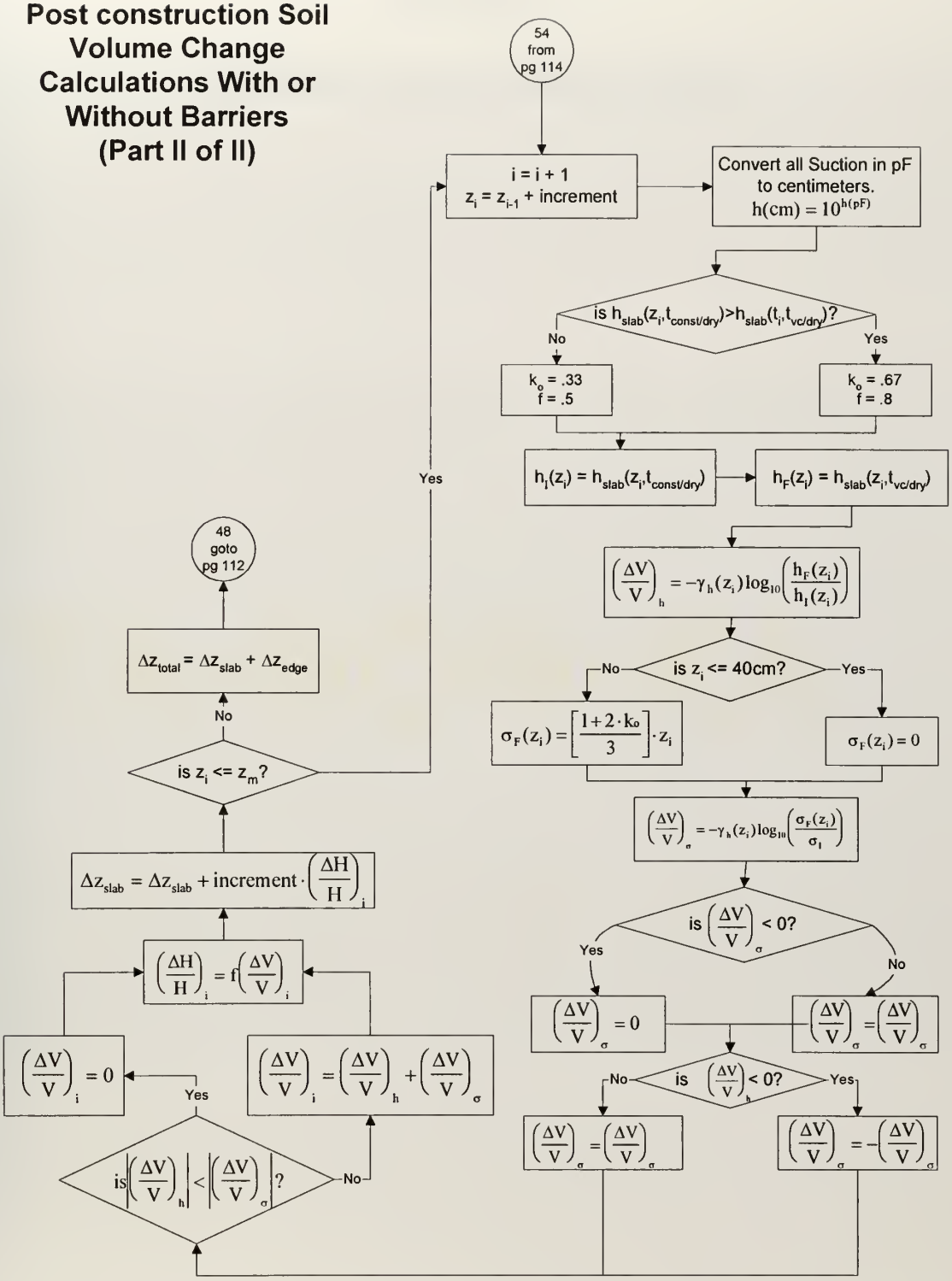

# APPENDIX B

## SOFTWARE PROGRAM DESIGN LAYOUT

# Program Design Layout

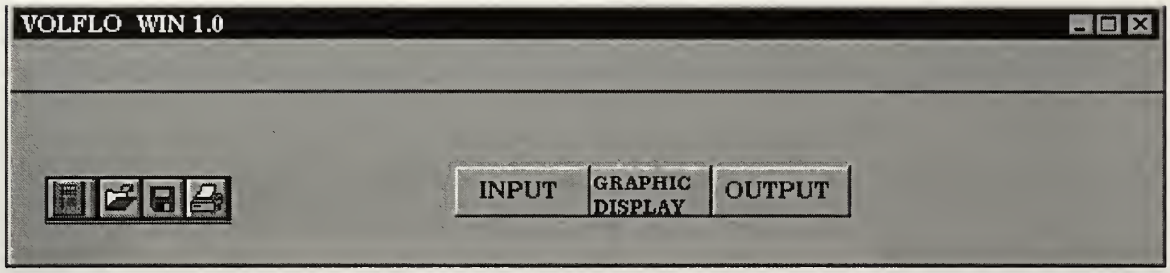


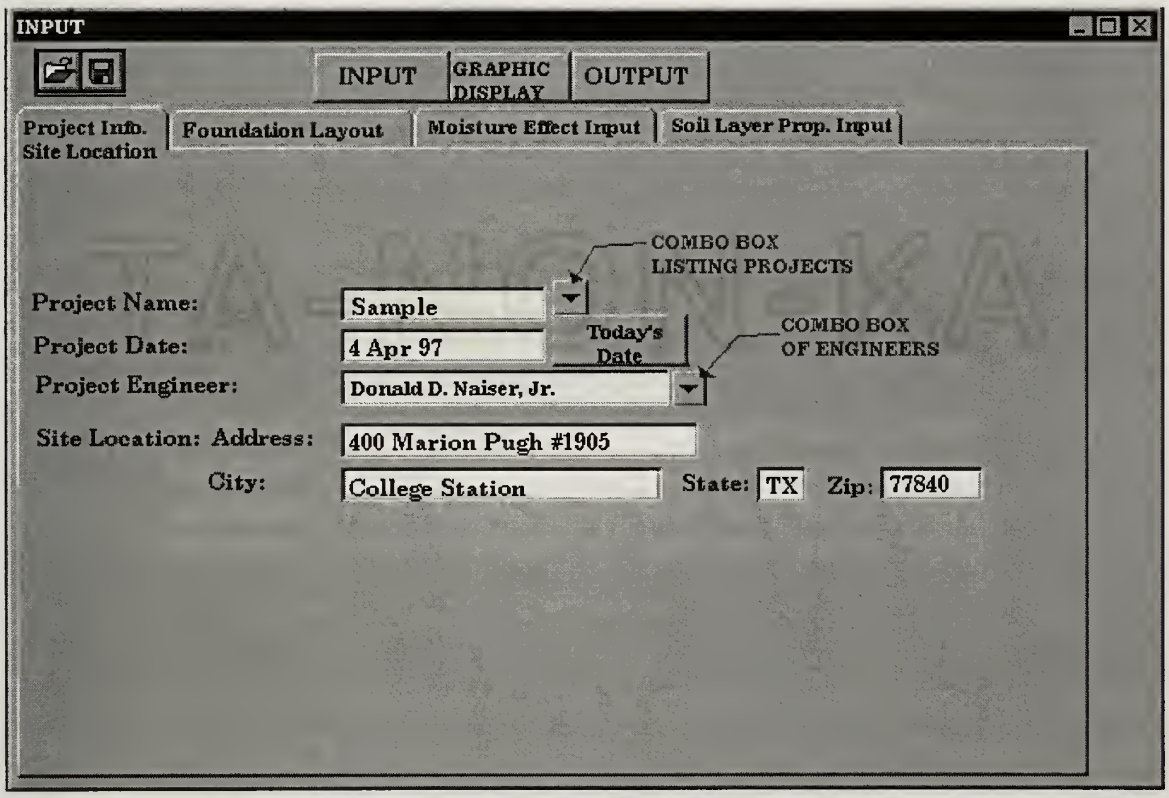

# Program Design Layout

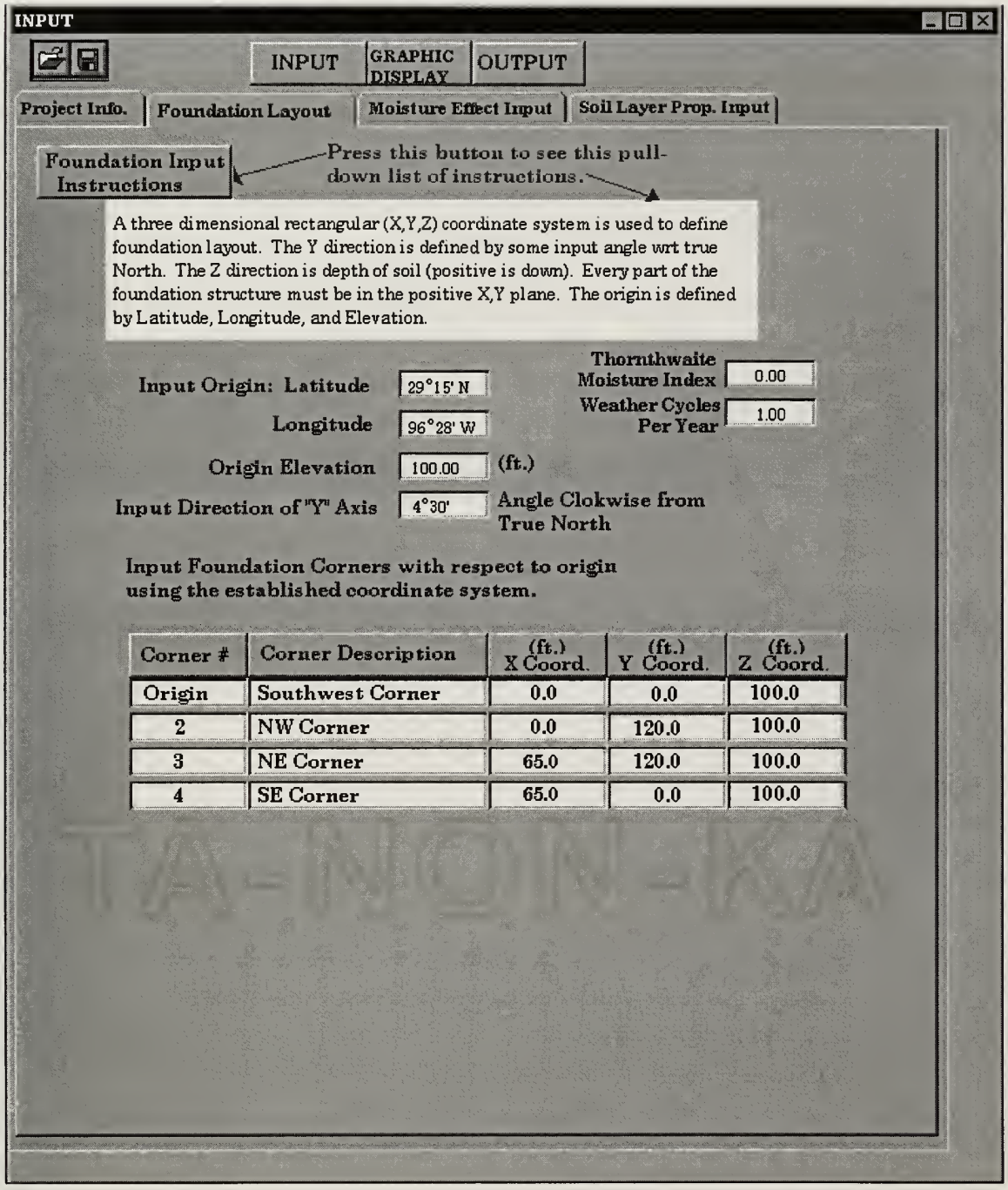
INPUT
INPUT
GRAPHIC DISPLAY
OUTPUT
Project Info.
Foundation Layout
Moisture Effect Input
Soil Layer Prop. Input
Foundation Input Instructions
Press this button to see this pull-down list of instructions.
A three dimensional rectangular (X,Y,Z) coordinate system is used to define foundation layout. The Y direction is defined by some input angle wrt true North. The Z direction is depth of soil (positive is down). Every part of the foundation structure must be in the positive X,Y plane. The origin is defined by Latitude, Longitude, and Elevation.
Input Origin: Latitude
29°15' N
Longitude
96°28' W
Origin Elevation
100.00
(ft.)
Input Direction of "Y" Axis
4°30'
Angle Clokwise from True North
Thornthwaite Moisture Index
0.00
Weather Cycles Per Year
1.00
Input Foundation Corners with respect to origin using the established coordinate system.
Corner # | Corner Description | (ft.) X Coord. | (ft.) Y Coord. | (ft.) Z Coord.
Origin | Southwest Corner | 0.0 | 0.0 | 100.0
2 | NW Corner | 0.0 | 120.0 | 100.0
3 | NE Corner | 65.0 | 120.0 | 100.0
4 | SE Corner | 65.0 | 0.0 | 100.0

# Program Design Layout

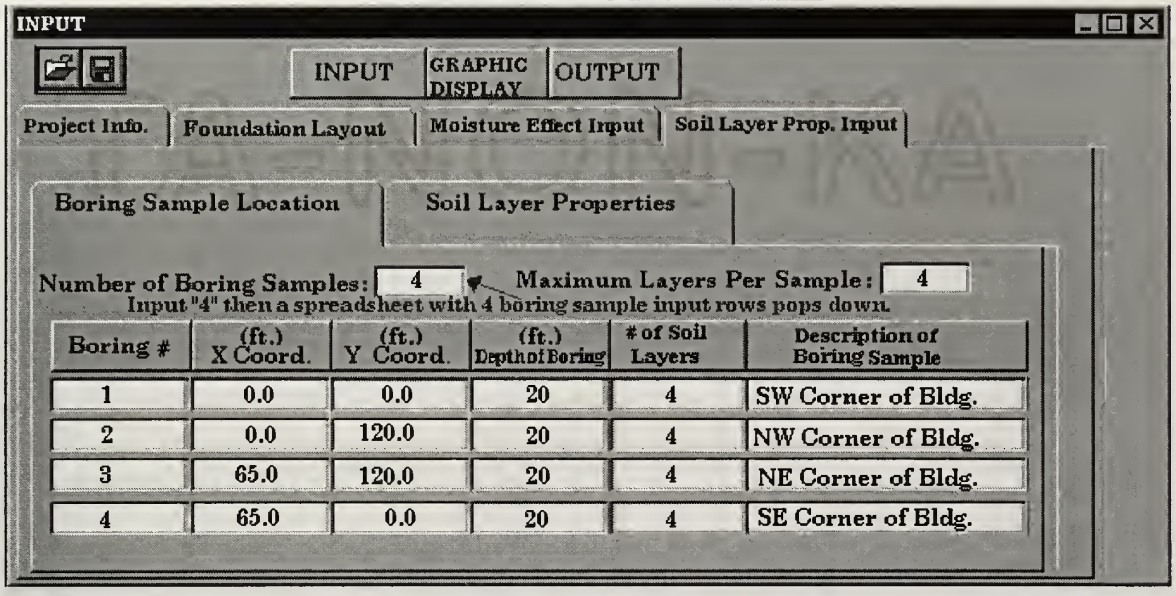
INPUT
INPUT
GRAPHIC DISPLAY
OUTPUT
Project Info.
Foundation Layout
Moisture Effect Input
Soil Layer Prop. Input
Boring Sample Location
Soil Layer Properties
Number of Boring Samples: 4
Maximum Layers Per Sample: 4
Input "4" then a spreadsheet with 4 boring sample input rows pops down.
Boring # | (ft.) X Coord. | (ft.) Y Coord. | (ft.) Depth of Boring | # of Soil Layers | Description of Boring Sample
1 | 0.0 | 0.0 | 20 | 4 | SW Corner of Bldg.
2 | 0.0 | 120.0 | 20 | 4 | NW Corner of Bldg.
3 | 65.0 | 120.0 | 20 | 4 | NE Corner of Bldg.
4 | 65.0 | 0.0 | 20 | 4 | SE Corner of Bldg.

# Program Design Layout

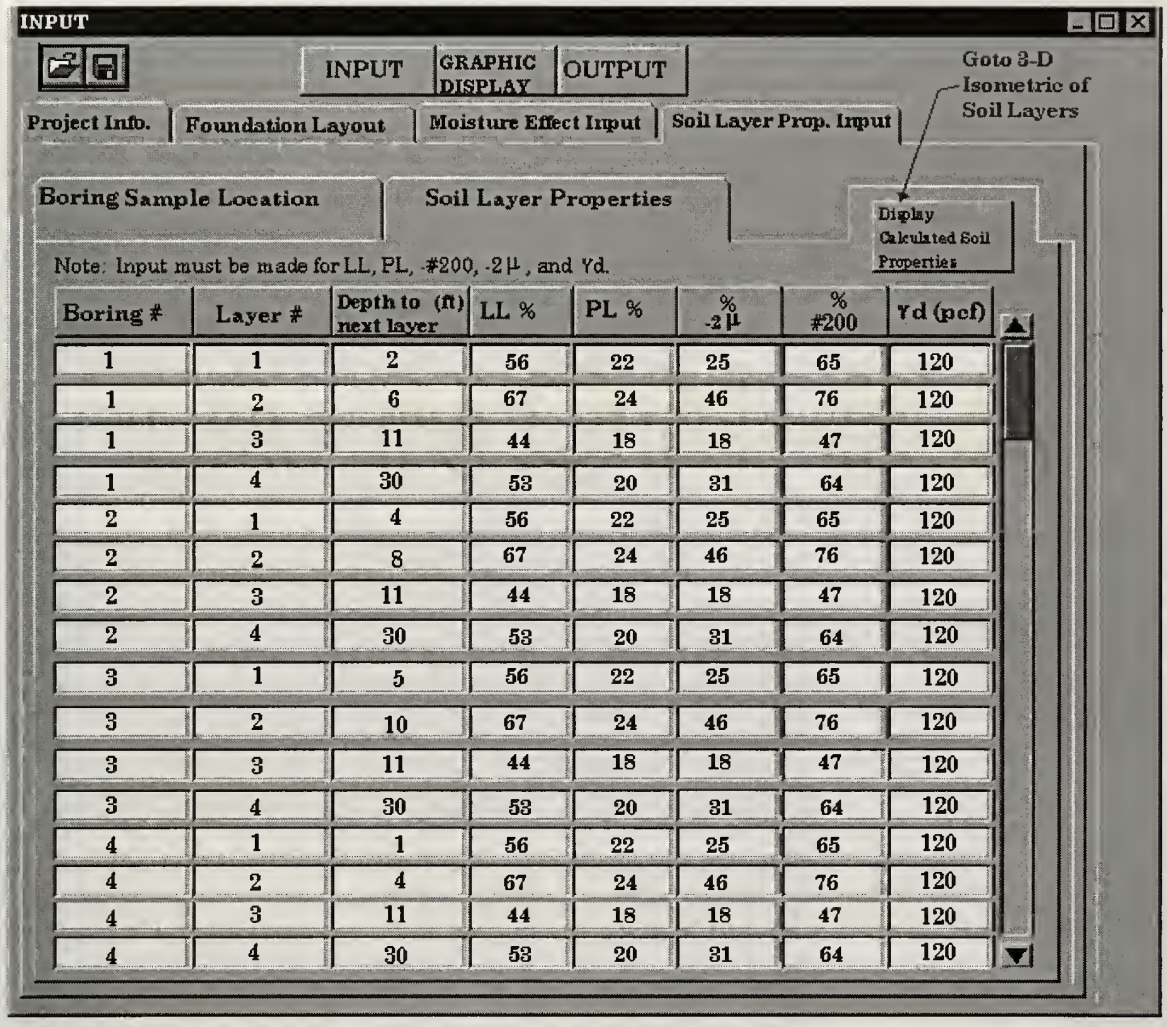


| Boring # | Layer # | Depth to (ft) next layer | LL % | PL % | % -2μ | % #200 | Yd (pcf) |
|---|---|---|---|---|---|---|---|
| 1 | 1 | 2 | 56 | 22 | 25 | 65 | 120 |
| 1 | 2 | 6 | 67 | 24 | 46 | 76 | 120 |
| 1 | 3 | 11 | 44 | 18 | 18 | 47 | 120 |
| 1 | 4 | 30 | 53 | 20 | 31 | 64 | 120 |
| 2 | 1 | 4 | 56 | 22 | 25 | 65 | 120 |
| 2 | 2 | 8 | 67 | 24 | 46 | 76 | 120 |
| 2 | 3 | 11 | 44 | 18 | 18 | 47 | 120 |
| 2 | 4 | 30 | 53 | 20 | 31 | 64 | 120 |
| 3 | 1 | 5 | 56 | 22 | 25 | 65 | 120 |
| 3 | 2 | 10 | 67 | 24 | 46 | 76 | 120 |
| 3 | 3 | 11 | 44 | 18 | 18 | 47 | 120 |
| 3 | 4 | 30 | 53 | 20 | 31 | 64 | 120 |
| 4 | 1 | 1 | 56 | 22 | 25 | 65 | 120 |
| 4 | 2 | 4 | 67 | 24 | 46 | 76 | 120 |
| 4 | 3 | 11 | 44 | 18 | 18 | 47 | 120 |
| 4 | 4 | 30 | 53 | 20 | 31 | 64 | 120 |

# Program Design Layout

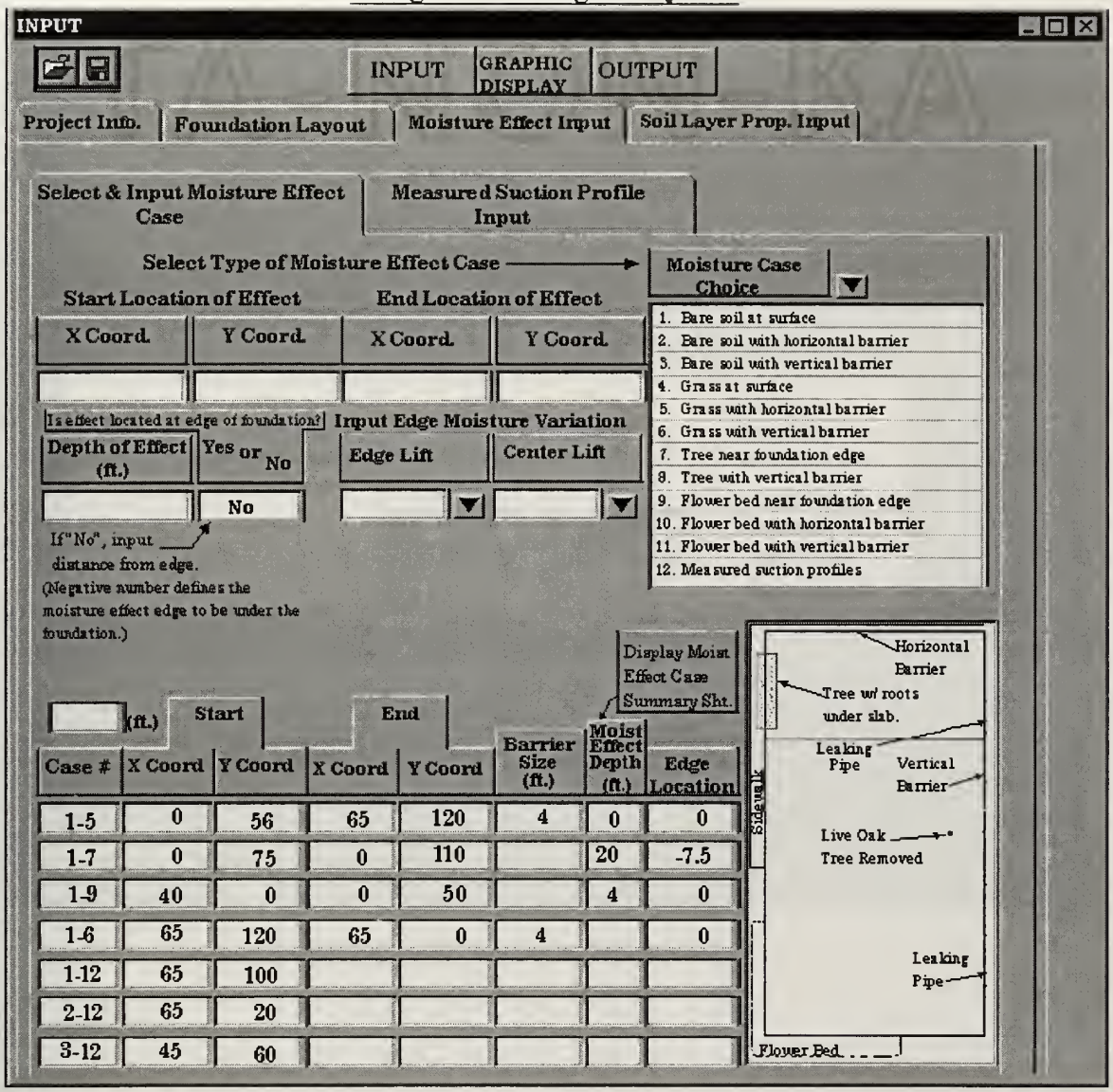

# Program Design Layout

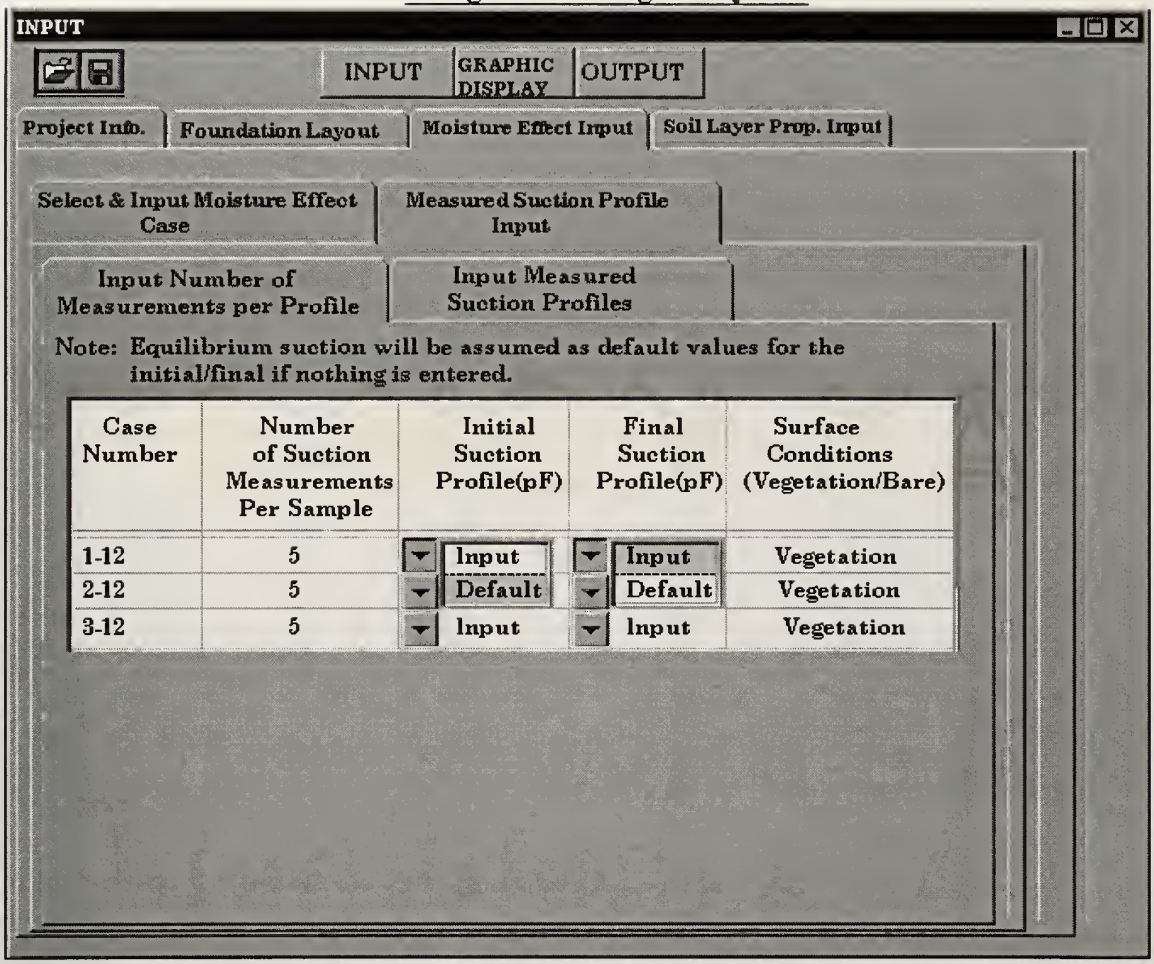
INPUT
INPUT
GRAPHIC DISPLAY
OUTPUT
Project Info.
Foundation Layout
Moisture Effect Input
Soil Layer Prop. Input
Select & Input Moisture Effect Case
Measured Suction Profile Input
Input Number of Measurements per Profile
Input Measured Suction Profiles
Note: Equilibrium suction will be assumed as default values for the initial/final if nothing is entered.
Case Number
Number of Suction Measurements Per Sample
Initial Suction Profile(pF)
Final Suction Profile(pF)
Surface Conditions (Vegetation/Bare)
1-12 5 Input Input Vegetation
2-12 5 Default Default Vegetation
3-12 5 Input Input Vegetation

# Program Design Layout

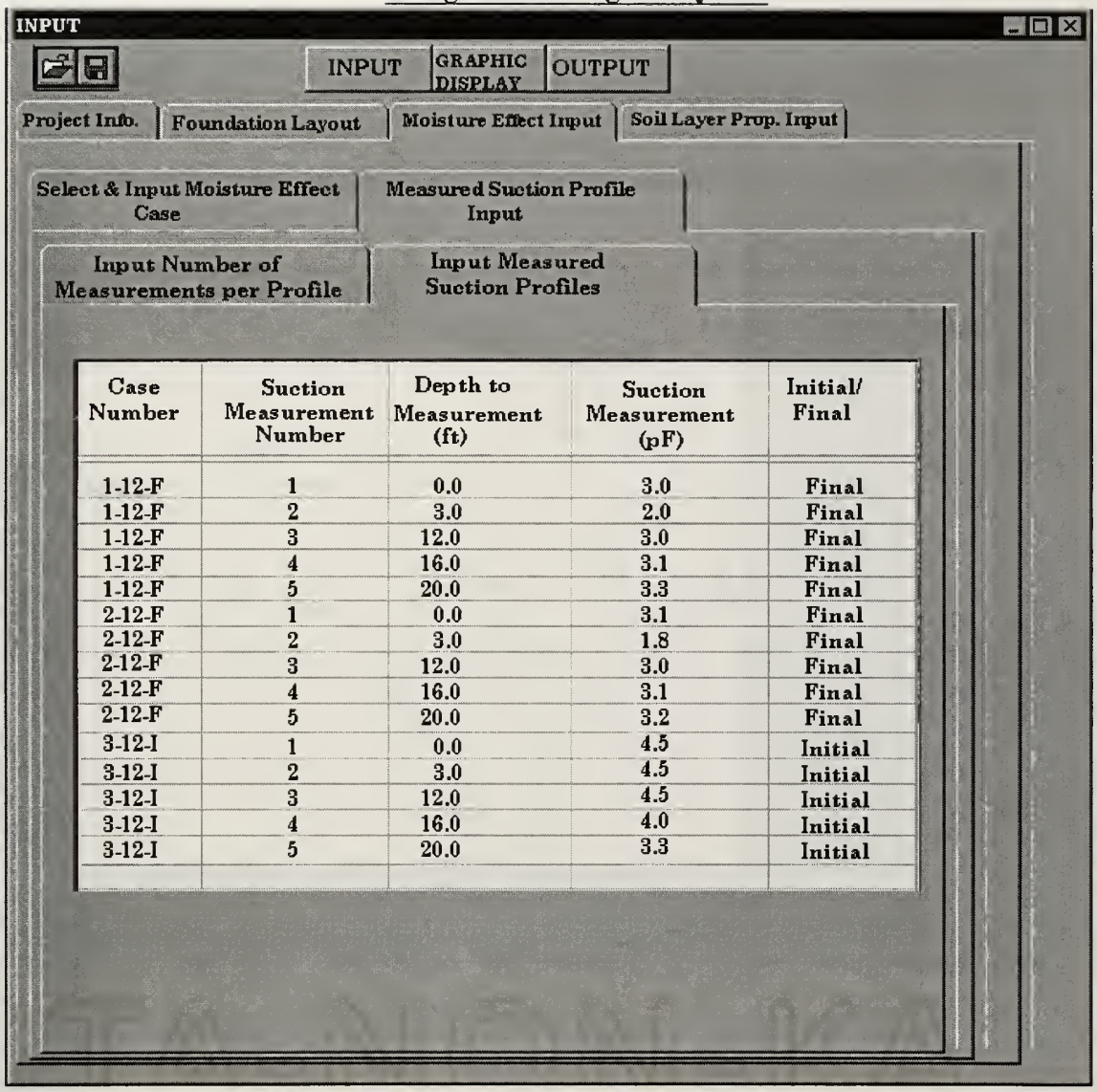


| Case Number | Suction Measurement Number | Depth to Measurement (ft) | Suction Measurement (pF) | Initial/ Final |
|---|---|---|---|---|
| 1-12-F | 1 | 0.0 | 3.0 | Final |
| 1-12-F | 2 | 3.0 | 2.0 | Final |
| 1-12-F | 3 | 12.0 | 3.0 | Final |
| 1-12-F | 4 | 16.0 | 3.1 | Final |
| 1-12-F | 5 | 20.0 | 3.3 | Final |
| 2-12-F | 1 | 0.0 | 3.1 | Final |
| 2-12-F | 2 | 3.0 | 1.8 | Final |
| 2-12-F | 3 | 12.0 | 3.0 | Final |
| 2-12-F | 4 | 16.0 | 3.1 | Final |
| 2-12-F | 5 | 20.0 | 3.2 | Final |
| 3-12-I | 1 | 0.0 | 4.5 | Initial |
| 3-12-I | 2 | 3.0 | 4.5 | Initial |
| 3-12-I | 3 | 12.0 | 4.5 | Initial |
| 3-12-I | 4 | 16.0 | 4.0 | Initial |
| 3-12-I | 5 | 20.0 | 3.3 | Initial |

# Program Design Layout

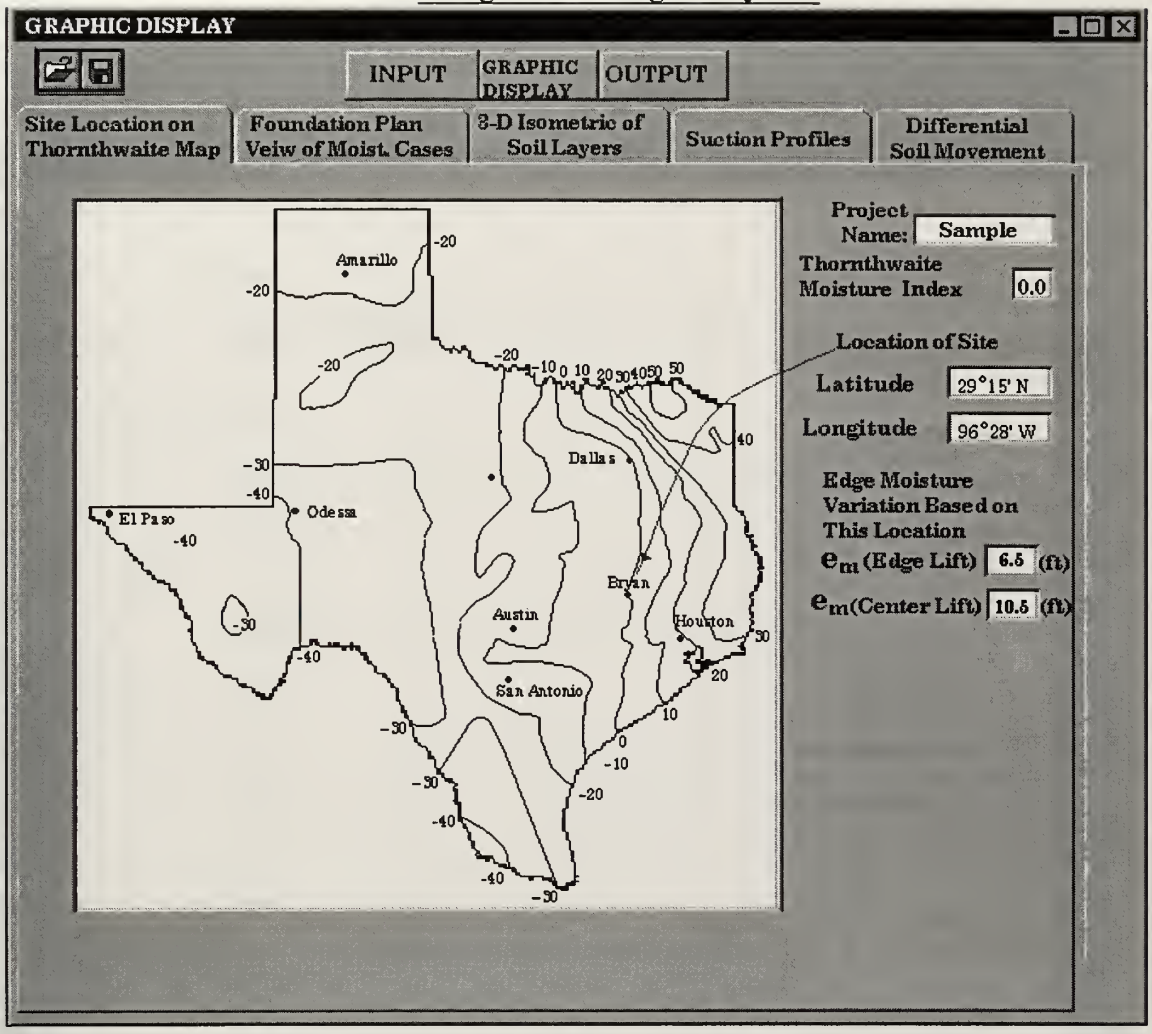

## Program Design Layout

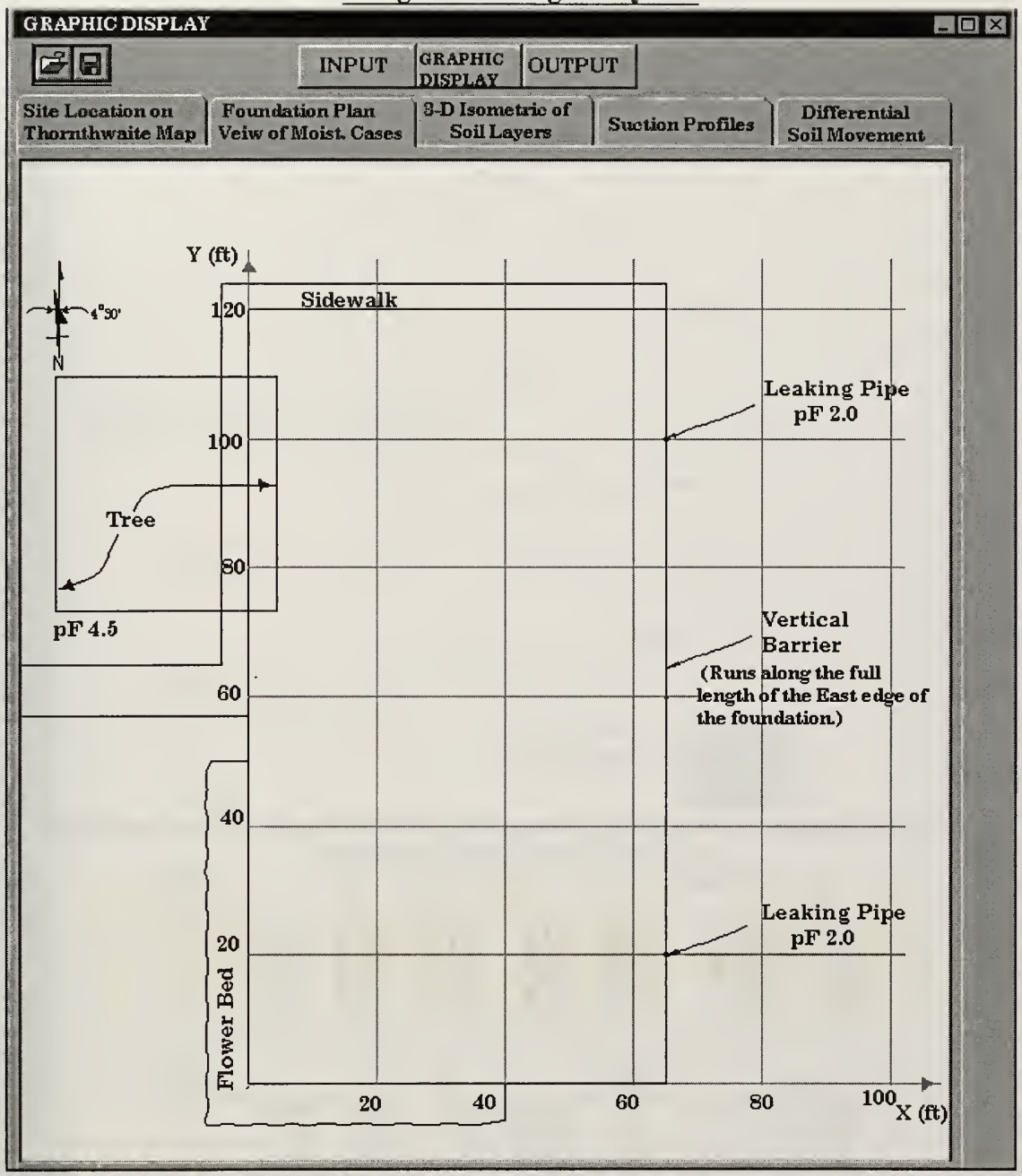

# Program Design Layout

GRAPHIC DISPLAY

INPUT | GRAPHIC DISPLAY | OUTPUT

Site Location on Thornthwaite Map | Foundation Plan Veiw of Moist. Cases | 3-D Isometric of Soil Layers | Suction Profiles | Differential Soil Movement

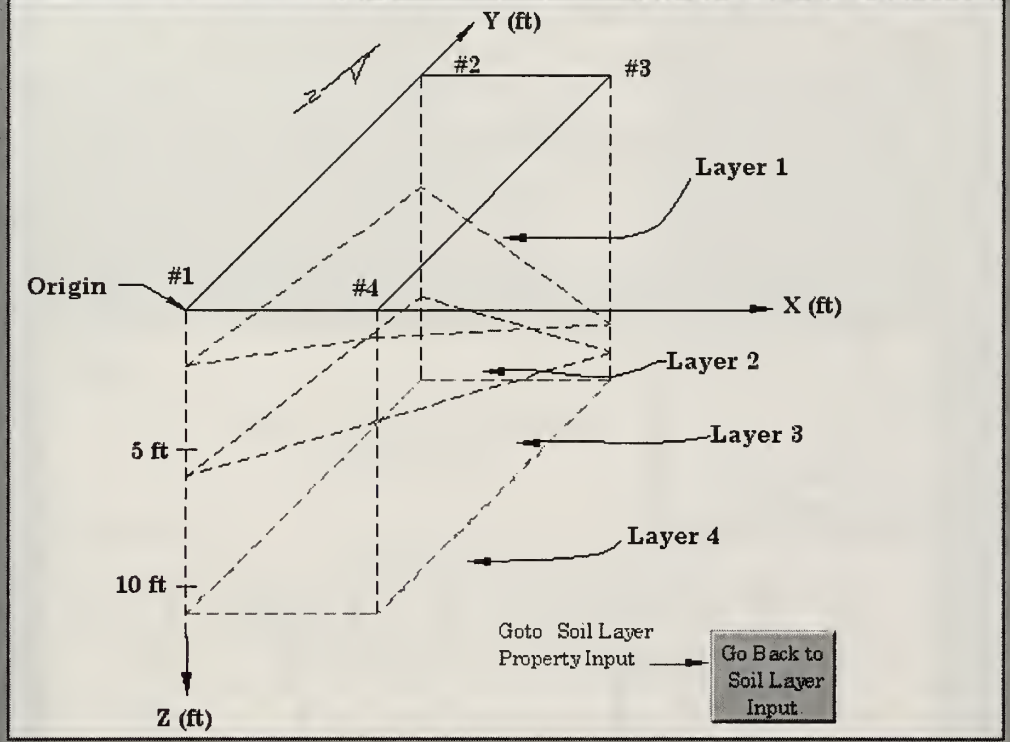


## Summary of Soil Layer Properties

| Soil Layer # | %LL | %PL | %-#200 % | %-2μ | %PI | %Fine Clay | CEC |
|---|---|---|---|---|---|---|---|
| 1 | 56.0% | 22.0% | 65.0% | 25.0% | 34.0% | 38.46% | 37.21 |
| 2 | 67.0% | 24.0% | 76.0% | 46.0% | 43.0% | 60.53% | 41.20 |
| 3 | 44.0% | 18.0% | 47.0% | 18.0% | 26.0% | 38.30% | 29.42 |
| 4 | 53.0% | 20.0% | 64.0% | 31.0% | 33.0% | 48.44% | 33.28 |

| Soil Layer # | Ac | CEA | $\gamma_{h100}$ % | $\gamma_h$ | $\gamma_d$ lbs/ft$^3$ | S | $\alpha$ cm$^2$/s |
|---|---|---|---|---|---|---|---|
| 1 | 0.8840 | 0.9674 | 0.163 | 0.062692 | 120 | -11.11 | 0.003936 |
| 2 | 0.7104 | 0.6806 | 0.163 | 0.098658 | 120 | -9.70 | 0.003268 |
| 3 | 0.6789 | 0.7682 | 0.163 | 0.062426 | 120 | -13.28 | 0.004289 |
| 4 | 0.6813 | 0.6871 | 0.163 | 0.078953 | 120 | -11.53 | 0.003805 |

| Soil Layer # | p cm$^2$/s | $k_o$ cm/s | TMI | n cycles/yr | $e_m$ Center Lift ft | $e_m$ Edge Lift ft |
|---|---|---|---|---|---|---|
| 1 | 0.000681 | 2.96E-06 | 0 | 1 | 10.2 | 6 |
| 2 | 0.000648 | 2.81E-06 | 0 | 1 | 7.6 | 5 |
| 3 | 0.000621 | 2.70E-06 | 0 | 1 | 10.5 | 6.5 |
| 4 | 0.000635 | 2.76E-06 | 0 | 1 | 9.5 | 5.9 |

# Program Design Layout

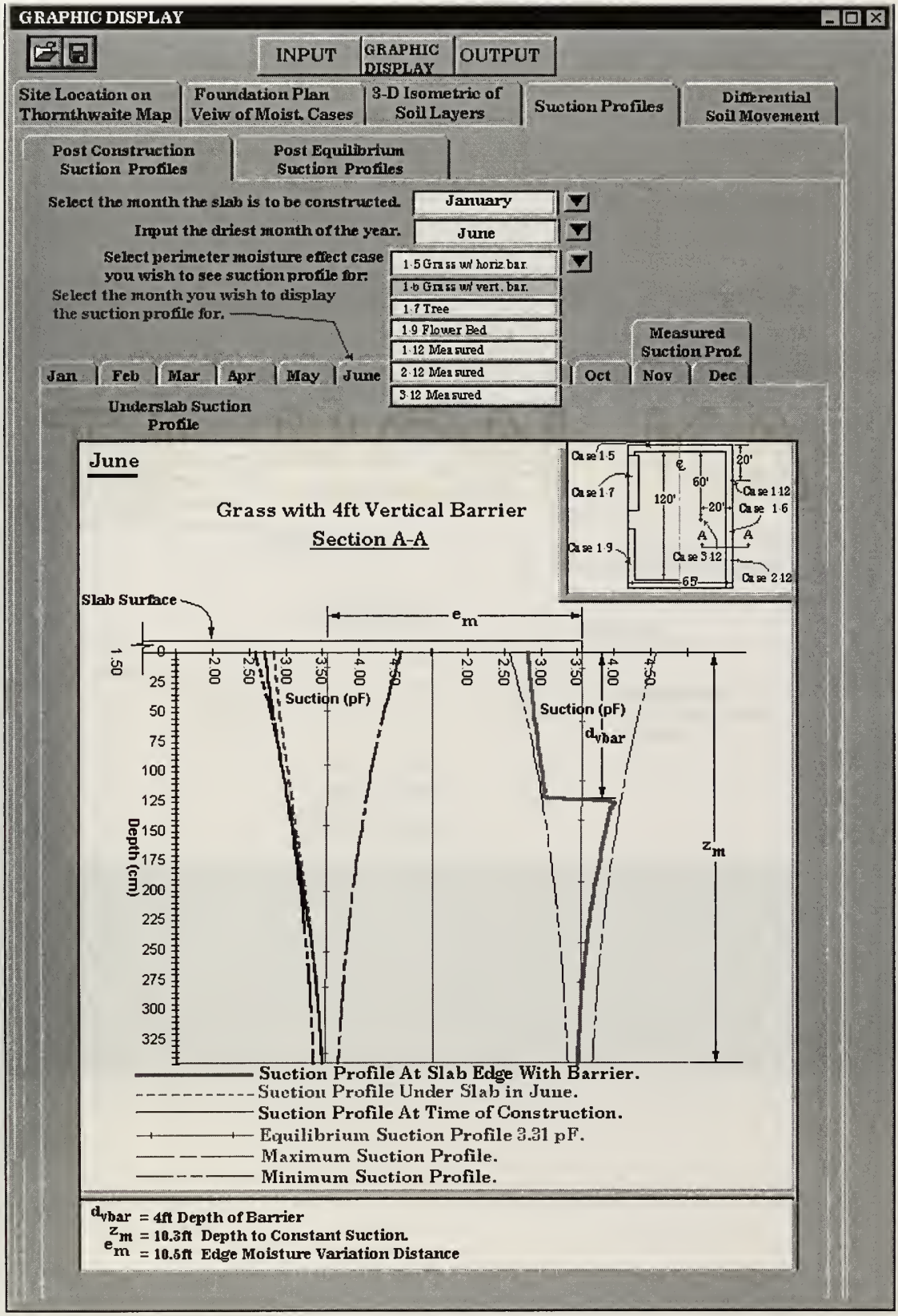

# Program Design Layout

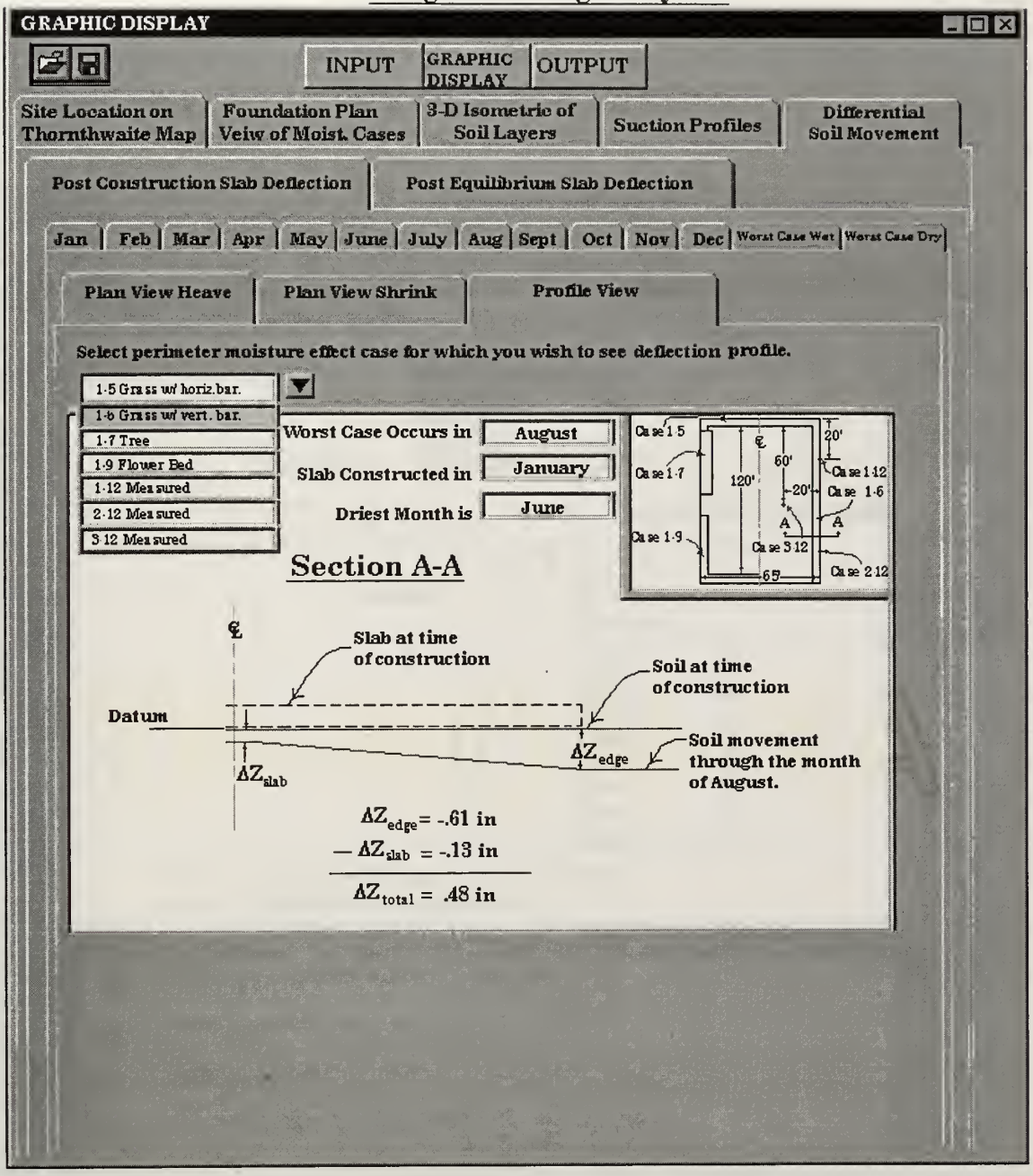

# Program Design Layout

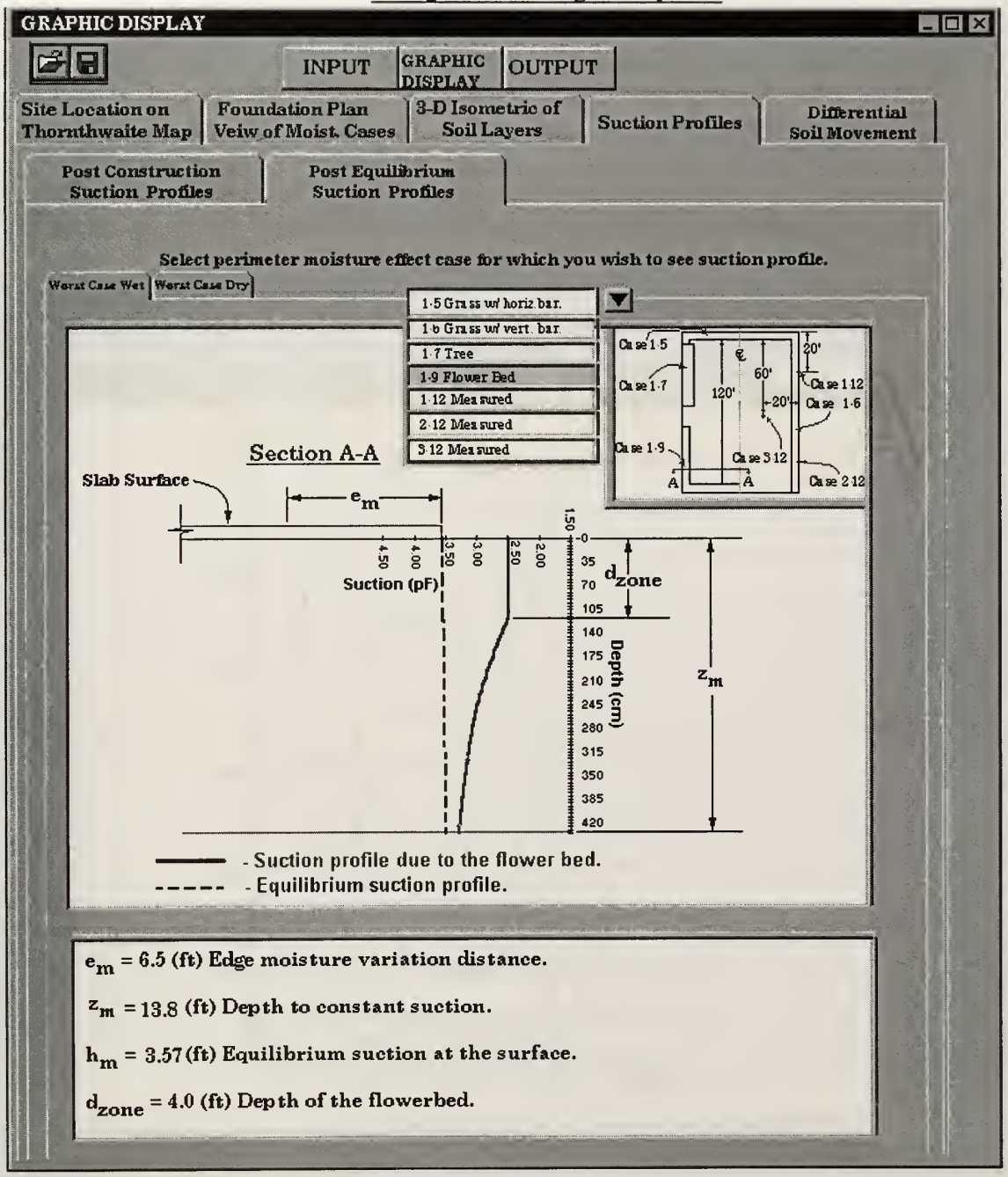

# Program Design Layout

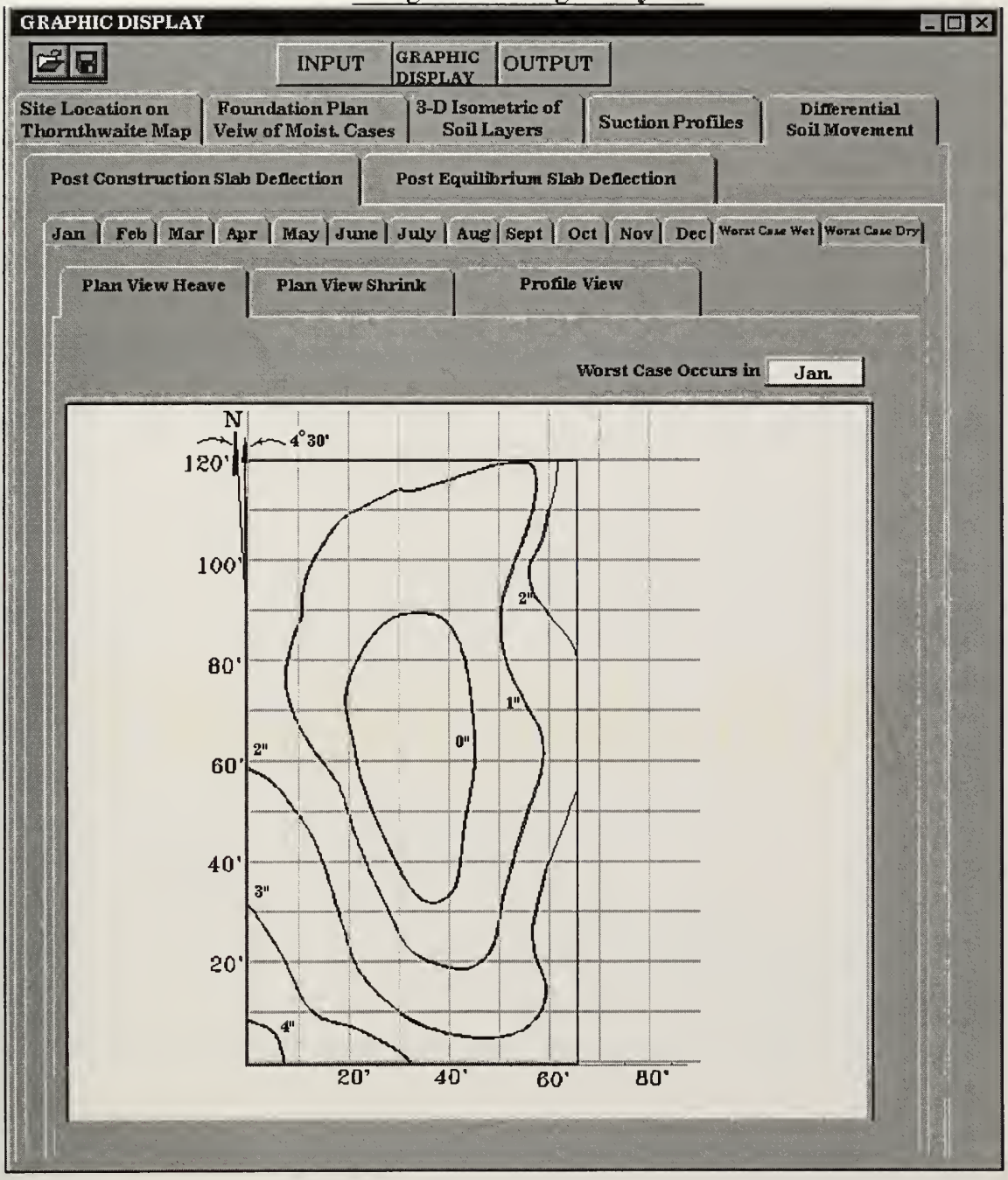

# APPENDIX C

## SITE PLAN OF MOISTURE EFFECT CASES USED IN SAMPLE CALCULATIONS

# Program Design Layout

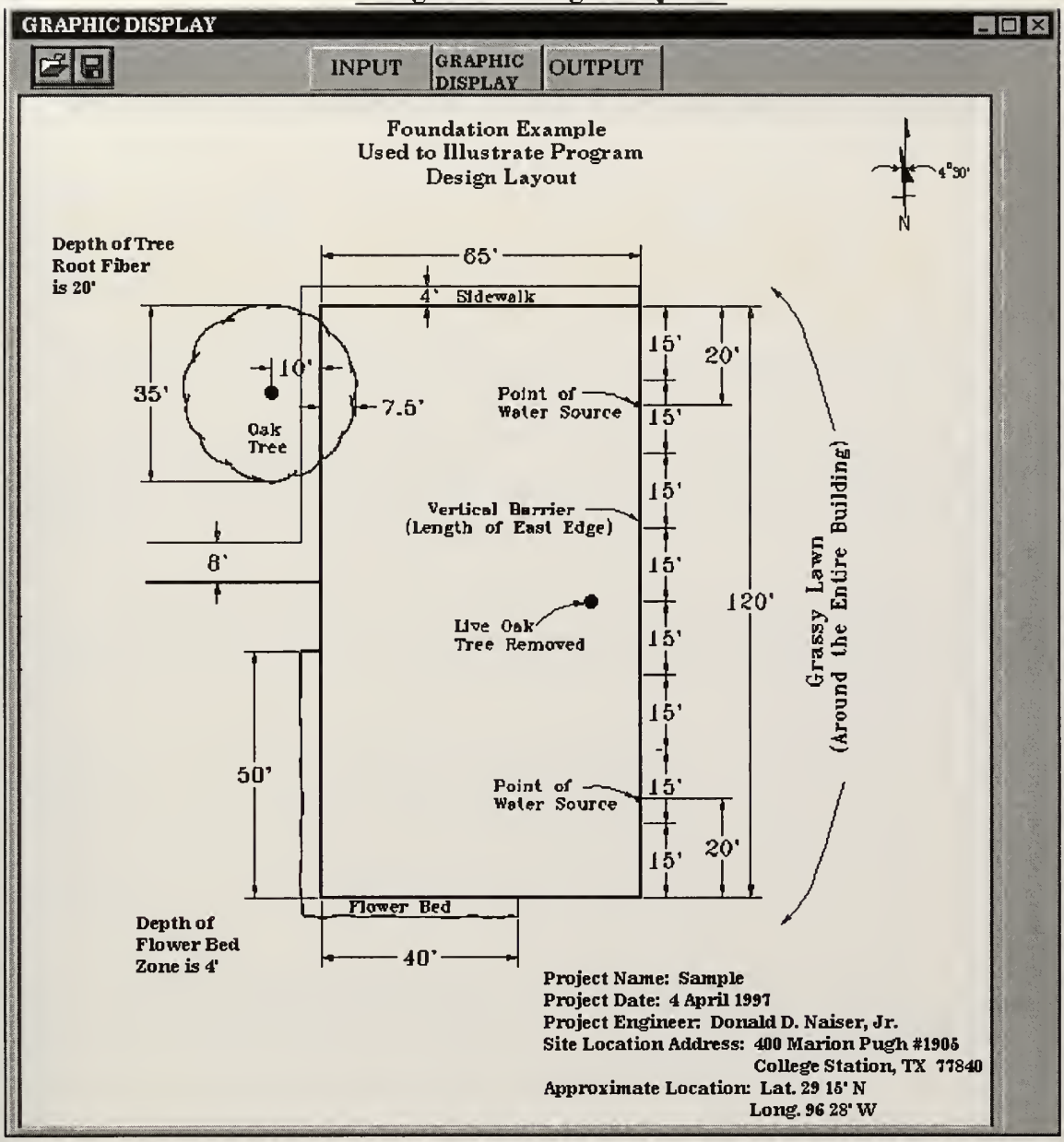

# APPENDIX D

## REQUEST FOR PERMISSION TO USE COPYRIGHTED MATERIAL

**Donald D. Naiser, Jr.**
**400 Marion Pugh #1905**
**College Station, Texas 77840**

August 27, 1997

Permissions Department
John Wiley & Sons, Inc.
605 Third Avenue
New York, NY 10158-0012

**REQUEST TO USE FIGURES COPIED FROM *SOIL MECHANICS* 1969**

I am a master of science candidate at Texas A&M University and I will be finalizing my thesis in the next two weeks. Our library sends our theses to University Microfilms Inc., for preparation of a microfilm copy of the document. As I am sure you are aware, UMI retains the right to sell both hard and microfilm copies of the document.

My reason for writing is to request permission to use the figures listed below exactly as they appear in *SOIL MECHANICS*, by Lambe and Whitman, copyrighted by John Wiley & Sons, Inc., 1969. With your permission, I will use the following figures in my thesis:

1. Figure 4.7 "The structure of serpentine." Found on page 47.
2. Figure 4.8 "The structure of kaolinite." Found on page 47.
3. Figure 4.9 "The structure of pyrophyllite." Found on page 47.
4. Figure 4.10 "The structure of muscovite." Found on page 47.
5. Figure 4.11 "Sheet silicate minerals." Found on page 48-49.
6. Figure 5.9 "Soil particles with water and ions." Found on page 55.

One chapter in my thesis describes the magnitude of the problem of designing foundations built on expansive soils. The figures described above will be used to illustrate the molecular structure of fine grained soil particles. The thesis has been accepted and the author proofs indicate a 1997 publication date. The thesis title is *PROCEDURES TO PREDICT VERTICAL DIFFERENTIAL SOIL MOVEMENT FOR EXPANSIVE SOILS.*

Please inform me of any necessary action to prevent future publication complications. I can be contacted by phone at home (409) 543-8412 or at work (409) 845-9919. Thank you very much for your effort in resolving these issues.

Sincerely,

Donald D. Naiser, Jr.

# VITA

Donald David Naiser, Jr. is a citizen and resident of the United States of America, whose permanent mailing address is,

Rt. 3 Box 203-C

El Campo, Texas 77437.

He obtained his Bachelor of Science degree in Civil Engineering, from Texas A&M University in 1991.

Since graduating from Texas A&M University, he has been commissioned as a United States Naval Officer as a member of the Civil Engineer Corps. His time served in the Navy has been exclusively with the SEABEES performing contingency construction training as well as constructing naval facilities. His tour highlights have been as the Officer In Charge of the Elevated Causeway System (ELCAS) in Amphibious Construction Battalion ONE and as the Officer In Charge of Construction Battalion Unit 418.

In 1996 he was accepted at Texas A&M University to pursue studies toward the degree of M.S. within the Geotechnical branch of Civil Engineering.

In 1997 he became registered as a professional engineer in the state of Washington.

"Blessed are the people whose leaders can look destiny in the eye without flinching but also without attempting to play God.", Henry Kissinger. His career interests include achieving excellence through leadership in any Christian form.

20 SINFS
1/99 22527-157

DUDLEY KNOX LIBRARY
3 2768 00360253 3